

LAND USE BASED FLOOD HAZARD ANALYSIS FOR THE MEKONG DELTA

Zur Erlangung des akademischen Grades eines

DOKTOR-INGENIEURS

von der Fakultät für

Bauingenieur-, Geo- und Umweltwissenschaften

des Karlsruher Instituts für Technologie

genehmigte

DISSERTATION

von

MSc. Vu, Hoang Thai Duong

aus Dong Nai, Vietnam

Tag der Mündlichen Prüfung :	28.03.2018
Hauptreferent:	Prof. Dr.-Ing. Dr. h.c. mult. Franz Nestmann (Karlsruher Institut für Technologie)
Korreferent:	Assoc. Prof. Dr.-Ing. Trinh Cong Van (Mekong Water Innovation Institute, Vietnam) Prof. Dr.-Ing. Stefan Hinz (Karlsruher Institut für Technologie)

Karlsruhe, 2018

“Where there’s a will, there’s a way”

Proverb

Acknowledgments

The dissertation is a yield of my research efforts at the Institute for Water and River Basin Management (IWG) – Karlsruhe Institute of Technology (KIT), Germany. Herewith, I would like to express my deep grateful to the supervisors, my doctor fathers: Prof. Franz Nestmann (IWG) and Prof. Stefan Hinz (IPF) in Germany; Prof. Trinh Cong Van (MWI), Vietnam who fulfill excellent advisory works and always stand aside me to help anytime.

Especially, I greatly appreciate the KAAD organization, Herr Dr. Geiger, Frau Bialas, Frau Wend for their great supports and warm encouragements during my research period in Germany.

Many thanks from me to the colleagues at the IWG for providing me a friendly and professional working environment at the institute. Particularly, Dr. Oberle is like a big brother of mine, who supports not only in academic issue but also give me advises for my daily matters, besides Karin and Sandra are so lovely to support me in administration works.

I am full of thanks to the experts and colleagues at the German Aerospace Center (Dr. Kuenzer, Frau Huth), Germany; the National Institute for Agro-Environment sciences (Dr. Sakamoto), Japan; the Institute for Water and Environment Research (Director Dr. Bảo, Mr. Quyét, Mr. Cường, Ms. Vân, Ms. Hà); The Mekong Water Innovation Institute (Mr. Thiện, Mr. Tiến), the Southern Institute of Water Resources Planning (Mr. Nam, Ms. Hằng, Ms. Đường), the Southern Institute of Water Resources Research (Mr. Trung, Mr. Vinh), Vietnam, Danish Hydraulic Institute (DHI), Denmark for their kindly supports, comments, and also providing precious data and software license to implement this study.

Through this occasion, I am appreciated very much the BMBF, Prof. Dr. Furrer (PTKA) for offering us great chances to help in uprising the living conditions of Vietnamese people, particularly for the Mekong delta, a countryside with fundamental existence worth of the Motherland. My best regards to the enthused KIT colleagues: Prof. Norra, Prof. Fink, Dr. Klinger, Dr. Schenk, Dr. Seidel, Dr. Kron, Dr. Boersig, Mr. Wilhelms, Ms. Gonzales, who support very much within the ViWaT Mekong project.

Besides, I would like to express my best regards to the doctoral candidates (Mr. Dũng Trần and Ms. Ngân Lê in the Wageningen University) who accompany me on the same route and overcome together difficulties and obstacles.

I also want to thank to all KAAD-scholars fellows: Vân Anh, Nguyệt, Dũng, Chi, Lưu, Thắng, Khánh, Bashar, Teddy, Zan, etc, who have shared with me unforgettable memories in Germany.

Last but not least, I would love to spare the sweetest words for my family: my parents, my brothers and sisters, for my wife Rose who always love and support me in such a long time that I have to stay far away from them.

Karlsruhe, 2018

Vu Hoang Thai Duong

Kurzfassung

Das Mekong-Delta nimmt für die Republik Vietnam einen sehr hohen Stellenwert in Bezug auf Natur, Wirtschaft, Politik, Menschen, Landwirtschaft, Fischerei, Geopolitik und vielen anderen Bereichen ein. Der sogenannte Dreifachreis (auch Herbst-Winter-Ernte oder Third Crop genannt) wurde in den letzten Jahren für das Mekong-Delta in den stark überfluteten Gebiete durch umschlossene Kompartimenten wie Halbdeichstrukturen (zum Schutz der Reisfelder vor Hochwasser (von Juli bis Mitte August) sowie Volldeichmessungen (zum vollständigen Schutz der Reisfelder während der Hochwassersaison) schnell ausgebaut. Der Reisanbau hat daher Auswirkungen auf die Hochwassersituation in den flußabwärts gelegenen Gebieten.

Diese Studie zielt darauf ab, die Auswirkungen von Deichmessungen auf Hochwasser in den Mekong-Flüssen zu analysieren, indem das 1D-Hydraulikmodell MIKE11 sowie Fernerkundungsprodukte (MODIS-Satellit) verwendet werden. Um diese Einflüsse umfassend zu erforschen, wurde mit dem Hydraulikmodell MIKE11 die Auswirkungen von mehreren Volldeichkompartimenten auf das Hochwasser entlang der Hauptflüsse basierend auf einem Geographical Impact Factor (GIF) analysiert. Der Autor fand heraus, daß verschiedene geografische Kompartimente unterschiedliche Einflüsse auf das Hochwasserniveau entlang des Mekong haben.

Fernerkundungsprodukte wurden eingesetzt, um die Veränderung der Landnutzungsgebiete im Mekong-Delta von 2000 bis 2017 zu analysieren. Außerdem wurde von MODIS Satellitenprodukte eine komplette Datenbank von Hochwasserverteilungskarten (476 Karten) im Mekong-Delta während der Hochwassersaison 2000 bis 2017 interpretiert. Darüber hinaus wurden die Satellitenprodukte einschließlich Landnutzung und Hochwasserkarten in MD zu weiteren Untersuchungen des Mekong Delta für die Öffentlichkeit online zur Verfügung gestellt

Die Simulation funktioniert für ein großes und komplexes Flussnetz, da das Mekong-System viele Anstrengungen und Erfahrungen der Ingenieure erfordert, die nicht leicht zu bewältigen sind. Daher wurde eine einfache Methode zur Interpretation des Hochwasserstandes entlang der Mekong Flüsse entwickelt, um Ingenieuren ein schnelles Werkzeug zur Bewertung der Auswirkungen von Deichkonstruktionen für Landnutzungszwecke auf Hochwasserregime zur Verfügung zu stellen.

Im Bereich Hydraulik wurde ebenfalls eine Empfehlung zum Reisanbau in den Gebieten vom Mekong-Delta abgegeben, welche den Anwendern die Möglichkeit bieten soll, die Ausrichtung der landwirtschaftlichen Entwicklung gegenüber dem Hochwassermanagement zu steuern.

Abstract

The Mekong Delta holds substantial worth for the Socialist Republic of Vietnam because of its contributions in regards to nature, the economy, politics, the people, agriculture, fishery, geopolitics, and numerous others. An intensive rice-based production strategy was issued by the Government of Vietnam to support the growth of so-called triple rice (also named Autumn-Winter crop or Third Crop) within the Mekong Delta. This required the rapid construction in recent years of a multitude of compartments enclosed by semi-dyke structures (to protect rice fields from flood water from July until mid-August) and full-dyke measures (to protect the rice fields fully during flood season) within the frequently high flooding areas. Consequently, these structures have significantly impacted the flood situation in the areas downstream.

This study is aimed at analyzing the impact of dyke measures on flood water in the Mekong rivers by applying a 1D hydraulic model MIKE11 and remote sensing products, such as a MODIS satellite. To explore these influences comprehensively, MIKE11 was used to analyze the impacts of several full-dyke compartments on the flood water along the main rivers based upon a Geographical Impact Factor (GIF). It has been figured out that that different geographical compartments cause different rates of influences on the flood water level along Mekong Rivers.

Remote sensing products were collected and analyzed the change of land use areas in the Mekong Delta from 2000 to 2017. Additionally, a full database of flood distribution maps (476 maps) in the Mekong Delta (MD) during flooding seasons from 2000 to 2017 was prepared and interpreted using MODIS satellite products. The satellite products including the land use and flood maps in the MD are available to serve further researches about the Mekong Delta.

Simulation for a large and complex river network such as the Mekong River system requires engineers with significant experience. Therefore, a simple method for interpolation of flood water level along the Mekong River was also developed (FLEM model) to provide engineers a quick tool to evaluate the impacts of dyke construction for land use purposes on flood regimes.

A recommendation about the areas of rice cultivation in the Mekong Delta was also offered in terms of a hydraulic sector to support administrators in developing a comprehensive plan to manage the orientations of agricultural development in relation to flood management for the Mekong Delta.

Table of contents

1. Introduction	1
1.1. Problem description.....	2
1.2. Objectives of the study	5
1.3. Research questions.....	5
1.4. Approaches.....	6
1.5. Structure of the Dissertation	10
2. Analysis the land use change versus flooding situation in the MD using remote sensing technology.....	11
2.1. Overview of remote sensing technology	11
2.2. Selection of appropriate remote sensing sensor.....	12
2.2.1. Multi-criteria analysis for satellite selection.....	14
2.2.2. MODIS satellite	16
2.3. Time series of flood monitoring in the MD	18
2.3.1. Algorithms for flood mapping.....	18
2.3.2. Flood extent analysis.....	24
2.3.3. Flood map accuracy analysis	26
2.3.3.1. In comparison with higher resolution SAR satellite products	26
2.3.3.2. Field trip to An Giang and Dong Thap province.....	31
2.3.4. Discussion about MODIS flood maps	32
2.3.5. The relationship between flood levels vs flooded area.....	32
2.4. Land use analysis for Mekong delta	33
2.4.1. Algorithm for land use mapping.....	33
2.4.2. Land use change analysis in the Mekong delta	42
2.4.3. Land use product accuracy analysis.....	44
2.4.3.1. MODIS land use vs statistical data	44
2.4.3.2. Compare MODIS land use map interpreted by Duong vs Dr. Sakamoto.	46
2.4.3.3. Field trip to An Giang and Dong Thap province	47
2.4.4. Discussion land use change in MD.....	48

2.4.5.	Effect of triple rice cropping to local farmers:.....	48
2.5.	Discussion.....	49
3.	Analysis the impact of land use change versus flooding situation in the MD using numerical modelling.....	51
3.1.	Identification the factors of hydraulic change in the Mekong delta	52
3.1.1.	Water level change	53
3.1.2.	Flood inflow rates change	55
3.2.	Analysis the impact of land use change based on numerical modelling.....	56
3.2.1.	Hydraulic model MIKE11 description.....	56
3.2.1.1.	Building geometry network for Mekong delta	56
3.2.1.2.	Calibration validation works	60
3.2.2.	Numerical modelling for land use change scenarios.....	70
3.2.2.1.	Impact of dyke measurement on historical floods	70
3.2.2.2.	Geographical impact factor (GIF) analysis	73
3.2.2.2.1.	Influence of GIF at a location to different positions on Mekong Rivers.....	75
3.2.2.2.2.	Influence of full-dyke system at each compartment at different locations ...	77
3.3.	Discussion.....	79
4.	Application of GIF and remote sensing into flood monitoring and land use management for the MD.....	80
4.1.	Optimization the area for triple rice cropping in the MD	80
4.2.	Application of GIF for flood level prediction in the MD	81
4.2.1.	Interpolation of flood level for flood in 2011	87
4.2.2.	Interpolation of flood level for flood in 2012	89
4.2.3.	Interpolation of flood level for flood in 2013	91
4.2.4.	Interpolation of flood level for flood in 2014	93
4.2.5.	Interpolation of flood level for flood in 2015	95
4.2.6.	Interpolation of flood level for flood in 2016	97
4.2.7.	Interpolation of flood level for flood in 2017	99
4.3.	Implementation of online information system.....	103
4.4.	Discussion.....	106
5.	Conclusion and outlooks.....	108
5.1.	Conclusions.....	108
5.2.	Outlooks.....	109
6.	References.....	110

7. Appendix.....	119
7.1. Day of Year (DOY) Calendar	119
7.2. Telemetry data from MRC website	121
7.3. Accuracy analysis for Land use flood map by MODIS satellite	122
7.3.1. The accuracy of total rice in year and aquaculture areas vs statistical data	122
7.3.2. Accuracy analysis of Triple rice cropping area.....	125
7.4. Flood distribution in Mekong Delta - MODIS satellite.....	127
7.4.1. Flood distribution in 2001	127
7.4.2. Flood distribution in 2002	129
7.4.3. Flood distribution in 2003	131
7.4.4. Flood distribution in 2004	133
7.4.5. Flood distribution in 2005	135
7.4.6. Flood distribution in 2006	137
7.4.7. Flood distribution in 2007	139
7.4.8. Flood distribution in 2008	141
7.4.9. Flood distribution in 2009	143
7.4.10. Flood distribution in 2010	145
7.4.11. Flood distribution in 2011	147
7.4.12. Flood distribution in 2012	149
7.4.13. Flood distribution in 2013	151
7.4.14. Flood distribution in 2014	153
7.4.15. Flood distribution in 2015	155
7.4.16. Flood distribution in 2016	157
7.4.17. Flood distribution in 2017	159
7.5. Accuracy analysis of flood maps from MODIS satellite.....	161
7.5.1. Comparison with flood maps by ENVISAT-ASAR Satellite	161
7.5.2. Comparison with flood map of TERRA-X-Scan SAR satellite	166
7.5.3. Comparison with flood map of TSX Strip satellite	170
8. Information about the author.....	173

List of figures

Figure 1.1. Map of the Mekong Delta.....	1
Figure 1.2. Examples of semi-dyke and full-dyke structures in Dong Thap (A) and An Giang (B);	3
Figure 1.3. Impacts of dyke system on flood extents in 2000 and 2011	3
Figure 1.4. The relationship of dyke compartments vs flood water change in Mekong delta	5
Figure 1.5. The combination of flood factors (1.5a) and the study coordination of MD (1.5b).....	6
Figure 1.6. Cross sections at Tan Chau and Chau Doc gauges on Mekong and Bassac Rivers... ..	7
Figure 1.7. Observed rainfall data at the Tan Chau and Chau Doc gauges during rainy season ..	7
Figure 1.8. Land use based flood hazard analysis for the Mekong delta.....	9
Figure 2.1. Principles about active and passive remote sensing (NASA website, 2017)	11
Figure 2.2. The range of electromagnetic spectrum.....	12
Figure 2.3. Pictures of popular satellites	13
Figure 2.4. Image of the website used to access MODIS Satellite images.....	18
Figure 2.5. Processing of flood mapping.....	19
Figure 2.6. Example of the process for cloud removal	20
Figure 2.7. Flood distribution (rising stage) in 2000 from DOY145 to DOY233	22
Figure 2.8. Flood distribution (peak and falling stages) in 2000 from DOY241 to DOY361	23
Figure 2.9. Relationship between water level at Tan Chau gauge and flooded area in 2000	24
Figure 2.10. Flooded area in Mekong delta from 2000 to 2017	24
Figure 2.11. Maximum flood extension in MD from 2000 to 2017	25
Figure 2.12. Maximum flood extension in An Giang province from 2000 to 2017	25
Figure 2.13. Comparison of flooded maps between MODIS-Terra and Envisat-ASAR satellite ..	27
Figure 2.14. Agreement of flood maps by Envisat ASAR vs MODIS on 23.10.2007	28
Figure 2.15. Comparison of flooded maps between MODIS vs Terra SAR Scan satellite	29
Figure 2.16. Comparison of flood maps by Terra SAR-X vs MODIS on 25.09.2008	29
Figure 2.17. Agreement of flood maps by Terra SAR-X vs MODIS on 24.10.2010	30
Figure 2.18. Comparison of flooded maps between MODIS vs TSX strip	31
Figure 2.19. Field trip to An Giang and Dong Thap provinces during flood seasons	31

Figure 2.20. Relationship between water levels at Tan Chau and Chau Doc gauges vs flooded area in 2014	32
Figure 2.21. Relationship between water levels at Tan Chau and Chau Doc gauges vs flooded area in 2017	33
Figure 2.22. Flow chart showing the integrated algorithms of the wavelet-based filter	34
Figure 2.23. Flow chart showing the modification part for land use detection by Duong, 2017....	35
Figure 2.24. EVI series in the Mekong Delta from January 2013 to December 2017	36
Figure 2.25. The variation of observed EVI time series at the locations from 2013 to 2017	37
Figure 2.26. The variation of observed EVI time series at 4 locations in MD in 2017	39
Figure 2.27. Land use pattern in Mekong Delta	42
Figure 2.28. Area of triple rice cropping changes in upstream provinces from 2000 to 2017.....	42
Figure 2.29. The relationship between triple rice and flooded areas in An Giang province	43
Figure 2.30. Areas of triple rice cropping in An Giang province	43
Figure 2.31. Agreement between statistical data vs MODIS land use data	45
Figure 2.32. Agreement of triple rice area between statistical data and MODIS land use	46
Figure 2.33. Agreement about land use mapping in 2003 between Sakamoto vs Duong.....	46
Figure 2.34. Agreement of land use areas in 2003 between statistical data and MODIS	47
Figure 2.35. Field trip to the MD for ground true assessment	47
Figure 2.36. Activities of farmers for triple rice cropping	49
Figure 2.37. Dyke system calibration by MODIS flood maps	50
Figure 2.38. Dyke system in the MD after calibration.....	50
Figure 3.1. Mekong river basin (MRC, 2013) and maximum water level at Tan Chau.....	51
Figure 3.2. Flood hydrograph in 2000 vs 2011 at the Tan Chau gauge.	53
Figure 3.3. Studied locations on Mekong and Bassac river	53
Figure 3.4. Difference in water levels on the Mekong River	54
Figure 3.5. Difference in water levels on the Bassac River	54
Figure 3.6. Flood flow distribution to the Mekong Delta in 2000 vs the flood in 2011	55
Figure 3.7. Typical floodplain description compartment (Approach 1).....	57
Figure 3.8. Typical floodplain compartment (Approach 2).....	57
Figure 3.9. Detailed description of additional storage of link channel in MIKE11.....	58
Figure 3.10. Mekong River network in MIKE 11	59
Figure 3.11: Chart for hydraulic model calibration and validation.....	60
Figure 3.12. Hydraulic gauges in Mekong Delta	61
Figure 3.13. Model calibration of water level with high flood in 2000.....	63

Figure 3.14. Model calibration of water level with high flood in 2011.....	64
Figure 3.15. Hydraulic model validation of water level with medium flood in 2013	66
Figure 3.16. Hydraulic model validation of water level with low flood in 2012	67
Figure 3.17. Agreement of flood maps in 2011 to hydraulic models and satellite products	69
Figure 3.18. Difference in water levels on the Mekong River (SC1 vs SC3).....	70
Figure 3.19. Difference in water levels on the Bassac River (SC1 vs SC3).....	71
Figure 3.20. Difference in water levels on the Mekong River (SC2 vs SC4).....	71
Figure 3.21. Difference in water levels on the Bassac River (SC2 vs SC4).....	71
Figure 3.22. Difference in water levels in inland areas in DTM and TGLX (SC2 vs SC4).....	72
Figure 3.23. Mekong Delta with 22 compartments (A) and 10 examined locations (P).....	74
Figure 3.24. GIF of compartment A10 on flood water level along Mekong and Bassac rivers	76
Figure 3.25. GIF of compartment A20 on flood water level along Mekong and Bassac rivers	76
Figure 3.26. Geographical impact factors on Tan Chau water level (left) and Chau Doc water level (right) vs total flood discharge into Mekong Delta measured at the Tan Chau and Chau Doc gauges	77
Figure 3.27. Geographical impact factors on Vam Nao water level (left) and on Long Xuyen water level (right) vs total flood discharge into the Mekong Delta measured at the Tan Chau and Chau Doc gauges	78
Figure 3.28. Geographical impact factors on Cao Lanh water level (left) and on Can Tho water level (right) vs. total flood discharge into the Mekong Delta measured at the Tan Chau and Chau Doc gauges	78
Figure 4.1. Vulnerability analysis of dyke measures for triple rice cropping in the MD	80
Figure 4.2. Approach of FLEM model (interpolation method).....	81
Figure 4.3. Impacts of land use on flood water on the Mekong River.....	84
Figure 4.4. Impacts of land use on flood water on the Bassac River.....	85
Figure 4.5. Flood extension on 29.09.2011.....	88
Figure 4.6. Interpolation of flood water level along Mekong and Bassac rivers on 29.09.2011.....	88
Figure 4.7. Flood extension on 30.09.2012.....	90
Figure 4.8. Interpolation of flood water level on main rivers for small flood on 30.09.2012.....	90
Figure 4.9. Flood extension on 02.10.2013.....	92
Figure 4.10. Interpolation of flood water level along main rivers on 02.10.2013.....	92
Figure 4.11. Flood extension on 11.08.2014.....	94
Figure 4.12. Interpolation of flood water level along main rivers on 11.08.2014.....	94
Figure 4.13. Flood extension on 16.08.2015.....	96
Figure 4.14. Interpolation of flood water level along main rivers on 16.08.2015.....	96

Figure 4.15. Flood extension on 06.10.2016.....	98
Figure 4.16. Interpolation of flood water level along main rivers on 06.10.2016.....	98
Figure 4.17. Flood extension on 10.10.2017.....	100
Figure 4.18. Interpolation of flood water level along main rivers on 10.10.2017.....	100
Figure 4.19. Interpolation of unavailable water level along the main rivers on 29.09.2011.....	101
Figure 4.20. Interpolation of unavailable water level along the main rivers on 10.10.2017.....	102
Figure 4.21. Personal website.....	103
Figure 4.22. Database menu of the website.....	103
Figure 4.23. Details of GIS menu.....	104
Figure 4.24. Detail of Remote Sensing – Land Use.....	104
Figure 4.25. Detail of Remote Sensing – Flood Menu.....	105
Figure 4.26. Hydraulic Simulation Menu.....	105
Figure 4.27. Sea level Rice Scenarios.....	106
Figure 4.28. Salinity Simulation Menu.....	106
Figure 7.1. Online observed water level and discharge at Tan Chau guage on MRC website. .	121
Figure 7.2. Flood distribution in Mekong delta in 2001 – MODIS satellite.....	128
Figure 7.3. Flood distribution in Mekong delta in 2002 – MODIS satellite.....	130
Figure 7.4. Flood distribution in Mekong delta in 2003 – MODIS satellite.....	132
Figure 7.5. Flood distribution in Mekong delta in 2004 – MODIS satellite.....	134
Figure 7.6. Flood distribution in Mekong delta in 2005 – MODIS satellite.....	136
Figure 7.7. Flood distribution in Mekong delta in 2007 – MODIS satellite.....	138
Figure 7.8. Flood distribution in Mekong delta in 2007 – MODIS satellite.....	140
Figure 7.9. Flood distribution in Mekong delta in 2008 – MODIS satellite.....	142
Figure 7.10. Flood distribution in Mekong delta in 2009 – MODIS satellite.....	144
Figure 7.11. Flood distribution in Mekong delta in 2010 – MODIS satellite.....	146
Figure 7.12. Flood distribution in Mekong delta in 2011 – MODIS satellite.....	148
Figure 7.13. Flood distribution in Mekong delta in 2012 – MODIS satellite.....	150
Figure 7.14. Flood distribution in Mekong delta in 2013 – MODIS satellite.....	152
Figure 7.15. Flood distribution in Mekong delta in 2014 – MODIS satellite.....	154
Figure 7.16. Flood distribution in Mekong delta in 2015 – MODIS satellite.....	156
Figure 7.17. Flood distribution in Mekong delta in 2016 – MODIS satellite.....	158
Figure 7.18. Flood distribution in Mekong delta in 2017 – MODIS satellite.....	160
Figure 7.19. Comparison of flood mapping between Envisat ASAR vs MODIS on 14.08.2007. .	161
Figure 7.20. Comparison of flood mapping between Envisat ASAR vs MODIS on 19.07.2007. .	161

Figure 7.21. Comparison of flood mapping between Envisat ASAR vs MODIS on 11.09.2007 .	162
Figure 7.22. Comparison of flood mapping between Envisat ASAR vs MODIS on 18.09.2007 .	162
Figure 7.23. Comparison of flood mapping between Envisat ASAR vs MODIS on 16.10.2007 .	163
Figure 7.24. Comparison of flood mapping between Envisat ASAR vs MODIS on 23.10.2007 .	163
Figure 7.25. Comparison of flood mapping between Envisat ASAR vs MODIS on 01.11.2007 .	164
Figure 7.26. Comparison of flood mapping between Envisat ASAR vs MODIS on 20.11.2007 .	164
Figure 7.27. Comparison of flood maps by Envisat ASAR vs MODIS on 27.11.2007	165
Figure 7.28. Comparison of flood mapping between Envisat ASAR vs MODIS on 06.12.2007 .	165
Figure 7.29. Comparison of flood mapping between Terra SAR-X vs MODIS on 23.08.2008...	166
Figure 7.30. Comparison of flood mapping between Terra SAR-X vs MODIS on 25.09.2008...	167
Figure 7.31. Comparison of flood mapping between Terra SAR-X vs MODIS on 28.10.2008...	168
Figure 7.32. Comparison of flood mapping between Terra SAR-X vs MODIS on 30.11.2008...	169
Figure 7.33. Comparison of flood mapping between Terra SAR-X vs MODIS on 30.8.2010.....	170
Figure 7.34. Comparison of flood mapping between Terra SAR-X vs MODIS on 10.9.2010.....	170
Figure 7.35. Comparison of flood mapping between Terra SAR-X vs MODIS on 24.10.2010...	171
Figure 7.36. Comparison of flood maps between Terra SAR-X vs MODIS on 04.11.2010.....	171
Figure 7.37. Comparison of flood mapping between Terra SAR-X vs MODIS on 15.11.2010...	172
Figure 7.38. Comparison of flood mapping between Terra SAR-X vs MODIS on 26.11.2010...	172

List of tables

Table 2.1. Specification of common satellites	14
Table 2.2. A short list of potential satellites.....	15
Table 2.3. Rate of weighting factor	15
Table 2.4. Multi-criteria analysis for satellite selection	16
Table 2.5. MODIS specification	16
Table 2.6. MODIS bands	17
Table 2.7. The decrease of flooded area in An Giang province	26
Table 2.8. Comparison of flooded maps between MODIS-Terra vs Envisat-ASAR satellite	27
Table 2.9. Comparison of flooded maps between MODIS vs Terra SAR Scan satellite	28
Table 2.10. Comparison of flooded maps between MODIS-Terra vs TERRA-TSX strip.....	30
Table 2.11. Agreement of land use areas in 2003 between statistical data and MODIS as well as Sakamoto and MODIS –Duong	47
Table 3.1. Probability of flood event in Mekong Delta	52
Table 3.2. Water level flood 2000 (WL00) and flood 2011 (WL11) on the Mekong River	54
Table 3.3. Water level of flood 2000 (WL00) and flood 2011 (WL11) on the Bassac River	54
Table 3.4. Observed flood inflow to the Mekong Delta.....	55
Table 3.5. Description of the MIKE 11 for Mekong River network (Source: Duong, 2016)	60
Table 3.6. Results of calibration and validation in flood 2011, 2012, and 2013	68
Table 3.7. Simulated scenarios	70
Table 3.8. Water level difference between SC2 vs SC4 at studied points by inland gauges	72
Table 3.9. Areas of the compartments (ha).....	74
Table 3.10. Scenarios of dyke measurement locations in the Mekong Delta	75
Table 3.11. Flood discharge to the Mekong Delta via Tan Chau and Chau Doc gauges.....	77
Table 4.1. Water level baseline (Z_baseline) & water level max (Z_total) on the Mekong River .	83
Table 4.2. Water level baseline (Z_baseline) and water level max (Z_total) on the Bassac River	83
Table 4.3. Additional water level (ΔZ) due to dyke measurement at the compartments	86
Table 4.4. Calculation for flood interpolation on 29.09.2011	87
Table 4.5. Interpolation of maximum water level along the main rivers on 29.09.2011.....	87

Table 4.6. Calculation for flood interpolation on 30.09.2012	89
Table 4.7. Interpolation of water level along the main rivers for flood on 30.09.2012	89
Table 4.8. Calculation for flood interpolation on 2.10.2013	91
Table 4.9. Interpolation of flood water along main rivers on 2.10.2013	91
Table 4.10. Calculation for flood interpolation on 11.08.2014	93
Table 4.11. Interpolation of flood water along main rivers on 11.08.2014	93
Table 4.12. Calculation for flood interpolation on 16.8.2015	95
Table 4.13. Interpolation of water level along the main rivers for flood on 16.8.2015	95
Table 4.14. Calculation for flood interpolation on 06.10.2016	97
Table 4.15. Interpolation of flood water along main rivers on 06.10.2016	97
Table 4.16. Calculation for flood interpolation on 10.10.2017	99
Table 4.17. Interpolation of water level along the main rivers on 10.10. 2017	99
Table 7.1. DOY for normal year	119
Table 7.2. DOY for leap year	120
Table 7.3. Comparison of total rice area between MODIS and statistical data in the MD	122
Table 7.4. Comparison of aquaculture area between MODIS and statistical data in the MD	124
Table 7.5. Total area of inland aquaculture by statistical data	124
Table 7.6. Comparison of Triple rice cropping between MODIS vs Statistical data	125

Abbreviations

CC	Climate change
LU	Land use
SLR	Sea level rise

Organization

DHI	Danish Hydraulic Institute, Denmark
DLR	German Aerospace Center, Germany
GSO	General Statistics Office of Vietnam, Vietnam
IWG	Institute for Water and River Basin Management, Germany
IMH	Institute of Meteorology and Hydrology, Vietnam
IWER	Institute for Water and Environment Research, Vietnam
KAAD	Catholic Academic Exchange Service, Germany
KIT	Karlsruhe Institute of Technology, Germany
MOST	Ministry of Science and Technology, Vietnam
MRC	Mekong River Commission
MWI	Mekong Water Technology Innovation Institute, Vietnam
NASA	National Aeronautics and Space Administration, USA
NIES	National Institute for Environmental Studies, Japan
SIWRP	Southern Institute for Water Resources Planning, Vietnam
SIWRR	Southern Institute of Water Resources Research, Vietnam
TLU	Thuyloi University (Water Resources University), Vietnam

Region

MD	Mekong Delta
LXQ	Long Xuyen Quadrangular (Tứ giác Long Xuyên)
PoR	Plain of Reeds (Đồng Tháp Mười)

GIS and Remote sensing terms

ASAR	Advanced Synthetic Aperture Radar
DEM	Digital elevation map
DOY	Day of year
DVEL	Difference Value between EVI and LSWI
ENVI	ENvironment for Visualizing Images
EVI	Enhanced vegetation index
LSWI	Land Surface Water Index
GIF	Geographical Impact Factor
GIS	Geographical Information System
GPS	Global positioning system
MODIS	Moderate-resolution Imaging Spectroradiometer
NDVI	Normalized difference vegetation index
NIR	Near-infrared
SWIR	short-wave infrared

Hydraulic and hydrological terms

E	Nash-sufficient index
HD	Hydraulic dynamics
Q	Discharge (m ³ /s)
WL	Water level (m)

Project acronyms

ViWaT	Vietnam Water Technology
WISDOM	Water related Information System for the Sustainable Development of MD

1. Introduction

The Mekong Delta (MD) possesses a short geological history due to its creation approximately 10,000 years ago, whereas the building and transformation of the surrounding areas need to be understood as continuous processes (Nestmann et al., 2017). It is the third largest delta plain in the world (Coleman & Roberts, 1989) and is located at the downstream end of the Mekong River basin covering 40,816 km², 13 provinces and 17,660 thousand inhabitants (GSO, 2016). It has substantial worth for the Socialist Republic of Vietnam due to the significant contributions it offers in regards to nature, the economy, politics, the people, agriculture, fishery, geopolitics, and numerous other areas.

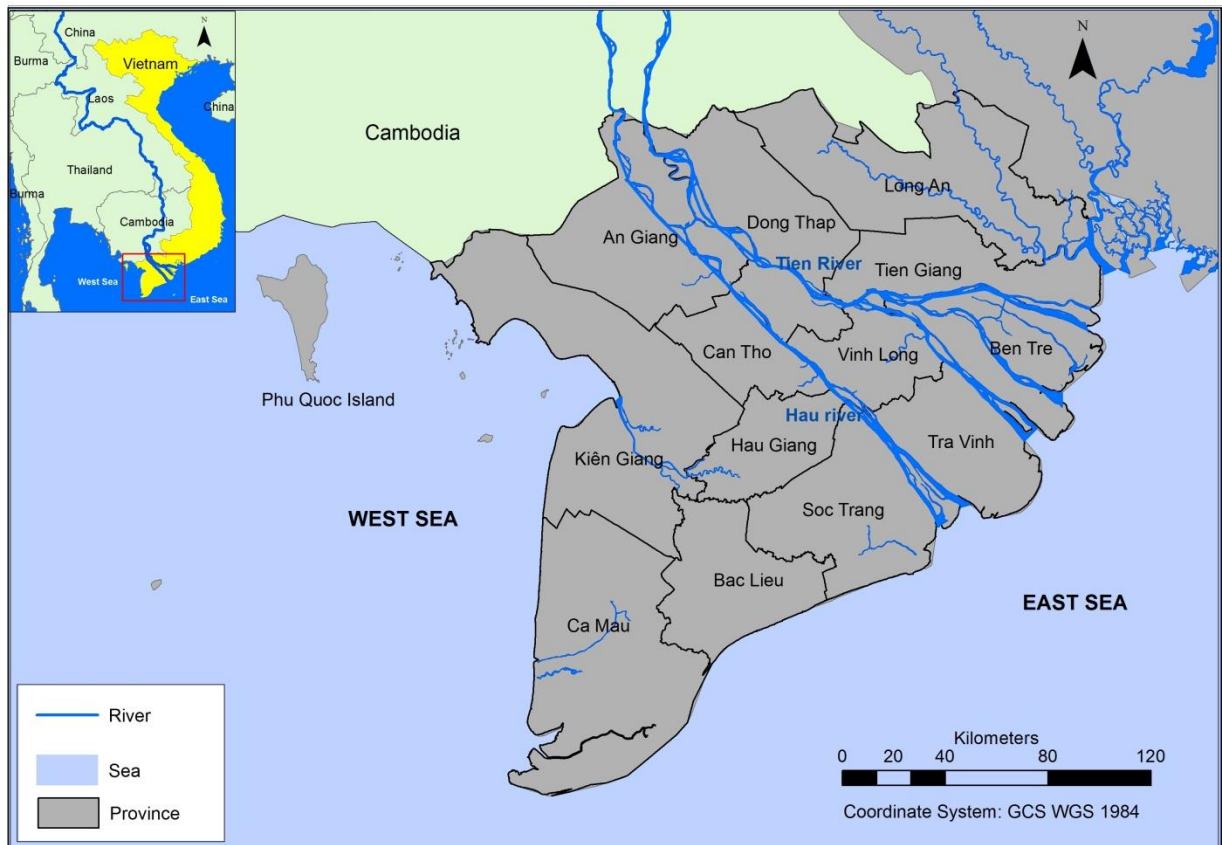


Figure 1.1. Map of the Mekong Delta

As a result of the transport processes of extremely fine-grained material from the upper Mekong River, the delta body could continue to grow. However, the processes described have also been influenced by man-made activities, which have created negative effects on the former "quasi-equilibrium state." The expansion of barriers in the middle parts of the Mekong River has been the strongest destabilizing influence on the entire MD (Nestmann et al., 2017; Li et al., 2017). Global climate change also negatively affects the quasi-balance of the delta. In the long term, this effect might result, in the coming century, in a measurable increase in backwater within the delta.

As a result of climate change, conditions in the Mekong catchment area, annual precipitation distributions and intensities as well as the entire evapotranspiration are changing. The intensity of drought and flood periods will increase the impact of the sediment transport mechanism even more due to increased irregularities. In other words, the MD has to face severe challenges relating to the loss of land, river embankment, coastal erosion, salinity intrusion, land subsidence, and flooding. This dissertation is focused on examining the flood management issue in the Mekong Delta.

1.1. Problem description

Due to the natural topography of flat and low-lying land with an area of only 5% of the entire Mekong River basin, vast amounts of water from the entire basin area must flow through the delta, which causes severe floods annually from July to December with a flood depth in the range of 0.5 to 4.0 m (Hoa, Shigeko, Huu Nhan & Thanh, 2008). Floods have been shown to have an important economic and social impact on the people living in the MD; each year floodwater inundates 1.9 million ha and affects the lives of more than 2 million people (Van , 2013). In fact, these floods are essential to food security, seasonal fishing, increased biodiversity, and as a conducive fertilizer by providing about one billion m³ of sediment (Kuenzer et al., 2013). The people in the delta have a tradition of living with the floods (Hoc, 2016), it is a hybrid policy that emphasizes a need to exploit flood waters while minimizing the negative impacts of flood hazards through flood avoidance, control, and drainage (Benedikter, 2013). However, extreme mainstream flood events may be destructive and cause enormous damage. Although extreme events leading to fatalities are relatively rare, they have occurred and resulted in the death of several hundred people. During the historic flood in 2000, more than 750 people died or were injured; the economic damage cost up to 4,600 billion. After the high flood in 2000, the flood in 2011 was of a smaller degree but still caused over 20 people to drown, 250,000 damaged embankments, 55 km of provincial roads and national highways being unpassable, and inundated 27,000 hectares of rice, and crops in which 10,000 ha crops were destroyed. After the historic flood that occurred in 2000, more infrastructures were strengthened including roads and irrigation works (Van T.C., 2013, Triet et al., 2017).

The agricultural situation in the MD has been developing for a long progress, in which there was a phase of restriction due to the Vietnam War and private trade was prohibited after the reunification in 1975 (Kakonen, 2006, 2008). Since the “Doi Moi” innovative policy in 1986 (Benedikter, 2013), the development of intensive rice cropping had been rapidly expanded in the MD. As a result, the delta is popularly known as the largest “rice bowl” of Vietnam (Le Coq, 2001, 2005). Agriculture and fisheries in the MD play an important function in acquiring foreign currency for Vietnam (Sakamoto et al., 2009). Therefore, cropping pattern areas in the MD have required an investment in dyke construction to extend the areas for rice practice from double crops to triple rice cropping, which are also called as “third crops” or “Autumn Winter crops”. This trend has pushed Vietnam to become one of the top rice exporting countries in the rice market worldwide (Nhat, 2011). In specific, yields reached 24.3 million tons in 2012, which is two times higher than 1995, which was 12.8 million tons (GSO, 2015). However, due to the intensive development of a full dyke system to protect the triple rice cropping from flood waters, especially in deep flooded zone of the Mekong Delta, such as the Long Xuyen quadrangle (LXQ) and the Plain of Reeds (PoR), the flood plains are increasingly restricted. This leads to higher water levels and increased flood risks in downstream areas of the Mekong River system (Van T.C., 2010).

Introduction



Figure 1.2. Examples of semi-dyke and full-dyke structures in Dong Thap (A) and An Giang (B);

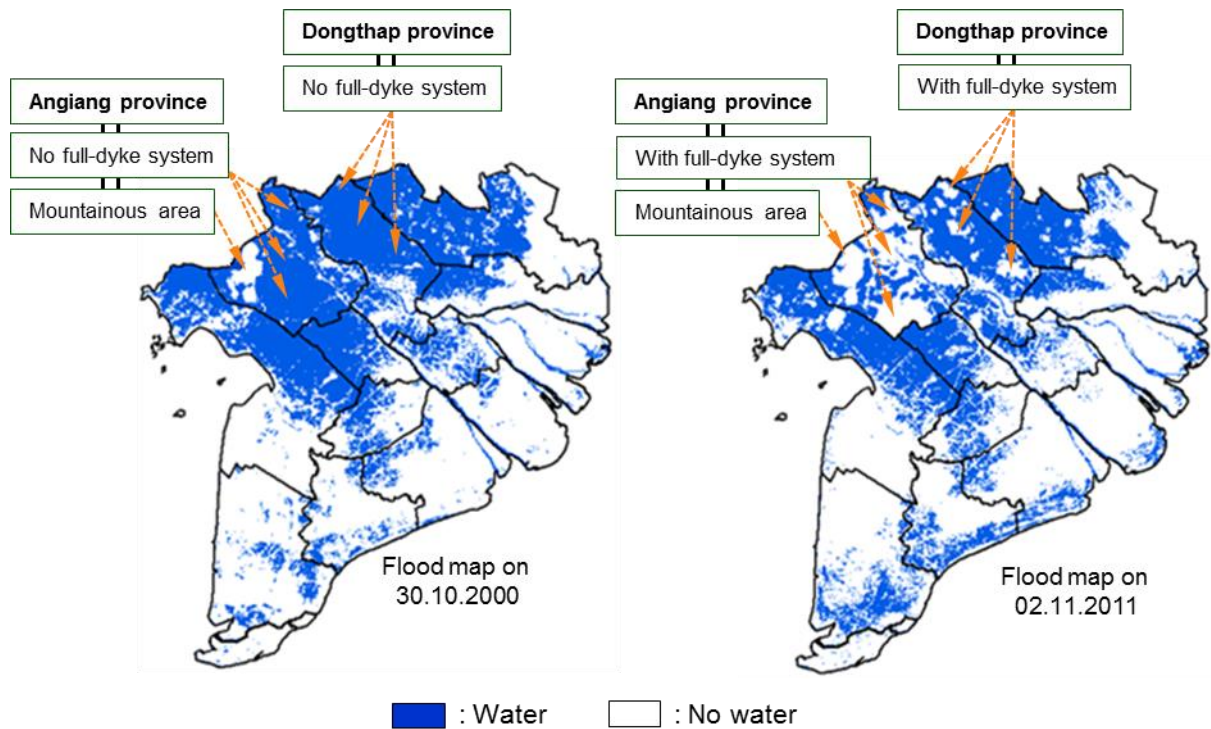


Figure 1.3. Impacts of dyke system on flood extents in 2000 and 2011

The flood prone area in the northern part of the MD has a total area of around 1.9 million ha. According to the Worldfish Center, (2002), the regions were classified based on the flood depth: a deep flood zone (> 2.0 m), a semi-deep flood zone (1.0 - 2.0 m), and a shallow flood zone (0.5 - 1.0m). Figure 1.2 A and B show some examples of semi-dyke and full-dykes systems; the dyke structures were constructed in the LXQ and POR that prevented the flood into the rice fields during flood season. An Giang and Dong Thap provinces are located in the deep flood zone. However, as shown in figure 1.3, the “dry areas” in 2011 due to the full-dyke system in An Giang and Dong Thap provinces were flood areas in 2000.

Floods in the Mekong delta are considered as a “float water season” or a “beautiful flood” (Kuenzer et al., 2013). They are not perceived as only a risk, but they also bring many benefits to the people. Hence, to be able to manage a flood and serve the sustainable development of the

economic society in the region, it is necessary to develop a comprehensive management plan based on a scientific basis and research as well as effective tools with the appropriate accuracy.

Numerous studies about flooding in MD have been carried out thanks to the rapid development of technologies and computer sciences. As satellite remote sensing is a valuable tool for flooding monitoring, Kuenzer et al., (2013) studied the flooding times series based on Envisat-ASAR-WSM 150m (from 2007 to June 2011) to identify the impacts of artificial dykes to flood patterns in the MD. On the other hand, Sakamoto et al. (2009, 2007, 2009) developed algorithms for detecting temporal changes in the farming system and the extent of annual flooding in MD based mainly on optical resolved MODIS images captured from 2000 to 2007. With the grant from the BMBF, the WISDOM project was designed and implemented an Information System for the Mekong Delta, which examined information from the fields of hydrology, sociology, information technology, and earth observations. The integration of such data will enable an end-user of the system to perform analyses on very specific questions; thus, it will supply an end-user with a tool to inform regional planning activities (DLR, 2017). Many remote sensing products, such as MODIS, ENVISAT ASAR, Terra SAR X, and Landsat, were utilized to analyze land use cover, flooding, wetland loss, water quantity monitoring, and turbidity in the MD.

In the hydraulic sector, plenty of numerical models have been invented to serve many purposes. For instance, flood distribution and areas exposed to flood inundations were evaluated by Bates Anderson, Price, Hardy, and Smith (1996), Aronica, Henkin, and Beven (1998), Jain, Singh, Jain, and Lohani (2005), Fluet-Chouinard, Lehner, Rebelo, and Hamilton (2014), and Manfreda, Samela, Gioia, Consoli, Iacobellis, Giuzio, Cantisani, and Sole (2015). Models for flood estimation were created by the USDA Soil Conservation Service (SCS) (1972), Feldman (2000), Rigon, Bertoldi, and Over (2006), Fiorentino, Gioia, Iacobellis, and Manfreda (2006, 2011), Beven (2012), and Iacobellis, Castorani, DiSanto, and Gioia (2015). Models dealing with dam and reservoir management were developed by Johnson, Stedinger, and Staschus (1991), Mizyed, Loftis, and Fontane (1992), Crawley and Dandy (2016), Oliveira and Loucks (1997), Gioia et al., (2016), and Sordo-Ward, Gabriel-Martin, Bianucci, and Garrote (2017). Models dealing with optimization techniques for dam or reservoir operations were also created by several research teams (Esat & Hall, 1994; Wardlaw & Sharif, 1999; Teegavarapu & Simonovic, 2002; Chen, 2003; Kim, Heo, & Jeong, 2006). Models for sediment transport were carried out by Wolanski et al. (1996, 1998), Tamura et al. (2010), Mikhailov and Arakelyants, (2010), Hung et al. (2012), Manh et al (2013, 2014), and Ngoc (2016).

In flooding projections, hydrodynamics models have been widely applied to simulate flood distribution and to project future patterns according to the changes in boundary conditions. Dung (2011) established an automatic calibration for flood simulation in the MD during his PhD study; a study by Tri et al. (2012) revealed the impacts of dykes on flooding regimes for LXQ under the dyke system in 2011 and a scenario of boundary conditions in 2000 based on Hec-ras 1D model. Apart from this, Hoa et al. (2007, 2008) reported the impacts of man-made dyke system on floods that occurred in 1996, 2000 and 2007 based on MIKE GIS. In addition, the relation of land-use patterns over the last decade with flooding regimes in the MD was also studied by a combination of hydraulic modelling and satellite products (Duong, Nestmann, Van, Oberle, & Nam, 2014). In addition, Dang, Cochrane, Mauricio, and Van (2017) analyzed the situation of flood water on the Mekong River after the dyke construction in the MD, dam construction in the upstream Mekong River, land subsidence, and any rise in the sea water level. Moreover, the impacts of dyke constructions on flood dynamics were also confirmed and quantitated by Tran & Weger (2017) and Triet et al. (2017).

Based on the inherited results from previous researches, the impacts of dyke measurements at different locations in the MD on the flood water level were analyzed comprehensively by Duong et al. (2016). Also, simulation works for a large and complex river network such as the Mekong River system, but it requires a lot of effort and experiences from the engineers, so not everyone can handle it. Therefore, a simple method to forecast the flood water level along the Mekong Rivers should be developed to provide engineers an alternative tool to evaluate the impacts of dyke construction on the flood water along the Mekong Rivers. A recommendation about the areas for triple rice cultivation in the Mekong delta should be also figured out to support administrators in developing a comprehensive plan to balance the agricultural development versus the flood management for the Mekong Delta.

1.2. Objectives of the study

- To find out the relationships between flooding hazards and the construction of dyke measurements for land-use purposes
- Different levels of flood hazards will be predicted and determined that correspond to different dyke measurement scenarios
- Identify a scientific base for developing a near real-time flood monitoring in the Mekong Delta based on hydraulic modelling and satellite products to support decision-makers in flood management for the MD

1.3. Research questions

As a result, the overall objective of this research is to investigate the spatial and temporal interactions of land-use changes and the inter-boundary water resources management in the Mekong Delta. The following questions will be addressed:

- How is the development of the triple rice cropping area impacting the flooding situation in MD in recent years?
- What are the effects of dyke measurements for triple rice cropping on different types of the flood areas in the Mekong delta?
- What are the impacts of a full-dyke compartment at a specific location on flood water levels along the Mekong River (see Figure 1.4a), and what are the impacts of full-dyke compartments at various locations on flood water levels depending on their position (see Figure 1.4b)?

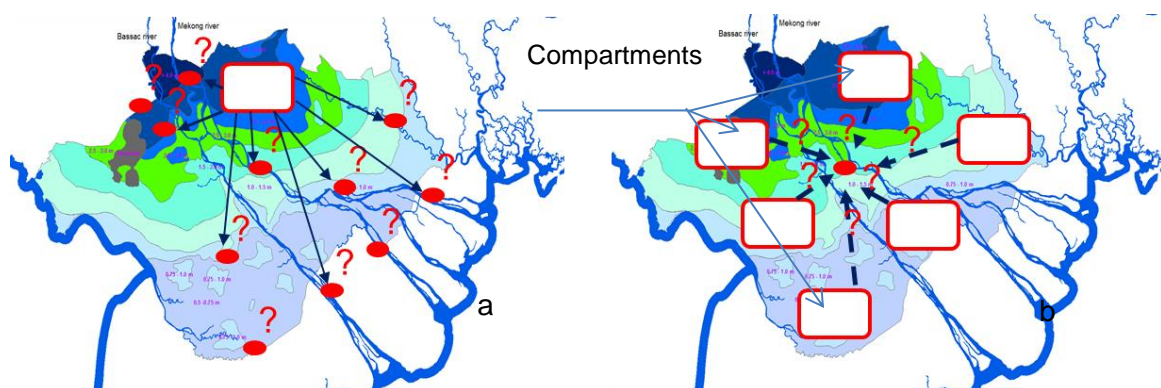


Figure 1.4. The relationship of dyke compartments vs flood water change in Mekong delta

1.4. Approaches

According to research conducted by Kuenzer et al, (2013), flooding in the Mekong Delta is defined by a complex interaction between four influencing factors, which are:

- Component 1 (CP1): flood inflow is mainly induced by the flood flow on the Mekong River and overland flow;
- Component 2 (CP2): short-term flooding due to extreme local rainfall;
- Component 3 (CP3): tidal flooding is mainly related to high tides during the spring tides;
- Component 4 (CP4): flooding due to human activities in the MD.

Flood occurrences are always triggered by a combination of several of the four factors mentioned above, as can be seen in Figure 1.5a.

Base on the natural boundary conditions of the Mekong Delta, this research assumed a coordination scheme with a Y axial along the Mekong River and an X axial along the Long Thanh Lo Gach Canal in Dong Thap and Long An province, as can be seen in Figure 1.5b. It is also assumed that a full-dyke system was constructed at the compartment A_1 , compartment A_2 , A_3, \dots, A_n . The coordinators of these compartments are expressed as $A_1(x,y)$, $A_2(x,y)$, $A_3(x,y), \dots, A_n(x,y)$.

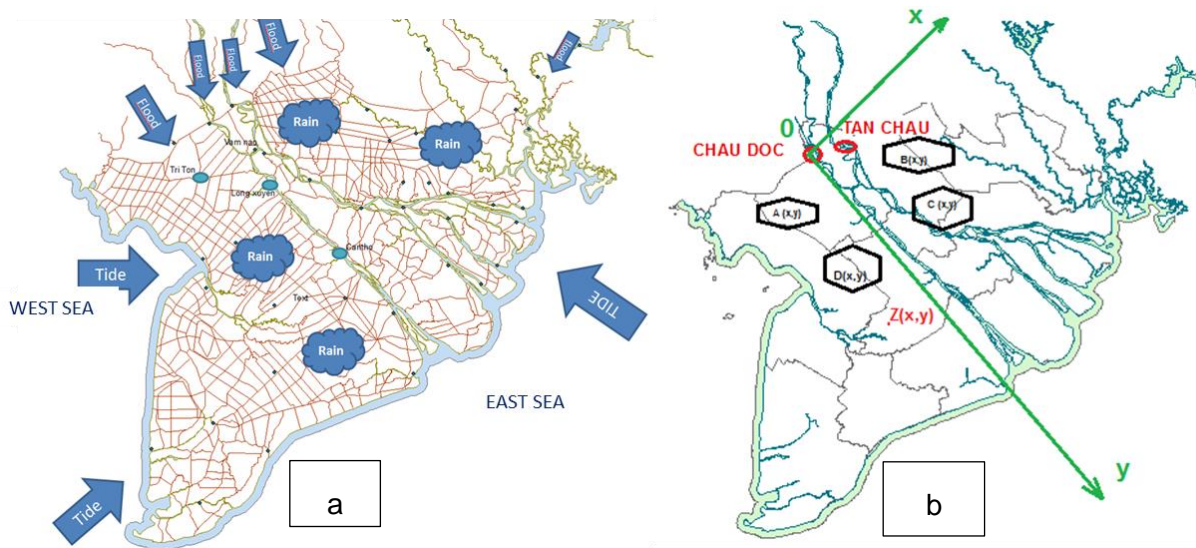


Figure 1.5. The combination of flood factors (1.5a) and the study coordination of MD (1.5b)

In other words, the water level at a certain location $Z(x,y)$ will be a function of the four factors of flooding, which include flood inflow, local rainfall, tides, and terrain (DEM):

$$Z(x,y) = f(\text{flood inflow}, \text{local rainfall}, \text{tide}, \text{DEM}) \quad [1-1]$$

Therefore:

- Flood inflows (CP1):** Flooding enters into the MD through four main ways including i) the Mekong River; ii) the Bassac River; iii) border overflow in the Plain of Reeds (PoR), and iv) border overflow in the Long Xuyen quadrangle (LXQ). Thus, the percentage of flood flow distribution focuses mostly on two major rivers. Due to the development of a dyke system in the original flood plains in Cambodia, flood overflow from the Great Mekong River into the PoR and LXQ areas in 2011 decreased significantly in comparison with flooding in 2000 (Duong, Nestmann, Van, Oberle, & Nam, 2014).

Introduction

In this study, we assume that the dyke system will be constructed completely along the borders to PoR and LXQ, and then, the overflow discharge into PoR and LXQ might be neglected. As a result, flood inflows will enter the MD through only two main ways via the Mekong and Bassac Rivers. Water levels and discharge from the Mekong and Bassac Rivers are continuously monitored by the Tan Chau and Chau Doc gauges, as illustrated in Figure 1.6, which shows cross sections of the Mekong and Bassac Rivers at the gauges.

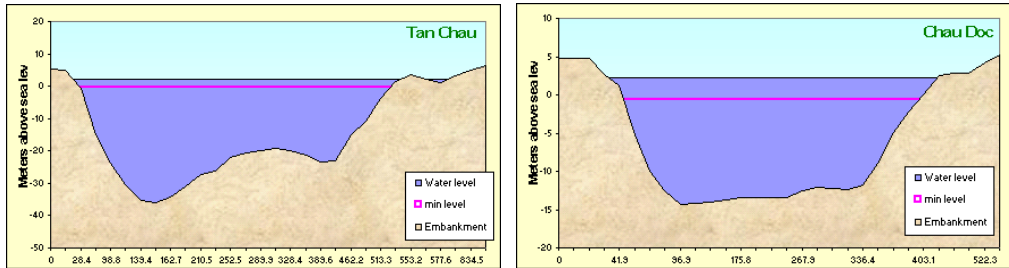


Figure 1.6. Cross sections at Tan Chau and Chau Doc gauges on Mekong and Bassac Rivers
(Source: Mekong River Commission, 2017)

- ii) **Local rainfall (CP2):** The rainy season runs annually from May to December, and the flooding season occurs during the same time period in the MD. Rainfall plays an important role in creating flooding in the upstream countries along the main Mekong River, such as China, Lao, Cambodia. As shown in Figure 1.7, rainfall data were recorded from 1st June to 31st October from 2009 to 2017 (Mekong River Commission, 2017), and the rainfall volume at Tan Chau and Chau Doc did not vary by very much. However, there were different types of flooding from 2009 to 2017 (Mekong River Commission, 2017) due to the flood inflows. In particular, the flooding in 2010 and 2016 were considered low floods due to the water level at Tan Chau in those years, which was 3.2m and 3.01m. In contrast, the rainfall data at Tan Chau in 2010 and 2016 were 1053 mm and 802 mm, which was higher than the recorded rainfall in 2011 with 782mm. While flooding in 2011 was considered high with Tan Chau receiving 4.86m. Therefore, it can be determined that local rainfall only plays a minor role in the flooding situation in the MD.

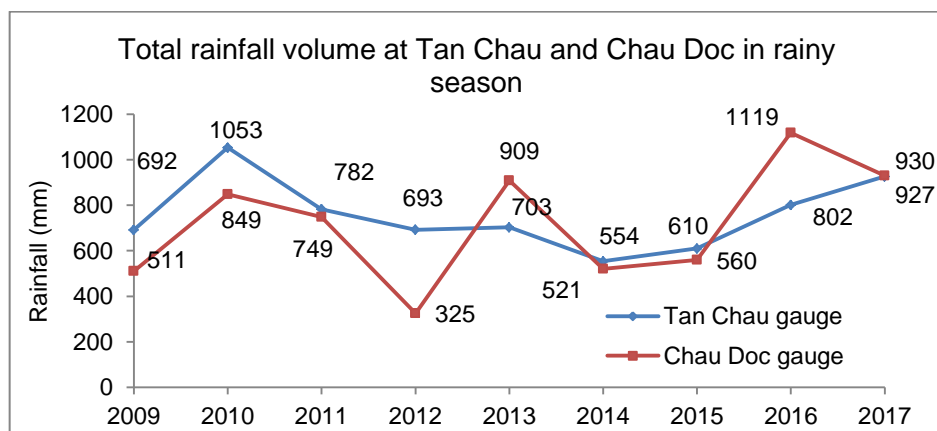


Figure 1.7. Observed rainfall data at the Tan Chau and Chau Doc gauges during rainy season
(Source: Mekong River Commission, 2017)

- iii) Tidal effect (CP3): The MD is a low lying land area, which experiences strong effects from the East Sea and the West Sea. Most of the area is only several meters above sea level, so the high water level of an East Sea tide can result in a tidal effect as far away as the Mekong Delta area and along its main rivers. However, the tide is not significant because of its characteristic with spring and neap tides only occur once each month while the flooding lasts for four months. As a result of the climatic variations, scientists estimate a worldwide annual rise in sea level of around 3 mm/a. In the long term, this effect might pose a more serious challenge in the coming century by resulting in measurable backwater in the delta. However, this effect could be mitigated in the long term through appropriate infrastructure measures (Nestmann et al., 2017). Therefore, the impact of tides on the flood situation in the MD is also considered a minor factor.
- iv) Terrain change due to dyke structures (CP4): Terrain in the Mekong Delta changed to include full dyke rings that serve the triple rice cropping areas in the flooded zones of PoR and LXQ. These compartments took away room for the flood water, and consequently, they caused the flood waters in downstream areas to increase (Duong et al., 2014). However, the locations of each compartment in the MD caused different rates on flood water levels on Mekong Rivers (Duong et al., 2016). Therefore, the geographical factor of the compartment for the triple rice area is a dynamic variant.

Terrain = f (fixed DEM, geographical location of the compartment)

Therefore, Formula 1-1 will be rewritten as:

$$Z(x, y) = f(\{inflow_{(Tanchau, Chaudoc)} | Geographical dyke | observed (DEM, Rain, Tide)\}) \quad [1-2]$$

or

$$Z(x, y) = f\{inflow_{(Tanchau, Chaudoc)}; \sum_1^n A_i(x, y); observed (DEM, Rain, Tide)\} \quad [1-3]$$

In which:

- $f\{inflow_{(Tanchau, Chaudoc)}\}$ is the observed data in near real-time, which is obtained by obtaining data related to the water levels and discharge on the Mekong and Bassac Rivers hourly by accessing the MRC website.
- $\sum_1^n A_i(x, y)$ is the total dyke measurements in the MD.
- Observe DEM, rain, tide represent existing observed data of DEM, rainfall and tide as compared to previous years, which enable a comparison to the present situation, to understand the impacts on flooding.

Figure 1.8 presents the process of analyzing the relationship between flood monitoring and land use change in the MD.

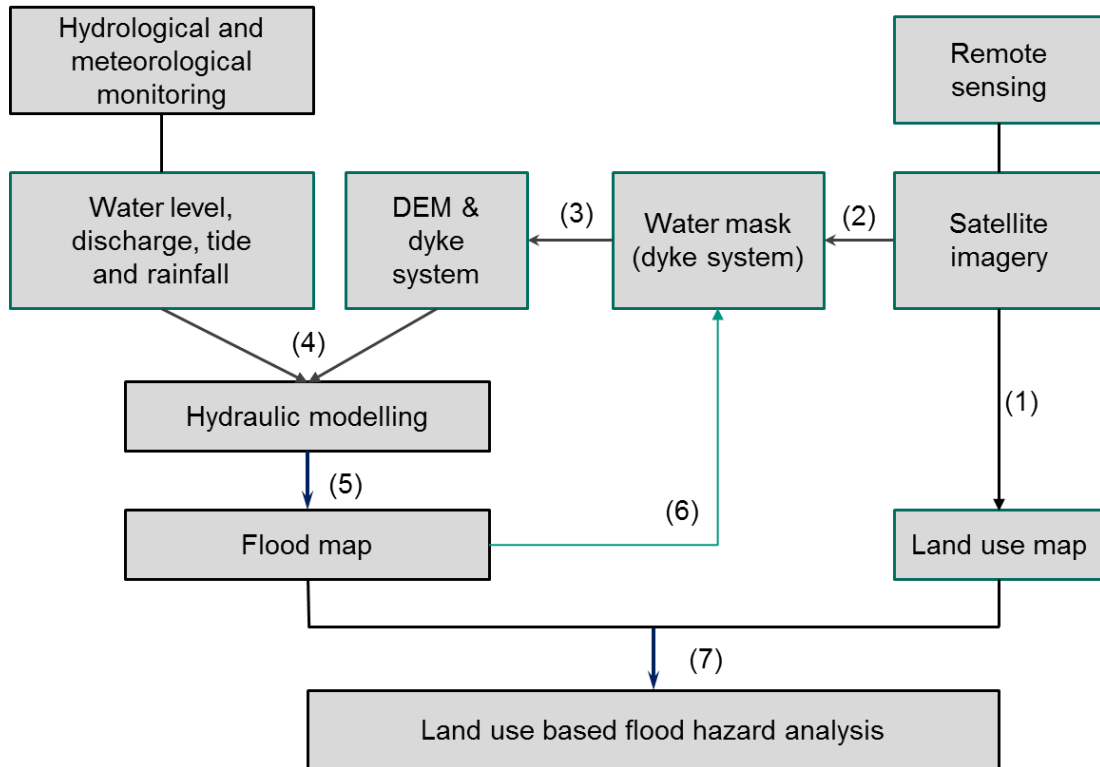


Figure 1.8. Land use based flood hazard analysis for the Mekong delta

It includes 6 steps as follows:

- Step 1: the time series satellite imageries will be collected for interpretation in years of land use map to analyze the change of land use in the last decade.
- Step 2: the satellite products will be also interpreted into daily flood extension (water mask).
- Step 3: the water masks present the information related to the flood distribution in the MD in regards to “wet” and “dry” areas. Dry areas in the flooded zone will indicate areas that are protected by “dyke system” against flood water.
- Step 4: The input data for the hydraulic model include i) terrain, area and location of dyke system, ii) hydrological and meteorological data of water level, discharge, tide and rainfall. The online data of boundary conditions of flood inflows and water level at the Tan Chau and Chau Doc stations could be collected on the Mekong River Commission website <http://ffw.mrcmekong.org/>.
- Step 5: Hydraulic model is applied to simulate the historical floods in the Mekong delta.
- Step 6: flood maps from hydraulic modelling shall be calibrated and validated based on the water masks from the satellite data and hydrological data at gauge stations in the MD.
- Step 7: Several scenarios of dyke measurements in different types of flooding will be simulated using a hydraulic model to identify the relationship between dyke measurements and flood hazards. Hence, a land use based flood analysis model will be

developed to identify the flood hazards based on the dyke measurements for future land use in the Mekong Delta.

1.5. Structure of the dissertation

The thesis includes 6 chapters, which are described as below.

- Chapter 1 commences an exploration of the intensive development of agricultural and aquaculture in recent years and its consequences. The objectives and the methodology of the research are generally stated.
- Chapter 2 discusses about the application of remote sensing technology to analyze land use change and the subsequent impacts on the flooding situation in the Mekong Delta over the last decade.
- Chapter 3 examines the application of hydraulic modelling 1D to analyze the impacts of various dyke measurements for land use purposes on flooding areas in the MD. The land use based flood model analysis, which has been referred to as the geographical impact factor (GIF), was established to evaluate the impact of dyke measurements on flood water levels along the Mekong Rivers.
- Chapter 4 describes the application of GIF on land use management and flood level forecasting for the Mekong Delta.
- Chapter 5 presents a detailed conclusion, which essentially corresponds to all of the findings and contributions of the dissertation and the outlooks for further studies.
- Appendix: All calculations including remote sensing and hydraulic modelling and the statistical data related to this study are collected and presented in the Appendix.

2. Analysis the land use change versus flooding situation in the MD using remote sensing technology

Satellite remote sensing is a valuable tool for objectively detecting inundated areas. Therefore, many studies have been undertaken in this field for a variety of purposes, such as studies of paddy fields as crop-production areas (Sarp & Erenner, 2008; Sakamoto et al., 2007, 2009; Cotlier, Brisco, Mondino, & Balparda, 2011; Hauser et al., 2017), analyses of wetlands (Okotto, Raburu, Obiero, & Raburu, 2016; Shadaydeh, Zlinszkym, Kovacs, & Sziranyi, 2017), wild animals tracking (Yeap, Shephard, Le Souef, Warren, Groom, Dawson, Kirkbym, & Warren, 2015), fire detection and quantification (Kuenzer, Zhang, Tetzlaff, Wagner, & Voigt, 2008), natural disasters such as land subsidence assessment (Chatterjee, Roy, Dadhwal, Quang, & Saha, 2007; Shalajja et al., 2016), deforestation tracking (Hoa et al., 2017), drought (Xiaofeng et al. 2016; Dong, Li, Yuan, & Chen 2017) and flood monitoring (Brakenridge and Anderson 2006; Sakamoto et al., 2007, 2008; Kuenzer et al, 2013; Nigro et al. 2014; Ahmed et al., 2017).

The objective of this chapter is aimed at exploring the application of remote sensing technology in order to analyze the land use change and flood mapping for the MD. There are several types of satellite products with different resolutions, and a satellite product that is easy-to-access by download, free-of-charge, and acceptably accurate will be the most suitable tool for this study.

2.1. Overview of remote sensing technology

According to Zubair A. O., (2006), remote sensing is defined as a process that information is gathered about an object, area, or phenomenon without contact directly with it. Sensors are divided into two types of passive and active. Sensors provide their own source of energy called active while the ones rely on energy emitted from other sources, i.e. the sun, are called passive.

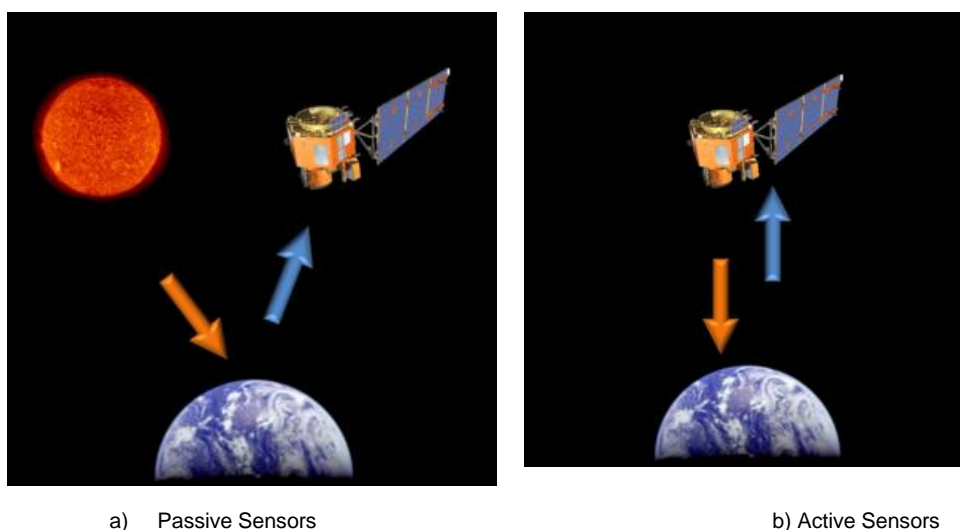


Figure 2.1. Principles about active and passive remote sensing (NASA website, 2017)

Analysis the land use change versus flooding situation in the MD using remote sensing technology

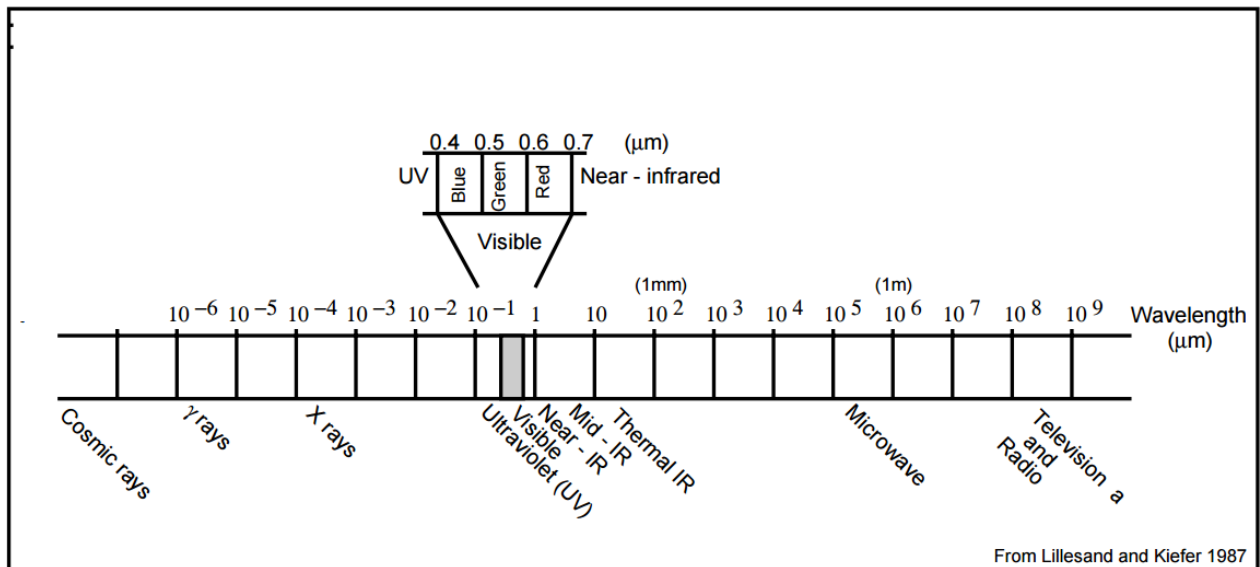


Figure 2.2. The range of electromagnetic spectrum

(Source: Lillesand and Kiefer, 1987)

Figure 2.2 shows the energy is emitted in various frequencies and wavelengths from large wavelength radio waves to shorter wavelength gamma rays. Radars emit microwave energy, a longer wavelength that is typically a few centimeters in length (Lillesand and Kiefer, 1987).

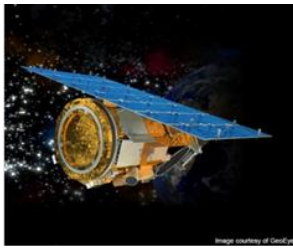
2.2. Selection of appropriate remote sensing sensor

The pictures and specifications of common satellites in the world are presented in Figure 2.4 and Table 2.1 below. The spatial resolution of both active and passive satellites varies from very high (with a pixel size of 0.6 m to 10 m), to high resolution (10 m – 60 m), to medium resolution (60 – 500 m), and low resolution (above 500 m).

The satellites with high spatial resolution include GeoEye-1, WorldView-1, Quickbird, IKONOS, NOAA19, ALOS 2, SPOT6, SPOT7. These satellite products are used for modelling terrain, digital elevation maps (DEM), street mapping, tree identification, and tracking important areas that require high accuracy. They demonstrate the objects on the ground clearly and easily for interpretation. The SPOT 1 - 4, Landsat 4-7, Envisat ASAR, MODIS satellites are convenient for the management of natural resources, land use detection, and monitoring flooding and drought on a provincial and regional scale.

Whereas, the lower resolution satellites have advantages due to their wide swaths and short time for revisits. A number of satellites with low resolution sensors include the Envisat Meris (1200 m) and the Meteosat (2500 m). These are valuable in tracking phenomenon fluctuations on a global scale, such as those necessary for natural disaster forecasting, survey of the ocean surface, and the earth's surface temperature and weather.

Analysis the land use change versus flooding situation in the MD using remote sensing technology



Geo Eye-1



Worldview-1



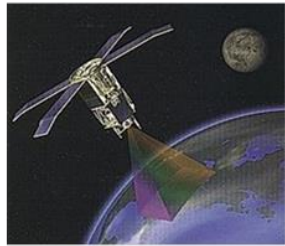
Ikonos



Quickbird



NOAA19



SeaStar



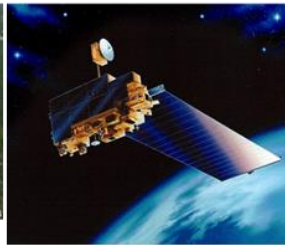
SPOT5



SPOT 7



ALOS 2



Landsat 7



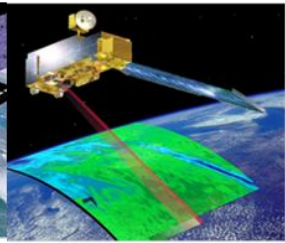
ENVISAT ASAR



Terra SAR-X



Radarsat



MODIS



Landsat 4,5



Meteosat



Sentinel-1



Sentinel-2



Sentinel-3

Figure 2.3. Pictures of popular satellites

(Source: the pictures collected from several sources on the internet)

Analysis the land use change versus flooding situation in the MD using remote sensing technology

Table 2.1. Specification of common satellites

Satellite	Sensor	Type	Resolution (m)	Band	Swath (km)	Revisit time (day)	Launched	Country
GEOEYE-1	PAN/MS	Optical	0.41 - 1.65	2	15.2	2-8	2008	USA
WORLDVIEW-1	PAN	Optical	0.46	1	17.6	1.7	2007	USA
QUICKBIRD	QBP	Optical	0.65	4	27	1-3	2001	USA
IKONOS	PAN/MS	Optical	1 (PAN)	4	11	3-5	1999	USA
NOAA19	AVHRR	Optical	1	7	3000	1	2009	USA
SeaStar	SeaWiFS	Optical	1.1	8	2800	1	1997	USA
SPOT 6-7	HRVIR	Optical	1.5 - 6	6	60	4-6	2012, 2014	France
FORMOSAT-2	PAN	Optical	2	5	24	1	2004	USA
SPOT5	PAN	Optical	2.5-5	6	120	2-3	2002	France
SPOT 1-3	HRV	Optical	10 (PAN)	3	60	4-6	1986, 1990,1993	France
SPOT 4	HRVIR	Optical	10 (PAN)	4	60	4-6	1998	France
ALOS	AVNIR-2	Optical	10	4	70	46	2006	Japan
Landsat 7	ETM+	Optical	15 (PAN)	8	185	16	1999	USA
Landsat 4,5	TM	Optical	30	7	185	16	1982, 1984	USA
MODIS	Aqua/Terra	Optical	461	36	2330	1	2000	USA
Meteosat 1	VISSR	Optical	2500	3	equator	30 (Minute)	2004	France
Sentinel 2	MSI	Optical	10	13		5	2015	EU and ESA
TerraSAR-X	SAR-X	Radar	1	1	10	2.5	2007	Germany
ALOS 2	PALSAR	Radar	1-3	4	70	46	2014	Japan
Radarsat	SAR	Radar	8	4	10	250	1995	Canada
ENVISAT	ASAR	Radar	90	15	3	150	2002	USA
Sentinel 1	SAR-C	Radar	9	1	80	1	2014	EU and ESA

Based on the objectives of this dissertation, which satellite will be the best option to apply for flood monitoring and land use detection for the Mekong Delta region?

To answer this question, a multi-criteria analysis (MCA) method was applied to analyze multi-criteria about the satellites.

2.2.1. Multi-criteria analysis for satellite selection

According to Rigo et al. (2005), MCA method was largely introduced after World War II. The main reasons for their success are as follows.

- growing urbanization and increased complexity of large infrastructural projects
- emancipation of different social groups, interests, and ideas
- call for more transparency and balance in all projects concerning the environment
- demand for cost optimization and good cost control
- logics of computerization, desire for programmable selection procedures

However, one should not use MCA to assess all satellites because it will make the evaluation become overly complicated. Therefore, a short list of the satellites with the most potential was chosen, which included Sentinel-1, Sentinel-2, Landsat 7, SPORT 5, ALOS 2, ENVISAT ASAR, MODIS and Radasat, as illustrated in Table 2.2.

Analysis the land use change versus flooding situation in the MD using remote sensing technology

Table 2.2. A short list of potential satellites

No.	Name	Sensor	Type	Resolution (m)	number of band	Revisit time (day)	swath (km)	Country	Lifetime
1	Sentinel 1	SAR-C	Radar	9	1	1	80	EU and ESA	2014 - now
2	Sentinel 2	MSI	Optical	10	13	5	-	EU and ESA	2015 - now
3	Landsat 7	ETM+	Optical	30	8	16	185	America	1999-now
4	SPOT 5	HRVIR	optical	5	4	3	60	France	2002-now
5	ALOS 2	PALSA	radar	10	4	46	70	Japan	2006-2011
6	ENVISAT	ASAR	radar	90	15	3	150	America	2002-2011
7	MODIS	Terra	Optical	461	36	1	2330	America	2000-now
8	Radarsat	SAR	radar	8	4	10	250	Canada	1995-2000

The criteria to select the most appropriate satellite included:

- Price: The satellite's images should be as cheap as possible.
- Revisit time: The satellite should have a short revisit time in order to monitor the study area continuously.
- Accessibility: The program should be easy-to-access by downloading and/or by purchasing the satellite products.
- Resolution: The satellite's images should have high resolution to ensure the preciseness of the interpreted products.
- Monitoring period: The expected period for the study of the land use change in the MD was covering a time period since 2000. Therefore, the lifetime of satellite should also include that time period, so it was active and in operation at that time.
- Cloud effects: The products should be affected by cloud covering in relation to noise as little as possible.

A weighting factor represented the importance of a particular criterion in the analysis in relation to the total of all the criteria. The most convenient way was to assign the weighting factors was based on a range from 0 to 1 for all criteria, such that that the sum of these factors equals 1. The total scores will then emerge in the same rating scale as the scores for each criterion, which gives the method more recognition and helps to avoid confusion.

Table 2.3. Rate of weighting factor

Criterion	Weighting factor (w.f)
Price	0.25
Accessibility	0.20
Revisit time (day)	0.15
Resolution (m)	0.15
Monitoring period	0.15
Cloud effect	0.10
Total	1.00

In Table 2.3, the price of the satellite product plays the most important factor, so it was rated with a w.f of 0.25. The accessibility criterion was 0.20; the criteria of revisit time, resolution and monitoring period were the same w.f of 0.15. Finally, the cloud effect was assigned a w.f of 0.1.

Analysis the land use change versus flooding situation in the MD using remote sensing technology

The rating scale from 0 to 10, with higher marks representing a better score, were marked for each satellite in the matrix, as shown in Table 2.4.

Table 2.4. Multi-criteria analysis for satellite selection

RATING 9-10: very good; 7-8: good; 5-6: fair; below 5: bad

No.	Criteria	Satellite	W.F	Satellite							
				Sentinel 1	Sentinel 2	Landsat 7	SPOT 5	ALOS	ENVISAT	MODIS	Radarsat
1	Price		0.25	10	10	10	6	6	10	10	6
2	Revisit time		0.20	10	9	7	9	5	8	10	7
3	Accessibility		0.15	10	10	9	8	7	8	10	7
4	Resolution		0.15	10	10	8	10	10	9	6	10
5	Monitoring period		0.15	3	3	8	10	7	7	10	10
6	Cloud effect		0.10	10	8	8	8	10	10	6	8
7	Total		1.00	8.95	8.55	8.45	8.3	7.1	8.7	9.0	7.75

As a result, the MODIS satellite was selected as the most appropriate solution since its product is free-of-charge, easy-to-access and easy to download its images; also, MODIS was launched in 2000 and has been in constant operation until now. With the highest score of 9.0, MODIS satellite was expected to meet the objectives of this research.

2.2.2. MODIS satellite

The moderate-resolution imaging spectro-radiometer (MODIS) is an optical sensor with two observing satellites of EOS AM and EOS PM, which are commonly known as Terra and Aqua. Terra and Aqua were launched into synchronous sub-recurrent orbit at an altitude of 705 km in December 1999 and May 2002, respectively (EOS, 2006). MODIS specifications are listed in Table 2.5.

Table 2.5. MODIS specifications

Specifications	
Orbit	705 km, 10:30 a.m. descending node (Terra) or 1:30 p.m. ascending node (Aqua), sun-synchronous, near-polar, circular
Scan rate	20.3 rpm, cross track
Swath	2330 km (cross track) by 10 km (along track at nadir)
Dimensions	
Telescope	17.78 cm diam. off-axis, afocal (collimated), with intermediate field stop
Size	1.0 × 1.6 × 1.0 m
Weight	228.7 kg
Power	162.5 W (single orbit average)
Data rate	10.6 Mbit/s (peak daytime); 6.1 Mbit/s (orbital average)
Spatial Resolution	250 m (bands 1–2) 500 m (bands 3–7) 1000 m (bands 8–36)
Temporal Resolution	1-2 days
Design life	6 years

(Source: https://en.wikipedia.org/wiki/Moderate_Resolution_Imaging_Spectroradiometer)

The instruments capture data in 36 spectral bands, which range in wavelength from 0.4 μm to 14.4 μm and are at varying spatial resolutions. Together, the instruments image the entire earth

Analysis the land use change versus flooding situation in the MD using remote sensing technology

every 1 to 2 days. They are designed to provide measurements for large-scale global dynamics including changes in earth's cloud cover, radiation budget, and processes occurring in the oceans, on land, and in the lower atmosphere (EOS, 2006).

Table 2.6. MODIS bands

Band	Wavelength (nm)	Resolution (m)	Description	Primary Use
1	620–670	250	RED	Land/Cloud/Aerosols
2	841–876	250	NIR (near-infrared)	Boundaries
3	459–479	500	BLUE SWIR (short-wave infrared)	Land/Cloud/Aerosols Properties
4	545–565	500		
5	1230–1250	500		
6	1628–1652	500		
7	2105–2155	500		
8	405–420	1000		
9	438–448	1000		
10	483–493	1000	Ocean Color/ Phytoplankton/ Biogeochemistry	
11	526–536	1000		
12	546–556	1000		
13	662–672	1000		
14	673–683	1000		
15	743–753	1000		
16	862–877	1000		
17	890–920	1000	Atmospheric Water Vapor	
18	931–941	1000		
19	915–965	1000		
20	3.660–3.840	1000	Surface/Cloud Temperature	
21	3.929–3.989	1000		
22	3.929–3.989	1000		
23	4.020–4.080	1000		
24	4.433–4.498	1000	Atmospheric Temperature	
25	4.482–4.549	1000		
26	1.360–1.390	1000	Cirrus Clouds Water Vapor	
27	6.535–6.895	1000		
28	7.175–7.475	1000		
29	8.400–8.700	1000	Cloud Properties	
30	9.580–9.880	1000	Ozone	
31	10.780–11.280	1000	Surface/Cloud Temperature	
32	11.770–12.270	1000		
33	13.185–13.485	1000	Cloud Top Altitude	
34	13.485–13.785	1000		
35	13.785–14.085	1000		
36	14.085–14.385	1000		

(Source: https://en.wikipedia.org/wiki/Moderate_Resolution_Imaging_Spectroradiometer)

Analysis the land use change versus flooding situation in the MD using remote sensing technology

In this study, only the product MOD09A1: MODIS/TERRA SURFACE REFLECTANCE 8-DAY L3 GLOBAL 500 M SIN GRID V004 was applied. MOD09A1 composite products the best surface spectral-reflectance data for each 8-day period. The MODIS/Terra products can be easily downloaded for the MD region via the website <http://reverb.echo.nasa.gov/reverb/>

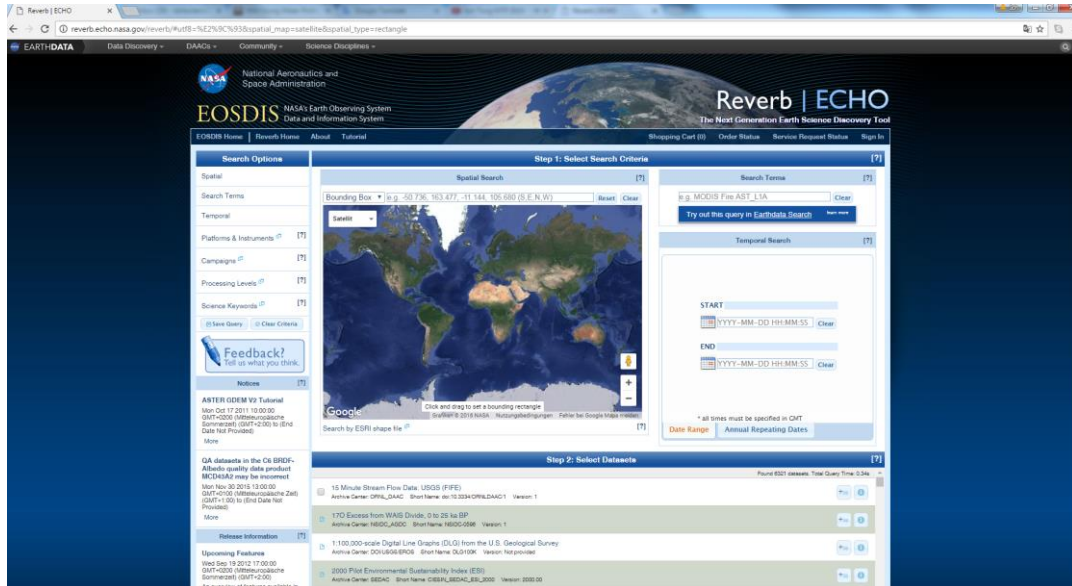


Figure 2.4. Image of the website used to access MODIS Satellite images (<http://reverb.echo.nasa.gov/reverb/>)

2.3. Time series of flood monitoring in the MD

2.3.1. Algorithms for flood mapping

The images of MODIS/Terra were downloaded for monitoring flooding situations from 2000 to 2017. Flooding maps are processed according to an algorithm developed by Sakamoto et al. (2007).

The algorithm includes 10 steps as shown in Figure 2.5 below. The author did make some different points when compared with Sakamoto, which are as follows.

- The author used only the products of MODIS/Terra MOD09A1 to decrease the volume of works while Sakamoto used MODIS/Terra (MYD09Q1 and MOD09A1) products together to increase observed input data volume.
- In Step 3 of Figure 2.5, the missing pixels due to cloud coverage are being replaced by extracting the pixels from the next acquisition time. This method is described clearly in Figure 2.6, and in the author's point of view, it is simpler than the smoothed indexes method performed by Sakamoto et al. (2007, 2009).

After downloading the images, the preparation works are processed including image format conversions, mosaicking, and spatial resizing. The map projection is converted to Universal Transverse Mercator (Zone 48N). The steps for flood map interpretation are presented in the following.

- Step 1: According to Table 2.6, land and surface water shall reflex from band 1 to band 7. Therefore, band 1 and band 2 have a resolution of 250m while band 3 to band 7 have resolution of 500m. Thus, to unify the pixel resolution in calculations, a 250-m resolution is

Analysis the land use change versus flooding situation in the MD using remote sensing technology

produced by re-sampling the 500-m resolution MOD09A1 product by the nearest-neighbor method (Sakamoto et al. 2009).

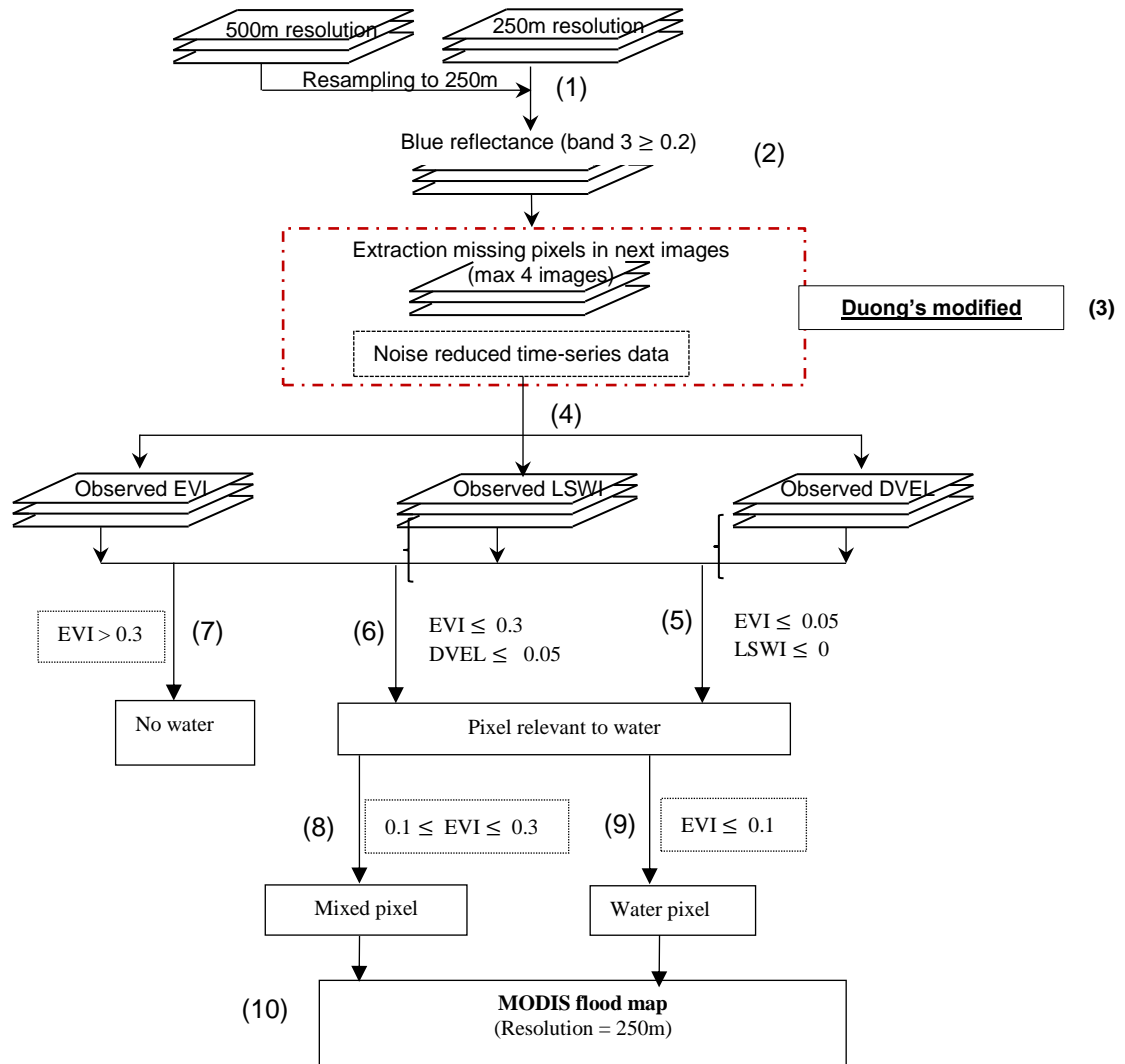


Figure 2.5. Processing of flood mapping

(Source: Sakamoto et al., 2007)

- **Step 2:**
The surface reflectance data input is systematically pre-processed with atmospheric correction and an eight-day composition. However, the images included noise components due to cloud cover, viewing angle, the mixed-pixel effect, and the effect of bidirectional reflectance distribution. Clouds were detected based on the pixel value of blue-band reflectance (band 3) ≥ 0.2 .
- **Step 3:**
Flooding in the MD occurs slowly and gently while the period of rice cropping often lasts for three months. Therefore, it is assumed that the pixel value in the next images did not vary by very much. The pixel in the next eight-day images was extracted to provide for the missing data due to cloud coverage for the current image. To ensure accuracy, it is recommended to use the time span of four images or a time period of 32 days. Figure 2.6.a below presents the progress of noise removal for the image DOY289 in 2017 by

Analysis the land use change versus flooding situation in the MD using remote sensing technology

using the next three images of DOY297, DOY305, DOY313 to provide the missing pixels for the image of DOY289.

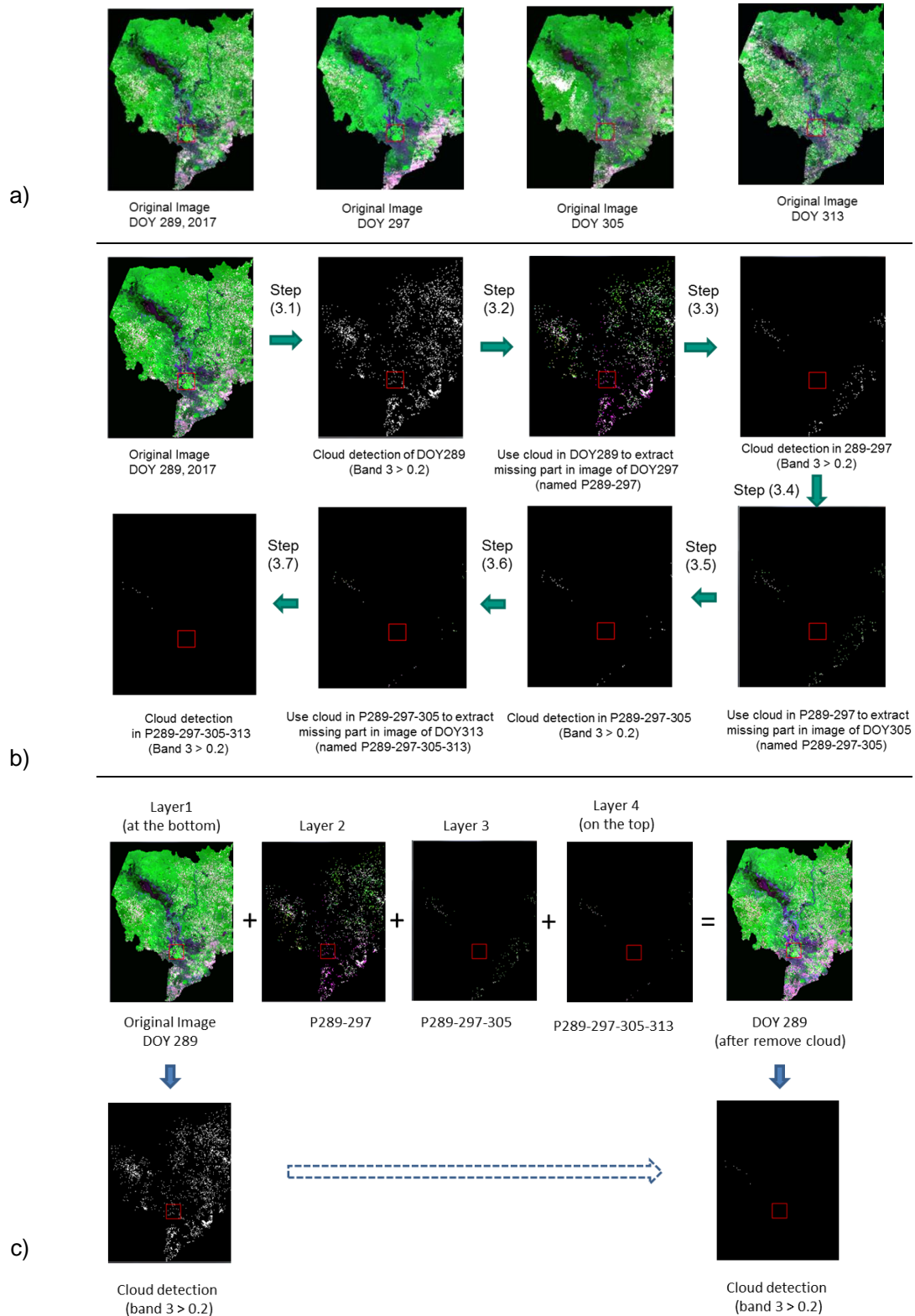


Figure 2.6. Example of the process for cloud removal

- a) the 4 continuous images of DOY289, DOY297, DOY305, DOY313; b) Cloud detection and mask applying for extracting for the next images; c) Mosaicking for the Image DOY289

Analysis the land use change versus flooding situation in the MD using remote sensing technology

- The cloud detection for the Image DOY289 is shown in Figure 2.6.b, and the cloud detected throughout Step 3.1 was quite a lot. This cloud cover was used as a mask to extract the pixel in Image DOY297 by the Step 3.2 and named as P289-297. Afterwards, clouds were detected based on the pixel value of blue-band reflectance ≥ 0.2 for P289-297 in Step 3.3, and the detected cloud in Step (3.3) was much less than the cloud cover in Step 3.1. Then, the cloud 289-297 was used to extract the pixel in Image DOY305 in Step 3.4, which was named as P289-297-305. Similarly, the Steps 3.5, 3.6, and 3.7 were performed the same way as Steps 3.1, 3.2, 3.3 to detect clouds and extract the missing pixels in DOY313 for the creation of P289-297-305 and P289-297-305-313.
- In Figure 2.6.c, the images are mosaicked together in the exact order: Layer 1 is DOY289 at the bottom; Layer 2 is the P289-297; Layer 3 is the P289-297-305; and Layer 4: P289-297-305-313 is on the top. Image DOY289 after removing cloud has close to no noise of clouds.

- Step 4: Calculating the indexes:

- Enhanced vegetation index:

$$EVI = 2.5 \frac{NIR - RED}{NIR + 6RED - 7.5BLUE + 1} \quad [2-1]$$

- Land surface water index:

$$LSWI = \frac{NIR + SWIR}{NIR - SWIR} \quad [2-2]$$

- Difference value between EVI and LSWI:

$$DVEL = EVI - LSWI \quad [2-3]$$

In accordance with the pioneering method described by Xiao et al. (2005, 2006), DVEL was used in the present study to discriminate between water-related pixels and non-flood pixels.

- Step 5 and Step 6: Detection of pixel relevant to water

If the observed EVI was less than or equal to 0.05, and the LSWI was less than or equal to 0, such pixels were determined to be a Water-related pixel. Similarly, if the observed DVEL was less than 0.05, and the observed EVI was less than or equal to 0.3, the pixel was determined as a water-related pixel.

- Step 7: Detection of non-flood pixel

If the EVI was greater than 0.3, the pixel was categorized as a non-flood pixel.

- Step 8 and Step 9: Classification of pixel related to water into flood and mixture.

Water-related pixels were divided into flood and mixture based on the value of EVI. According to Sakamoto et al. (2007), EVI in homogeneous open-water areas, such as large lakes and the sea, is generally lower than that in mixed-pixels, which refers to a mix of water, vegetation, and soil coverage. Thus, it is assumed that the observed EVI of the water-related pixels can be used as a criterion for discriminating between flooding and

Analysis the land use change versus flooding situation in the MD using remote sensing technology

mixture. If the observed EVI was less than or equal to 0.1, the water-related pixels were defined as flood pixels. If the observed EVI was greater than 0.1 and less than or equal to 0.3, these pixels were defined as mixed-pixels.

- Step 10: An eight-day composite MODIS image was interpreted into a flood map with three classes that included non-flood pixel, flood and mixed-pixels.

Annual flooding season in the Mekong Delta often occurs from early June through the end of December. Therefore, the images from DOY145 to DOY361 were interpreted into flood maps to monitor the entire flooding season for eighteen years from 2000 to 2017. Figure 2.7 and Figure 2.8 show examples of flood distribution in the MD in 2000. Flooding distribution in areas are presented in the Appendix 7.4 of this thesis.

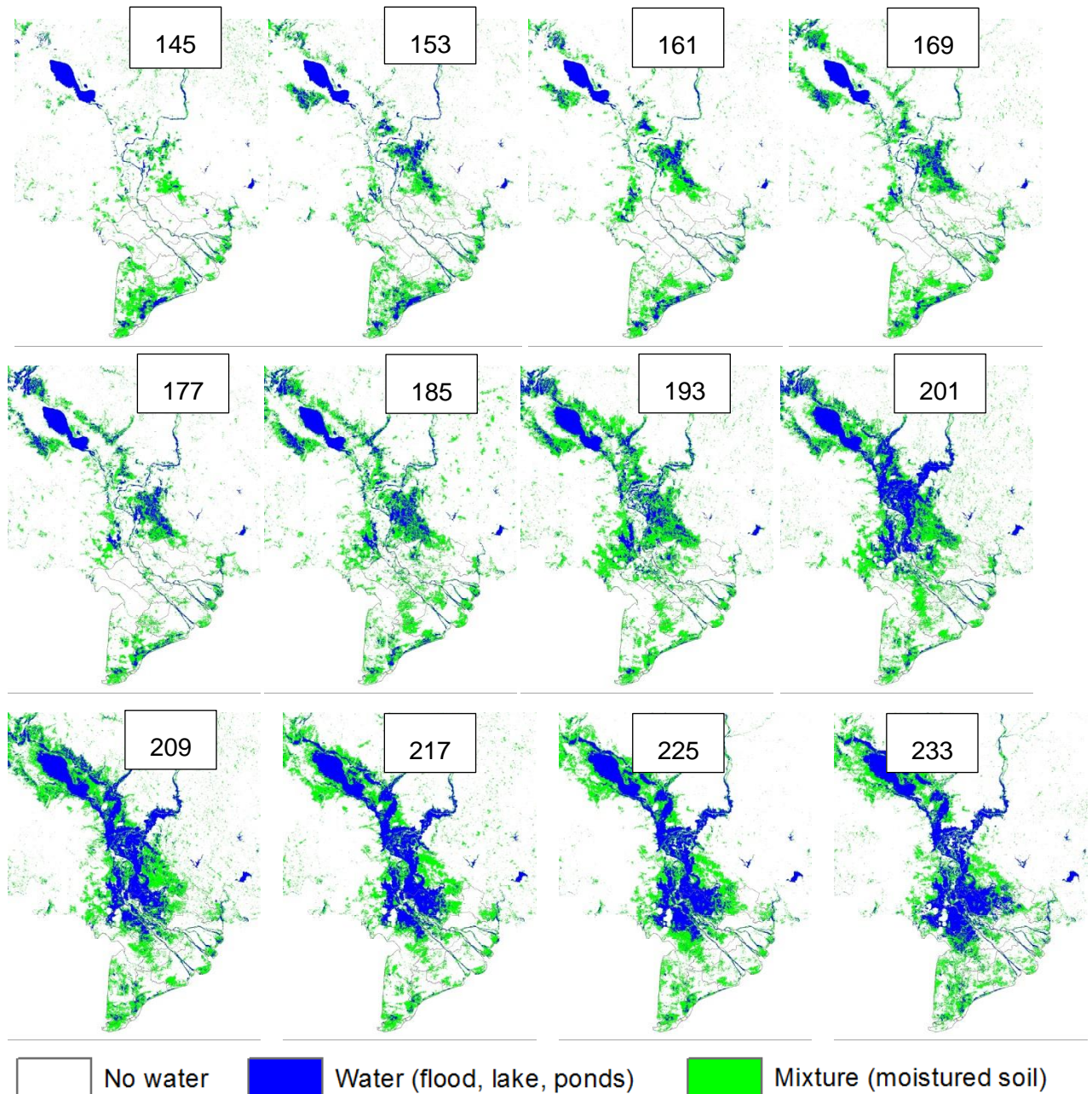


Figure 2.7. Flood distribution (rising stage) in 2000 from DOY145 to DOY233

Analysis the land use change versus flooding situation in the MD using remote sensing technology

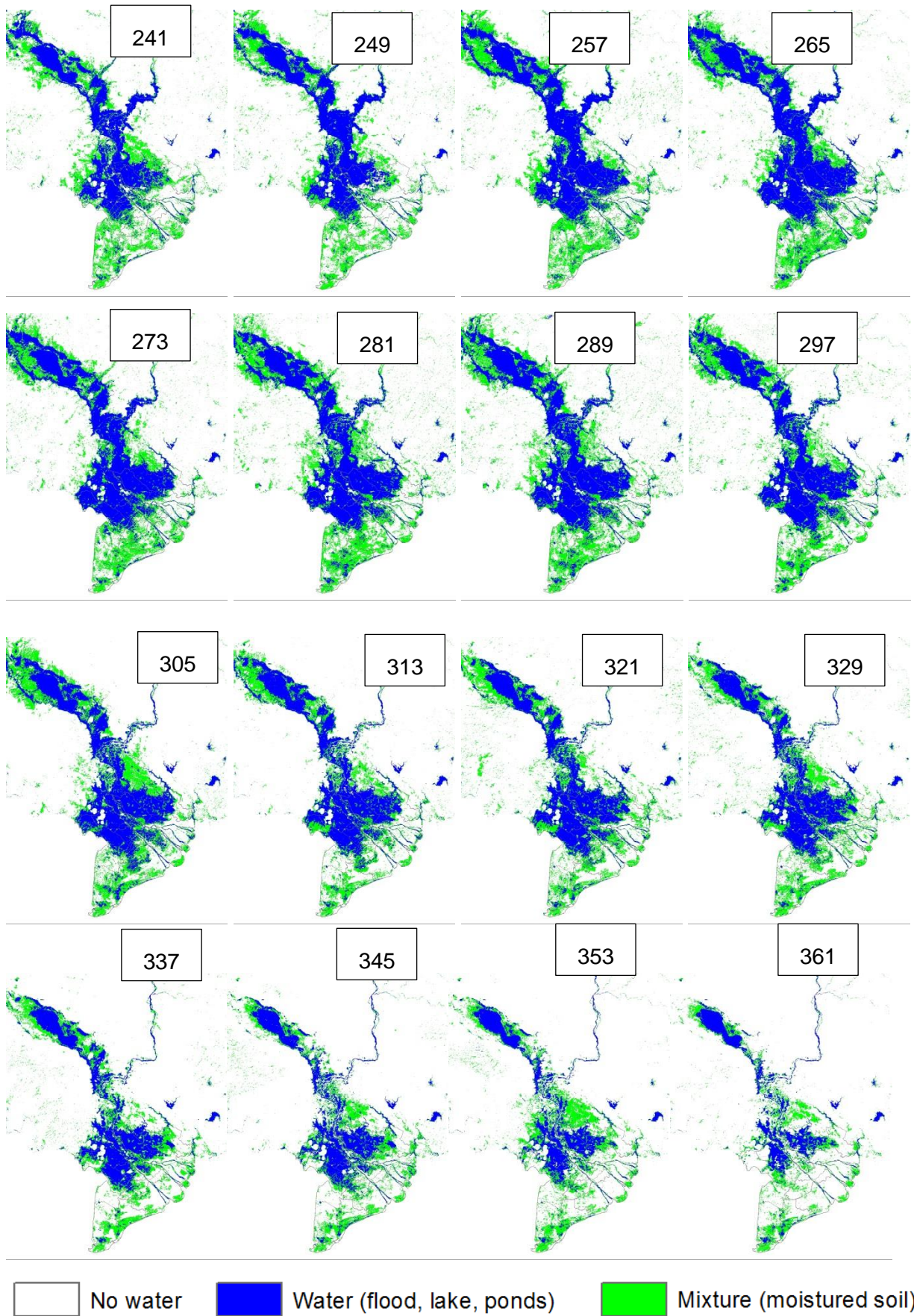


Figure 2.8. Flood distribution (peak and falling stages) in 2000 from DOY241 to DOY361

2.3.2. Flood extent analysis

The inundation areas were used to analyze the impact of full-dyke constructions in upstream provinces based on the flooding situation in the MD. The area of flood extension has a relationship with Mekong River inflow, which was measured at the Tan Chau gauge during flooding in 2000, as can be seen in Figure 2.9. When the water level at Tan Chau increased, the area of flooding also increased, and the date with the maximum flooded area is identified based on this relationship. For example, in 2000, the max flooded area was on 1.11.2000 even though the peak of the flood level was on 22.9.2000. This can be explained by the fact that flooding in the MD occurred slowly, which meant a longer time of flooding that covered a large part of the delta.

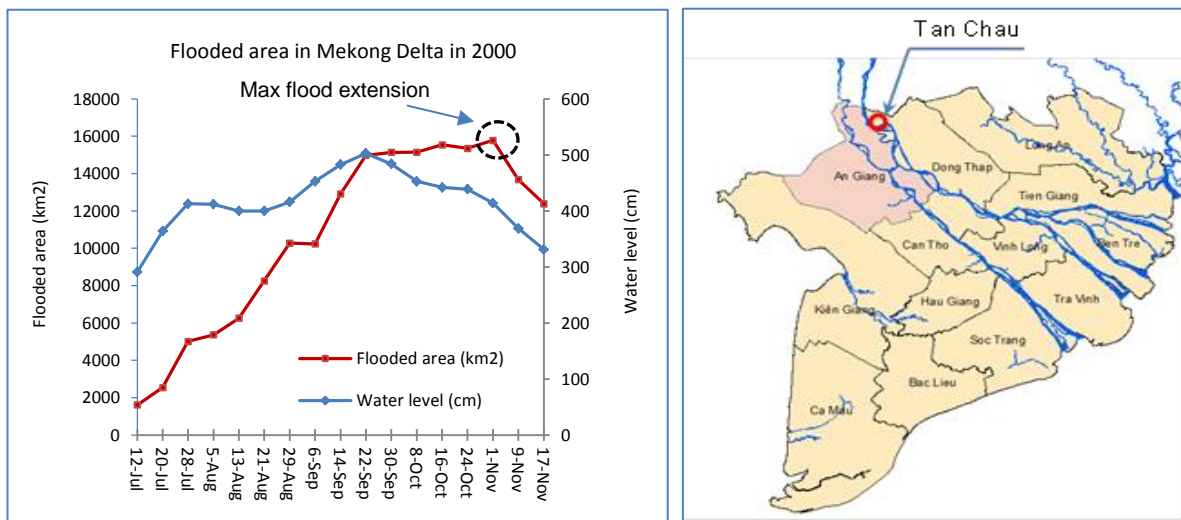


Figure 2.9. Relationship between water level at Tan Chau gauge and flooded area in 2000

Doing the same process for other floods from 2001 to 2017, the areas of flood extension are shown in Figure 2.10 below. It can be seen that the time of maximum flooding extension in MD occurs annually from the 8th of October through the 9th of November each year

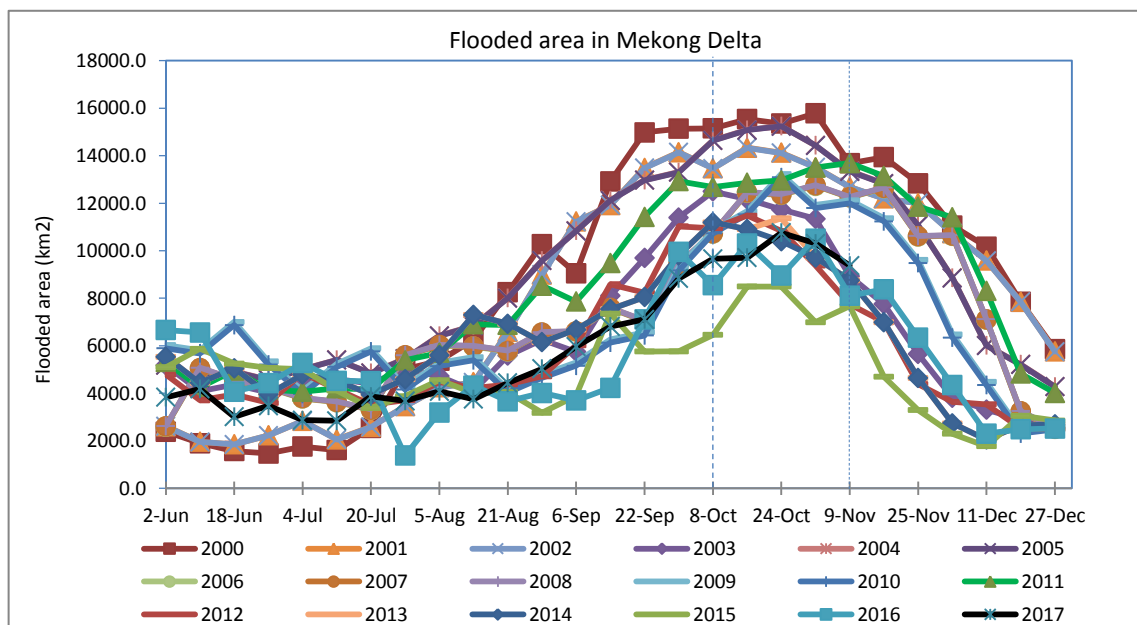


Figure 2.10. Flooded area in Mekong delta from 2000 to 2017

Analysis the land use change versus flooding situation in the MD using remote sensing technology

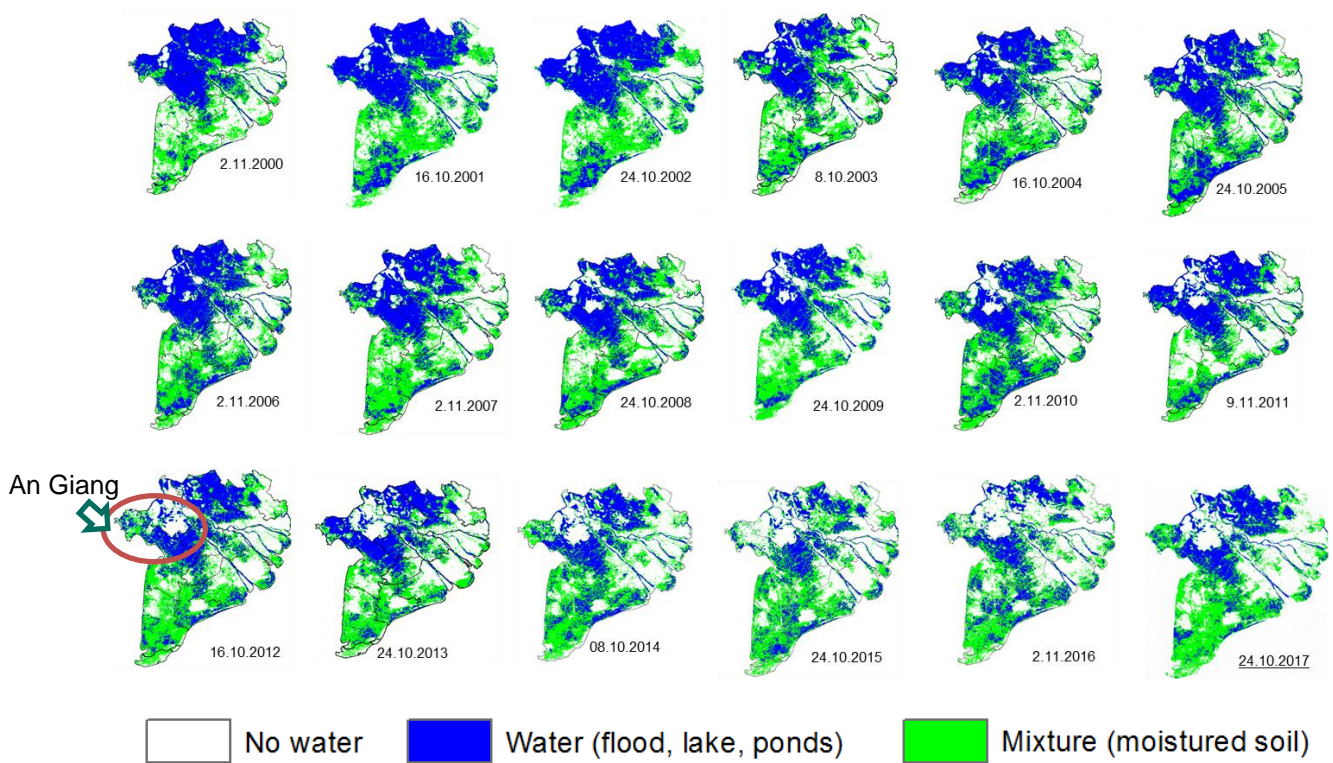


Figure 2.11. Maximum flood extension in MD from 2000 to 2017

Figure 2.11 presents the maximum flood extension from 2000 to 2017. This illustrates that the flooding area in An Giang province decreased slightly from 2000 to 2005, and after that, it decreased rapidly from 2006 to 2013 and kept decreasing slightly until 2017. Figure 2.12 below provides details.

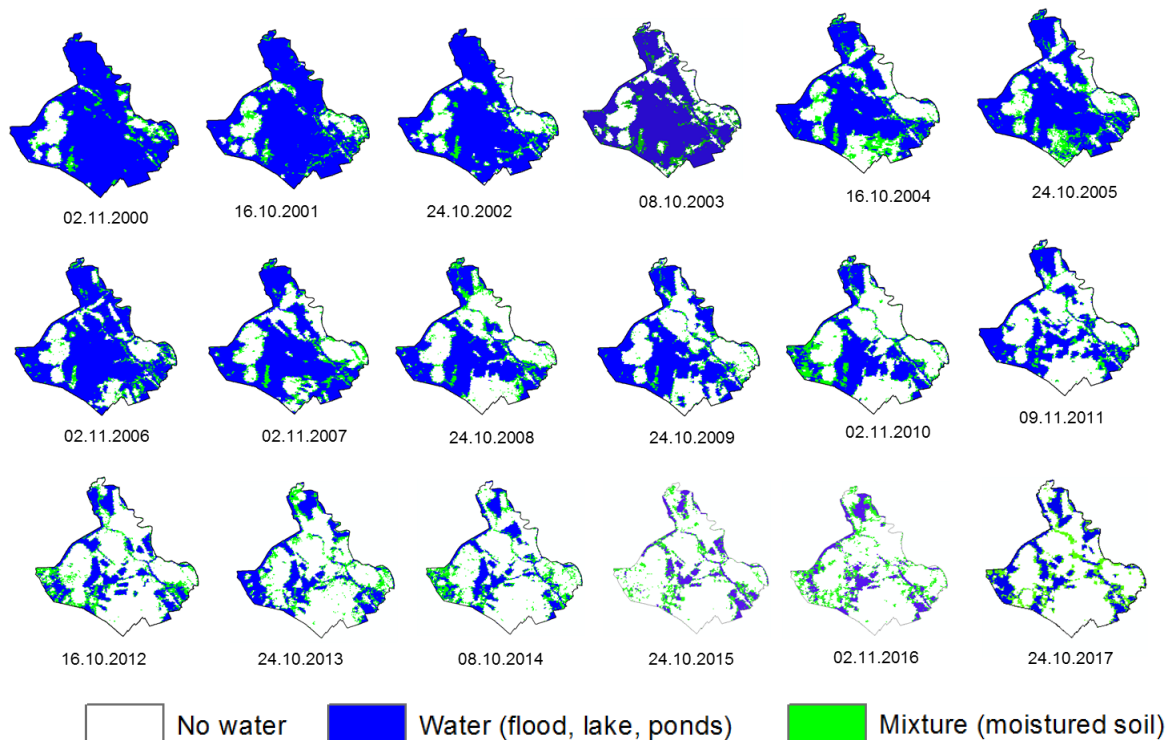


Figure 2.12. Maximum flood extension in An Giang province from 2000 to 2017

Analysis the land use change versus flooding situation in the MD using remote sensing technology

Table 2.7. The decrease of flooded area in An Giang province

No.	year	Dry area (km ²)	Wet area (km ²)	% dry	% wet	WL Tan Chau (cm)
1	2000	423	3105	12%	88%	506
2	2001	494	3034	14%	86%	478
3	2002	706	2822	20%	80%	482
4	2003	811	2717	23%	77%	405
5	2004	1023	2505	29%	71%	441
6	2005	882	2646	25%	75%	435
7	2006	776	2752	22%	78%	417
8	2007	1058	2470	30%	70%	408
9	2008	1482	2046	42%	58%	377
10	2009	1482	2046	42%	58%	409
11	2010	1835	1693	52%	48%	320
12	2011	1835	1693	52%	48%	486
13	2012	2187	1341	62%	38%	319
14	2013	2117	1411	60%	40%	433
15	2014	2293	1235	65%	35%	371
16	2015	2646	882	75%	25%	243
17	2016	2470	1058	70%	30%	309
18	2017	2787	741	79%	21%	326

The inundation area in An Giang province has been decreasing significantly over the years. As calculated in Table 2.7, the wet area in 2000 was 3,105 km², which accounts for 88% area of the province. However, that decreased to 48% in 2011 and 21% in 2017, respectively. This is the main consequence of full-dyke construction for the triple rice cropping areas in An Giang province. Also, there has been a decrease in the flood discharge in the Mekong River in recent years due to the construction of hydropower dams upstream in the Mekong River (ICEM, 2009).

2.3.3. Flood map accuracy analysis

To evaluate the accuracy of MODIS flood maps, there were two approaches performed.

- Compare the MODIS flood maps with the flood maps from radar satellites that have higher resolutions. Herein, the water masks from ENVISAT ASAR, Terra SAR X, and Terra TSX strip were kindly provided in 2015 by Dr. Kuenzer (DLR) to serve the calibration purpose.
- Field trip to detect the footprint of floods and land use surveys in Dong Thap province and An Giang province.

2.3.3.1. In comparison with higher resolution SAR satellite products

Synthetic Aperture Radar (SAR) is the most effective sensor in detecting flooded areas under cloud cover. Satellite images acquired using RADARSAT, JERS-1, ERS-1/2, and ENVISAT have previously been used to detect inundated areas in a variety of ways (Haruyama & Shida, 2006; Henry, Chastanet, Fellah, & Desnos, 2006; Heremans et al., 2005; Hirose et al., 2001; Ishitsuka et al., 2003; Laugier et al., 1997; Liew et al., 1998; Nguyen & Bui, 2001; Wang, 2004; Wang, Colby, & Mulcahy, 2002). When using a pointing device and the selectable sensor mode, ENVISAT enables the frequent monitoring of a ground surface at a large scale.

In this research, the water masks from Envisat ASAR, Terra X Scan and TSX strip were used to calibrate the MODIS flood maps. The water masks from SAR radars were collected from the

Analysis the land use change versus flooding situation in the MD using remote sensing technology

database within the Wisdom Project in Germany (DLR, 2015), the resolution of these radar satellites are shown as follows.

- Envisat Asar: The resolution of the water masks is 88 m.
- Terra X Scan: The resolution of water masks is 8 m.
- Terra TSX Strip: The resolution of water masks is 3.75 m.

Table 2.8 shows a comparison between MODIS and Envisat ASAR for thirteen flood maps from 14 June 2007 to 6 December 2007.

Table 2.8. Comparison of flooded maps between MODIS-Terra vs Envisat-ASAR satellite

Date	MODIS (resolution: 461 m)	ENVISAT-ASAR (resolution: 88 m)	Relative difference (%)
	Flood area (km ²)	Flood area (km ²)	
14-Jun-2007	193.03	331.72	42%
3-Jul-2007	194.53	286.02	32%
19-Jul-2007	280.99	339.06	17%
14-Aug-2007	3007.21	1481.11	51%
23-Aug-2007	3424.24	2820.80	18%
11-Sep-2007	4105.45	3279.24	20%
18-Sep-2007	4875.92	3478.79	29%
16-Oct-2007	8179.41	6161.54	25%
23-Oct-2007	8179.41	6175.89	24%
1-Nov-2007	8615.70	7828.04	9%
20-Nov-2007	8681.71	6414.45	26%
27-Nov-2007	7764.04	6232.64	20%
6-Dec-2007	7354.85	5622.16	24%

Area of comparison = 15.078 km²

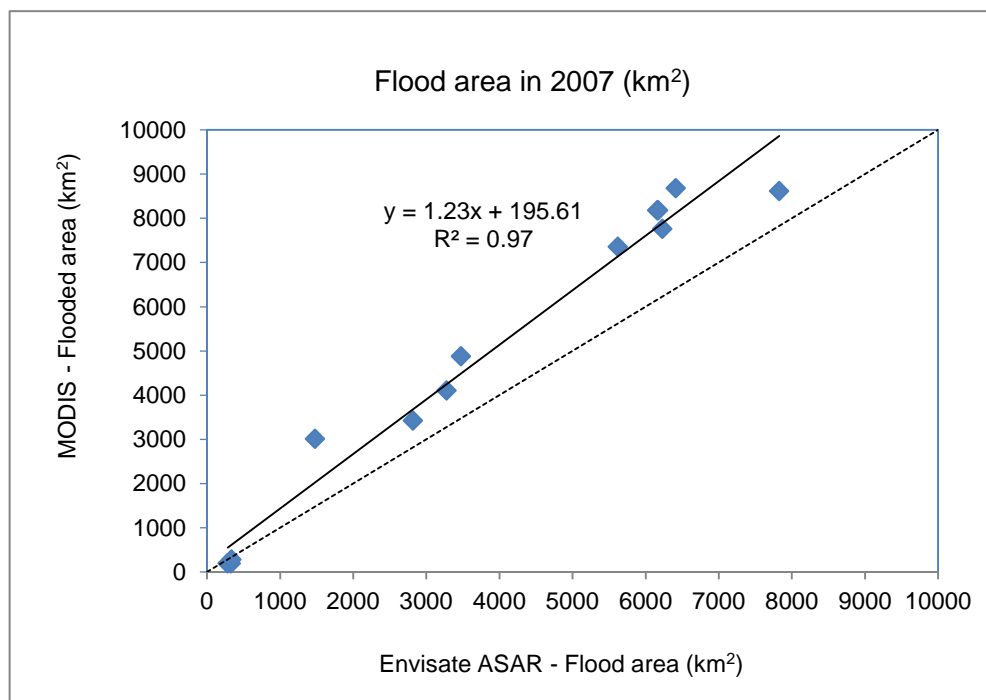


Figure 2.13. Comparison of flooded maps between MODIS-Terra and Envisat-ASAR satellite

Analysis the land use change versus flooding situation in the MD using remote sensing technology

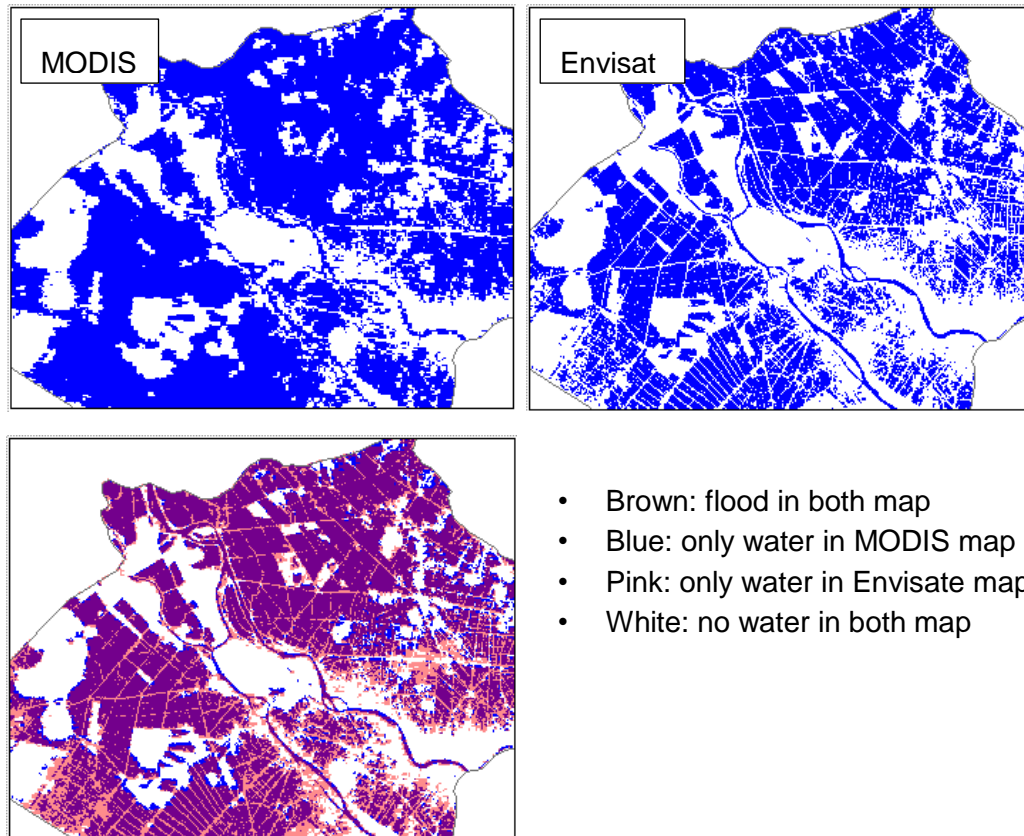


Figure 2.14. Agreement of flood maps by Envisat ASAR vs MODIS on 23.10.2007

The relative difference ranges depending on the stage of the flood. In the rising stage, the relative difference varies from 51% to 32%. However, in the peak flood period, it varies from 20% to 9%. Figure 2.13 shows the agreement about the accuracy of the flood maps from MODIS and Envisat ASAR during the flood season for 2007, which is expressed as $R^2 = 0.97$. Figure 2.14 presents an example of comparison between the flood maps of those satellites on 23.10.2007.

Similarly, the comparison between MODIS and Terra X Scan water masks were also conducted for five products during the flood in 2008. The area of comparison is 12.619 km²; the relative difference ranges from 5% during the peak of the flooding to 45% during the early stage of flooding. This demonstrated even better agreement with a $R^2 = 0.99$, which is illustrated in Table 2.9, Figure 2.15 and Figure 2.16 that all show the agreement between the MODIS flood maps and the Terra X Scan flood maps.

Table 2.9. Comparison of flooded maps between MODIS vs Terra SAR Scan satellite

Date	MODIS	TERRA-X-ScanSAR	Relative difference (%)
	(resolution: 461 m) Flood area (km ²)	(resolution: 8m) Flood area (km ²)	
19-Aug-2010	273.31	493.51	45%
23-Aug-2008	4717.18	4226.15	10%
25-Sep-2008	6401.44	5752.16	10%
28-Oct-2008	7612.01	6941.31	9%
30-Nov-2008	6627.05	6275.38	5%

Area of comparison = 12.619 km²

Analysis the land use change versus flooding situation in the MD using remote sensing technology

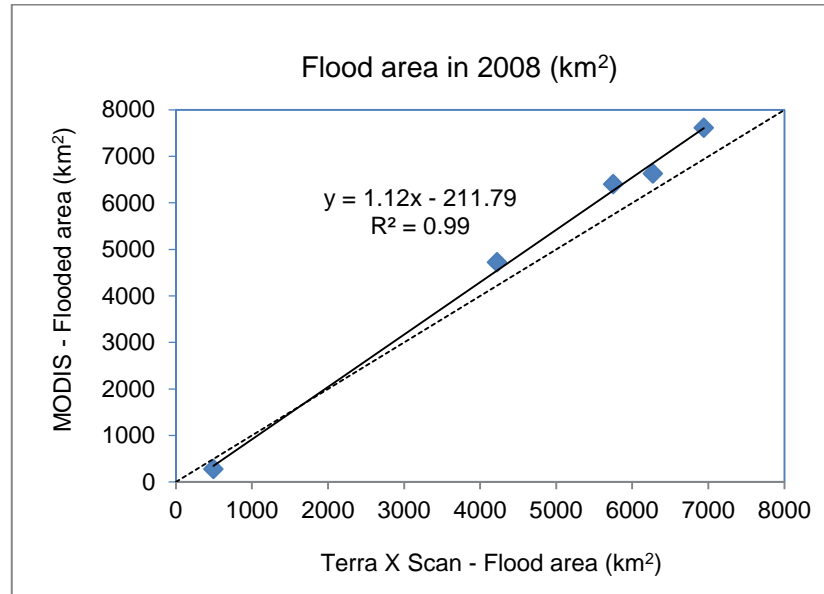


Figure 2.15. Comparison of flooded maps between MODIS vs Terra SAR Scan satellite

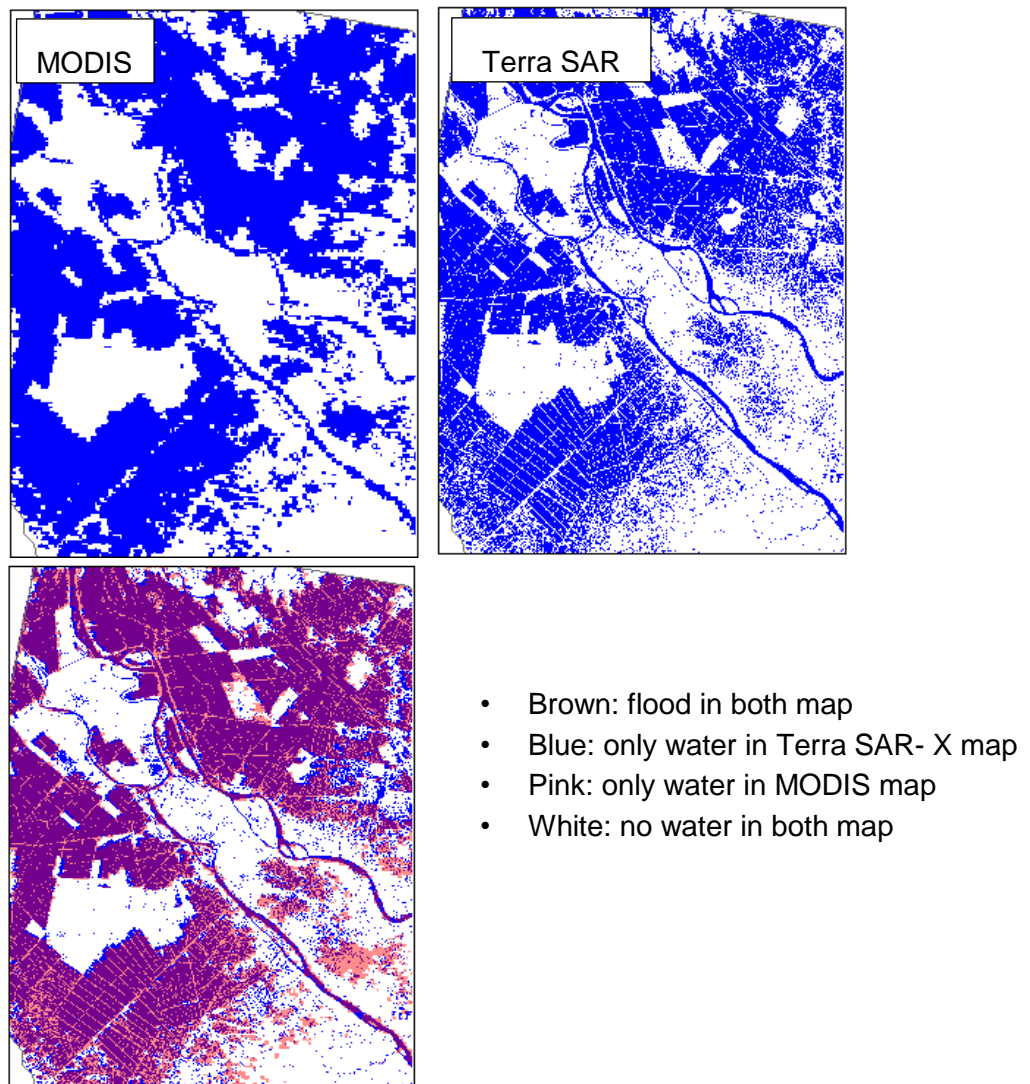


Figure 2.16. Comparison of flood maps by Terra SAR-X vs MODIS on 25.09.2008

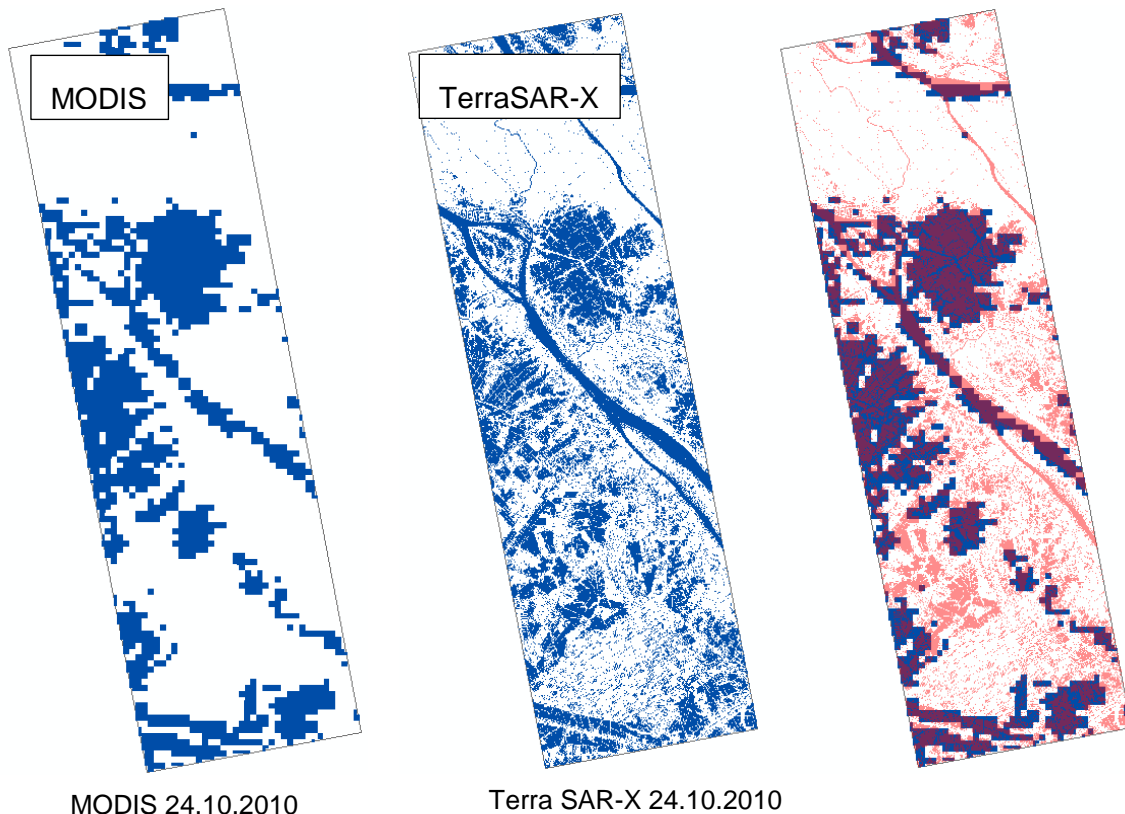
Analysis the land use change versus flooding situation in the MD using remote sensing technology

Finally, a comparison between MODIS and Terra TSX strip maps with a resolution of 3.75 was carried out for nine products during the flooding in 2010. The area of comparison is smaller in scale by representing only 946 km². Therefore, the relative difference ranges from 6% during the peak of flooding to 84% during the early stage of flooding. However, the agreement between MODIS and TSX strip flood maps was quite good with R² = 0.95. Table 2.10 and Figure 2.17 and 2.18 show the agreement between MODIS flood maps and Terra TXS flood maps.

Table 2.10. Comparison of flooded maps between MODIS-Terra vs TERRA-TSX strip

Date	MODIS	TERRA-TSX strip	Relative difference (%)
	(resolution: 461 m) Flood area (km ²)	(resolution: 3.75 m) Flood area (km ²)	
18-Jun-2010	24.52	152.79	84%
30-Aug-2010	69.50	180.85	62%
10-Sep-2010	108.72	150.88	28%
24-Oct-2010	513.79	421.10	18%
4-Nov-2010	513.62	446.70	13%
15-Nov-2010	368.94	392.31	6%
26-Nov-2010	268.54	325.03	17%
18-Dec-2010	74.16	155.76	52%
29-Dec-2010	40.73	129.26	68%

Area of comparison: 946 km²



Brown: flood in both map; Blue: only water in Terra SAR- X map

Pink: only water in MODIS map; White: no water in both map

Figure 2.17. Agreement of flood maps by Terra SAR-X vs MODIS on 24.10.2010

Analysis the land use change versus flooding situation in the MD using remote sensing technology

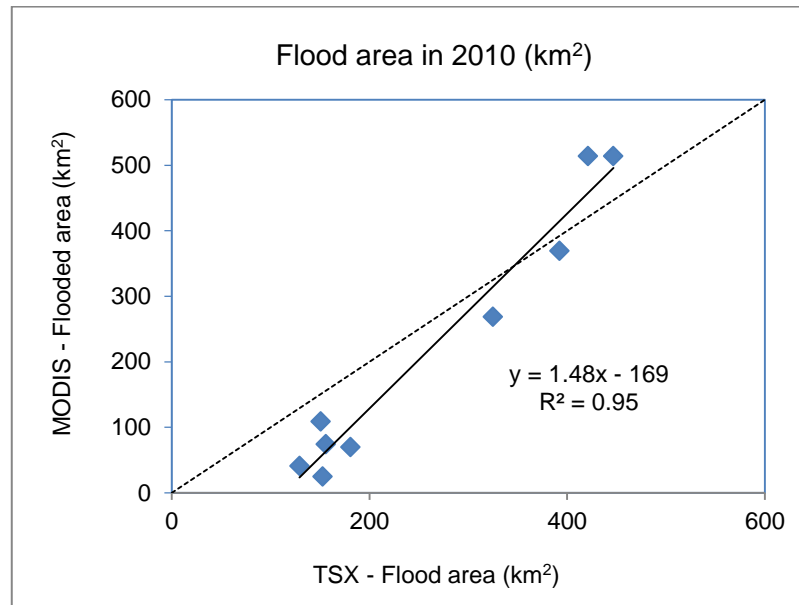


Figure 2.18. Comparison of flooded maps between MODIS vs TSX strip

In conclusion, the MODIS flood maps possessed a high level of agreement with SAR products with $R^2 = 0.99, 0.97, \text{ and } 0.95$, respectively.

2.3.3.2. Field trip to An Giang and Dong Thap province in the flood season

The field trips to the flooded zones in An Giang and Dong Thap province were conducted during the flood season in November 2013 and October 2014 to identify footprints of the floods in comparison with the MODIS flood maps from 14 November 2013 and 23 October 2014, which can be seen in Figure 2.19. The pictures were taken in Long Xuyen, Tinh Bien, An Giang province and Cao Lanh, Tam Nong district, Dong Thap province.

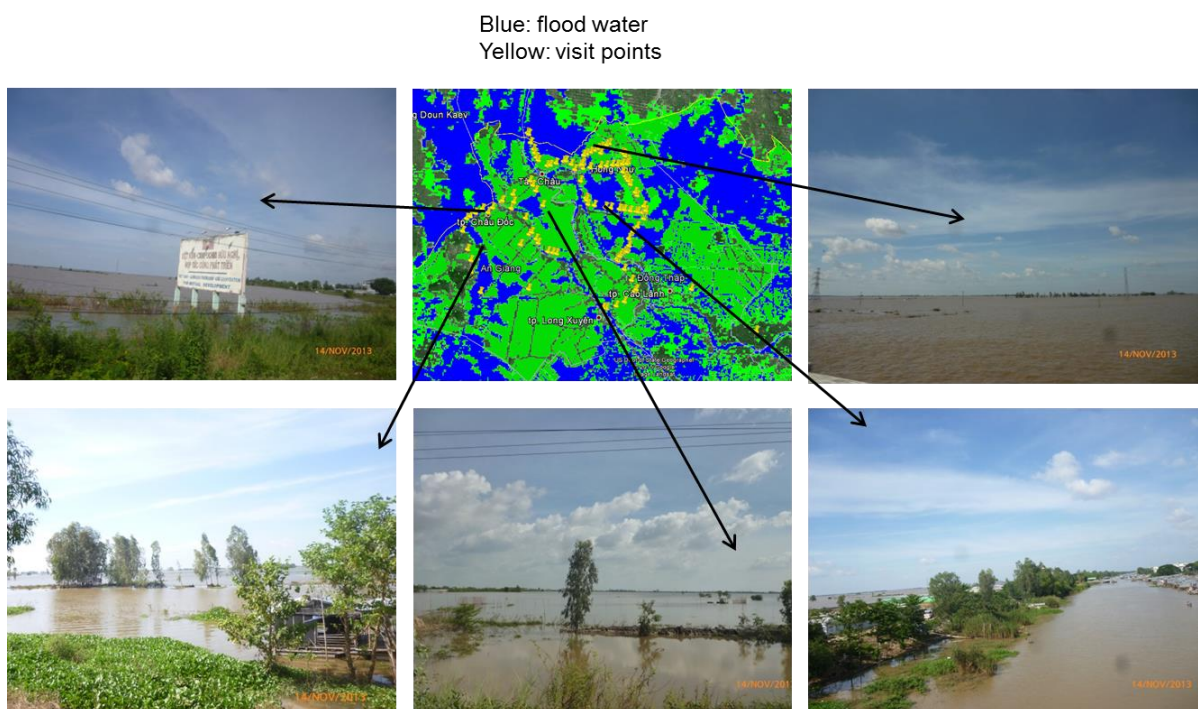


Figure 2.19. Field trip to An Giang and Dong Thap provinces during flood seasons

2.3.4. Discussion about MODIS flood maps

The MODIS flood maps show good agreement with the water masks from the SAR products. Specifically, they show the agreement of $R^2 = 0.97$ in comparison with Envisat ASAR (88m) $R^2=0.99$, and in comparison with Terra SAR-X (8m) $R^2=0.95$, and in comparison with Terra TSX (3.75m). Besides, MODIS flood maps have a high correspondence with hydrographs at the Tan Chau and Chau Doc gauges when compared with the flood area extension in the An Giang province. Finally, the footprints of the flood were also confirmed via field trips to the MD.

In conclusion, MODIS flood maps were appropriate to monitor flooding in the MD because the topography in the MD was very large and flat.

2.3.5. The relationship between flood levels vs flooded area

Flood waters enter the MD via Mekong and Bassac rivers, and the discharges and water level are monitored at Tan Chau and Chau Doc gauges, as stated in Figure 2.20. and 2.21. Due to the both Mekong and Bassac Rivers flowing through An Giang province, the hydrograph at the Tan Chau and Chau Doc gauges shall be applied to evaluate with the flooded area in An Giang province to identify the correspondence between them.

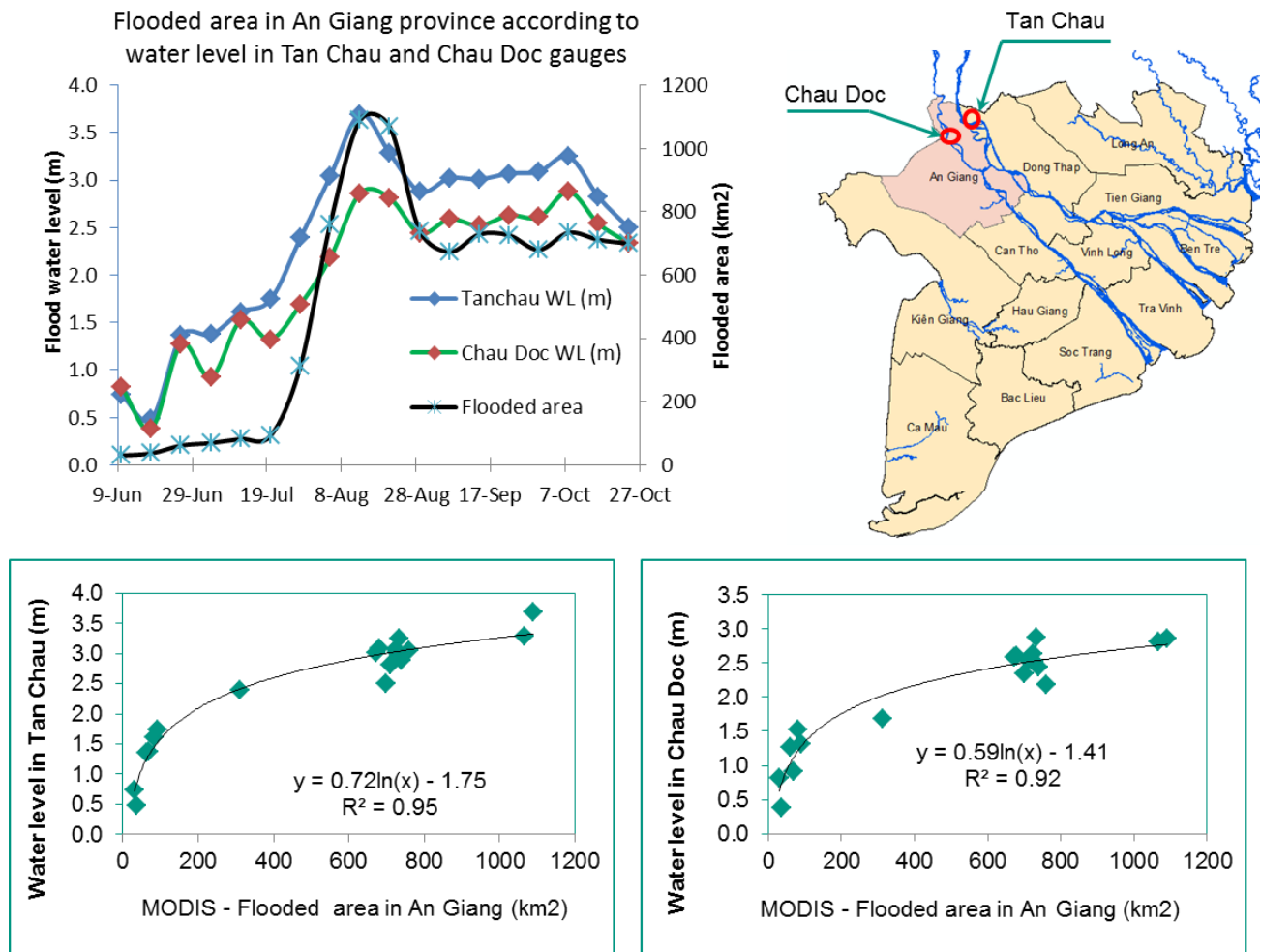


Figure 2.20. Relationship between water levels at Tan Chau and Chau Doc gauges vs flooded area in 2014

Analysis the land use change versus flooding situation in the MD using remote sensing technology

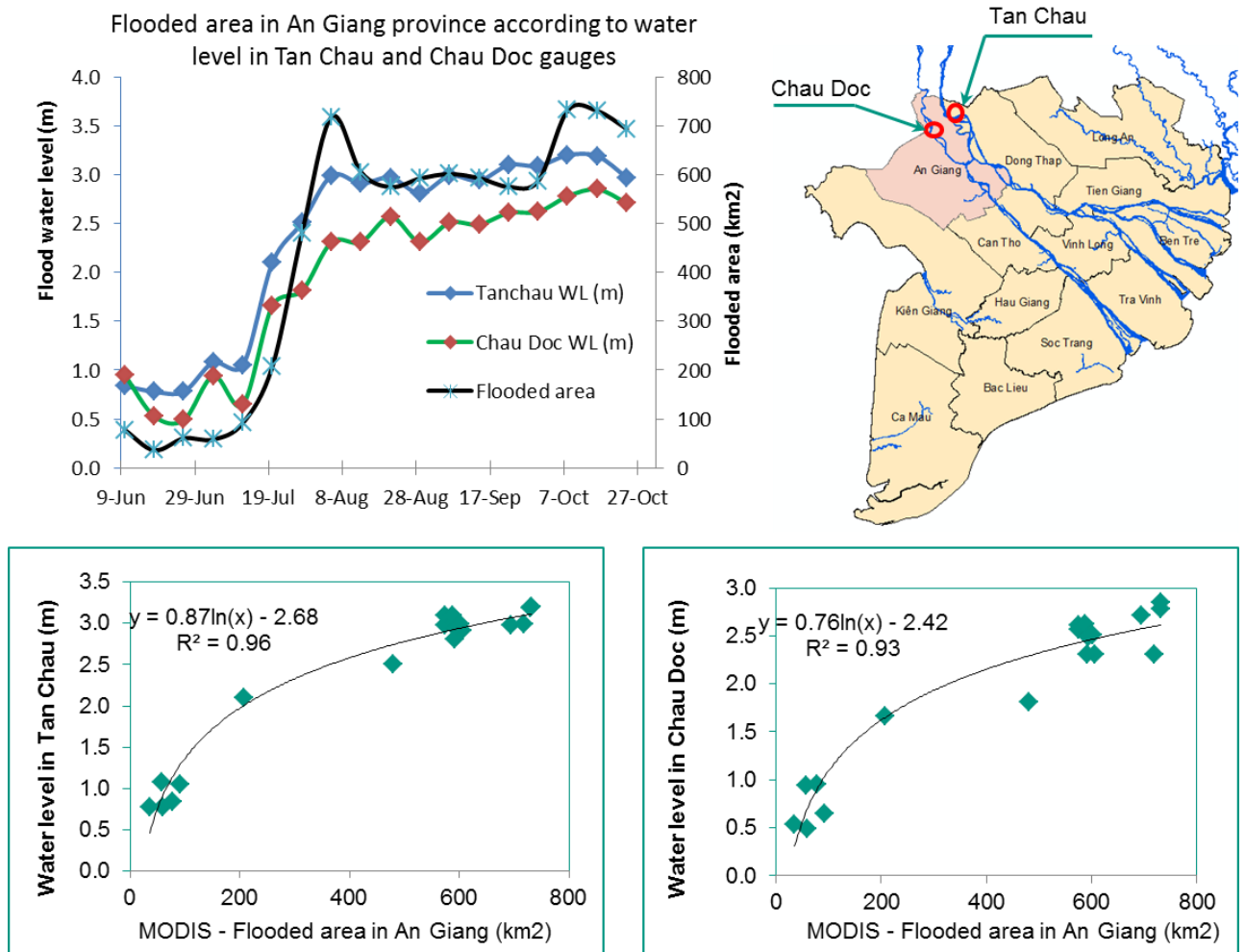


Figure 2.21. Relationship between water levels at Tan Chau and Chau Doc gauges vs flooded area in 2017

The correspondence between the flooding area and hydrographs was evaluated and confirmed with two floods in 2014 and 2017. The flooded area in An Giang province showed a high level of correspondence with the flood level at the Tan Chau Doc gauges with $R^2=0.96$ and 0.92 in 2014 and $R^2=0.96$ and 0.92 in 2017, respectively. When the flood level at Tan Chau and Chau Doc increased, the flooded area in the An Giang province also increased. Similarly, when the flood levels decreased, the area of flooding in the An Giang province also decreased.

2.4. Land use analysis for Mekong delta

Fortunately, land use maps in the MD were kindly provided by Dr. Sakamoto for the period from 2001 to 2012. Therefore, the authors analyses only included the land use maps for the year 2000 and from 2013 to 2017 to offer a comprehensive analysis about the change of agricultural development over the last decade.

2.4.1. Algorithm for land use mapping

Figure 2.22 shows the original algorithm for land use detection used by Sakamoto et al. (2009).

Analysis the land use change versus flooding situation in the MD using remote sensing technology

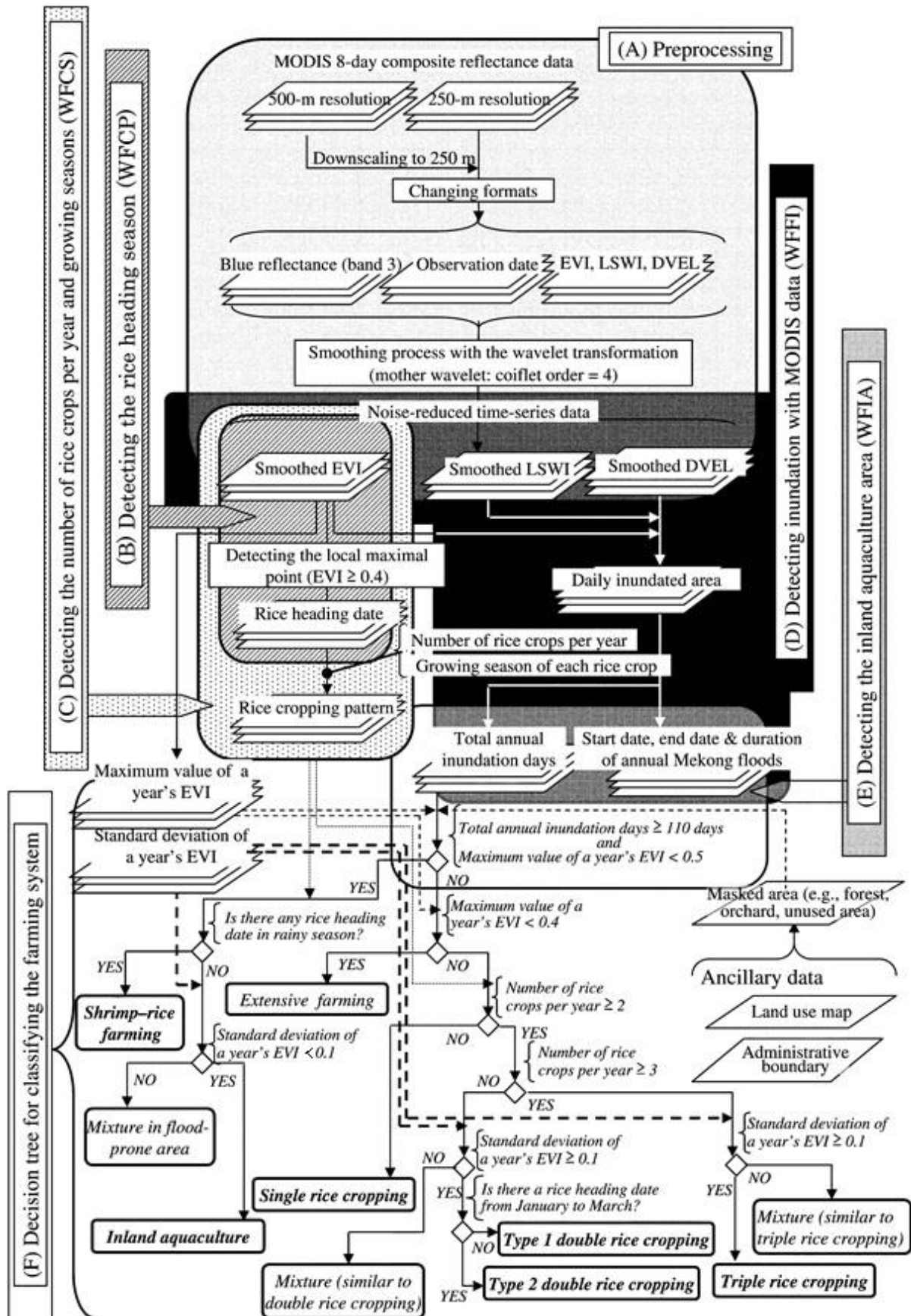


Figure 2.22. Flow chart showing the integrated algorithms of the wavelet-based filter

(Source: Sakamoto et al., 2009)

Analysis the land use change versus flooding situation in the MD using remote sensing technology

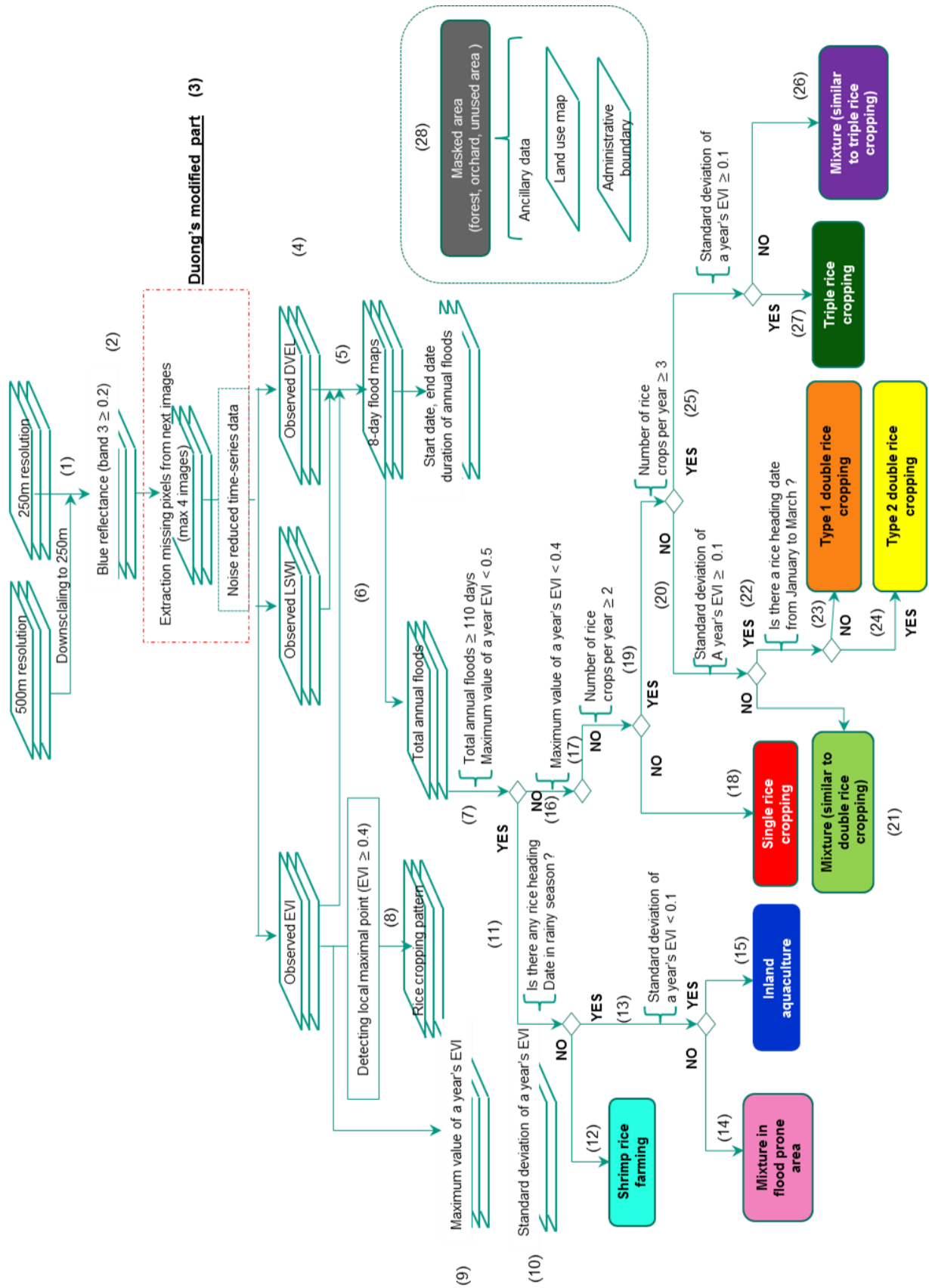


Figure 2.23. Flow chart showing the modification part for land use detection by Duong, 2017

Figure 2.23, in general, is similar to Figure 2.22. However, it presents the steps used to identify the land use items with an aim to support the readers' ease in following the process.

Analysis the land use change versus flooding situation in the MD using remote sensing technology

The process for land use map detection in MD includes 29 steps, which are listed below.

- Step 1 to Step 5: Describe the pre-processing procedures and flooding map interpretation for each eight-day image. These tasks were discussed in Section 2.3.1. Flood algorithms for flood maps detection were mentioned in this dissertation.

- Step 6: Yearly total annual flood

The start date, end date, and the duration of the annual Mekong floods were detected from the longest continuing period of flood. Because the floods often happen from June to December, the yearly annual flood is a sum of flood maps from DOY153 to DOY361, including both the mixture and flood situations. It can be expressed:

$$T = \text{Yearly total annual flood} = \sum \text{floods}(\text{DOY153} + \text{DOY161} + \dots + \text{DOY361})$$

- Step 7: Identify two conditions.

- Condition 1: the total annual of inundated days ≥ 110 days
- Condition 2: the pixels whose yearly maximum was $\text{EVI} < 0.5$

- Step 8: Detecting rice heading season by wavelet-based filter for crop phenology

According to Sakamoto et al. (2007), the EVI value gradually increased with rice growth; the rice heading dates are estimated by detecting local maximal in the observed EVI profile in which the observed EVI values were ≥ 0.4 .

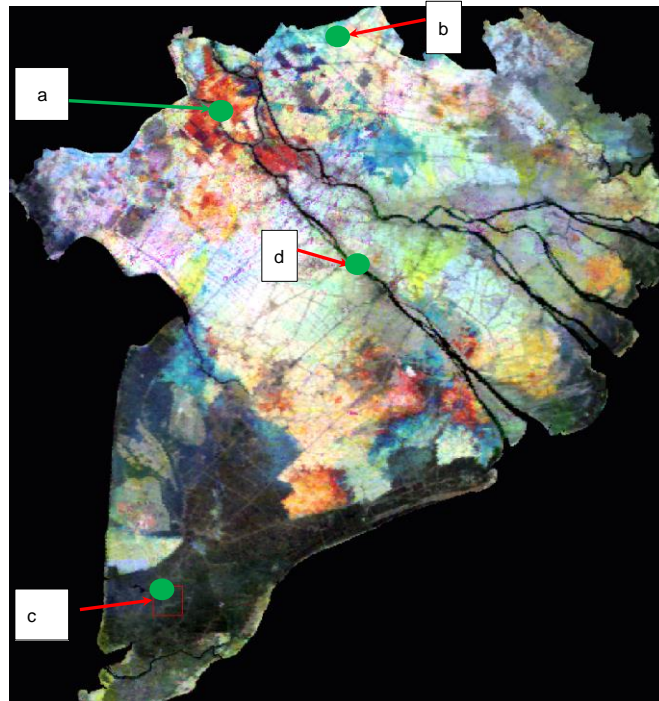


Figure 2.24. EVI series in the Mekong Delta from January 2013 to December 2017
(RGB composite created with the order of band 3, band 2, and band 1)

The time series indexes were processed from January 2013 to December 2017. Figure 2.24 shows the four locations of observed EVI time series in the MD. The EVI times series in the four locations are presented in Figure 2.25.

Analysis the land use change versus flooding situation in the MD using remote sensing technology

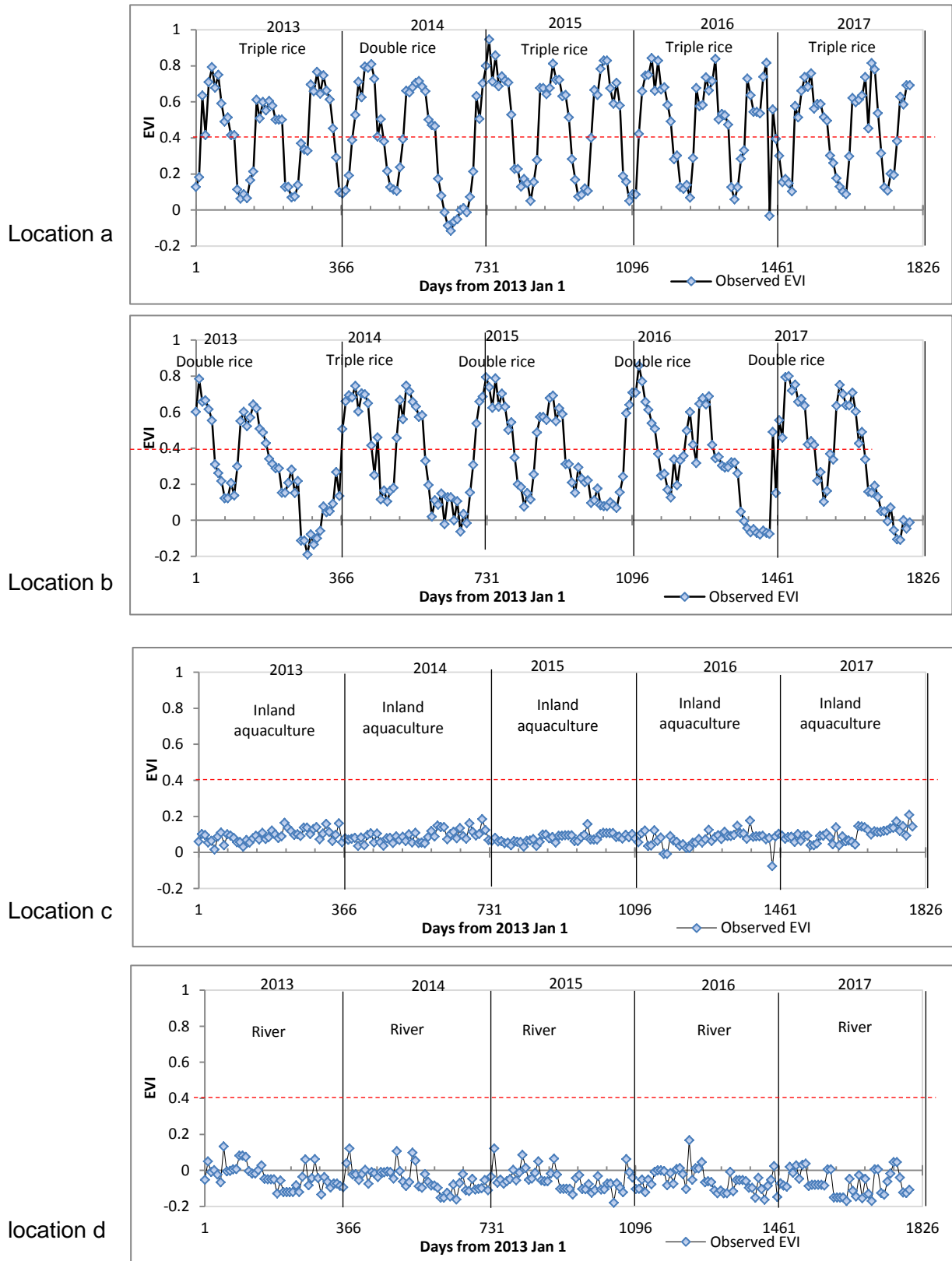


Figure 2.25. The variation of observed EVI time series at the locations a), b), c) and d) from 2013 to 2017. The number of rice crops per year and the growing seasons were measured from the observed EVI data. Figure 2.25 shows the different types of EVI series characteristics from 1.1.2013 to 18.11.17. Thus, the EVI series at the location a expresses the triple rice cropping in An Giang province with three peaks of EVI while the location b shows double

Analysis the land use change versus flooding situation in the MD using remote sensing technology

rice cropping in Dong Thap province, and location c is the area of inland aquaculture in Ca Mau province. Finally, location d shows the EVI in region of the Hau River. The EVI has very small value in relation to inland aquaculture and rivers.

- Step 9: Detecting maximum value of a year's EVI.

This step identified and selected the maximum EVI series value of a year from EVI of DOY001 to EVI of DOY361.

$$\text{Max_EVI_year} = \max(\text{EVI001}, \text{EVI009}, \dots, \text{EVI361})$$

- Step 10: Calculation of the standard deviation of a year's EVI.

This step can be easily processed using statistical math for an EVI series in a year.

- Step 11: Is there any rice heading date in the rainy season?

The rainy season in the MD starts in April (DOY97) and goes until the end of November (DOY329). The maximum EVI during that period was calculated to identify the rice heading date in the rainy season.

$$\text{Max_EVI_rainy} = \max(\text{EVI97}, \text{EVI105}, \dots, \text{EVI329})$$

- If $\text{max_EVI_rainy} \geq 0.4$, the pixel were defined as rice heading date in the rainy season.
 - If $\text{max_EVI_rainy} < 0.4$, the pixels were considered to show no rice heading date in the rainy season.
- Step 12: Shrimp Rice Farming detection

If the pixels met the two conditions in Step 10, but do not meet the condition in Step 11, meaning no rice heading date in the rainy season, they are classified as shrimp-rice farming.

- Step 13: Standard deviation of a year's EVI (Std_EVI_year) was classified into two classes.

- Class 1: $\text{Std_EVI_year} \geq 0.1$
 - Class 2: $\text{Std_EVI_year} < 0.1$

- Step 14: Mixture in flood prone area detection

If the pixels met the two conditions in Step 10 and also met the condition in Step 11, meaning that there were rice heading dates in the rainy season, but the standard deviation of a year's EVI ≥ 0.1 , which illustrates Class 1 in Step 13, they were classified as mixture in flood prone area.

- Step 15: Inland aquaculture detection

If the pixels met the two conditions in Step 10 and also met the condition in Step 11 and the standard deviation of a year's EVI < 0.1 , which illustrates Class 2 in Step 13, they were classified as inland aquaculture.

- Step 16: Maximum value of a year's EVI < 0.4

Analysis the land use change versus flooding situation in the MD using remote sensing technology

When the pixels do not meet the two conditions in Step 10, the maximum value of year's EVI in Step 8 were classified into two classes.

- If $\text{max_EVI_year} \geq 0.4$, the pixel were defined as rice heading date in a year.
- If $\text{max_EVI_year} < 0.4$, the pixels were considered no rice heading date in a year.

• **Step 17: Rice cropping classification**

Base on the rice cropping pattern in Step 7, it is strongly recommended to detect rice cropping period for each province to ensure the accuracy of the land use map since each province has a different rice cropping calendar due to its specific topography and water resources conditions.

The observed EVI time series in 2017 for four provinces are shown in Figure 2.26.

Thus,:

- **Location a:** Expressed triple rice cropping in An Giang province. The first rice crop was grown from January to April; the second rice crop was grown from May to August, and the triple crop was grown from September to December 2017.
- **Location b:** Showed double rice cropping in Dong Thap province in the dry season. Afterwards, most of the paddies located in the flood-prone area were submerged from August to December.
- **Location c:** Showed the area of double rice cropping in the rainy season in the Soc Trăng province; the first crop was grown in December 2016 to January 2017, and the second crop was grown from June to September 2017.
- **Location d:** the area of inland aquaculture in Ca Mau province

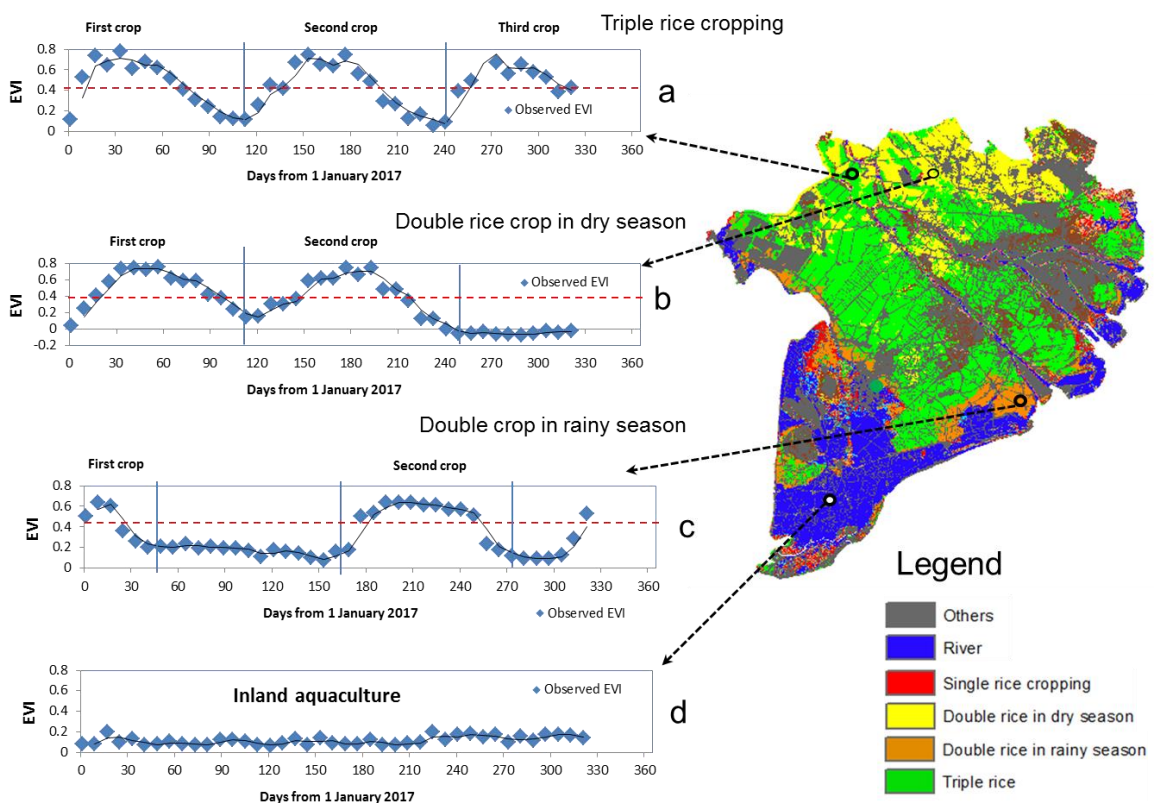


Figure 2.26. The variation of observed EVI time series at 4 locations in MD in 2017

Analysis the land use change versus flooding situation in the MD using remote sensing technology

Based on the period of cropping calendar, the max EVI was calculated for each province. This example below shows the calculations for the max EVI for three crops in the An Giang province:

- Crop 1: from 1 January (DOY001) to end of April (DOY113)

$$\text{Max_EVI_crop 1} = \max(\text{EVI001}; \text{EVI009}; \dots; \text{EVI113})$$

- Crop 2: from 1 May (DOY121) to end of August (DOY233)

$$\text{Max_EVI_crop 2} = \max(\text{EVI121}; \text{EVI129}; \dots; \text{EVI233})$$

- Crop 3: from 6 September (DOY249) to December (DOY353). Because the land use map 2017 was developed in November 2017, the EVI time series stopped at DOY321, as shown in Figure 2.22. However, it is also possible to determine the peak of EVI in October 2017.

$$\text{Max_EVI_crop 3} = \max(\text{EVI249}; \text{EVI257}; \dots; \text{EVI321})$$

If the max_EVI_crop 1 , max_EVI_crop 2 , $\text{max_EVI_crop 3} \geq 0.4$, the pixels were defined as rice heading date, and the rice cropping pattern was classified based on the number of crops per year.

$$\text{Total crops} = (\text{max}_{\text{EVI}_{\text{crop1}}} \geq 0.4) + (\text{max}_{\text{EVI}_{\text{crop2}}} \geq 0.4) + (\text{max}_{\text{EVI}_{\text{crop3}}} \geq 0.4)$$

- If total crops in year = 1, the pixel was defined as single rice cropping.
- If total crops in year ≥ 2 , the pixel was defined as double or triple rice croppings.

- Step 18: Single rice cropping detection

The pixel was defined as single rice cropping when the total crop in year = 1.

- Step 19, Step 20 & Step 21: Detection of mixture (similar to double rice cropping)

If the pixels in the total crops in year ≥ 2 , according to Step 20, but the standard deviation of a year's EVI < 0.1 , according to Step 21, the pixel was considered as mixture similar to double rice cropping.

- Step 19, Step 20 and Step 22: Detection of double rice cropping

If the pixels in the total crops in year ≥ 2 , according to Step 19, and the standard deviation of a year's EVI ≥ 0.1 , according to Step 20, the pixel was considered as double rice cropping, according to Step 22.

- Step 23 & Step 24: Detection of double rice cropping type 1 and type 2

- If there was no rice heading date from January to March ($\text{max_EVI_crop 1} = 0$), the pixel was considered as double rice cropping in rainy season (Type 1), according to Step 23.
- If there was a rice heading date from January to March ($\text{max_EVI_crop 1} = 1$), the pixel was considered as double rice cropping in dry season (Type 2), according to Step 24.

Analysis the land use change versus flooding situation in the MD using remote sensing technology

- Step 25, Step 26 & 27: Detection of triple rice cropping and mixture
 - If the pixels in the total crops in year ≥ 3 , according to Step 25, but the standard deviation of a year's EVI ≥ 0.1 , the pixel was considered as triple rice cropping, according to Step 27.
 - If the pixels in the total crops in year ≥ 3 , according to Step 25, however the standard deviation of a year's EVI < 0.1 , the pixel as considered as mixture similar to triple rice cropping, according to Step 27.
- Step 28: Mask area detection

As this study focused on shrimp farming and multiple rice cropping, other areas, such as orchards, unused land, and forests, were masked according to the 2002 ancillary use map. This mask layer was taken from the land use maps provided by Sakamoto in 2013.

The major farming systems determined by using the integrated algorithm were inland aquaculture, shrimp–rice farming, single rice cropping, Type 1 double rice cropping, Type 2 double rice cropping, and triple rice cropping. Inland aquaculture covered fields used only for raising fish or shrimp under extended waterlogged conditions. Shrimp–rice farming covered agricultural fields used for shrimp farming in the dry season and rice cropping in the rainy season. Single rice cropping implied that the farmer crops rice once a year. Type 1 double rice cropping implied that the farmer crops rice twice a year, mainly in the rainy season. Type 2 double rice cropping implied that the farmer crops rice twice a year, including in the dry season. Triple rice cropping implied that the farmer crops rice three times a year. These six categories were sufficient for identifying distinctive changes in farming across the whole of the MD. Four other categories - mixture 1, which was similar to double cropping, mixture 2, which was similar to triple cropping, and mixture 3 in annually flooded areas indicated that the objective pixels had no discriminating EVI feature probably due to mixed-pixel effects.

Farming systems in 2000 were also classified even though there was a lack of MODIS data from DOY001 to DOY 57. However, the authors used seven images from DOY001 to DOY57 in the year 2001 to apply for the year 2000. Figure 2.27 presents the land use maps in the MD from 2000 to 2017. Herein, only the main objects including triple rice cropping, double rice cropping, single rice, and inland aquaculture areas are presented in the legend. Other objects, such as mixture 1, mixture 2, mixture 3, and masks, are not presented in order to offer a simpler view of the land use.

Analysis the land use change versus flooding situation in the MD using remote sensing technology

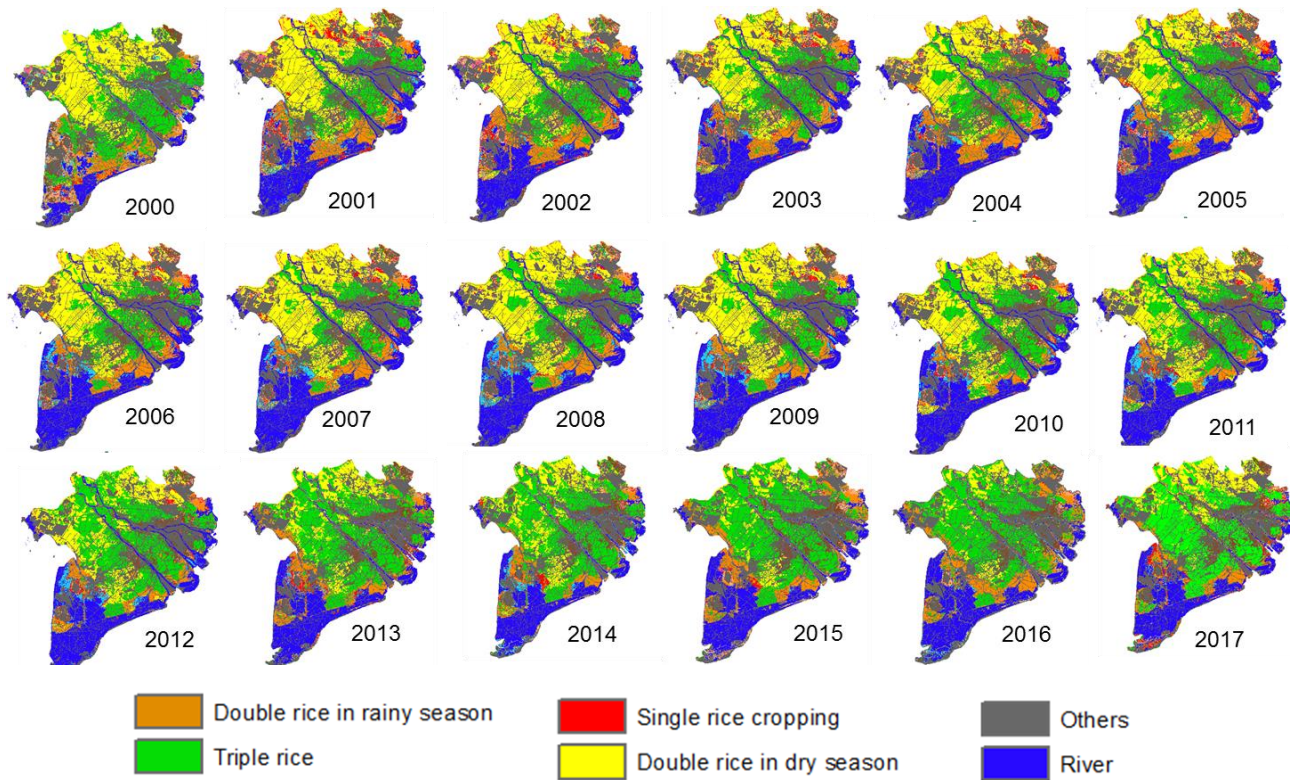


Figure 2.27. Land use pattern in Mekong Delta

(The maps from 2001 to 2012 were provided by Sakamoto (NIES, Japan); maps in 2000, 2013, 2014, 2015, 2016, 2017 were interpreted by Duong)

2.4.2. Land use change analysis in the Mekong delta

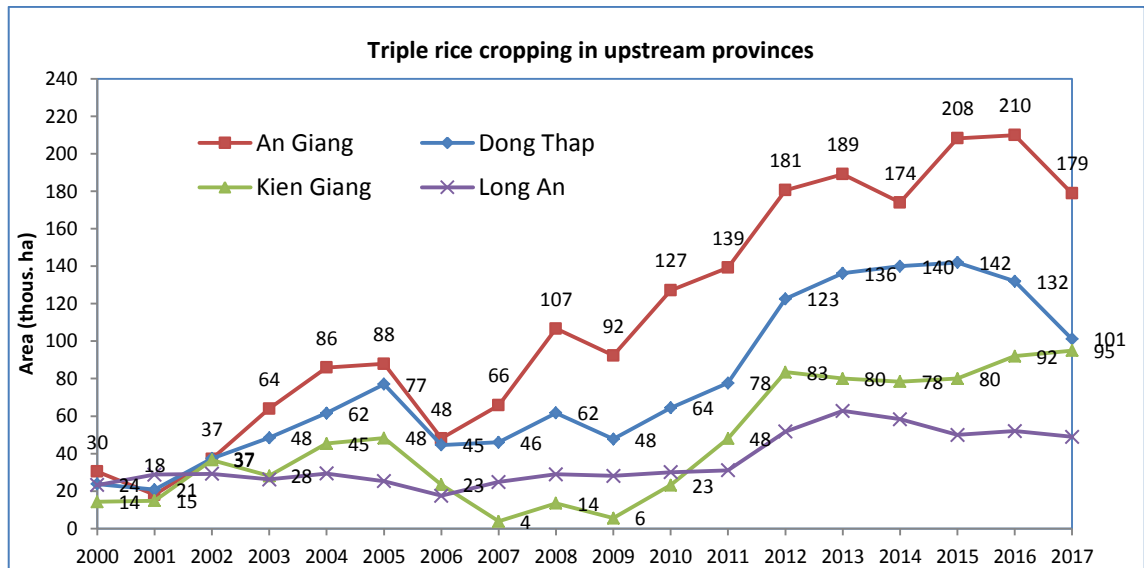


Figure 2.28. Area of triple rice cropping changes in upstream provinces from 2000 to 2017

Figure 2.28 illustrates the change in triple rice cropping area in the four upstream provinces of the upper part of the MD

- An Giang province: This is the best example of a focus on triple rice cropping development. Figure 2.29 shows the two opposing tendencies for the area of flooding versus the triple rice cropping area. Specifically, the flooded area in An Giang was 310

Analysis the land use change versus flooding situation in the MD using remote sensing technology

thousand ha in 2000, which accounted for 88% of the province area. Then, it reduced rapidly to 169 thousand ha (48%) in 2011 and 25% in 2017. This was the consequence of the full-dyke system for the development triple rice cropping areas in the An Giang province. As a result, the area for triple rice cropping increased continuously from 18 thousand ha in 2001 to 88 thousand ha in 2005. Afterwards, it decreased to 48 thousand ha in 2006 due to high floods. Then, it increased rapidly from 66 thousand ha in 2007 to 179 thousand ha in 2017, which was more than 2.5 times larger. This was due to the construction of the Bac Vam Nao sluice gates, which are scheduled to open for flooding every three-years in 2011, 2014, and 2017. Therefore, the triple rice cropping in 2014 and 2017 decreased slightly in comparison with the previous years of 2013 and 2016.

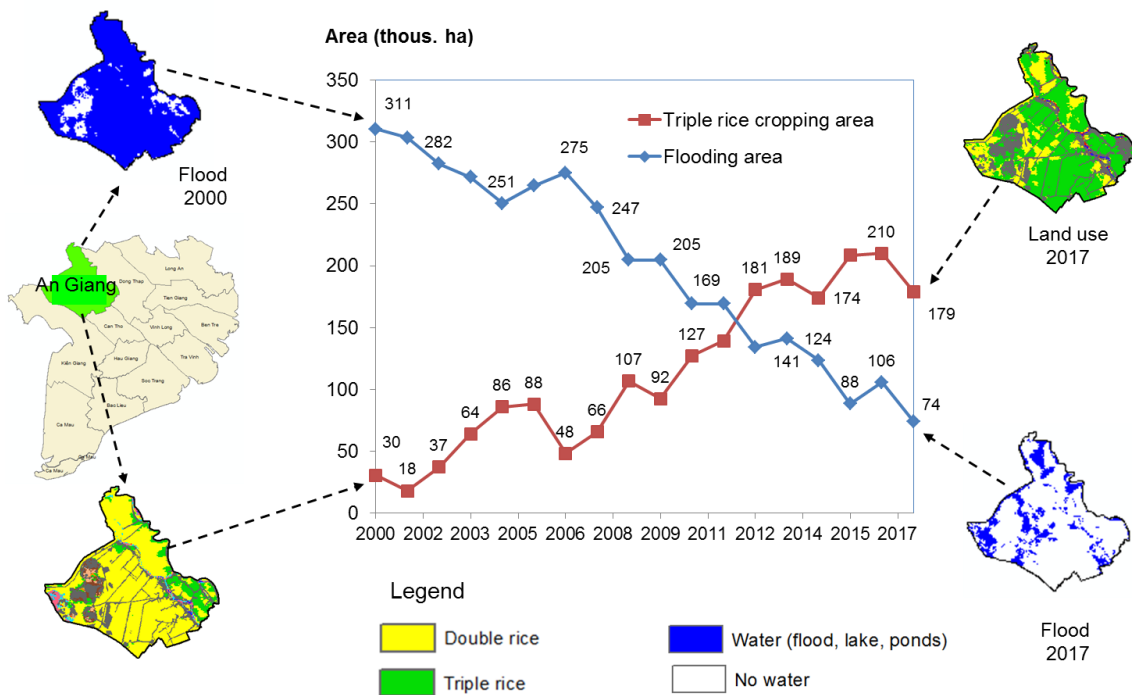


Figure 2.29. The relationship between triple rice cropping and flooded areas in An Giang province

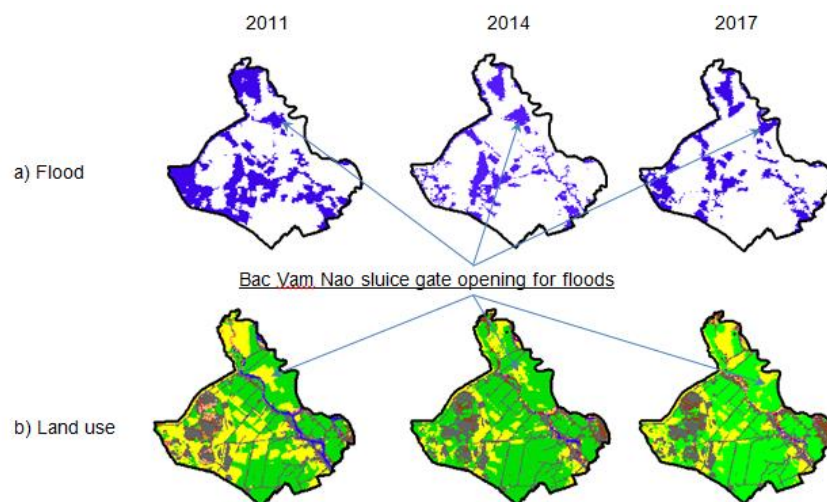


Figure 2.30. Areas of triple rice cropping in An Giang province

- a) Flood areas in 2011, 2014 and 2017 with the opening operation of the North Vam Nao sluice gates
- b) Land use in 2011, 2014 and 2017 in corresponding relation to the operation of the Vam Nao sluice gate

Analysis the land use change versus flooding situation in the MD using remote sensing technology

- Dong Thap province: The area for triple rice cropping increased slightly from 48 thousand ha in 2009 to 78 thousand ha in 2011. Then, it rapidly increased from 123 thousand ha in 2012 and kept on increasing slightly to 142 thousand ha in 2015. The area for triple rice cropping decreased in 2016 and 2017. This showed that the interest in triple rice cropping practice was influenced by the activities in the An Giang province in 2012. However, in recent years, the triple rice cropping area has decreased in Dong Thap. Through conversations with the local farmers, it was discovered that some of them are not interested in the triple rice cropping any more.
- Kien Giang province: The area for triple rice cropping increased very slightly from 14 thousand ha in 2000 to 45 thousand ha in 2005. Afterwards, it decreased rapidly in 2006 and 2007 because the farmers changed from rice cropping to shrimp farming. The attractiveness of triple rice cropping increased rapidly from 2010 at 6 thousand ha to 78 thousand ha in 2012. It has continued to increase slightly to 92 thousand ha in 2017.
- Long An province: The area of triple rice cropping seemed very constant since it increased very little from 14 thousand ha in 2000 to 45 thousand ha in 2005. Afterwards, it decreased rapidly in 2006 and 2007 because the farmers changed the rice cropping to shrimp farming. The attractive of triple rice cropping increased rapidly from 2010 from 6 thousand ha to 78 thousand ha in 2012. It has continued to increase slightly to 92 thousand ha in 2017.

2.4.3. Land use product accuracy analysis

To evaluate the accuracy of the MODIS land use maps:

- Compared MODIS land use map with statistical data
- Compared 01 MODIS land use map interpreted by Duong to the MODIS land use map kindly provided by Dr. Sakamoto
- Field trip to identify the triple rice area during the flooding season in Dong Thap province and An Giang province in November 2013 and October 2014

2.4.3.1. MODIS land use vs statistical data

The statistical data for the areas of rice and aquaculture were collected from 2000 to 2016 from the statistics books for 13 provinces in the Mekong Delta, including An Giang, Dong Thap, Long An, Kien Giang, Can Tho, Hau Giang, Ben Tre, Soc Trang, Tien Giang, Tra Vinh, Vinh Long, Bac Lieu and Ca Mau.

Analysis the land use change versus flooding situation in the MD using remote sensing technology

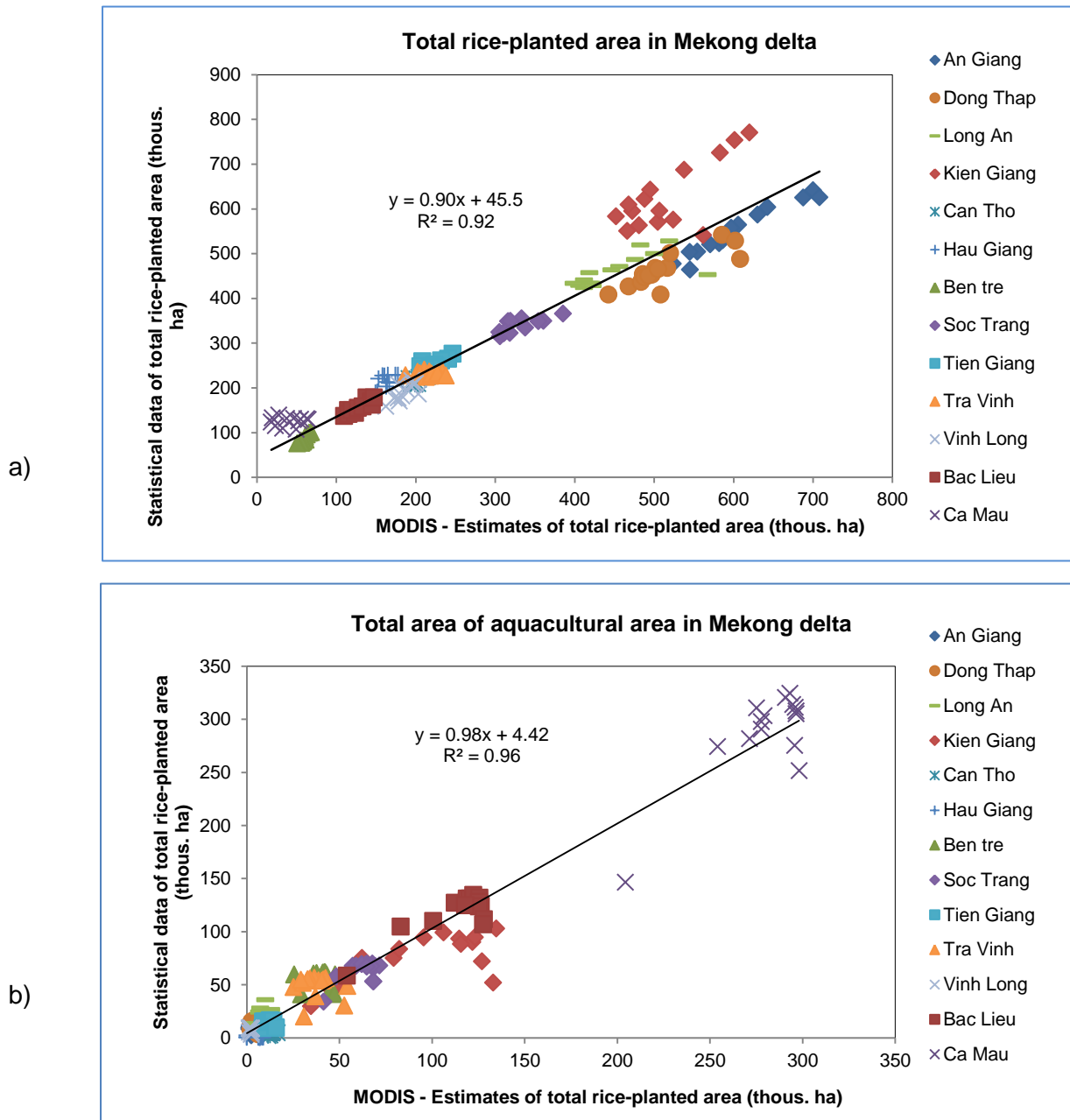


Figure 2.31. Agreement between statistical data vs MODIS land use data

a) Total rice-planted area in the MD; b) Aquaculture area in the MD

Figure 2.31 shows that the MODIS land use map showed a high level of agreement with the statistical data in regards to the total rice planted area and the total aquaculture area in the MD from 2000 to 2016 with the $R^2 = 0.92$ and 0.96 , respectively. Thus, the calculation of area in the MODIS land use maps was calculated as:

- Total rice planted area = single rice + 2 x double rice + 3 x triple rice (area)
- Total aquaculture area = Shrimp rice cropping + Inland aquaculture (area)

Due to the main objective of this research relating to the construction of full-dyke structures for triple rice cropping development in upstream provinces, it was necessary to assess the accuracy of the triple rice cropping area developed by the MODIS land use map in comparison with the statistical data.

Analysis the land use change versus flooding situation in the MD using remote sensing technology

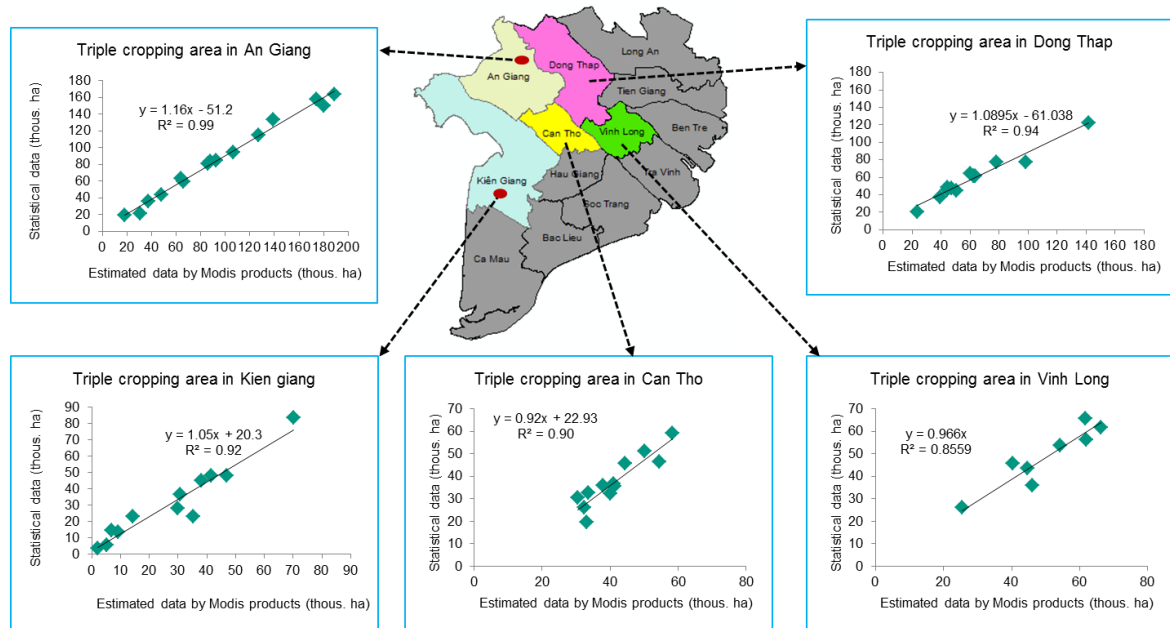


Figure 2.32. Agreement of triple rice cropping area between statistical data and MODIS land use

Figure 2.28 shows the comparison of triple rice cropping area between statistical data and MODIS land use in An Giang, Dong Thap, Kieng Giang, Vinh Long, and Can Tho provinces. The statistical data was also calculated from 2000 to 2016 to assist with the assessment. As a result, the MODIS triple rice area showed a high level of agreement with statistical data, $R^2 = 0.85$ to 0.99 respectively.

2.4.3.2. Compare MODIS land use map interpreted by Duong vs Dr. Sakamoto.

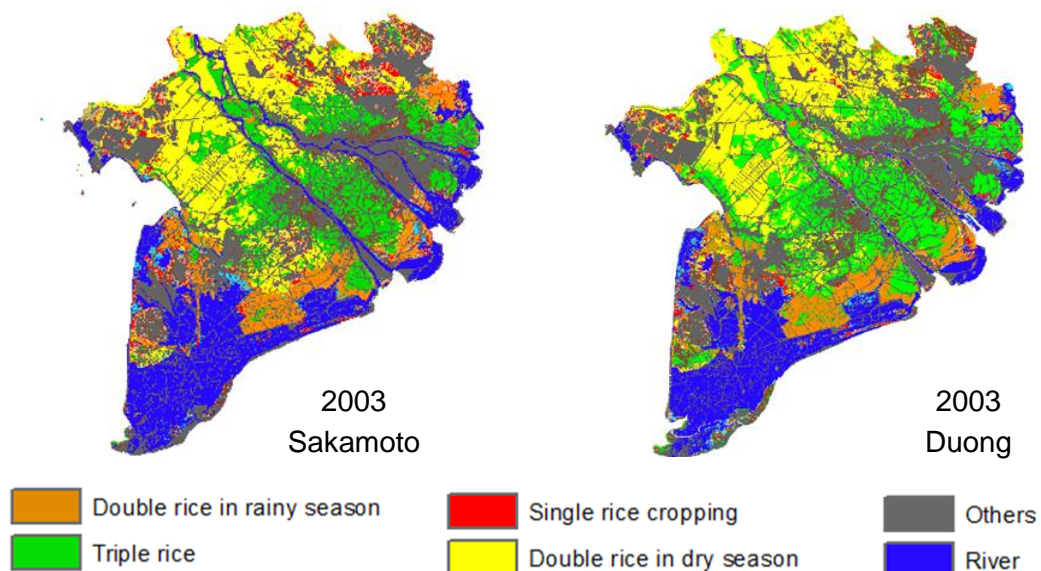


Figure 2.33. Agreement about land use mapping in 2003 between Sakamoto vs Duong

Due to the modification part of noise removal, it is necessary to make a comparison between the product by Sakamoto and the results from the authors to evaluate the appropriateness of the extraction method. Therefore, land use mapping in 2003 were performed to determine accuracy. It can be seen in Figure 2.29, Figure 2.30, and Table 2.11, the new method of noise removal used by the authors yielded quite similar results in comparison with Sakamoto's work and statistical data.

Analysis the land use change versus flooding situation in the MD using remote sensing technology

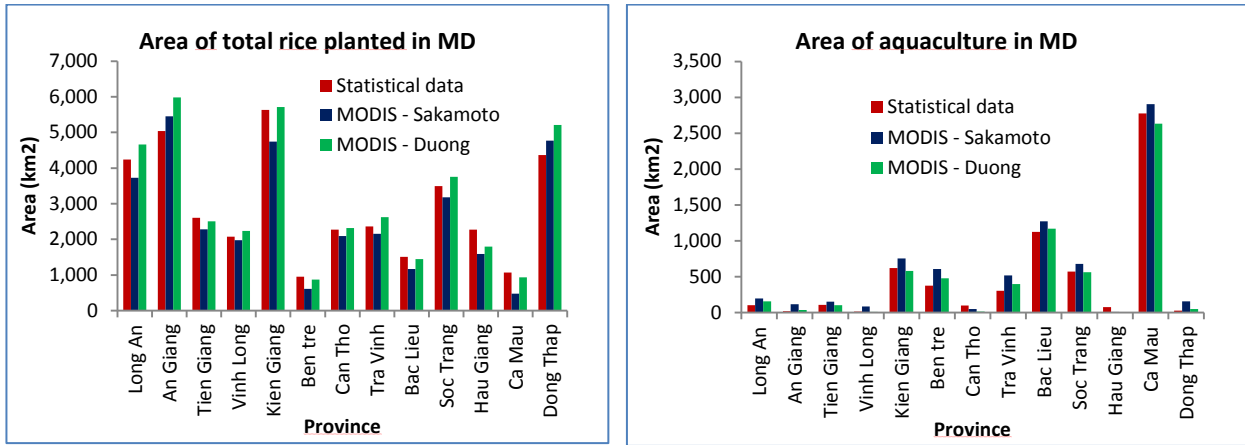


Figure 2.34. Agreement of land use areas in 2003 between statistical data and MODIS as well as Sakamoto and MODIS –Duong

Table 2.11. Agreement of land use areas in 2003 between statistical data and MODIS as well as Sakamoto and MODIS –Duong

Land use \ 2003	Statistical data (km ²)	Sakamoto (km ²)	Duong (km ²)	Relative difference	
				Sakamoto vs statistical data (%)	Duong vs statistical data (%)
Rice (km ²)	37.873	34.202	40.036	10%	5%
Aquaculture (km ²)	6.213	7.499	6.188	17%	0.41%

2.4.3.3. Field trip to An Giang and Dong Thap province

The field trips to the flooded zone in An Giang and Dong Thap province were conducted during flood season in November 2013 and October 2014 to identify the footprints of floods as well as the triple rice cropping area, which were protected against floods by full-dyke construction.

Green: rice ; Yellow: visit points

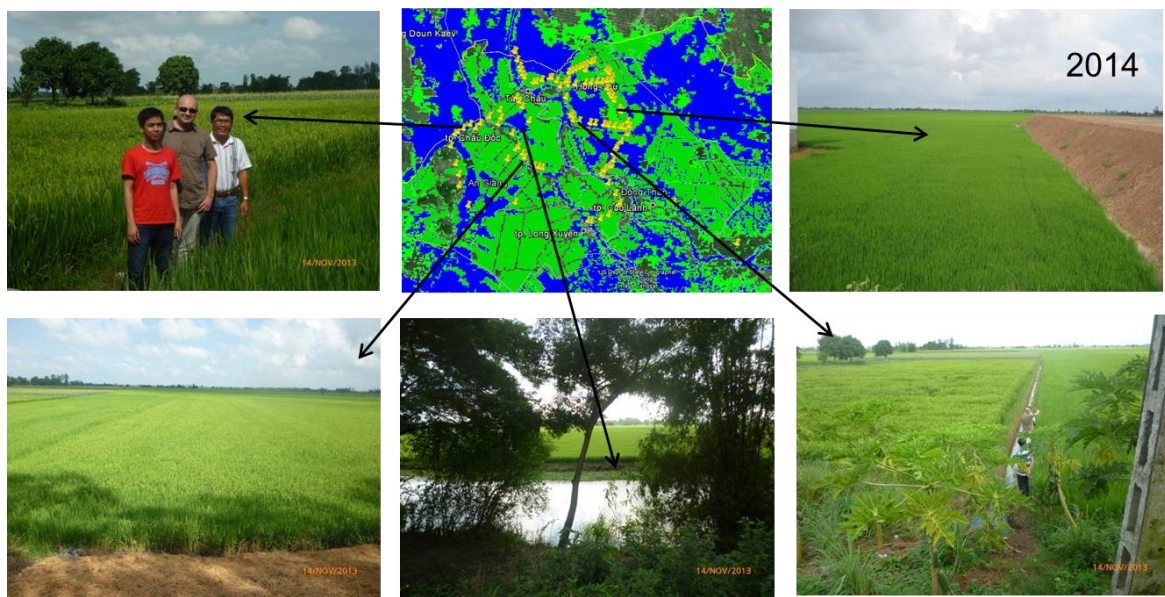


Figure 2.35. Field trip to the MD for ground true assessment

Analysis the land use change versus flooding situation in the MD using remote sensing technology

The pictures were taken in Long Xuyen, Tinh Bien, An Giang provinces as well as Cao Lanh, Tam Nong district, and Dong Thap province. In addition, the ground truth assessment by the confusion method should be applied for the land use map in 2018.

2.4.4. Discussion land use change in MD

MODIS land use maps showed good agreement with statistical data in provincial scale with $R^2 = 0.92$ for the annual total rice planted area and $R^2=0.96$ for the annual aquaculture area. The accuracy of MODIS land use map was acceptable for analyzing the change in land use in the Mekong Delta.

MODIS land use maps have more advantages when compared to statistical data due to its spatial visualization and convenience. Spatial visualization means that an individual can determine the locations for aquaculture and rice cropping cultivated while statistical data only provides an individual with the number. Moreover, it is convenient to get the land use data by using the MODIS product at the end of year while statistical data has to be surveyed and processed much later since it is often published one year later.

By applying remote sensing in land use detection, a significant savings on land use surveying could be realized. An Giang province is located in between the Tien and Hau Rivers; therefore, the full dyke construction for culverting of triple rice cropping in this province will cause a more significant impact on flooding situation as compared to other provinces.

2.4.5. Effect of triple rice cropping to local farmers:

In November 2013 and October 2014, the authors took a field trip to the An Giang and Dong Thap provinces to survey the footprints of floods and triple rice areas. Some conversations with local farmers were also conducted, in which the farmers in Tam Nong district and the Dong Thap province complained about the triple rice cropping pattern.

- The farmers had to work harder. In the past, they only cultivated from January to August, and after that, they lived on fishing during the flood seasons. On the other hands, their children do not want to work in the fields anymore due to the dirt and low income. The younger generation prefers to work in industrial parks. As a result, the older generation lacks the necessary manpower for cultivating the rice.
- Low price of rice that makes the farmers have low income.
- Total yields of triple rice cropping have the same or even lower yields when compared to double rice croppings in the past.
- Higher costs for seeds, fertilizer, and pesticide were experienced due to a lack of flooding and deposit of sediments.
- Soil and water pollution was a negative consequence to the increased use of fertilizers and chemical inputs.
- There are less fish during the flood seasons than before.

Figure 2.32 presents some of the necessary activities for the local farmers in Tam Nong district and in Dong Thap province (Images 2 and 4). Due to the full-dyke measurement (Image 1) the flood water cannot enter the rice fields which leads to the loss of fertile sediments for the fields (Manh, 2015). Consequently, the farmers have to spend more on pesticides (Image 6) and fertilizers (Image 3) which then results in water and soil pollution (Image 5). The quality of the rice decreases, and the net income for the farmers also decreases since they have to work harder.

Analysis the land use change versus flooding situation in the MD using remote sensing technology



Figure 2.36. Activities of farmers for triple rice cropping

However, the topic of triple rice development still is debated among farmers and scientists in several international and national conferences (Van, 2016). According to Tran and Weger (2017), the farmers in An Giang province, most often, oppose having their fields flooded because they prefer to earn additional income from a third rice crop. Nonetheless, the advantages of high dykes should be taken into account, including the flood protection that they provide for public infrastructure and homes.

2.5. Discussion

The construction of dyke measurements for triple rice cropping area in the An Giang and Dong Thap provinces have created more yields in rice productions. However, they have also caused changes in the annual flood distribution in the Mekong Delta. Room for flood water has been decreased during the flooding seasons in An Giang and Dong Thap provinces which has consequences in regards to the hydraulic and social needs within the occupied areas as well as in the downstream areas.

The land use and flooding maps have appropriate accuracy in comparison with statistical data and with radar satellite products. Also, they have shown correspondence between flood level in the Mekong Rivers. Additionally, the MODIS flooding and land use maps were also reconfirmed in terms of their appropriateness via field trips to the Mekong Delta.

A full database of MODIS flood distribution maps, which includes 476 maps, of the MD during flooding seasons and yearly land use maps (18 maps) from 2000 to 2017 were collected and interpreted from MODIS satellite products.

The products of MODIS satellite were valuable and suitable for monitoring flooding and land use changes for this large, flat area of the Mekong Delta. MODIS products will be used for input data within hydraulic modelling in the next chapters. Flood maps shall be used to present the daily water extension, and land use map will assist in identifying full-dyke locations as well as the

Analysis the land use change versus flooding situation in the MD using remote sensing technology

operation of sluice gates in the full-dyke areas, such as in North Vam Nao and in the An Giang province.

Additionally, flood maps from MODIS satellite were used to calibrate for the dyke system data, which were surveyed by the SIWRR.

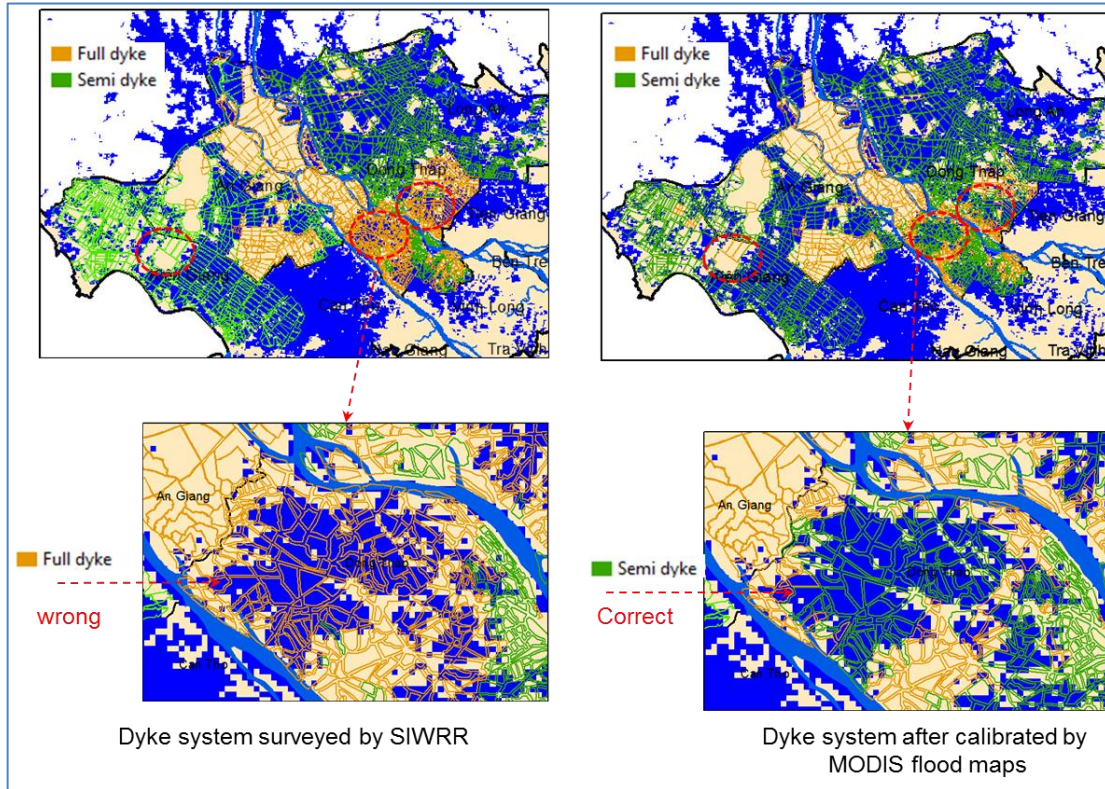


Figure 2.37. Dyke system calibration by MODIS flood maps

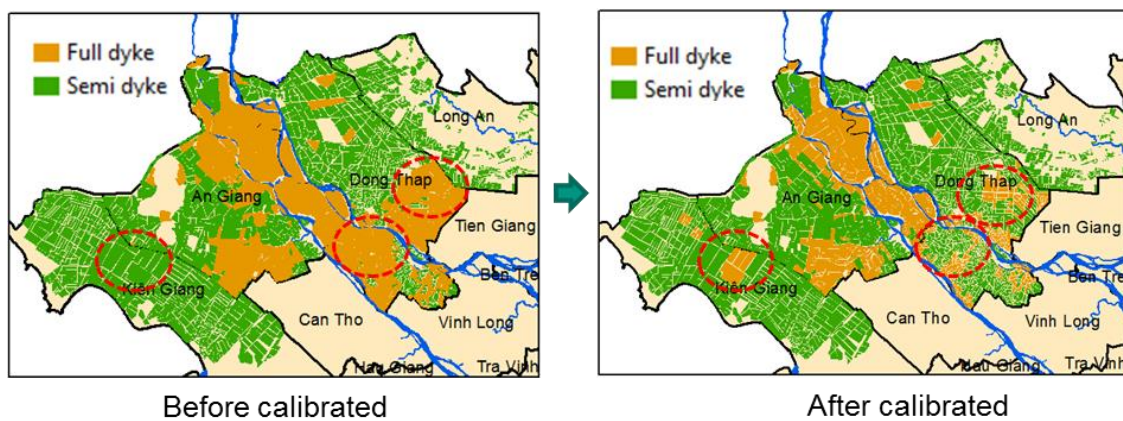


Figure 2.38. Dyke system in the MD after calibration

Figure 2.38 shows some of the mistakes made between semi-dykes and full-dykes in the Chau Phu district, in An Giang province, Lai Vung, Cao Lanh, Lap Vo, and Chau Thanh districts in the Dong Thap province and in Hon Dat district in Kien Giang province.

3. Analysis the impact of land use change versus flooding situation in the MD using numerical modelling

According to the approach of the PhD thesis presented in Figure 1.8, the daily water mask and observed hydrologic conditions shall be the input data for the numerical model to analyze the impact of dyke measurements for land use on the flooding situation in the MD. In this section, observed hydrologic data and numerical modelling were applied to analyze the change of flooding areas in the MD over the last decade due to the construction of dyke measurements upstream of the MD.

The flood area in the Mekong Delta is defined by a combination of four influences, which are (i) the flood inflow mainly induced by the flood flow on the Mekong River and overland flow, (ii) flood in the short-term due to high rainfall intensity, (iii) the tidal floods primarily during spring tide and with specific storm conditions, and (iv) flooding due to the development of human activities. Flood occurrences are triggered by a combination of several of these factors (Kuenzer et al., 2013).

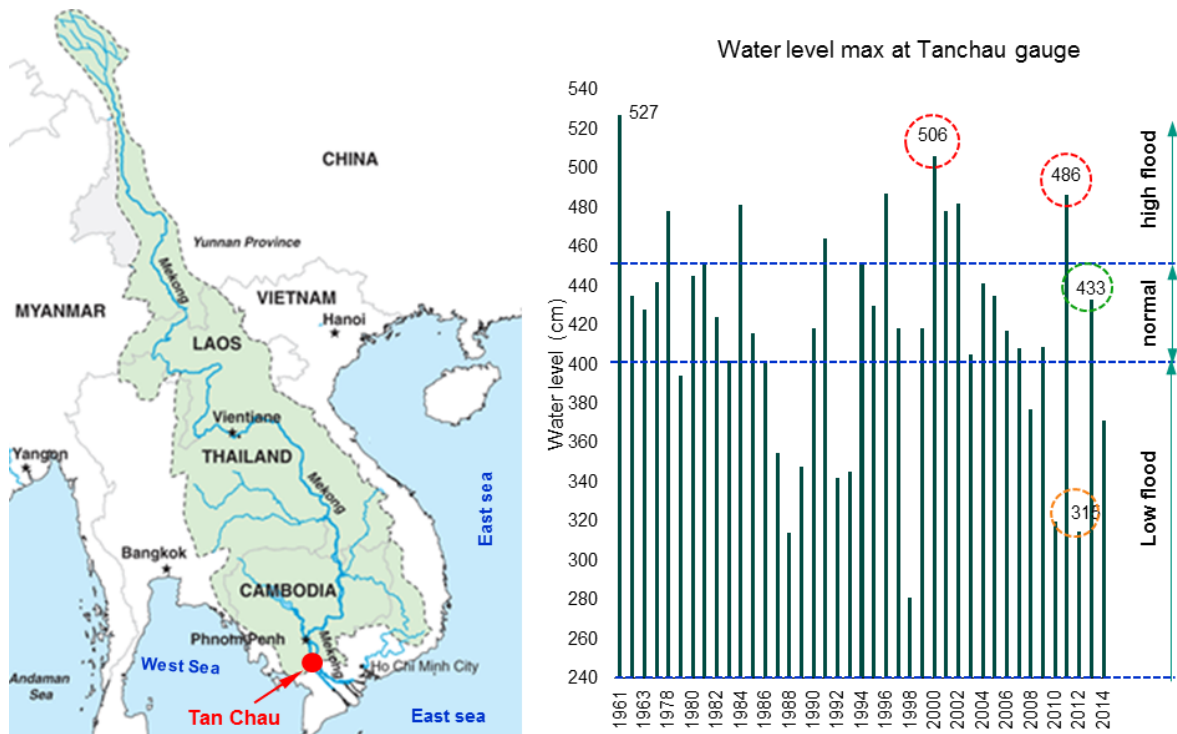


Figure 3.1. Mekong river basin (MRC, 2013) and maximum water level at Tan Chau

Flood magnitude in the Mekong Delta was classified by the water levels at the Tan Chau location, such that (i) when the water level was below 4 m, it was defined as a small flood; (ii) when the water level was between 4.0 m to 4.5 m, it was categorized as a normal flood; and (iii) when the water level was above 4.5m, it was considered as a high flood.

Analysis the impact of land use change versus flooding situation in the MD using numerical modelling

Figure 3.1 shows the observed water levels at the Tan Chau gauge from 1961–2014. Based on the data collection and the probability of flood events shown in Table 3.1, the four floods with $P=5\%$, $P=10\%$, $P = 40\%$ and $P = 97\%$ were selected for analysis as different typical types of floods in order to evaluate comprehensively the impacts of dyke measurement for land use on flooding situation in the MD.

Table 3.1. Probability of flood event in Mekong Delta

No.	P(%)	Z cm	Return period (year)	Study year
1	0.01	634.12	10000	
2	0.10	597.25	1000	
3	0.20	584.83	500	
4	0.33	575.35	303	
5	0.50	567.12	200	
6	1.00	552.51	100	
7	1.50	543.36	67	
8	2.00	536.55	50	
9	3.00	526.43	33	
10	5.00	512.63	20	~ Flood 2000
11	10.00	491.37	10	~ Flood 2011
12	20.00	465.65	5	
13	25.00	455.88	4	
14	30.00	447.12	3.3	
15	40.00	431.30	2.5	~ Flood 2013
16	50.00	416.54	2	
17	60.00	401.79	1.7	
18	70.00	385.99	1.4	
19	75.00	377.24	1.3	
20	80.00	367.50	1.2	
21	85.00	356.15	1.17	
22	90.00	341.87	1.11	
23	95.00	320.72	1.05	
24	97.00	307.00	1.03	~ Flood 2012
25	99.00	281.10	1.01	

3.1. Identification the factors of hydraulic change in the Mekong delta

According to the observed data from the Mekong River Commission (2015), there were two historic floods in the last decade, which occurred in 2000 and 2011, with a maximum water level at the Tan Chau gauge of 5.06 m and 4.86 m, respectively. There were changes in the water level along the main rivers as well as a change in discharge during these years. How did they change, and what are the reasons for these changes? These questions shall be clarified in the next section of this paper.

Analysis the impact of land use change versus flooding situation in the MD using numerical modelling

3.1.1. Water level change

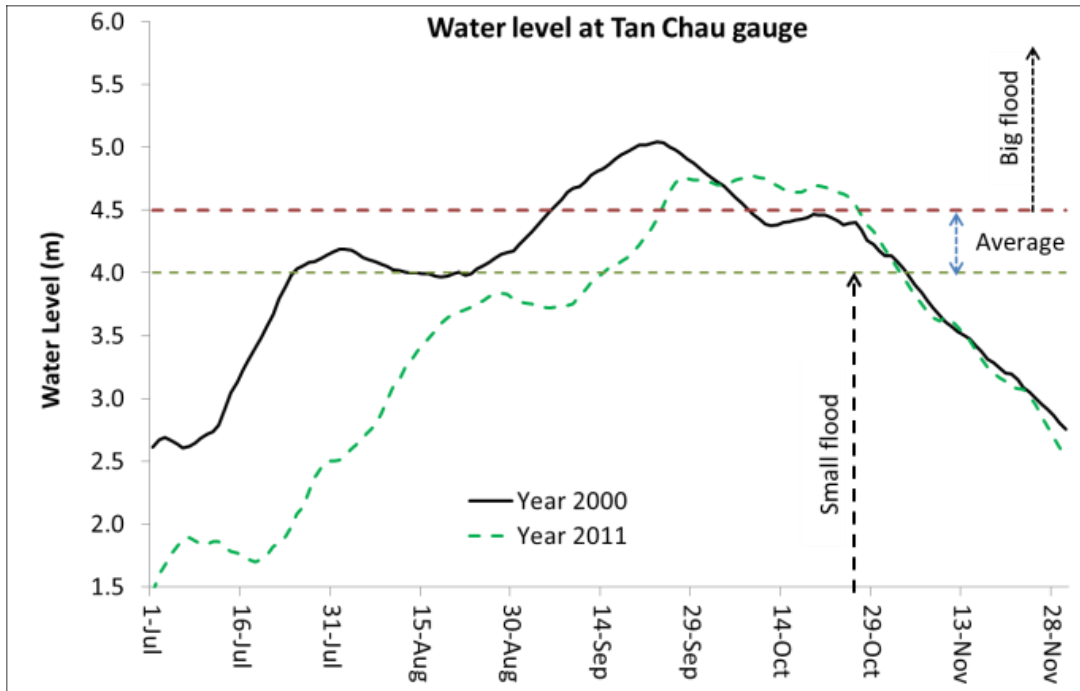


Figure 3.2. Flood hydrograph in 2000 vs 2011 at the Tan Chau gauge.

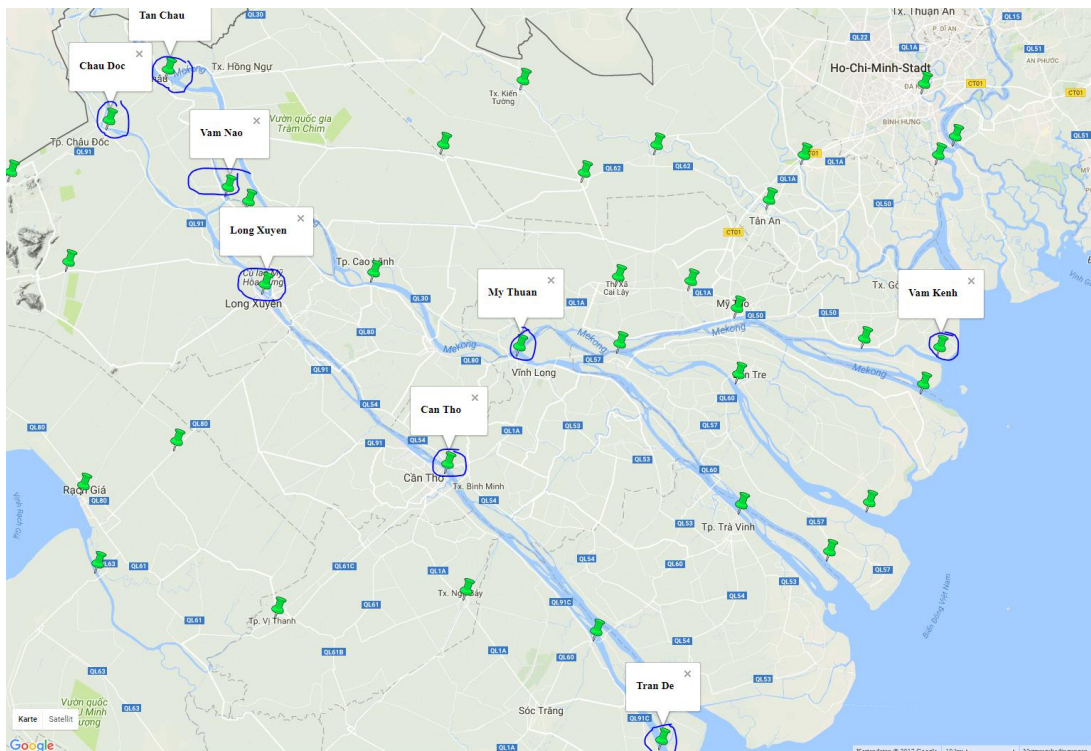


Figure 3.3. Studied locations on Mekong and Bassac river

(On Mekong river: Tan Chau, Vam Nao, Cao Lanh, My Thuan, Vam Kenh; On Bassac River: Chau Doc, Long Xuyen, Can Tho and Tran De)

Along the Mekong River, the flood peaked at the Tan Chau gauge in 2011 at 20 cm, which was lower as compared with the water level in 2000. However, the water level at the Vam Kenh gauge was 11 cm higher. Similarly, on the Bassac River, the flood peak at the Chau Doc gauge in 2011 at 63 cm lower than the water level in 2000, but the water level at the Tran De gauge was 64 cm higher, which is illustrated in Tables 3.2 and 3.3

Analysis the impact of land use change versus flooding situation in the MD using numerical modelling

Table 3.2. Water level flood 2000 (WL00) and flood 2011 (WL11) on the Mekong River

Gauge	Tan chau (cm)	Vam nao (cm)	Cao Lanh (cm)	My Thuan (cm)	Vam Kenh (cm)
WL00 (a)	506	373	267	180	170
WL11 (b)	486	360	267	203	181
(b) – (a)	-20	-13	0	+23	+11

Table 3.3. Water level of flood 2000 (WL00) and flood 2011 (WL11) on the Bassac River

Gauge	Chau Doc (cm)	Longxuyen (cm)	Can Tho (cm)	Tran De (cm)
WL00 (a)	490	263	179	170
WL11 (b)	427	281	215	234
(b) – (a)	-63	+18	+36	+64

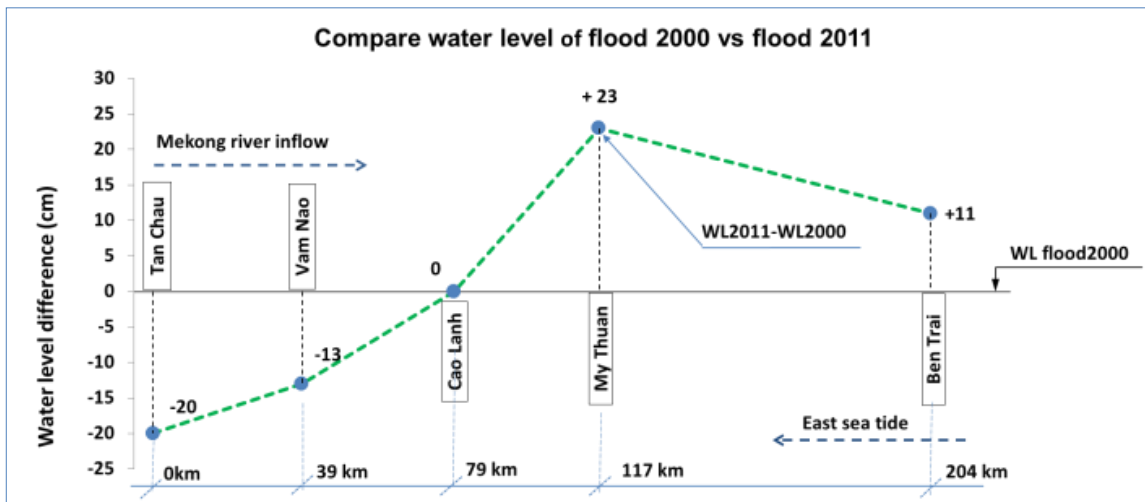


Figure 3.4. Difference in water levels on the Mekong River

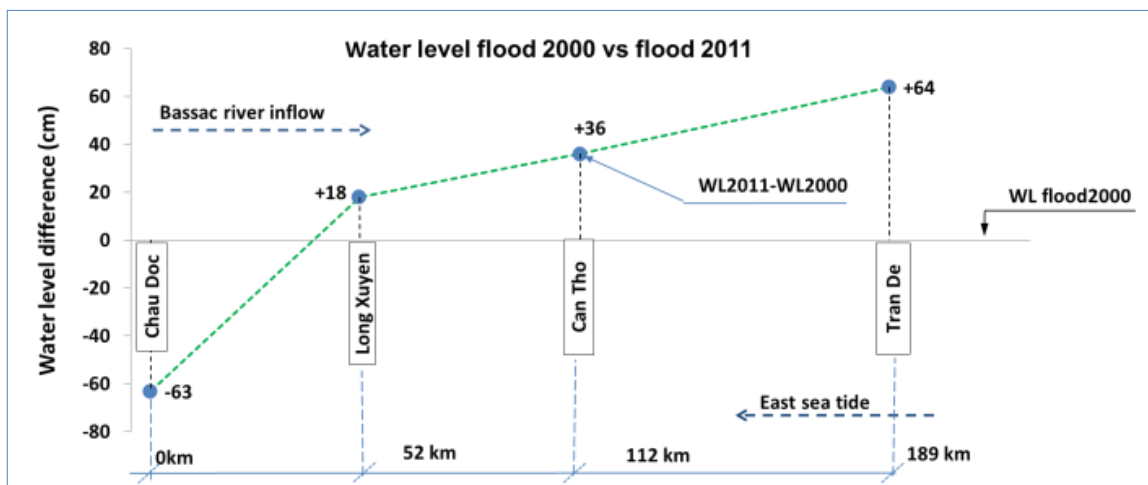


Figure 3.5. Difference in water levels on the Bassac River

The floodplain areas in upstream provinces decreased in combination with the water levels rising at the river mouths (Dang et al., 2017) and land subsidence effects (Minderhoud, Erkens, Pham, Bui, Erban, Kooi, & Stouthamer, 2017). The water levels in the middle regions of the MD

Analysis the impact of land use change versus flooding situation in the MD using numerical modelling

increased. For instance, the water levels at Cantho and My Thuan in 2011 were +23 cm and +36 cm higher than the water levels in 2000, which is shown in Figures 3.4 and 3.5.

3.1.2. Flood inflow rates change

According to Van (2013), flood inflows to the Mekong Delta occur through four components, which are the Mekong River flow, the Bassac River flow, the border overflow to the Plain of Reeds (PoR); and the border overflow to the Long Xuyen quadrangle (LXQ). The percentage of flood flow distribution focused mostly on the two major rivers, which are the Mekong and Bassac.

Due to the development of the dyke system in the original flood plains in Cambodia, flood overflow from the Great Mekong River into PoR and LXQ areas in 2011 decreased significantly. In contrast, flood flow distributed more through the main rivers, such as the Mekong and the Bassac, which is illustrated in Figure 3.6.

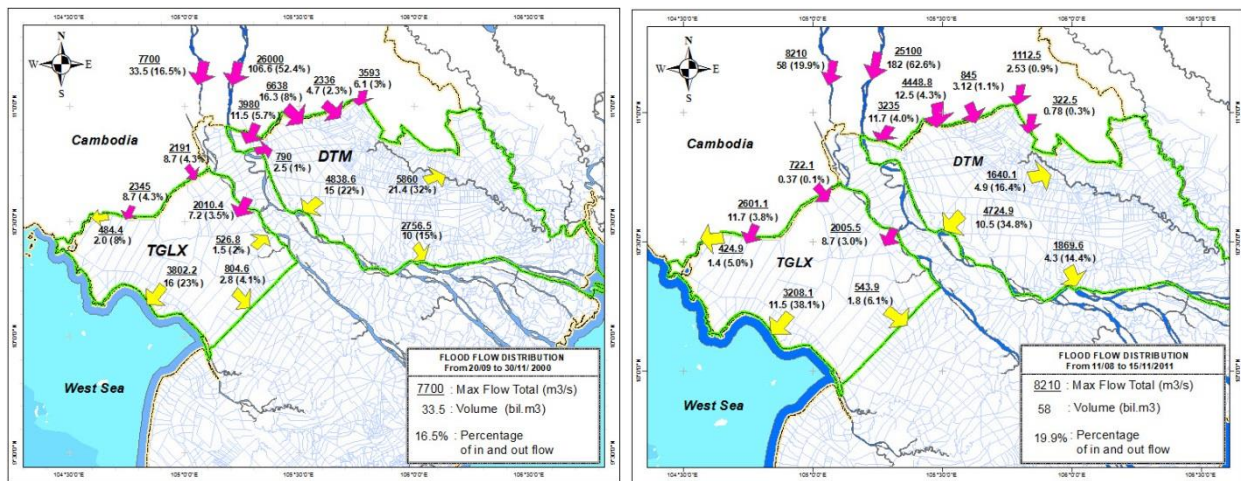


Figure 3.6. Flood flow distribution to the Mekong Delta in 2000 vs the flood in 2011

Table 3.4. Observed flood inflow to the Mekong Delta.

Location	Flood 2000		Flood 2011		Comparison (4) - (2)	Change
	bil. m3	%	bil. m3	%		
Tan Chau	234.5	57%	182.0	63%	+6 %	increase
Chau Doc	70.5	17%	58.0	20%	+3 %	increase
PoR	69	17%	30.6	11%	-6 %	decrease
LXQ	28.3	7%	12.1	4%	-3 %	decrease

Table 3.4 shows the change of flow distribution rate, particularly the flow rate through the Mekong River, which was measured at the Tan Chau gauge, and the Bassac river, which was measured at the Chau Doc gauge. In 2011, the flow increased +6% and +3% although the flood peak in 2011 was lower than the flood in 2000. In contrast, the inflow rate to the POR and LXQ decreased 6%, and TGLX decreased 3% further in 2011.

Discussion:

The rise of the water level in Can Tho and My Thuan combined with the decrease of discharge between the flood in 2000 and in 2011 was a combination of many factors, such as a rise in sea level, land subsidence, flood inflow rates, and dyke measurement. Therefore, to identify and quantify only the impact of the dyke measurement on the rise of water level, numerical modelling should be applied to identify the impact.

3.2. Analysis the impact of land use change based on numerical modelling

3.2.1. Hydraulic model MIKE11 description

To be compatible with the work from the Vietnamese institutions, the numerical 1D model MIKE 11 model developed by the Danish Hydraulic Institute was selected since it has the same features and is more convenient for the collection of data as well as allowing for the exchange of knowledge and experience with Vietnamese colleagues, who have also applied the software to serve for their studies of the Mekong floodplains (Dung et al., 2011; Dang et al., 2017; Tran & Weger, 2017; Triet et al., 2017).

MIKE 11, a one-dimensional hydrodynamic module (HD), was applied to simulate the Mekong Delta, one of the largest estuaries in the world with a highly complex hydraulic system (Dung et al., 2011). MIKE 11 uses an implicit, finite difference scheme for the computation of unsteady flows in rivers and estuaries, the model MIKE 11 applies the dynamic wave description and solves the vertically integrated equations of conservation of continuity and momentum using the “Saint Venant” equations, (DHI, 2004). The governing equations are:

$$\frac{\partial Q}{\partial x} + \frac{\partial A}{\partial t} = q \quad [3-1]$$

$$\frac{\partial Q}{\partial t} + \frac{\partial \left(\alpha \frac{Q^2}{A} \right)}{\partial x} + gA \frac{\partial h}{\partial x} + \frac{gQ|Q|}{C^2AR} = q \quad [3-2]$$

Where, Q= discharge; A= flow area; q= lateral inflow; h= stage above datum; C= Chezy resistance coefficient; R= hydraulic or resistance radius; and α = momentum distribution coefficient.

3.2.1.1. Building geometry network for Mekong delta

The Mekong River network in MIKE 11 is the property of Vietnamese Institutes; the researchers in those institutes had to spend a lot of time and efforts to build it for their own networks. That is why, it is impossible to share and/or provide it for a third party for any purpose. Due to that difficult condition, the author had to build a new Mekong River network after collecting the available shapefiles and cross sections, DEM, and hydrology data from relevant institutes such as IWER, SIWRP and SIWRR. Building the network, calibration, and validation work took two years to complete from October 2013 to October 2015.

Floodplain is an important characteristic to demonstrate the flooding situation in the MD. Hence, MIKE11 model has the capability to account in a realistic way for floodplain storage during flood events. There are two approaches for simulation of the floodplain in MIKE 11 for the Mekong Delta that the Vietnamese institutes often apply.

Approach 1: According to N.V. Dung (2011), most of the compartments represent a closed system surrounded by dykes and channels, so flood cells are modelled by artificial branches with low and wide cross sections linked to the channel by control structures. Here, weirs were used to represent dykes and dyke overflow, and sluice gates were used whenever information on existing sluice gates was available. Figure 3.11 illustrates this approach, which was initiated and generally applied by the Southern Institute of Water Resources Research (SIWRR) in Vietnam.

Analysis the impact of land use change versus flooding situation in the MD using numerical modelling

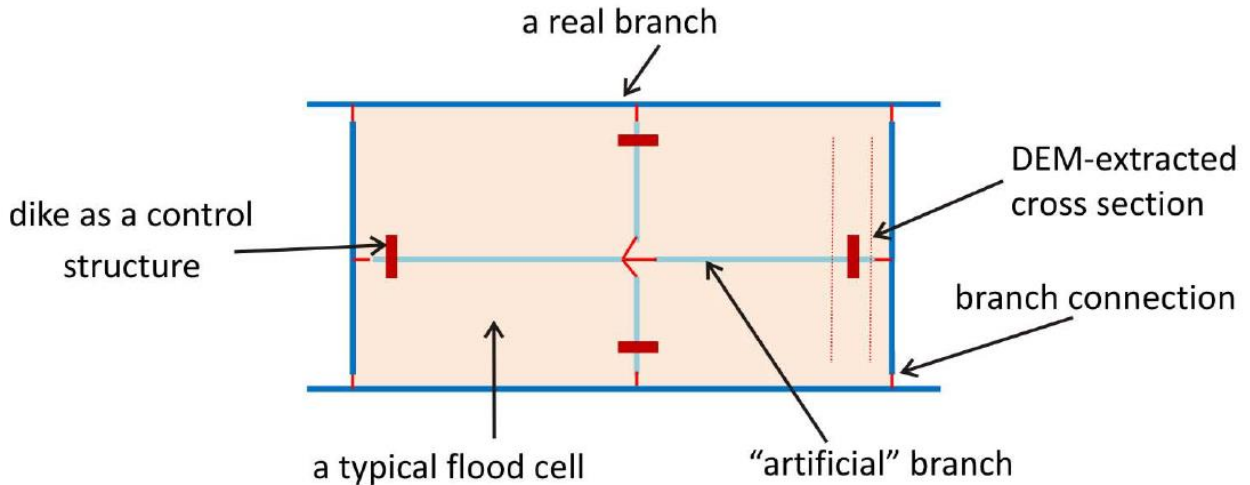


Figure 3.7. Typical floodplain description compartment (Approach 1)

(Source: N.V. Dung et al., 2011)

Approach 2: According to DHI (2004), the link-channel geometry comprises the definition of a longitudinal geometry of the embankment along the river typically.

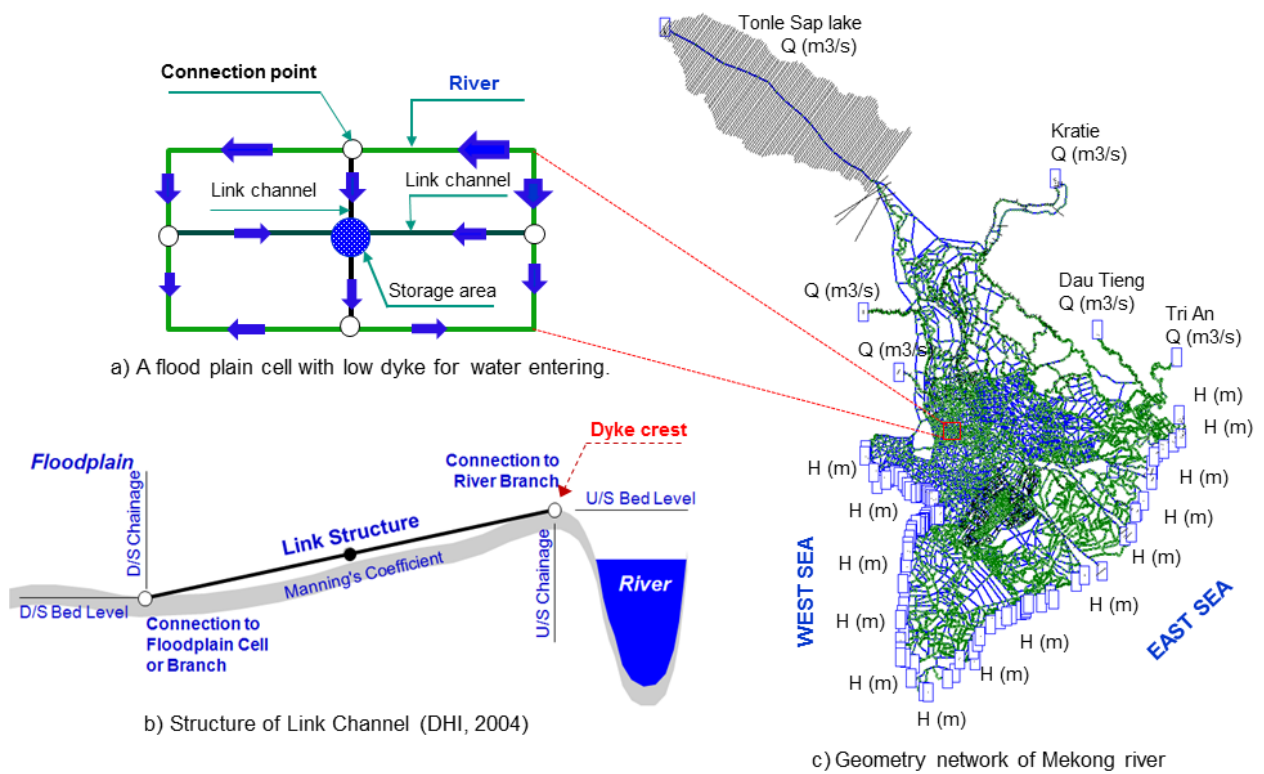


Figure 3.8. Typical floodplain compartment (Approach 2)

(Source: Duong et al., 2016)

The geometry is defined by the following parameters:

- Bed Level US: Upstream bed level of the link channel
- Bed Level DS: Downstream bed level of the link channel

Analysis the impact of land use change versus flooding situation in the MD using numerical modelling

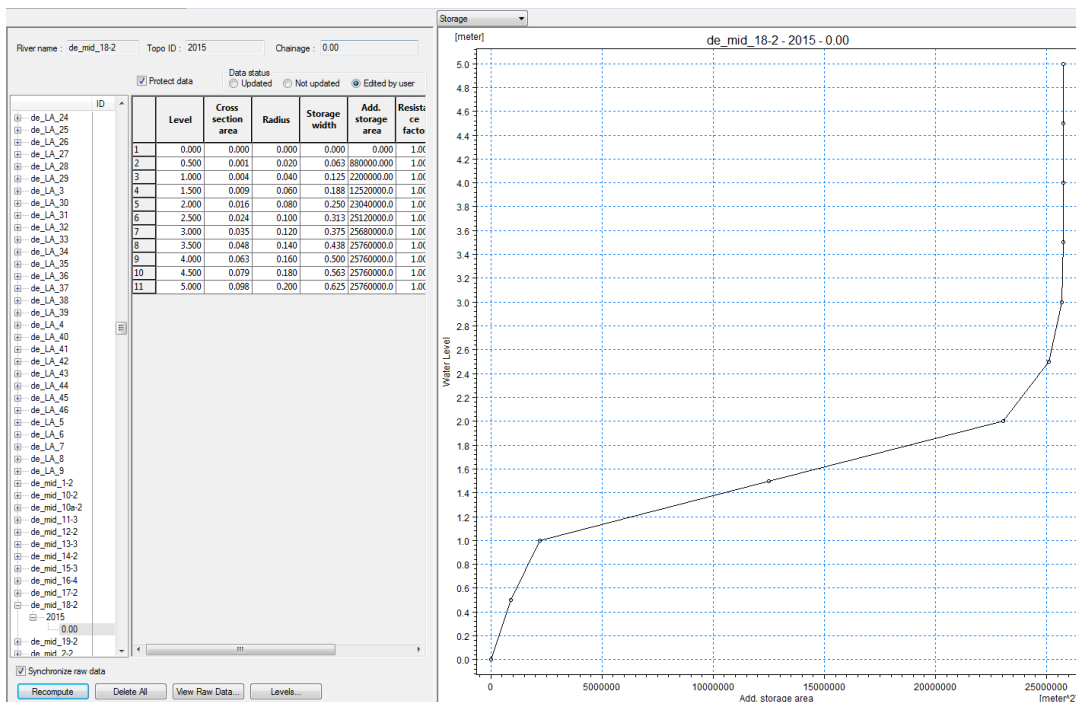
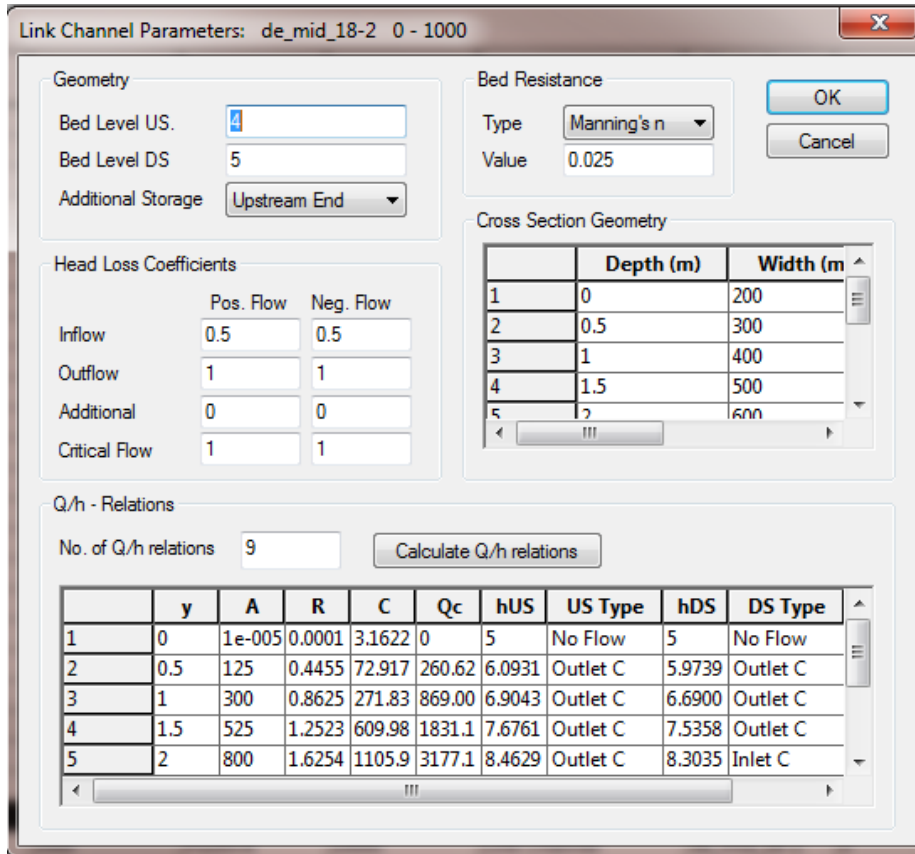


Figure 3.9. Detailed description of additional storage of link channel in MIKE11

Additional Storage: Link channels do not contain cross sections and do not contribute to the storage capacity at nodal points where the link connects to a main branch. The additional storage parameter can be used to avoid zero storage at nodal points to which only link channels and no regular channels are connected. The additional storage combo-box defines whether additional storage is to be added at the upstream, downstream, or both ends of the link channel. The actual storage is specified in the additional flooded area column of the processed data in a cross section

Analysis the impact of land use change versus flooding situation in the MD using numerical modelling

defined at the same location as the link channel. This approach is generally applied by the IWER, SIWRP, and TLU in Vietnam.

Although both approaches have good results after calibration, Approach 1 requires more work for preparation of the input data and more time for simulation (around 4-5 hours) due to the operation of numerous weirs and artificial branches for the flood plains. As a result, it requests more storage capacity for computation (around 2.1 GB /scenario). After carefully consideration, the author decided to follow Approach 2 to simulate the flood simulation for this study.

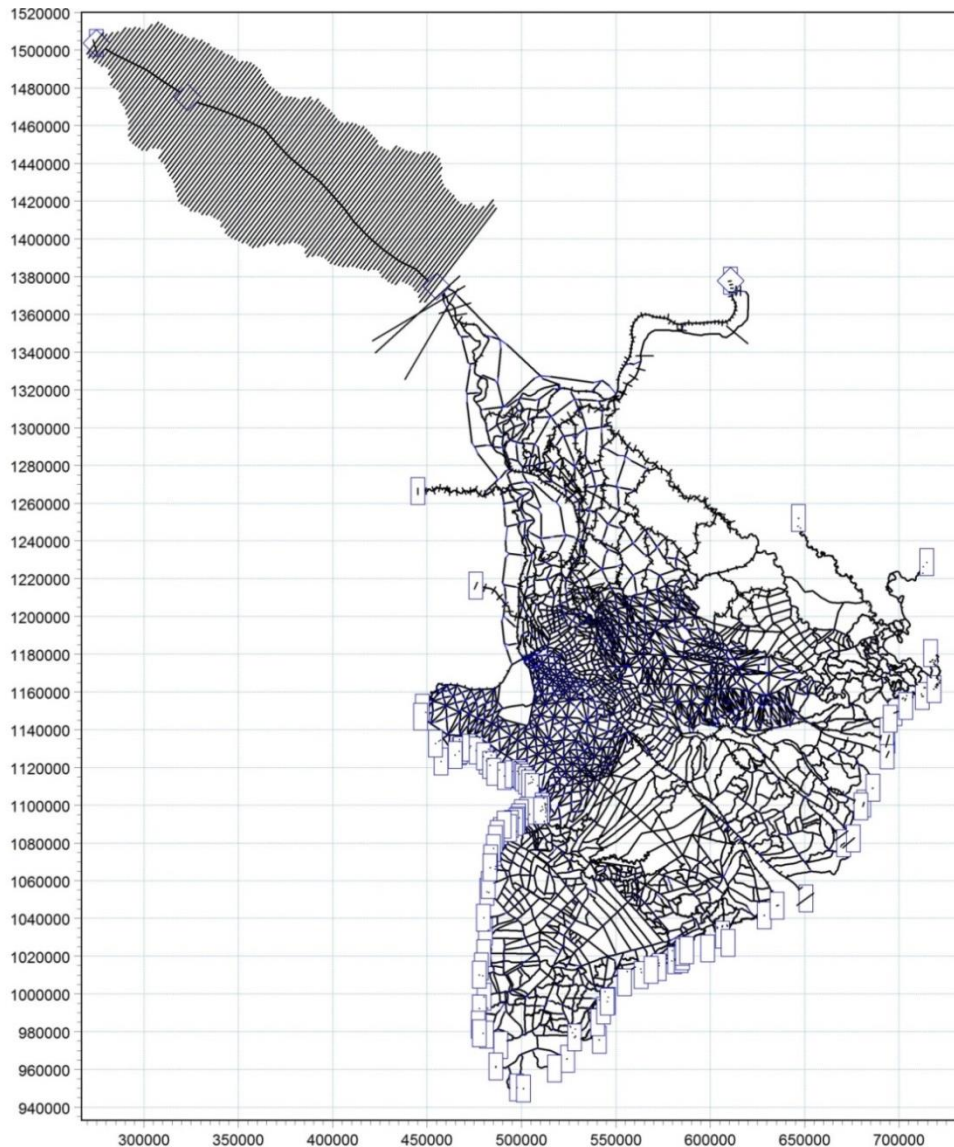


Figure 3.10. Mekong River network in MIKE 11

Figure 3.14 and Table 3.6 show the geometry and detailed elements of the Mekong River network, the scope of simulation includes the territories of Cambodia and Vietnam from Kratie and Tonle Sap Lake to the estuaries, which can be seen in Figure 3.10. The model consists of 35077 points, 2732 branches, 335 sub-basins for rainfall, and 419 floodplains.

Upstream boundaries included Kratie, Tonlesap Lake, Dau Tieng and Tri An reservoirs, and some small rivers in Cambodia. Downstream boundaries include all estuaries and coastal canals from the East Sea and West Sea from Vung Tau to Ha Tien.

Analysis the impact of land use change versus flooding situation in the MD using numerical modelling

Table 3.5. Description of the MIKE 11 for Mekong River network (Source: Duong, 2016)

Description	Quantity
Points	35077
Branches	2732
Total length of rivers and canals	~26.224 km
Link channels	1561
Control structures	09
NAM model sub-basin	335
Upstream boundary	7
Downstream boundary	92
Floodplain	419

The time for simulation of the Mekong River network takes around 50 minutes to simulate a flood period of six months (from 1st July to 31st December). Output results are normally 655 MB / scenario.

3.2.1.2. Calibration validation works

Measured flow parameters are necessary to calibrate an HN-Model. Calibration of models for flowing waters is done by comparing calculated and measured water surface levels and corresponding model adaptation generally by modification of surface roughness. Measured water levels, including those spreading laterally from the river axis, are needed to calibrate 1D-model, especially in areas with complex hydraulic conditions.

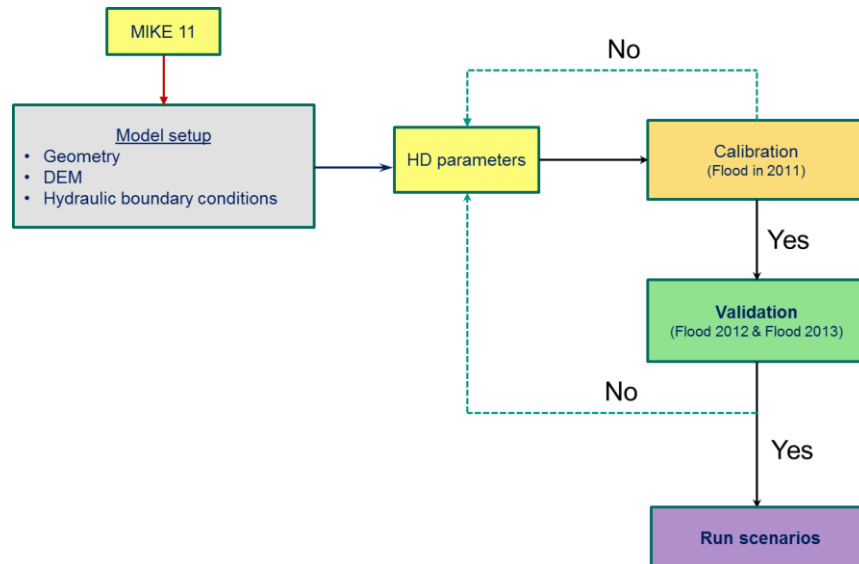


Figure 3.11: Chart for hydraulic model calibration and validation

The calibration of the channel/floodplain roughness coefficients for the MIKE 11 model are used to compensate the uncertainty of river cross-sectional geometries, river morphology, bed elevation approximation, and inflow boundary conditions. A trial and error method is used to adjust the floodplain roughness to best fit the observed stage and discharge measurements at multiple measured sites. Figure 3.16 shows the process for calibration and validation work for the numerical model MIKE11.

Analysis the impact of land use change versus flooding situation in the MD using numerical modelling

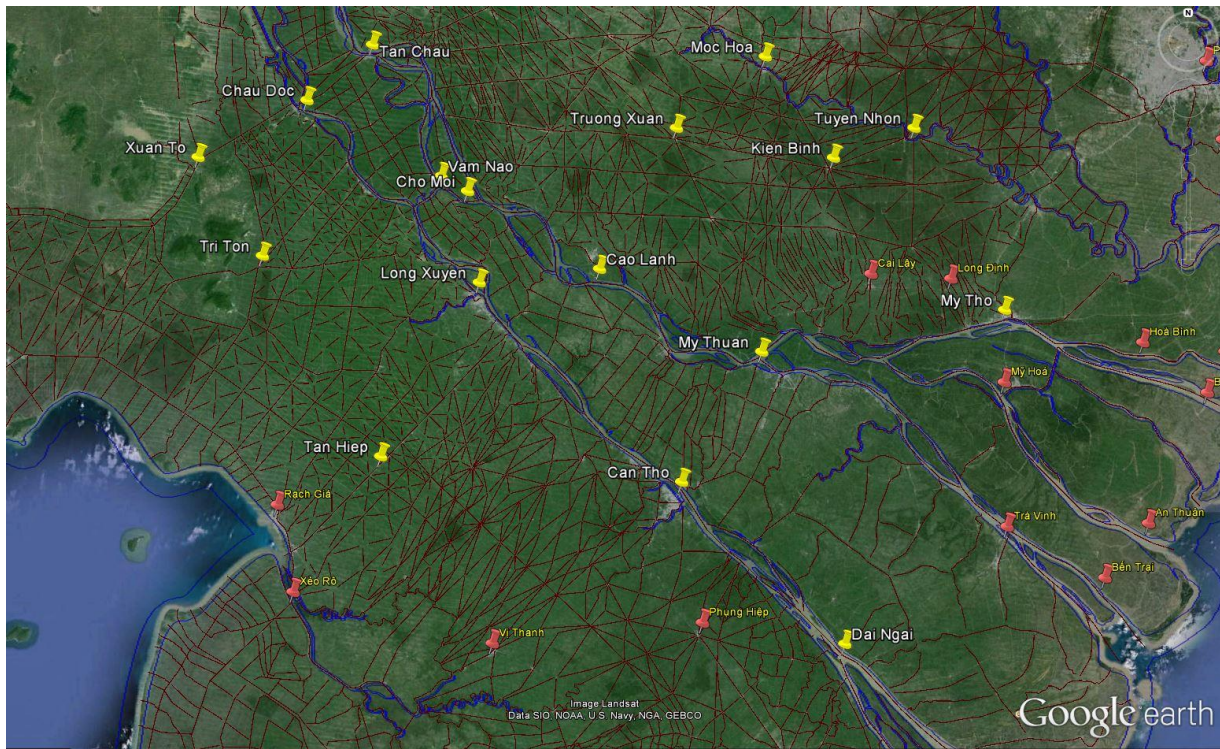


Figure 3.12. Hydraulic gauges in Mekong Delta

Figure 3.17 shows the locations of hydraulic gauges on the main rivers and inland canals. Depending on the collected data of water level and discharges, the MIKE 11 was calibrated and validated according to the following gauges:

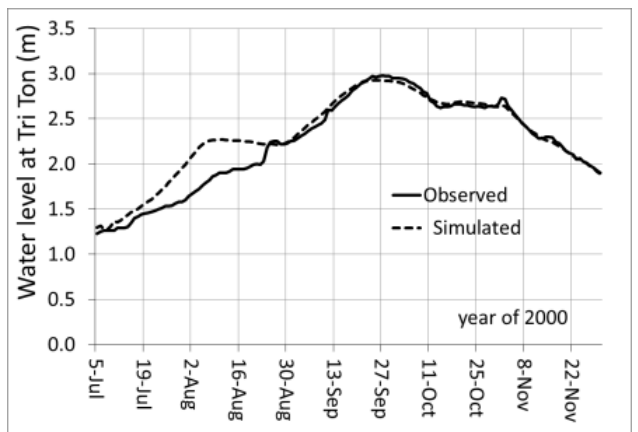
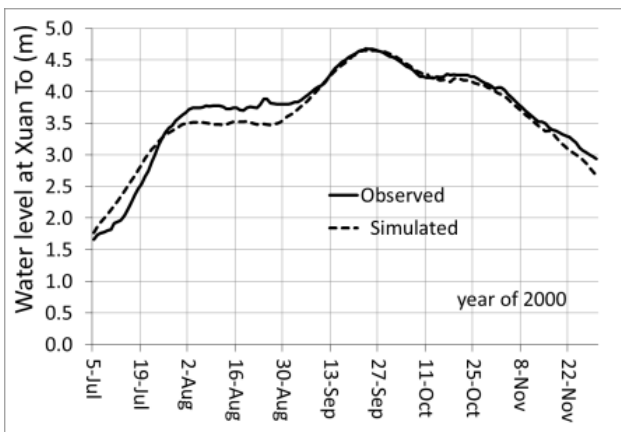
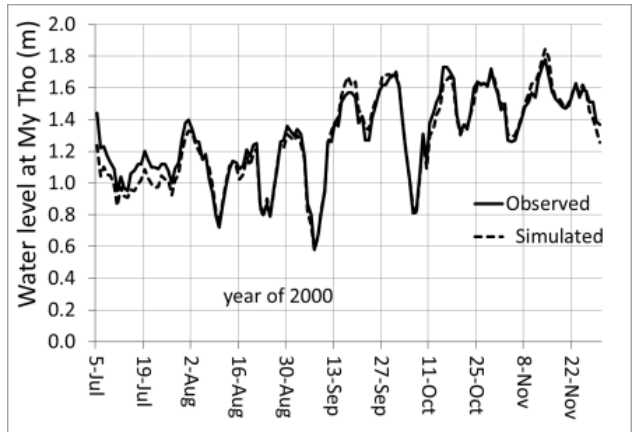
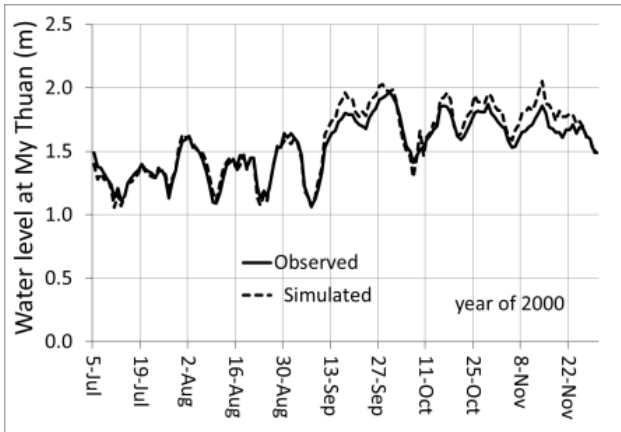
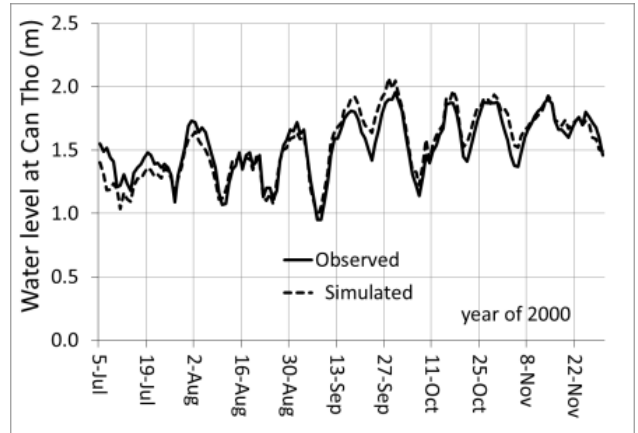
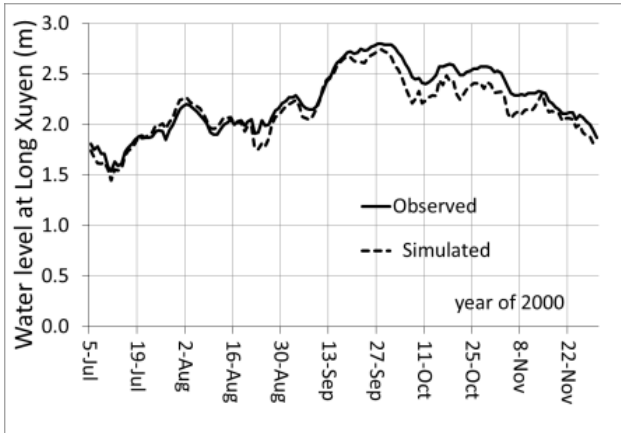
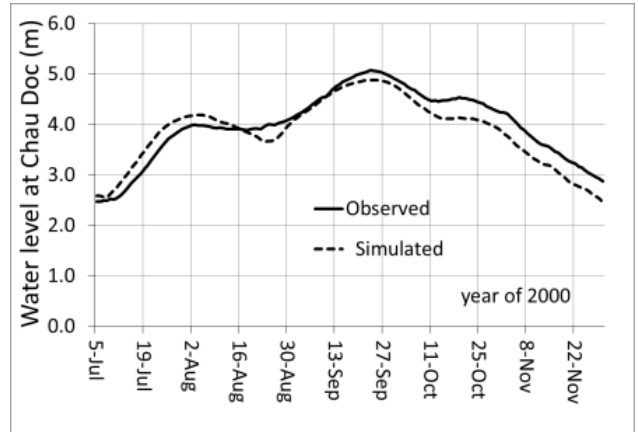
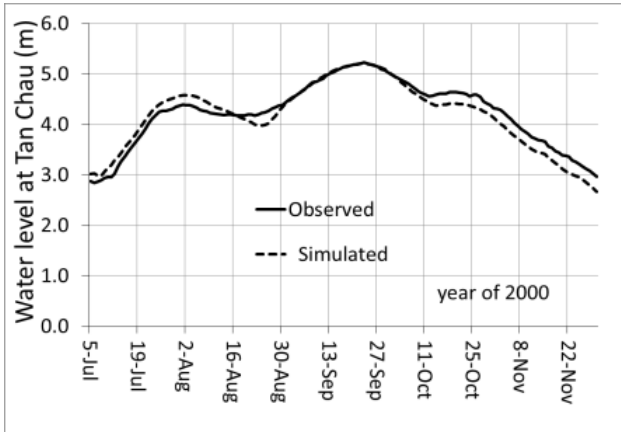
- On Mekong Rivers: Tan Chau (water level and discharge), Vam Nao (water level), Cao Lanh (water level), My Thuan (water level and discharge), and My Tho (water level).
- On Bassac Rivers: Chau Doc (water level and discharge), Long Xuyen (water level), Can Tho (water level and discharge), and Dai Ngai (water level)
- In the Plain of Reeds (PoR): only available data of water level for calibration and validation occurred at the gauges of Trung Xuan, Moc Hoa, Kien Binh, and Tuyen Nhon
- In the Long Xuyen Quadrangle (LXQ): only available data of water level for calibration and validation occurred at the inland gauges of Xuan To, Tri To, and Tan Hiep

The hydraulic model MIKE 11 was calibrated for water levels and discharge with the high floods in 2000 and 2011 by adjusting the hydraulic roughness coefficients (Manning's n). The ranges of hydraulic roughness were 0.016 – 0.028 for the main rivers, 0.022 – 0.027 for the branches, and 0.033 – 0.035 for the floodplains (Van, 2009). Then, the model was validated for accuracy for medium floods (2013) and small floods (2012).

The results of calibration and validation works are shown below in Figures 3.18 to 3.21. In general, the calibration and validation worked so that the MIKE 11 showed acceptable results on the main rivers. However, at the inland gauges in PoR and LXQ, the results only had a high level of accuracy with high floods in 2000 and 2011 whereas the accuracy decreased for validation with the medium flood in 2013 and the low flood in 2012 due to the impact of the riverbed roughness.

Analysis the impact of land use change versus flooding situation in the MD using numerical modelling

a) Calibration for high flood in 2000



Analysis the impact of land use change versus flooding situation in the MD using numerical modelling

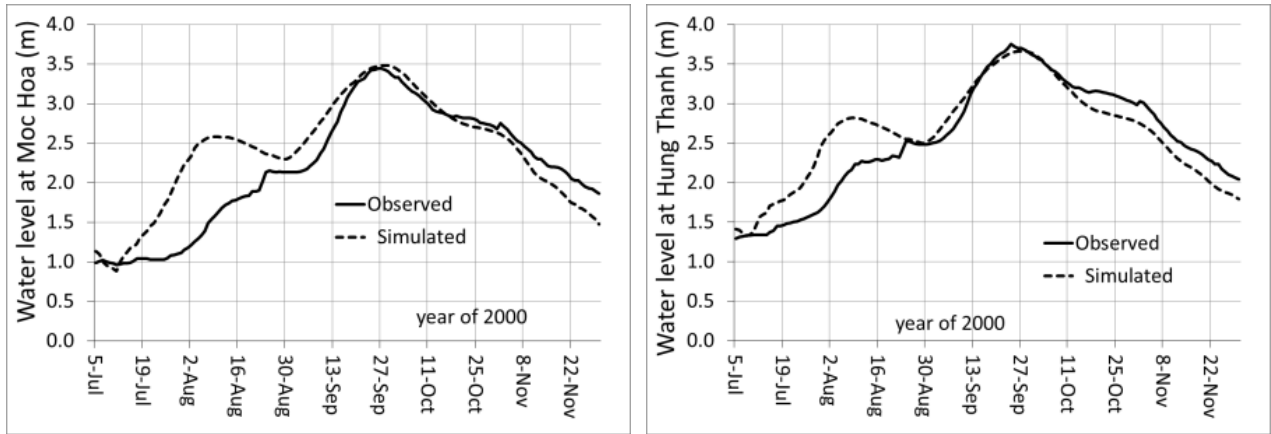
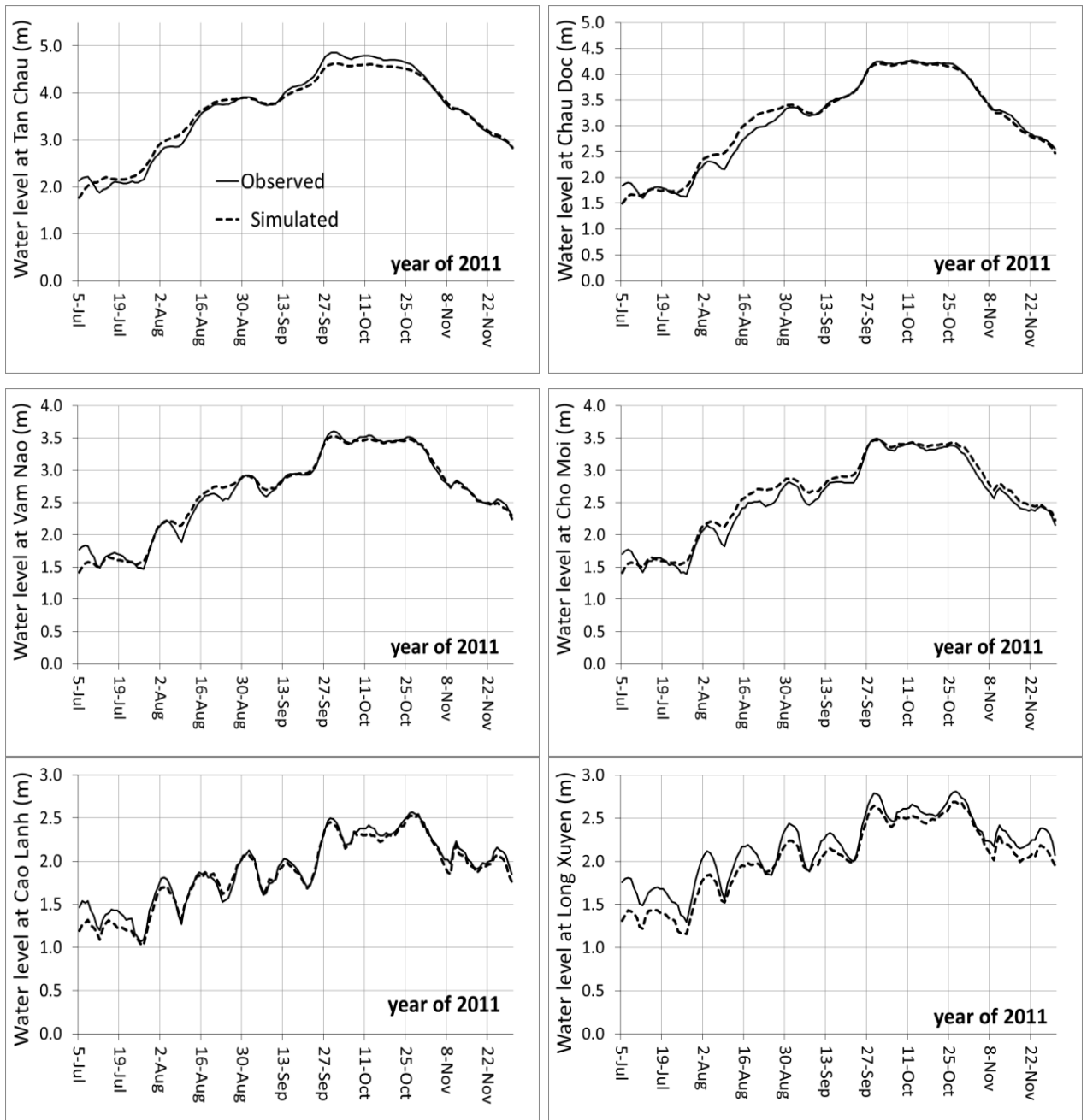


Figure 3.13. Model calibration of water level with high flood in 2000

b) Calibration for high flood in 2011



Analysis the impact of land use change versus flooding situation in the MD using numerical modelling

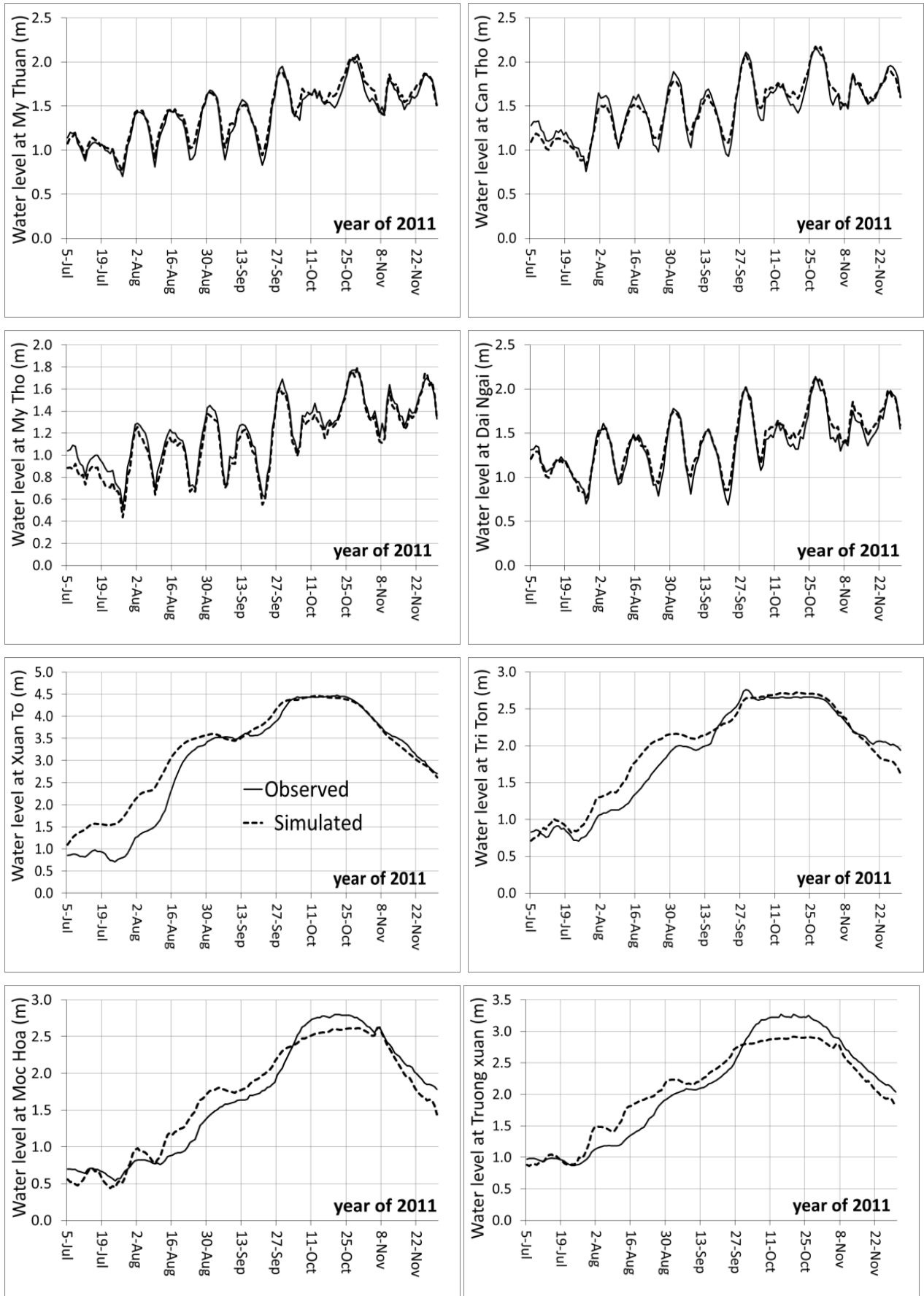
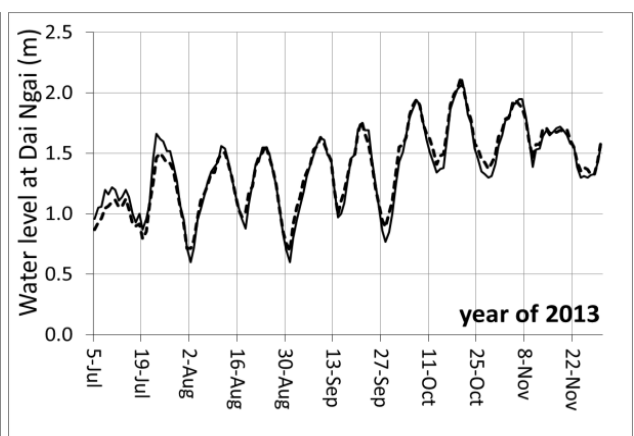
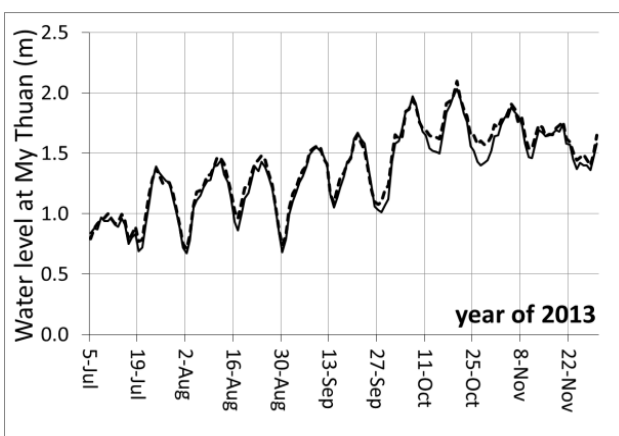
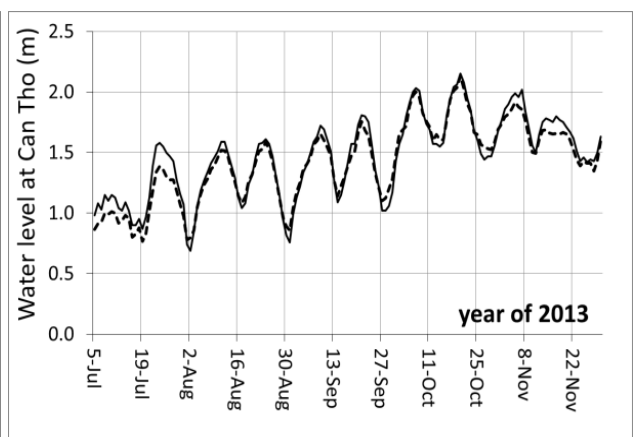
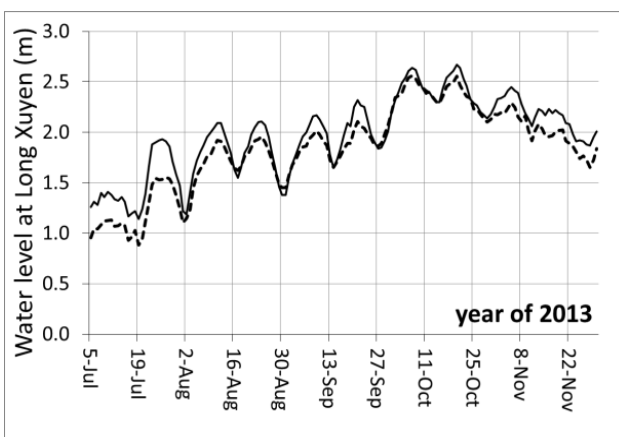
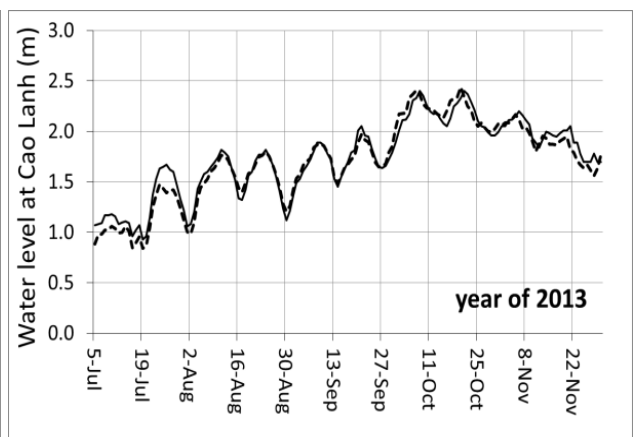
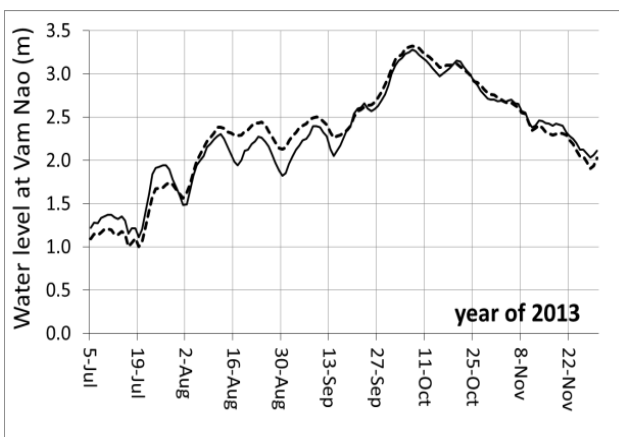
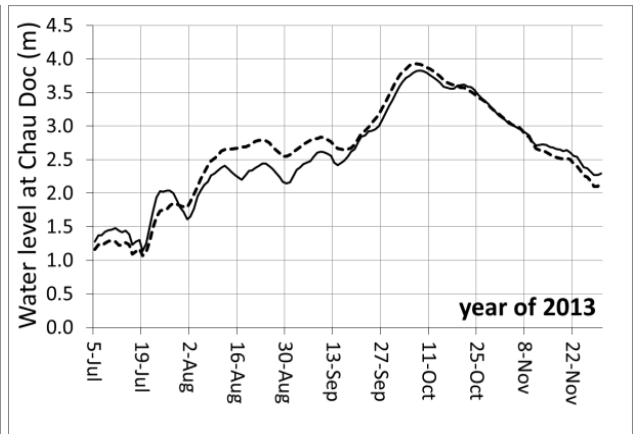
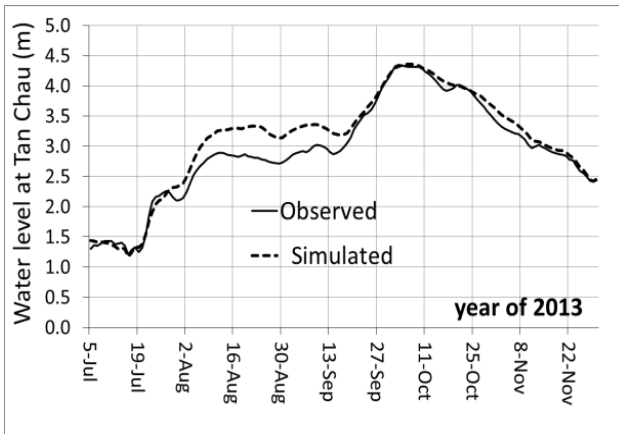


Figure 3.14. Model calibration of water level with high flood in 2011

Analysis the impact of land use change versus flooding situation in the MD using numerical modelling

c) Validation for medium flood in 2013



Analysis the impact of land use change versus flooding situation in the MD using numerical modelling

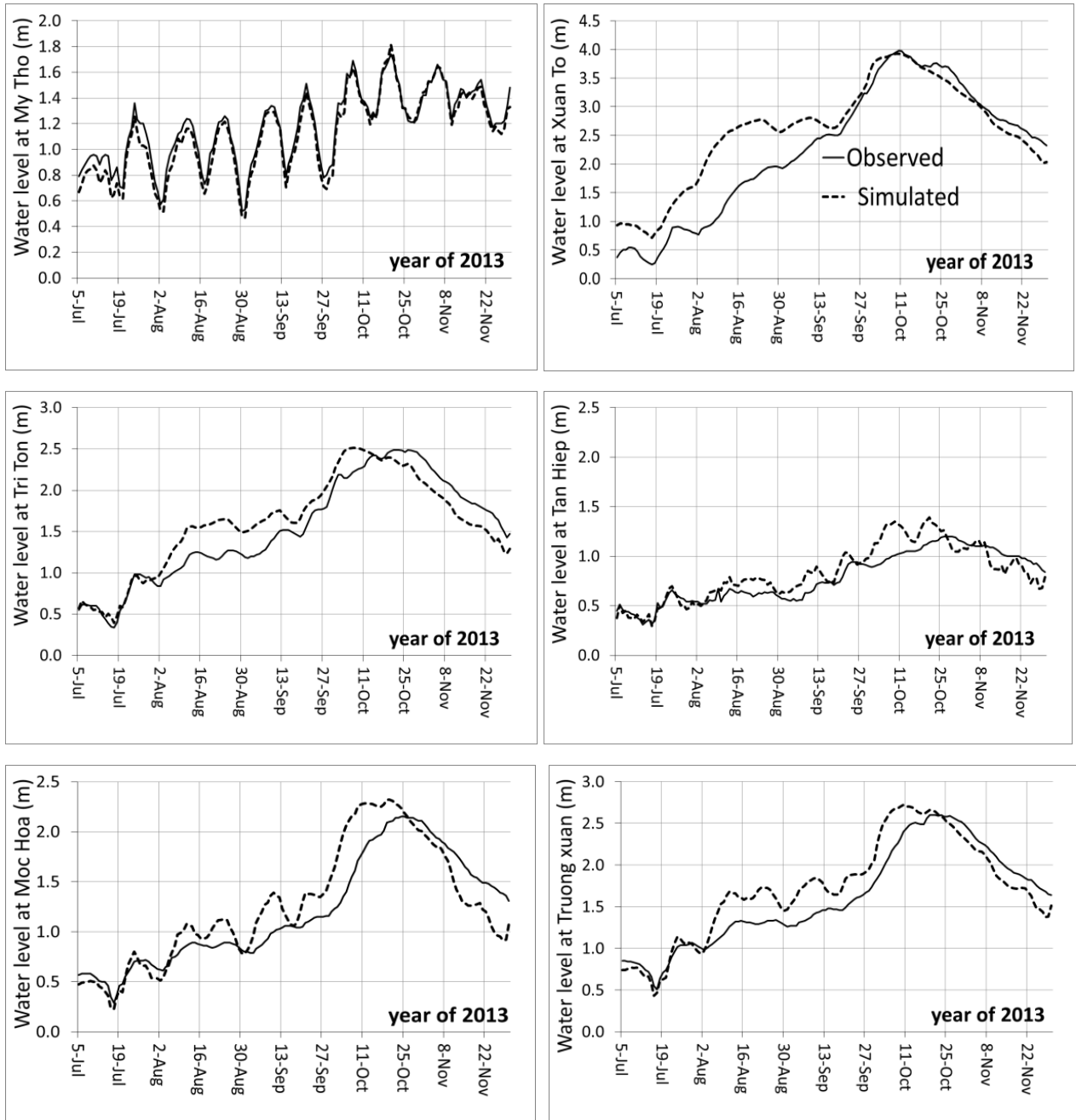
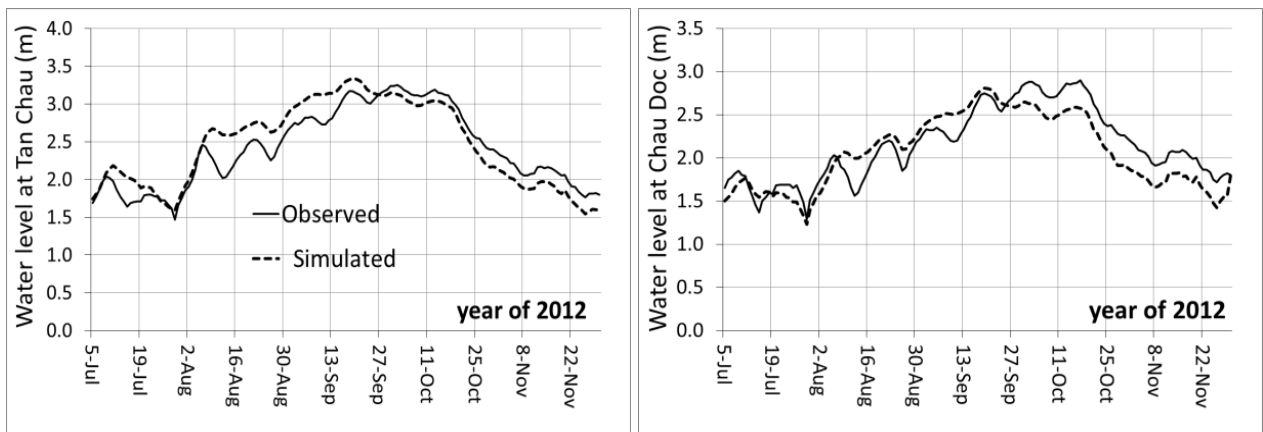


Figure 3.15. Hydraulic model validation of water level with medium flood in 2013

d) Validation for low flood in 2012



Analysis the impact of land use change versus flooding situation in the MD using numerical modelling

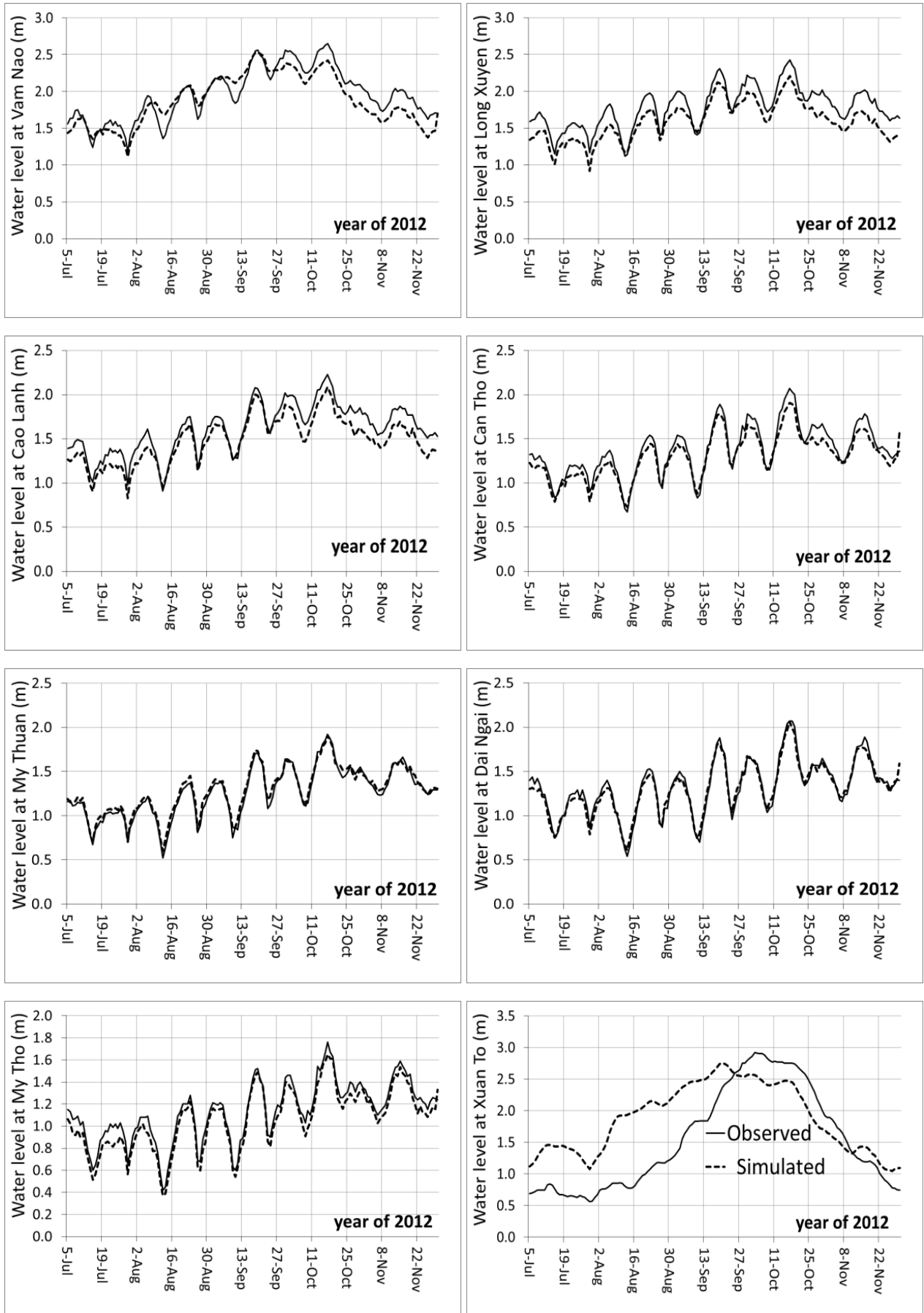


Figure 3.16. Hydraulic model validation of water level with low flood in 2012

Nash-Sutcliffe Index

The MIKE 11 model in the MD was calibrated by adjusting the hydraulic roughness coefficient (Manning's n) for each river and channel. The calibrating process was done based on the adjusting the value hydraulic roughness by the try-and-error method until the Nash-Sutcliffe Index value (E) meet the requirement of being close to nearly 1 (Tri et al., 2012).

The Nash–Sutcliffe Index (E) is defined as:

$$E = 1 - \frac{\sum_{t=1}^T (Q_0^t - Q_m^t)^2}{\sum_{t=1}^T (Q_0^t - \overline{Q_0})^2} \quad [3-3]$$

where Q_0 is the mean of observed data, and Q_m is modeled data. Q_0^t is observed data at time t.

Table 3.6. Results of calibration and validation in flood 2011, 2012, and 2013

No.	Station	High flood (2000)		High flood (2011)		Medium flood (2013)		Low flood (2012)	
		E	E	E	E	E	E	E	E
		Q (m ³ /s)	WL (cm)						
1	Tan Chau	0.8	0.91	0.85	0.98	0.86	0.92	0.73	0.8
2	Chau Doc	0.82	0.82	0.92	0.98	0.93	0.92	0.76	0.75
3	Vam Nao	0.86	-	0.81	0.98	0.73	0.94	0.75	0.78
4	Cho Moi	-	-	-	0.96	-	-	-	-
5	Long Xuyen	-	-	-	0.79	-	0.8	-	0.65
6	Can Tho	0.75	0.94	0.9	0.93	0.7	0.94	0.8	0.88
7	Dai Ngai	-	-	-	0.94	-	0.96	-	0.96
8	Cao Lanh	-	-	-	0.96	-	0.94	-	0.76
9	My Thuan	-	0.88	-	0.95	-	0.97	-	0.97
10	My Tho	-	0.97	-	0.93	-	0.93	-	0.9
11	Xuanto	-	0.94	-	0.88	-	0.76	-	0.60
12	Triton	-	0.9	-	0.92	-	0.71	-	0.72
13	Tan Hiep	-	0.65	-	0.65	-	0.85	-	0.66
14	Moc Hoa	-	0.69	-	0.94	-	0.76	-	0.63
15	Truong Xuan	-	0.8	-	0.91	-	0.81	-	-
16	Kien Binh	-	-	-	0.82	-	0.66	-	-
17	Tuyen Nhon	-	-	-	0.73	-	0.67	-	-
18	Cai Lay	-	-	-	0.66	-	0.68	-	-

where "-" means no valuable data for calibration and validation

Table 3.7 shows the accuracy in calibration of water levels (WL) and discharge (Q) at gauges on the Mekong River in locations such as Tan Chau and Chau Doc, Vam Nao, Long Xuyen, Cho Moi and Can Tho with E varying between 0.75 to 0.98. Whereas the calibration and validation of

Analysis the impact of land use change versus flooding situation in the MD using numerical modelling

water levels in inland canals faced more challenges with a lower Nash-Sutcliffe Index range from 0.63 to 0.98 depending on the type of flood.

Agreement between numerical flooding maps and satellite water maps

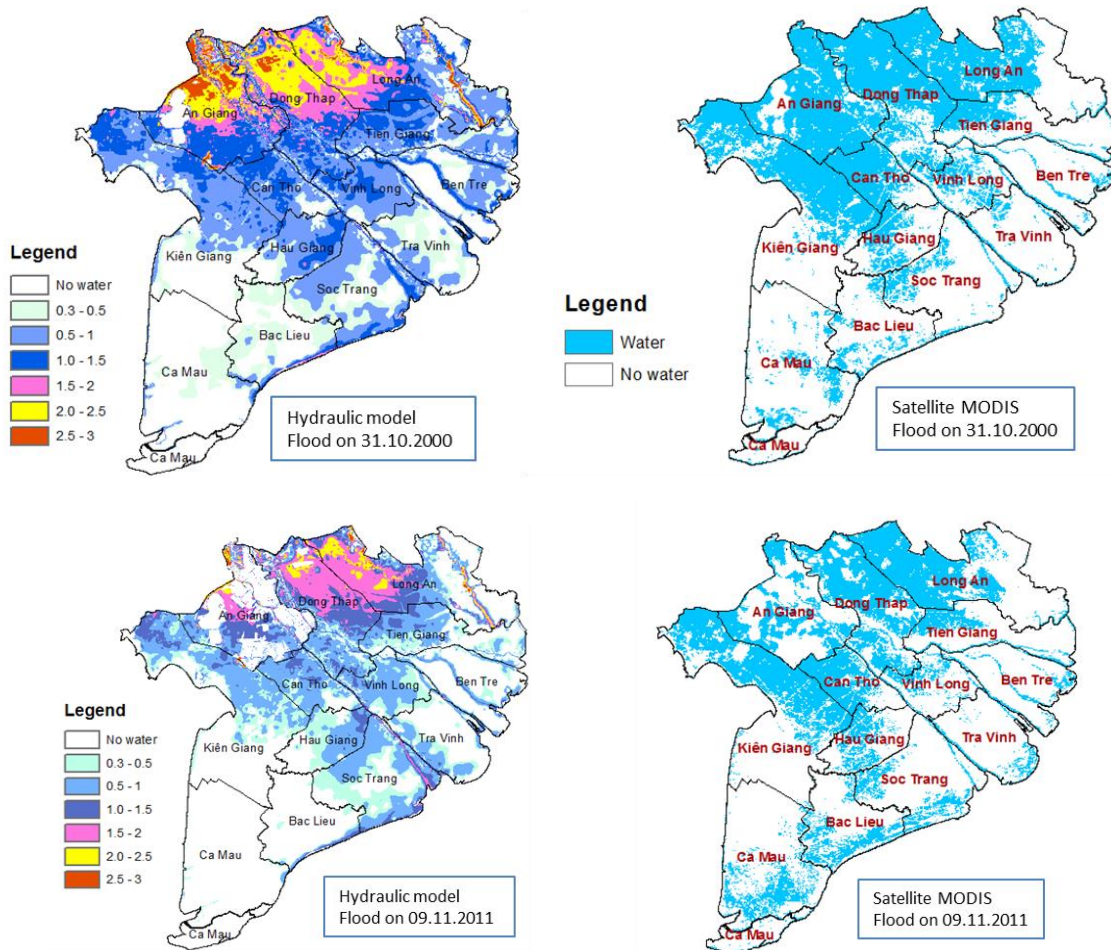


Figure 3.17. Agreement of flood maps in 2011 to hydraulic models and satellite products

The flood distribution was analyzed using hydraulic models and remote sensing for two high flood years in 2000 and 2011 with good agreement as illustrated in Figure 3.22. The map floods analyzed by MODIS products show the area of flooding while the ones carried out by hydraulic model (MIKE 11) state the water depth and flood distribution.

Discussion:

Calibration works were implemented for high floods in 2000 and 2011 while validation tasks were carried out for a medium flood (2013) and a low flood (2012). The accuracy and agreement have been evaluated through the Nash-Sutcliffe Index ranges between 0.98 to 0.65 and to compare with flood maps of MODIS flood maps. Due to the large and complex area of study with a dense network of Mekong River system, the 1D hydraulic model of MIKE11 is considered as an appropriate tool to simulate the flood hazards of a large and complex river network dominated by numerous hydraulic control structures such as the Mekong Delta. It demonstrated acceptable level of accuracy to hydraulic gauges and flood distribution as compared with flood mappings based on satellite products.

Analysis the impact of land use change versus flooding situation in the MD using numerical modelling

3.2.2. Numerical modelling for land use change scenarios

In this section, different scenarios of dyke measurements in the MD were simulated via numerical modelling to identify the impact of dyke impact factor on the rise of water level downstream, as many social media outlets have claimed.

3.2.2.1. Impact of dyke measurement on historical floods

To identify the impacts of dyke systems on triple crops and flood areas in the Mekong Delta, the developed scenarios include:

- Flood2000 (SC1): the dyke system in 2000 and upstream discharge and sea levels observed in 2000;
- Flood 2011 (SC2) the dyke system in 2011 and upstream discharge and sea levels observed in 2011;
- 2000on2011 (SC3): the dyke system in 2011 and upstream discharge and sea levels observed in 2000; and
- 2011on2000 (SC4): the dyke systems in 2000 and upstream discharge and sea levels in 2011.

Table 3.7. Simulated scenarios

Scenarios	Discharge Q (m3/s)	Water level (cm)	Actual status dykes
Flood 2000 (SC1)	Q2000	H2000	2000
Flood 2011 (SC2)	Q2011	H2011	2011
2000on2011 (SC3)	Q2000	H2000	2011
2011on2000 (SC4)	Q2011	H2011	2000

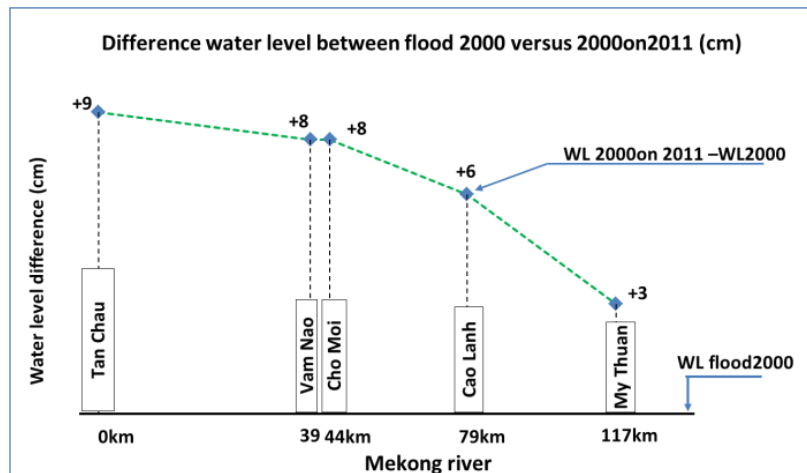


Figure 3.18. Difference in water levels on the Mekong River (SC1 vs SC3)

Comparison of SC1 to SC3: The impacts of dyke systems caused water flow to be distributed more into main rivers, and it made water levels along the main rivers increase. Particularly, the peak flood level at Chau Doc increased by 13cm, Tan Chau increased by 9 cm, Can Tho and My Thuan increased 5cm and 3 cm, respectively, in comparison with the actual flood of 2000, which can be seen in Figures 3.23 and 3.24.

Analysis the impact of land use change versus flooding situation in the MD using numerical modelling

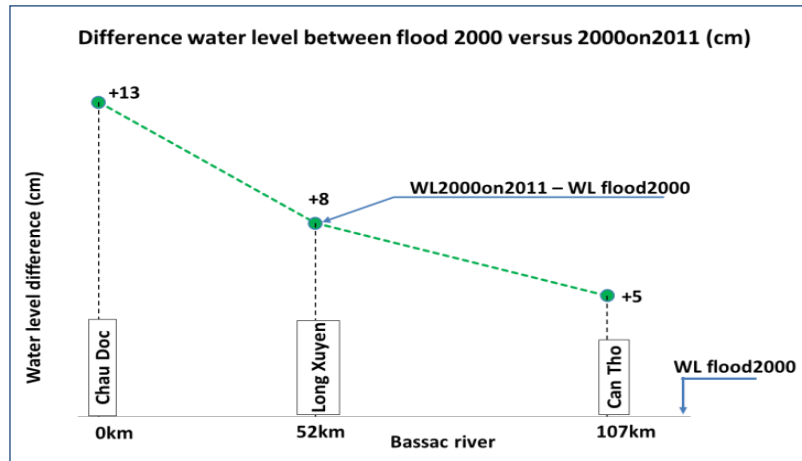


Figure 3.19. Difference in water levels on the Bassac River (SC1 vs SC3)

Comparison of SC2 to SC4: The scenario of the flood in 2011 with the dyke system in 2000 show that the water level on the major rivers was lower in comparison with the actual state in 2011, which is illustrated in Figures 3.25 and 3.26. Because there were no dyke systems for triple rice cropping, the flood water in SC4 distributed widely in inland areas, and it caused the water level to decrease in comparison with SC2, which can be seen in Table 3.9 and Figure 3.27.

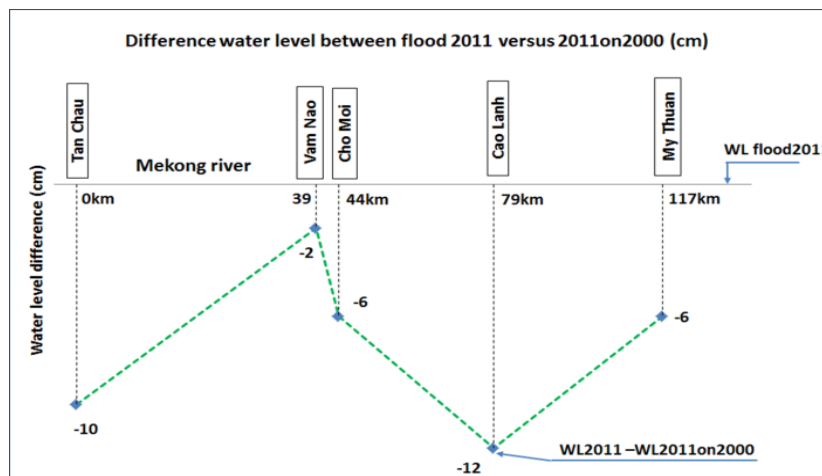


Figure 3.20. Difference in water levels on the Mekong River (SC2 vs SC4)

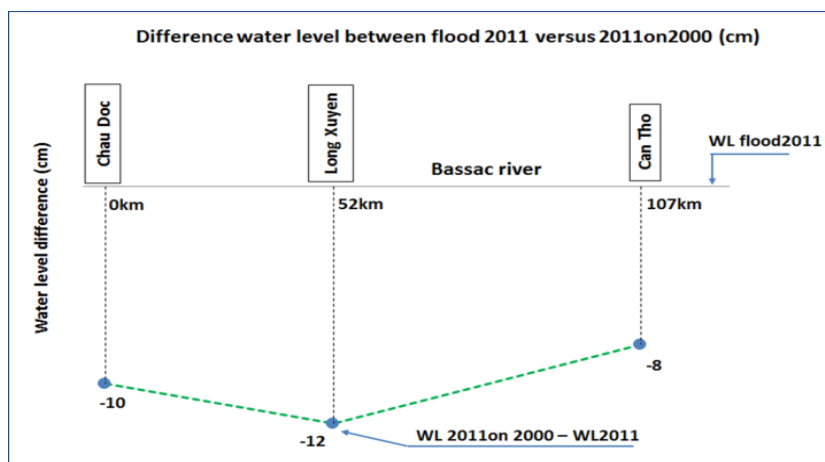


Figure 3.21. Difference in water levels on the Bassac River (SC2 vs SC4).

Analysis the impact of land use change versus flooding situation in the MD using numerical modelling

Table 3.8. Water level difference between SC2 vs SC4 at studied points by inland gauges

Location	Flood2011 (a) (cm)	2011on2000 (b) (cm)	(b) - (a) (cm)
<u>LXQ</u>			
Xuan To (9)	417	413	-4
Tri Ton (10)	270	266	-4
Tan Hiep (12)	211	199	-12
KH (11)	168	169	1
Thom Rom (13)	192	174	-18
KH3 (14)	145	128	-17
K8000 (16)	139	106	-33
<u>PoR</u>			
Cai Rung (20)	333	311	-22
Moc Hoa (21)	290	264	-26
Tuyen Nhon (25)	200	187	-13
Dong Tien 1 (22)	330	327	-3
K307 (23)	237	227	-10
Dong Tien 2 (24)	257	245	-12

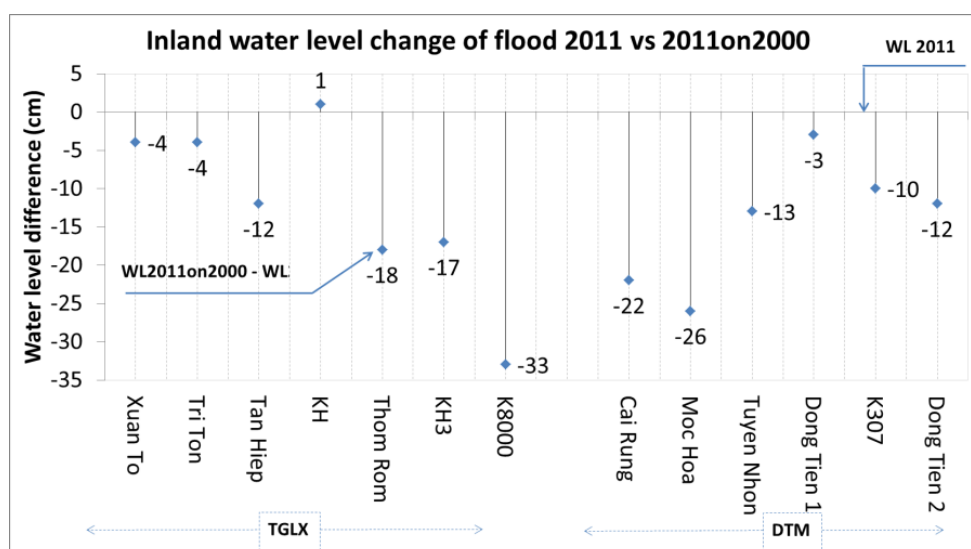


Figure 3.22. Difference in water levels in inland areas in DTM and TGLX (SC2 vs SC4).

Discussion:

The development of land use in the Mekong Delta in recent years has been caused great disruption in economic terms for Vietnam. However, it has also caused negative impacts to the annual flooding in the Mekong Delta. With the rapid development of triple rice cropping patterns, especially in the deep flooding zones in the LXQ and the PoR, the areas for floodplains have been intensively disrupted, which made water levels on the main rivers increase and caused negative impacts in downstream areas such as in Cantho City and My Thuan.

3.2.2.2. Geographical impact factor (GIF) analysis

In the upper Vietnamese delta, the impact of delta-based water infrastructure on hydrological areas has been more significant than other factors in the wet season, but the rise in sea level is the main factor in the dry season. In the wet season, dykes may not only affect water storage capacity but also water transfer capacity for the floodplains. Also, efforts to widen the current canal systems to mitigate the impact of dykes would have limited effect in relieving impacts.

The authors defined a new parameter to quantify the impact on land use for rice with full-dyke system at every compartment, which was defined as the geographical impact factor (GIF).

The GIF is defined as follows:

$$GIF_i = \frac{(Z_i - Z_{baseline})}{(Z_{total} - Z_{baseline})} \frac{1}{A_i} \quad (\text{unit: 1/ha}) \quad [3-4]$$

Where:

GIF_i : the geographical impact factor of compartment i in the flood area;

$Z_{baseline}$: water level at a considered point on Mekong river with no-dyke systems at 22 compartments (cm);

Z_i : water level at a considered point on Mekong river with full-dyke system at compartment i (cm);

Z_{total} : water level at a considered point due to full-dyke system at 22 compartments (cm);

A_i : area of compartment i (ha).

Based on the flood extent dated on 31.10.2000 from MODIS satellite, the delta is divided into 22 key compartments, in which each compartment is bounded by the main canals and rivers, which is illustrated in Figure 3.28. These compartments belong to four zones based on the hydrological characteristics of the watershed.

- The Long Xuyen Quadrangle (LXQ) includes six compartments (from A1 to A6) along the main canals of Tri Ton, Mac Can Dung, Rach Gia-Long Xuyen, and Cai San and the Bassac River.
- The Western region of the Bassac River (WBR) consists of three compartments (from A7 to A9) following the KH6 Canal, Thi Doi Canal, and the Omon-Xano system.
- The Middle zone is divided into three compartments (from A10 to A12) that are located in the middle region between the Mekong and the Bassac Rivers. They are divided along the Vam Nao River, Cai Tau Thuong Canal, and the Nha Man-Tu Tai River.
- The Plain of Reed (PoR) comprises 10 compartments (A13–A22) that are bounded by the main canals of Cai Co – Long Khot, Tan Thanh – Lo Gach, Cai Cai, Hong Ngu, Phuoc Xuyen, Thay Cai, Dong Tien, Nguyen Van Tiep, and the Mekong River and the Vam Co Tay River.

Analysis the impact of land use change versus flooding situation in the MD using numerical modelling

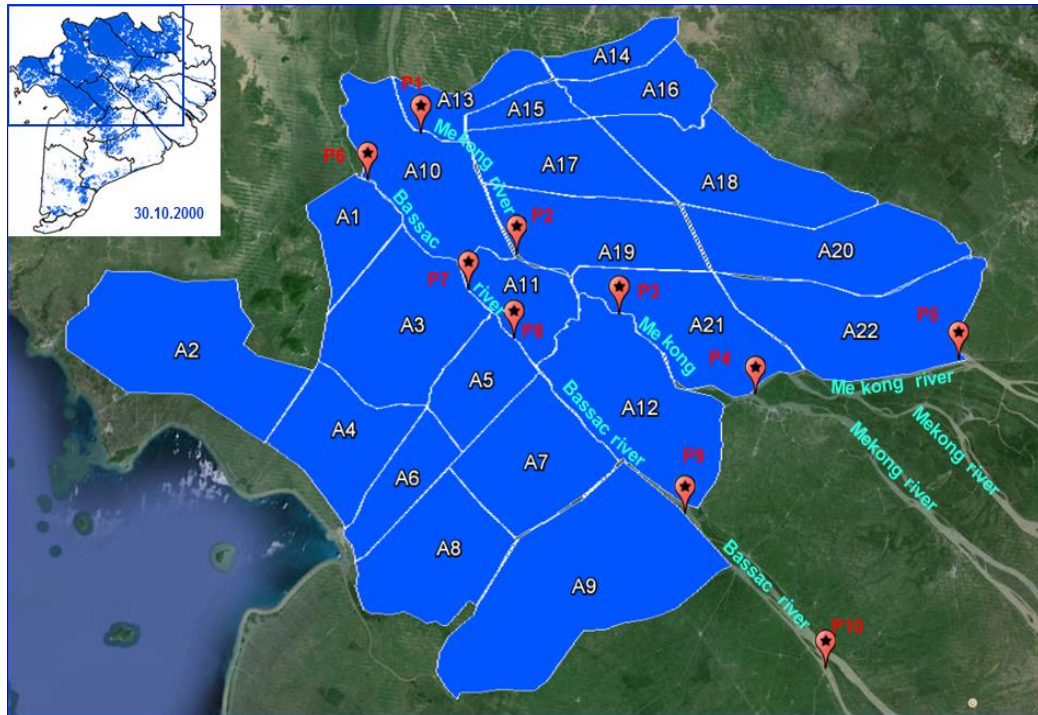


Figure 3.23. Mekong Delta with 22 compartments (A) and 10 examined locations (P).

The Table 3.10 represents the area of each compartment from A1 to A22 as well the total area of the whole 22 compartments, which is entitled A_{total} .

Table 3.9. Areas of the compartments (ha)

No.	Code	Name	Area (ha)	No.	Code	Name	Area (ha)
1	A1	LXQ1	33,202	13	A13	PoR1	26,803
2	A2	LXQ2	115,116	14	A14	PoR2	19,963
3	A3	LXQ3	90,837	15	A15	PoR3	16,593
4	A4	LXQ4	59,395	16	A16	PoR4	36,115
5	A5	LXQ5	38,531	17	A17	PoR5	55,050
6	A6	LXQ6	32,957	18	A18	PoR6	79,306
7	A7	WBR1	61,474	19	A19	PoR7	67,797
8	A8	WBR2	48,035	20	A20	PoR8	82,596
9	A9	WBR3	125,000	21	A21	PoR9	74,841
10	A10	MID1	77,102	22	A22	PoR10	95,553
11	A11	MID2	37,797	23	A_total	Total full dyke	1,337,000
12	A12	MID3	62,937				

MIKE11 is applied to simulate the impact of dyke construction on floods in the MD. Table 3.11 shows the 72 dyke scenarios included:

- No-dyke system in 22 compartments (three scenarios);
- 1 compartment with full-dykes, while other 21 compartments have no-dyke systems (66 scenarios); and
- All 22 compartments with full-dykes (three scenarios).

Analysis the impact of land use change versus flooding situation in the MD using numerical modelling

Table 3.10. Scenarios of dyke measurement locations in the Mekong Delta

Flood type	Scenarios	Discharge	Water level	Rainfall	Dyke system
		(m ³ /s)	(m)	(m)	
High flood	Baseline	Q_2011	H_2011	R_2011	No dyke at all compartments
	Full-dyke	Q_2011	H_2011	R_2011	Full-dyke at all compartments
	A ₁	Q_2011	H_2011	R_2011	Full-dyke at compartment A1, no-dyke system at A2 to A22
	A ₂	Q_2011	H_2011	R_2011	Full-dyke at compartment A2, no-dyke system at A1, A3 to A22
	A _i	Q_2011	H_2011	R_2011	Full-dyke at compartment A _i , no-dyke system at 21 other compartments (with i=3–22)
	<hr/>				
Medium flood	Baseline	Q_2013	H_2013	R_2013	No dyke at all compartments
	Full-dyke	Q_2013	H_2013	R_2013	Full-dyke at all compartments
	A ₁	Q_2013	H_2013	R_2013	Full-dyke at compartment A1, no-dyke system at A2 to A22
	A ₂	Q_2013	H_2013	R_2013	Full-dyke at compartment A2, no-dyke system at A1, A3 to A22
	A _i	Q_2013	H_2013	R_2013	Full-dyke at compartment A _i , no-dyke system at 21 other compartments (with i=3–22)
	<hr/>				
Low flood	Baseline	Q_2012	H_2012	R_2012	No dyke at all compartments
	Full-dyke	Q_2012	H_2012	R_2012	Full-dyke at all compartments
	A ₁	Q_2012	H_2012	R_2012	Full-dyke at compartment A1, no-dyke system at A2 to A22
	A ₂	Q_2012	H_2012	R_2012	Full-dyke at compartment A2, no-dyke system at A1, A3 to A22
	A _i	Q_2012	H_2012	R_2012	Full-dyke at compartment A _i , no-dyke system at 21 other compartments (with i=3–22)
	<hr/>				

3.2.2.2.1. Influence of GIF at a location to different positions on Mekong Rivers

To analyze the influences of full-dyke measurements on water levels along the main rivers, 10 positions were examined (Figure 3.28). These positions are located on the Mekong River (P1–P5) and the Bassac River (P6–P10).

The research investigated the impacts of several full-dyke compartments on flood water level along the Mekong and Bassac Rivers by exploiting a Geographical Impact Factor (GIF). By using a 1D hydrological model, the author found that different geographical compartments caused different rates of influences on the flood water level along the main rivers. Specifically, the full-dyke construction in the A10 compartment was very sensitive to water level changes in the Mekong and Bassac Rivers since these changes depended on the magnitude of the floods (Figure 3.29).

This compartment is the first area of the delta that receives flood water from upstream of the Mekong River, so the full-dyke system prevents the flood water from the Mekong River from entering the Bassac River. As a result, although the compartment increases the water level at Tan Chau (P1), a decrease in the river stage at Chau Doc (P6) was found. The same pattern of water level changes was also identified at Vam Nao (P2), but this no longer existed after Cao Lanh (P3). However, in the Bassac River, the water level changes remained until Dai Ngai (P10). Regarding the magnitude of the floods, GIF10 indicates a strong impact at A10 on water levels along the Mekong River in the case of a small flood. However, this tendency was reduced for the medium and high floods. On the Bassac River, the influence of A10 on water levels at Chau Doc (P6) was relatively high with high floods, but it decreased in the case of medium and small floods.

Analysis the impact of land use change versus flooding situation in the MD using numerical modelling

This impact showed similar results at the locations of Vam Nao (P7), Long Xuyen (P8) and Can Tho (P9) with decreasing values along the river.

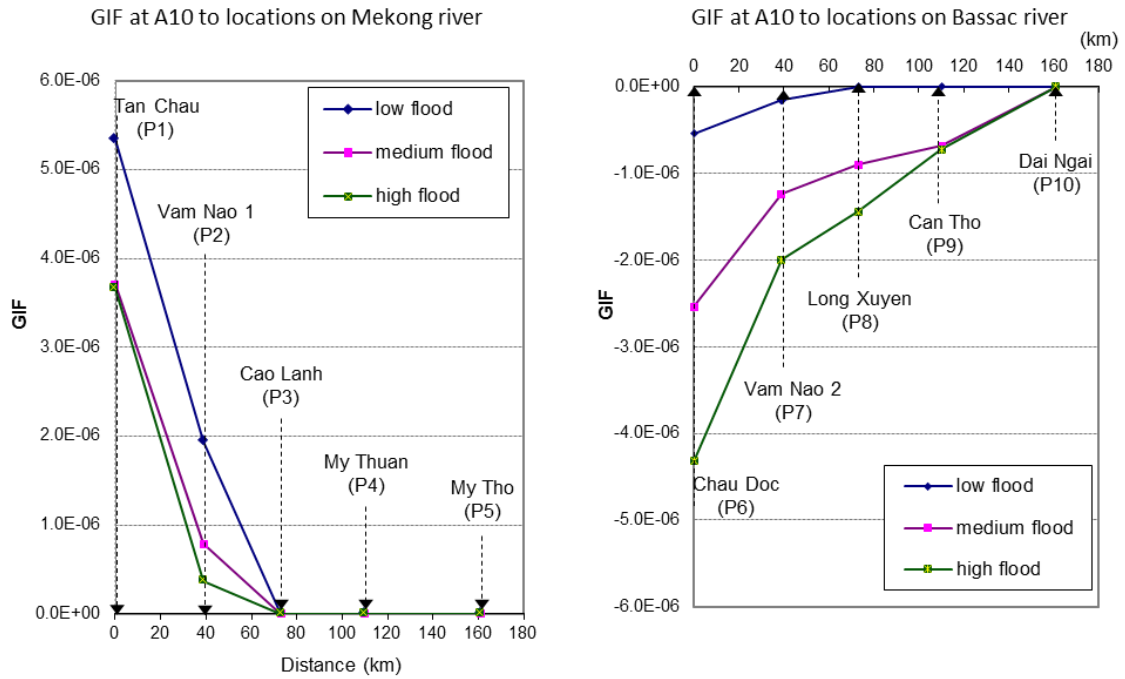


Figure 3.24. GIF of compartment A10 on flood water level along Mekong and Bassac rivers

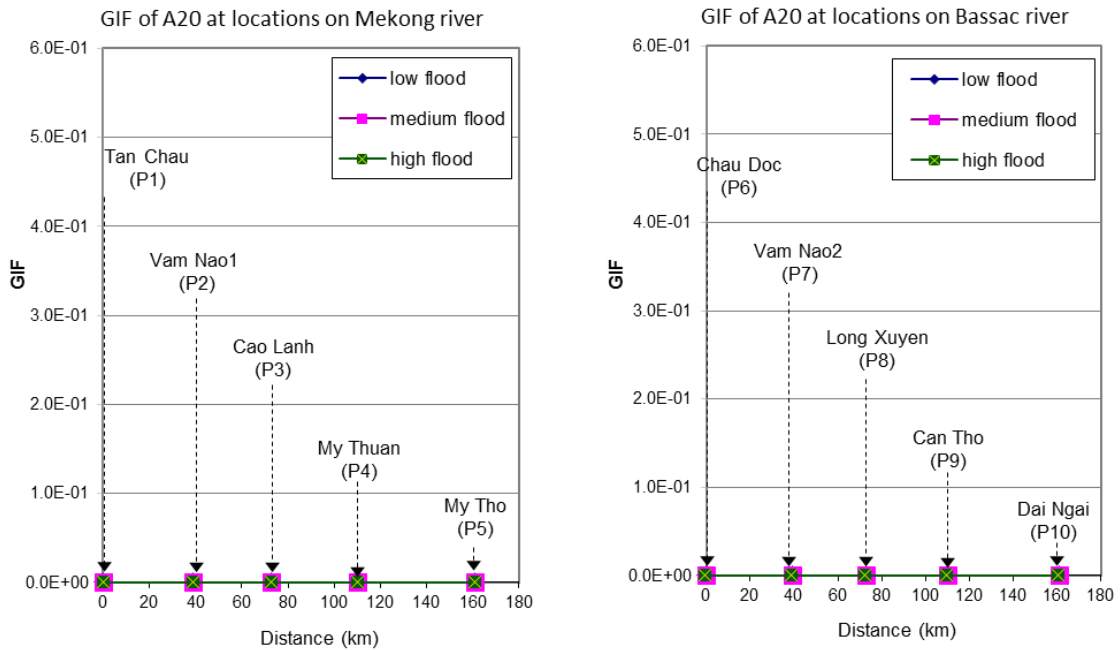


Figure 3.25. GIF of compartment A20 on flood water level along Mekong and Bassac rivers

The remaining compartments have different rates of impact on the water level along the Mekong and Bassac Rivers. For instance, the A20 compartment had no influence on water levels due to its distance far from the main rivers (Figure 3.30). In addition, the compartments A2, A4, A6, A8, A14, A16, and A18 indicated minor influence that are the same as that of compartment A20.

Analysis the impact of land use change versus flooding situation in the MD using numerical modelling

3.2.2.2. Influence of full-dyke system at each compartment at different locations

The geographical location of the full-dyke compartments and the magnitude of floods led to different levels of impact on the water levels at Tan Chau (P1), which can be seen in Figure 3.31. With low floods, the full-dyke compartments in most areas had little influence on the water level at Tan Chau, except for compartments A10, A11, and A15, which showed fairly high influence. The impacts decreased significantly for low to medium floods, but decreased slightly from medium to high floods. In contrast, the A17 compartment had quite a small impact during low floods, whereas the influence increased slightly with medium floods and increased rapidly with high floods. The findings implied that authorities should pause for consideration prior to implementing land use change for rice production based on full-dyke protection.

Table 3.11. Max flood discharge via the Mekong Delta measured at the Tan Chau and Chau Doc gauges

Year	Flood Classification	Tan Chau (m3/s)	Chau Doc (m3/s)	Total (m3/s)
2011	High flood	26100	8370	34470
2013	Medium flood	25200	7450	32650
2012	Low flood	20300	5610	25910

The full-dyke compartments also had an influence on water levels at Chau Doc (P6) at varying rates (Figure 3.31). Generally, most of compartments with full-dyke systems caused relatively low impacts on the water levels at this point. However, the A1 compartment caused a relatively high impact on the water level. This tendency was stable for small and medium floods but increases sharply with high floods. In contrast, the A10 compartment not only increased the water level at Tan Chau (P1), but also decreased the water level at Chau Doc (P6), because the full-dyke construction in this compartment prevented the flood water entering from the Mekong River into the Bassac River. This tendency is consistent with medium and high floods.

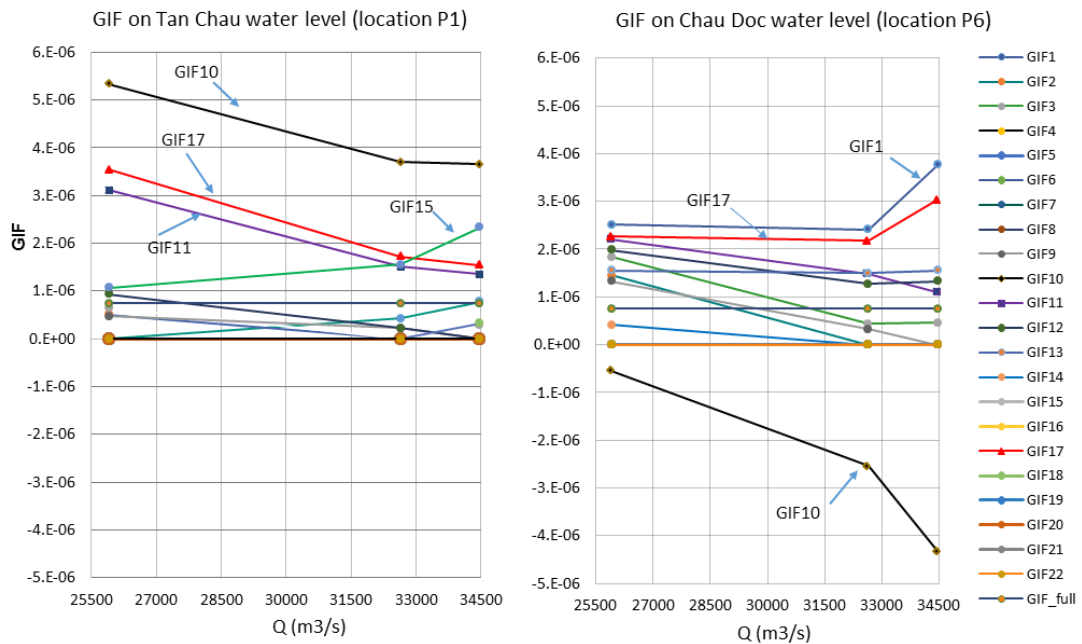


Figure 3.26. Geographical impact factors on Tan Chau water level (left) and Chau Doc water level (right) vs total flood discharge into Mekong Delta measured at the Tan Chau and Chau Doc gauges

Analysis the impact of land use change versus flooding situation in the MD using numerical modelling

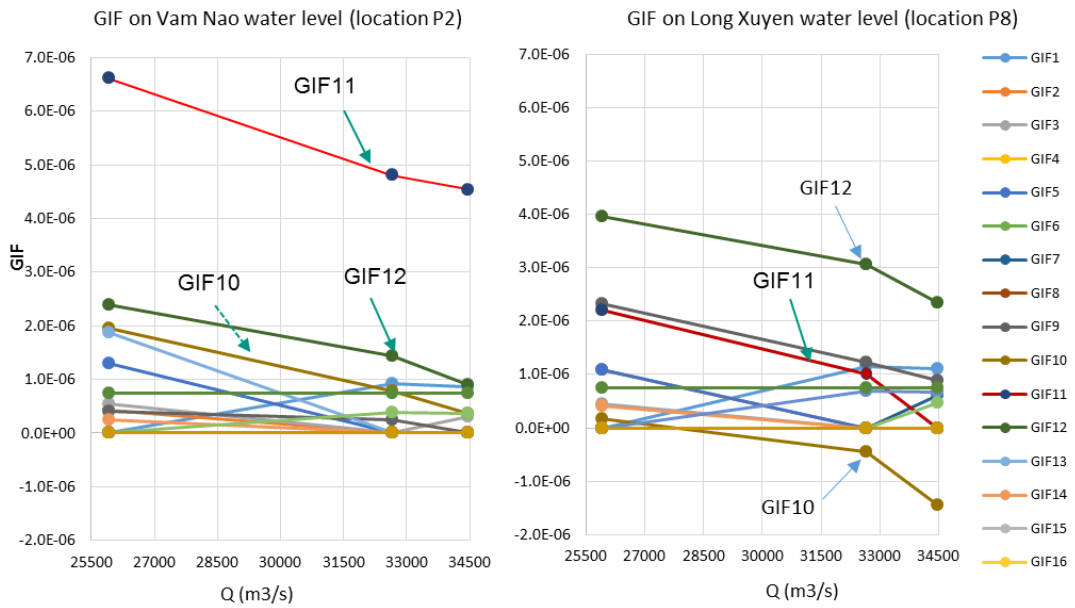


Figure 3.27. Geographical impact factors on Vam Nao water level (left) and on Long Xuyen water level (right) vs total flood discharge into the Mekong Delta measured at the Tan Chau and Chau Doc gauges

In Figure 3.32 and Figure 3.33, the construction of dyke measurements at compartments A11 and A12 were sensitive to changes in water levels at Cao Lanh (P3) whereas compartments of A9 and A11 strongly influenced the water level at Can Tho (P9). The A12 compartment caused a relatively high impact on Cao Lanh (P3) and Can Tho (P9) during low floods, but the impact decreased during the medium and high floods. The A11 compartment increased the water level at Cao Lanh (P3), but it decreased the water level at Can Tho (P9) due to the prevention of flood water moving from the Mekong River to the Bassac River.

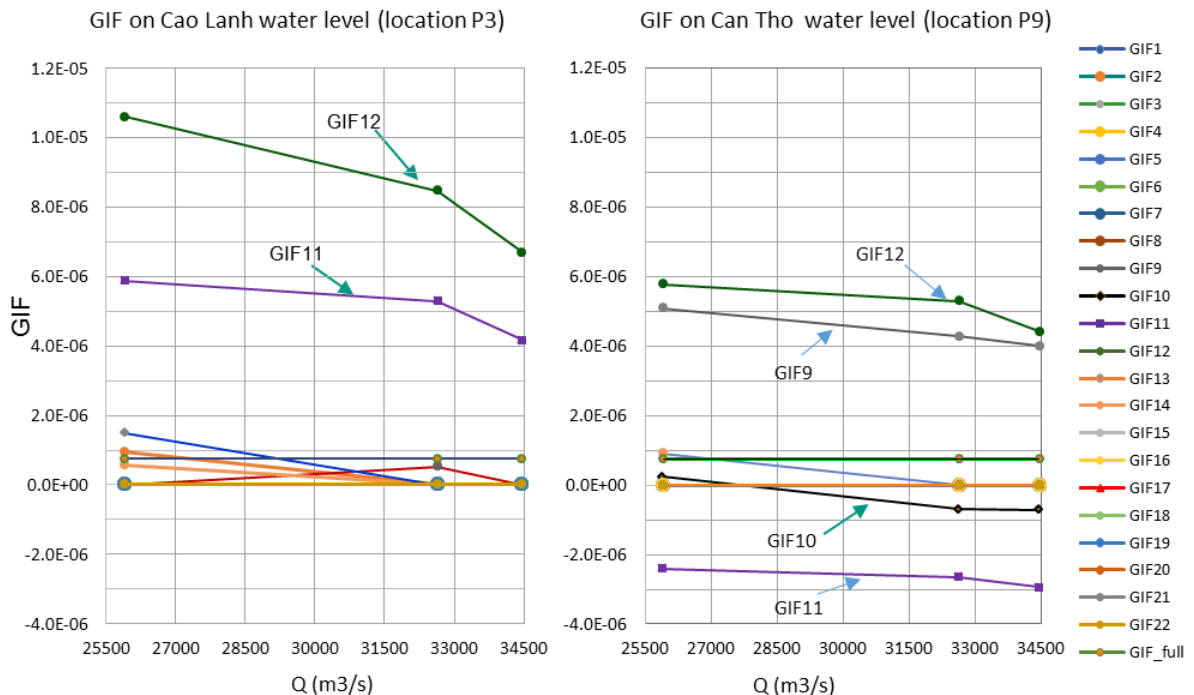


Figure 3.28. Geographical impact factors on Cao Lanh water level (left) and on Can Tho water level (right) vs. total flood discharge into the Mekong Delta measured at the Tan Chau and Chau Doc gauges

3.3. Discussion

Hydraulic model MIKE11 is an appropriate tool to simulate the flood hazards of a large and complex river network such as the Mekong Delta. It has acceptable accuracy to hydraulic gauges and flood distribution as compared with flood mappings based on satellite products.

A new database of Mekong network has been built in MIKE11 during the period of implementation for this dissertation. This Mekong network is a valuable property of the author that can simulate the Mekong river network faster and give higher accuracy in comparison with the current Mekong networks that belong to Vietnamese organizations.

The Geographical Impact Factor (GIF) could be used as an expression of the influence of dyke measurements on flood water levels along the main rivers. With different geographical locations of dyke compartments, different impacts on flooding situations along the main rivers were analyzed. In general, full-dyke measurements for land use purposes cause relatively minor impacts on the water level in the Mekong and Bassac Rivers. However, full-dyke measurements at multiple compartments in the middle zone (MID) indicated higher impacts on water levels at Tan Chau, Chau Doc, Cao Lanh, and Can Tho. Interestingly, the compartment A9 (Omon-Xano system) would be very sensitive to the increase of water levels at Can Tho if any full-dyke system was built in this area.

4. Application of GIF and remote sensing into flood monitoring and land use management for the MD

4.1. Optimization the area for triple rice cropping in the MD

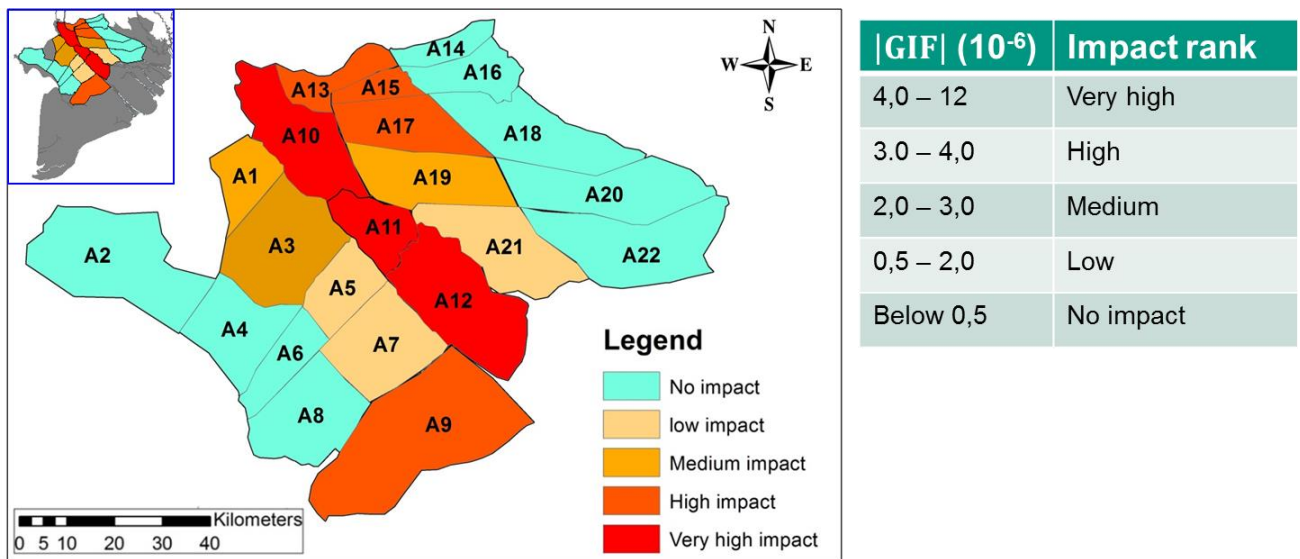


Figure 4.1. Vulnerability analysis of dyke measures for triple rice cropping in the MD

Based on the GIF, a vulnerability assessment is shown in Figure 4.1 for the impact of dyke measurement on triple rice cropping in the upstream provinces of the MD. The vulnerability of the compartments in terms of the hydraulic aspects was classified as follows.

- Very high vulnerability: This included compartment A10 due to its very high impact on flood waters in both the Mekong and Bassac Rivers. It is recommended to avoid cultivating triple rice croppings in this area.
- High vulnerability: This included the compartments of A11, A13, A15, A17 due to their impacts on flood waters in the Mekong River, and it is recommended to reduce the cultivation of triple rice cropping in these areas.
- Medium vulnerability: This included the compartments of A1, A19, A12 due to their local impacts on the Mekong and Bassac Rivers. The cultivation of triple rice cropping in these areas is acceptable to consider.
- Low vulnerability: This included the compartments of A3, A5, A7, A9, A21 due to their local impacts on the sections near the Mekong and Bassac Rivers. The cultivation of triple rice cropping in these areas is acceptable.
- No impact: This included the compartments of A2, A4, A6, A8 and A14, A16, A18, A20, A22. The construction of full-dyke measurements for triple rice cropping causes no impacts on the Mekong and Bassac Rivers.

However, Figure 4.1 shows the vulnerability analysis in terms of the hydraulic sector. Therefore, to have an overall assessment and recommendation for these areas in regards to triple rice cropping in the MD, an evaluation in terms of society and the economy should be undertaken.

4.2. Application of GIF for flood level prediction in the MD

Hydrodynamic models have been widely applied to simulate the flood distribution in order to project future patterns according to the changes in boundary conditions within the Mekong Delta (Tri et al., 2012). Flood water levels on the Mekong River play an important part in causing flooding in the downstream regions such as Can Tho City and My Thuan. However, there are only two hydrologic gauges at Tan Chau and Vam Nao on the Mekong River that offer online monitoring of the water level for the website hosted by the Mekong River Commission (MRC). Therefore, it is necessary to develop a tool to forecast the water level at any location along the Mekong and Bassac Rivers, which represents a total length of approximately around 400km.

In another hand, simulation works for a large and complex river network as the Mekong River system requires a lot of effort and experiences from the engineers, so not everyone can handle it. Besides, the capacity of the computer including the software and hardware need to be improved to meet the demand of a quick calculation time. In another hand, there is also a method to simplify the workloads of computation by application the GIF. Therefore, an interpolation method so-called FLEM “Flood level estimation method” was developed in this study to meet the mentioned request based on flood maps from remote sensing products and GIF, database of 1D-model and online data of discharge and water level from upstream Mekong river via the MRC website.

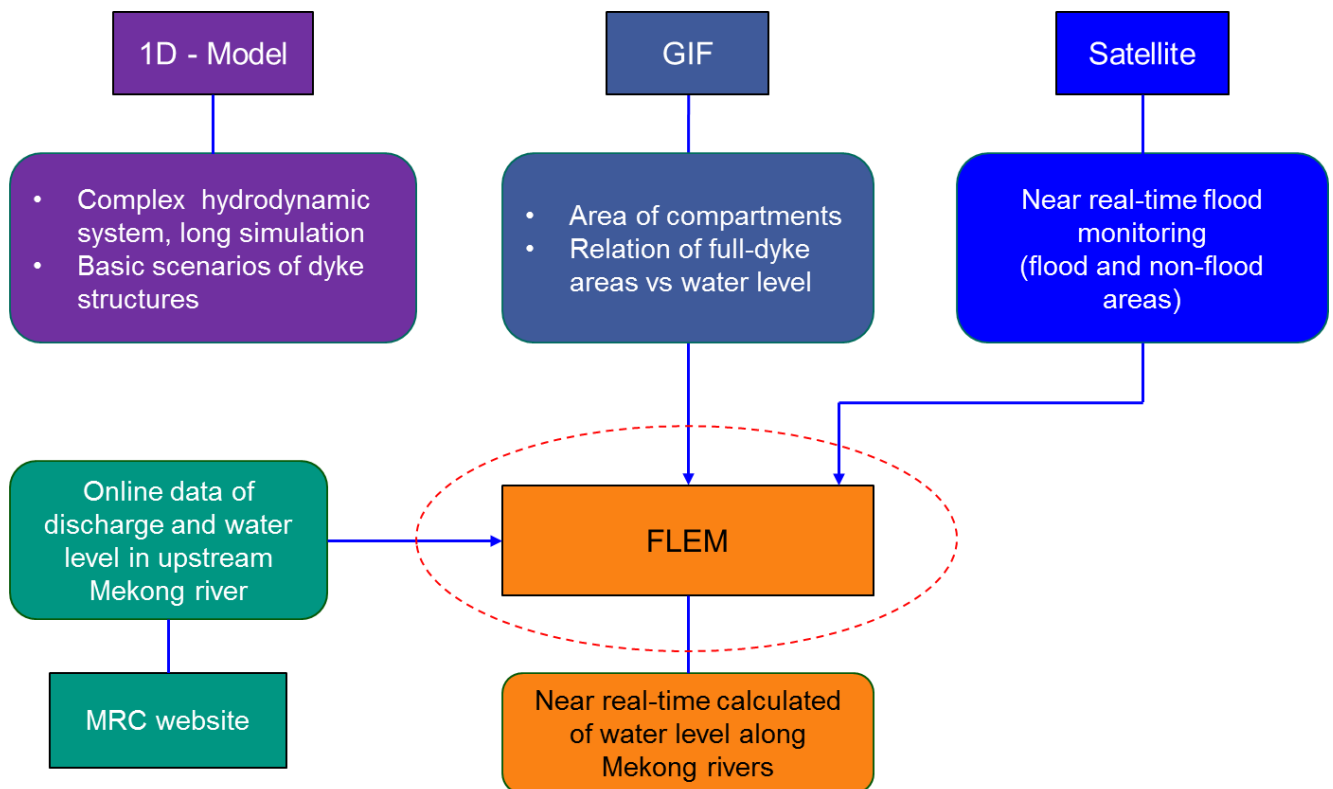


Figure 4.2. Approach of FLEM model (interpolation method)

Figure 4.2 presents the flow chart of FLEM model for calculation of water level along Mekong and Bassac rivers that is fast, precise and easy to practise based on the database of 1D Model, GIF and satellite products.

In general, water level at a considered location on Mekong river shall be calculated as (Z_j):

$$Z_j = Z_{baseline} + \Delta Z_j \quad [4-1]$$

$$\Delta Z_j = k_c \left(\Delta Z_1 \frac{A_1^*}{A_1} + \Delta Z_2 \frac{A_2^*}{A_2} + \dots + \Delta Z_n \frac{A_n^*}{A_n} \right) \quad [4-2]$$

$$\Delta Z_i = Z_i - Z_{baseline} \quad [4-3]$$

$$\Delta Z_{total} = Z_{total} - Z_{baseline} \quad [4-4]$$

where:

Z_j : Water level at the considered location j on the Mekong and Bassac rivers (m)

ΔZ_j : Additional water level due to full-dyke system at the considered location j (m).

$Z_{baseline}$: Water level at considered point with no-dyke system at all 22 compartments (m)

Z_i : Water level at considered point with full-dyke system at Compartment i (m).

Z_{total} : Water level at considered point due to full-dyke system at all 22 compartments (m)

ΔZ_i : Additional water level due to full-dyke system at compartment i (m).

A_i : Area of the compartment i (ha).

A_i^* : Area of full-dyke system in the compartment i (ha).

k_c : Adjustment coefficient, it is preliminary calculated in the Equation [4-5].

$$k_c = \frac{\Delta Z_{total}}{\Delta Z_1 + \Delta Z_2 + \dots + \Delta Z_n} \quad [4-5]$$

The results of the interpolation method were calibrated for the different types of floods in 2011 (high flood), in 2012 (low flood), and in 2013 (medium flood) with an accuracy from 90% to 96% in comparison with observed hydraulic data at the Tan Chau, Vam Nao, Cao Lanh and My Thuan gauges. Afterwards, this method was applied to interpolate the water level on the Mekong River for the floods in 2014, 2015, 2016, and 2017, respectively.

Application of GIF and remote sensing into flood monitoring and land use management
for the MD

Table 4.1. Water level baseline (Z_baseline) and water level max (Z_total) on the Mekong River

Z_baseline at gauge Total discharge (m ³ /s)	Tan Chau (m)	Vam Nao (m)	Cao Lanh (m)	My Thuan (m)
25910	3.229	2.367	1.930	1.871
32650	3.894	2.907	2.176	2.006
34470	4.350	3.275	2.350	2.049

Z_total at gauge Total discharge (m ³ /s)	Tan Chau (m)	Vam Nao (m)	Cao Lanh (m)	My Thuan (m)
25910	3.399	2.559	2.02	1.865
32650	4.248	3.228	2.328	2.026
34470	4.737	3.606	2.536	2.088

Table 4.2. Water level baseline (Z_baseline) and water level max (Z_total) on the Bassac River

Z_baseline at gauge Total discharge (m ³ /s)	Chau Doc (m)	Long Xuyen (m)	Can Tho (m)	Dai Ngai (m)
25910	2.750	1.867	1.730	2.071
32650	3.550	2.202	1.872	2.080
34470	4.083	2.442	1.936	2.100

Z_total at gauge Total discharge (m ³ /s)	Chau Doc (m)	Long Xuyen (m)	Can Tho (m)	Dai Ngai (m)
25910	2.870	2.108	1.843	2.050
32650	3.798	2.458	2.025	2.084
34470	4.327	2.714	2.120	2.110

Application of GIF and remote sensing into flood monitoring and land use management for the MD

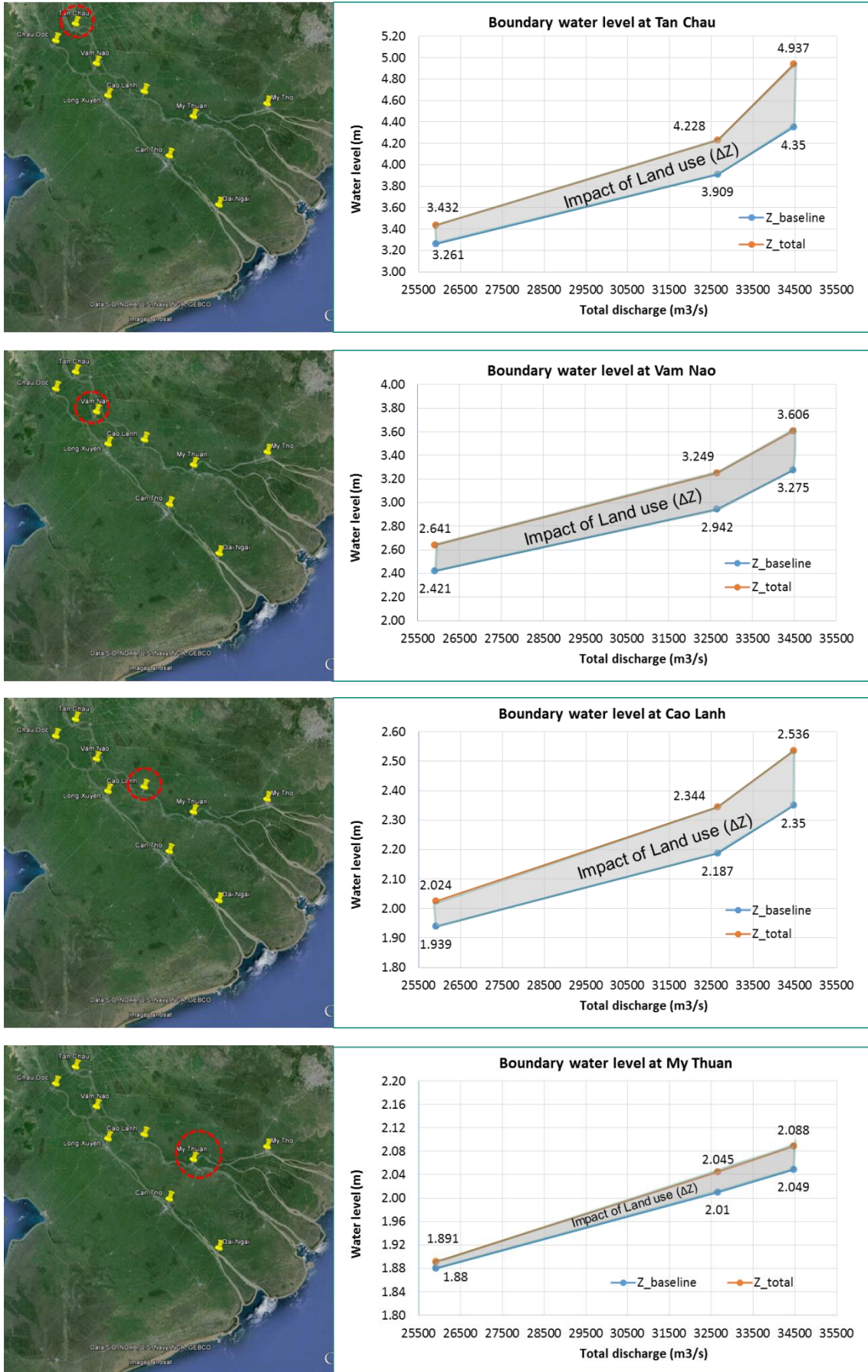


Figure 4.3. Impacts of land use on flood water on the Mekong River

Application of GIF and remote sensing into flood monitoring and land use management for the MD

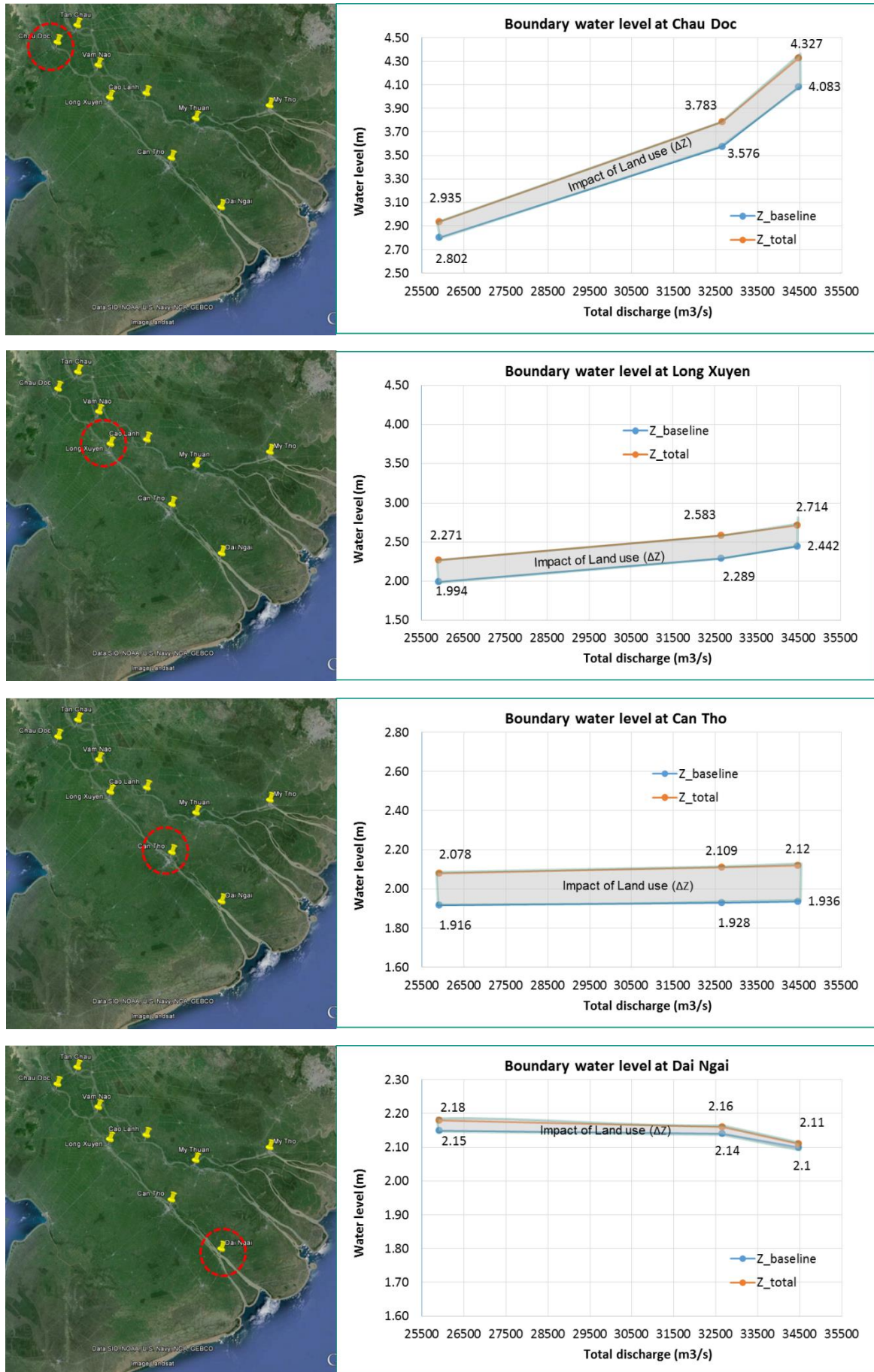


Figure 4.4. Impacts of land use on flood water on the Bassac River

Application of GIF and remote sensing into flood monitoring and land use management for the MD

Table 4.3. Additional water level (ΔZ) due to dyke measurement at the compartments on the Mekong River

ΔZ LOOKUP AT Tan Chau (cm)																							
Total discharge (m3/s)	Compartment (ha)	A1	A2	A3	A4	A5	A6	A7	A8	A9	A10	A11	A12	A13	A14	A15	A16	A17	A18	A19	A20	A21	A22
	25910		0	1	1	0	0	0	0	0	1	7	2	1	0	0	1	0	1	0	0	0	0
32650		0.5	0	0	0	0	0	0	0	1	10	2	1	0	0	1	0	3	0	0	0	0	0
34470		1	0	1	0	0	0	0	0	0	11	2	0	0	0	1	0	5	1	0	0	0	0
ΔZ LOOKUP AT Vam Nao (cm)																							
25910		0	1	1	0	1	0	0	0	2	3	4	3	1	0	0	0	0	0	0	0	0	0
32650		1	0	0	0	0	0	0	0	2	2	5	3	0	1	0	0	2	1	0	0	0	0
34470		2	0	1	0	0	0	0	0	0	5	2	0	0	1	0	4	1	0	0	0	0	0
ΔZ LOOKUP at Cao Lanh (cm)																							
25910		0	1	0	0	0	0	0	0	0	2	6	0	0	0	0	0	0	0	0	0	1	0
32650		0	0	0	0	0	0	0	0	1	0	3	8	0	0	0	0	0	0	0	0	0	0
34470		0	0	0	0	0	0	0	0	0	3	8	0	0	0	0	0	0	0	0	0	0	0
ΔZ LOOKUP at My Thuan (cm)																							
25910		0	0	0	0	0	0	0	0	0	0	1	0	0	0	0	0	0	0	0	0	0	0
32650		0	0	0	0	0	0	0	0	0	0	1	0	0	0	0	0	0	0	0	0	0	0
34470		0	0	0	0	0	0	0	0	0	0	3	0	0	0	0	0	0	0	0	0	0	0
on the Bassac River																							
ΔZ LOOKUP at Chau Doc (cm)																							
Total Discharge (m3/s)	Compartment (ha)	A1	A2	A3	A4	A5	A6	A7	A8	A9	A10	A11	A12	A13	A14	A15	A16	A17	A18	A19	A20	A21	A22
	25910		1	2	2	0	0	0	0	0	2	-0	1	1.5	0.5	0.1	0	0	1.5	0	0	0	0
32650		2	0	1	0	0	0	0	0	1	-5	1.4	2	1	0	0	0	3	0	0	0	0	0
34470		3	0	1	0	0	0	0	0	0	-8	1	2	1	0	0	0	4	0	0	0	0	0
ΔZ LOOKUP at Long Xuyen (cm)																							
25910		0	3	1	0	1	0	0	0	7	0.3	2	6	0	0.2	0	0	0	0	0	0	0	0
32650		1	0	0	0	0	0	0	0	4	-0.9	1	5	0	0	0	0	1	0	0	0	0	0
34470		1	0	0	0	0	0	1	0	3	-3	0	4	0	0	0	0	1	1	0	0	0	0
ΔZ LOOKUP at Can Tho (cm)																							
25910		0	0	0	0	0	0	0	0	7	0.2	-1	4	0	0.2	0	0	0	0	0	0	0	0
32650		0	0	0	0	0	0	0	0	8	-0.8	-1.5	5	0	0	0	0	0	0	0	0	0	0
34470		0	0	0	0	0	0	0	0	9	-1	-2	5	0	0	0	0	0	0	0	0	0	0
ΔZ LOOKUP at Dai Ngai (cm)																							
25910		0	0	0	0	0	0	0	0	0	0.1	-1	-1	0	0.1	0	0	0	0	0	0	0	0
32650		0	0	0	0	0	0	0	0	2	-0.6	-1	0	0	-0.7	0	0	0	0	0	0	0	0
34470		0	0	0	0	0	0	0	1	0	-1	0	0	0	0	0	0	0	0	0	0	0	0

Application of GIF and remote sensing into flood monitoring and land use management for the MD

4.2.1. Interpolation of flood level for flood in 2011

Table 4.4. Calculation for flood interpolation on 29.09.2011

Q_{\max} Tan Chau = 26100 (m^3/s), Q_{\max} Chau Doc = 8370 (m^3/s); $Q_{\text{total}} = 34470$ (m^3/s)

Compartment	Wet area (ha)	Dry area A^*i (ha)	Total area A_i (ha)	A^*i/A_i	Mekong river				Bassac river			
					ΔZ_i Tanchau (cm)	ΔZ_i Vam Nao (cm)	ΔZ_i Cao Lanh (cm)	ΔZ_i My Thuan (cm)	ΔZ_i Chau Doc (cm)	ΔZ_i Long Xuyen (cm)	ΔZ_i Can Tho (cm)	ΔZ_i Dai Ngai (cm)
A1	9,225	24,004	33,229	0.722	1	2	0	0	3	1	0	0
A2	93,843	21,342	115,186	0.185	0	0	0	0	0	0	0	0
A3	31,126	59,686	90,811	0.657	1	1	0	0	1	0	0	0
A4	47,633	11,801	59,434	0.199	0	0	0	0	0	0	0	0
A5	15,547	22,979	38,526	0.596	0	0	0	0	0	0	0	0
A6	27,015	5,946	32,961	0.180	0	0	0	0	0	0	0	0
A7	60,974	11,538	72,512	0.159	0	0	0	0	0	1	0	0
A8	47,944	24,949	72,893	0.342	0	0	0	0	0	0	0	0
A9	53,375	108,537	161,912	0.670	0	0	0	0	0	3	9	1
A10	23,811	53,235	77,046	0.691	11	0	0	0	-8	-3	-1	0
A11	3,504	34,243	37,748	0.907	2	5	3	0	1	0	-2	-1
A12	51,969	47,692	99,661	0.479	0	2	8	3	2	4	5	0
A13	18,686	9,971	28,657	0.348	0	0	0	0	1	0	0	0
A14	19,480	483	19,963	0.024	0	0	0	0	0	0	0	0
A15	8,726	7,846	16,572	0.473	1	1	0	0	0	0	0	0
A16	35,306	741	36,047	0.021	0	0	0	0	0	0	0	0
A17	42,916	12,150	55,065	0.221	5	4	0	0	4	1	0	0
A18	74,283	5,216	79,499	0.066	1	1	0	0	0	1	0	0
A19	59,197	8,613	67,811	0.127	0	0	0	0	0	0	0	0
A20	51,320	31,276	82,595	0.379	0	0	0	0	0	0	0	0
A21	39,991	34,828	74,819	0.465	0	0	0	0	0	0	0	0
A22	28,394	67,188	95,582	0.703	0	0	0	0	0	0	0	0
F_full	0	1,448,527	1,448,527	1	39	33	19	4	24	27	22	0
			sum_ A_i (i=1-22)		22	16	11	3	7	8	11	0
			$K_c = F_{\text{full}} / \text{sum}(A1:A22)$		1.77	2.06	1.73	1.33	6.00	3.38	2.00	0

Table 4.5. Interpolation of maximum water level along the main rivers on 29.09.2011

Flood on 29.09.2011	Gauge	Distance (km)	Z_baseline (m)	ΔZ_{2011} (m)	Interpolation (m)	Observed water level (m)	Agreement (%)
Mekong river	Tan Chau	0	4.350	0.391	4.741	4.86	98%
	Vam Nao	39	3.275	0.384	3.659	3.59	98%
	Cao Lanh	72	2.350	0.195	2.545	2.50	98%
	My Thuan	115	2.049	0.026	2.075	1.95	94%
Bassac River	Chau Doc	0	4.083	0.042	4.125	4.22	98%
	Long Xuyen	76	2.442	0.238	2.680	2.79	96%
	Can Tho	113	1.936	0.205	2.141	2.11	99%
	Dai Ngai	160	2.100	0.000	2.100	2.02	96%

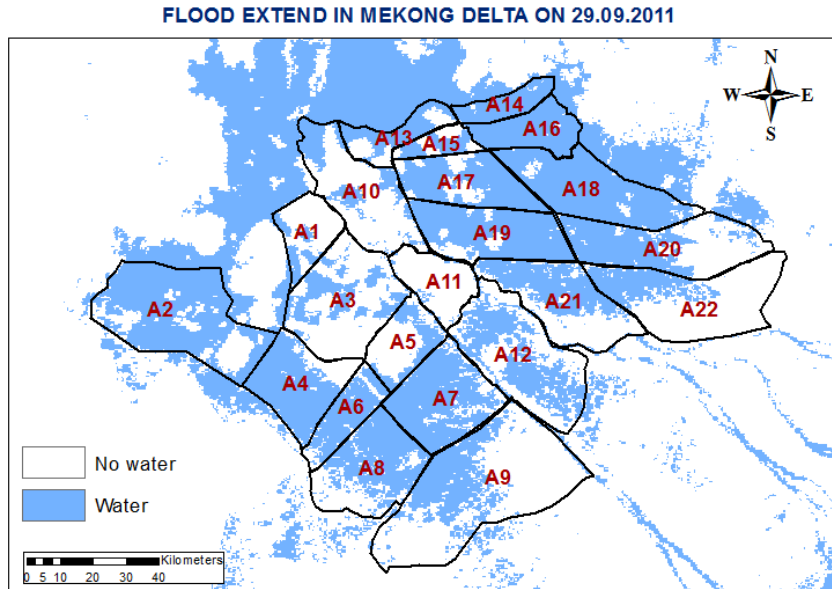


Figure 4.5. Flood extension on 29.09.2011

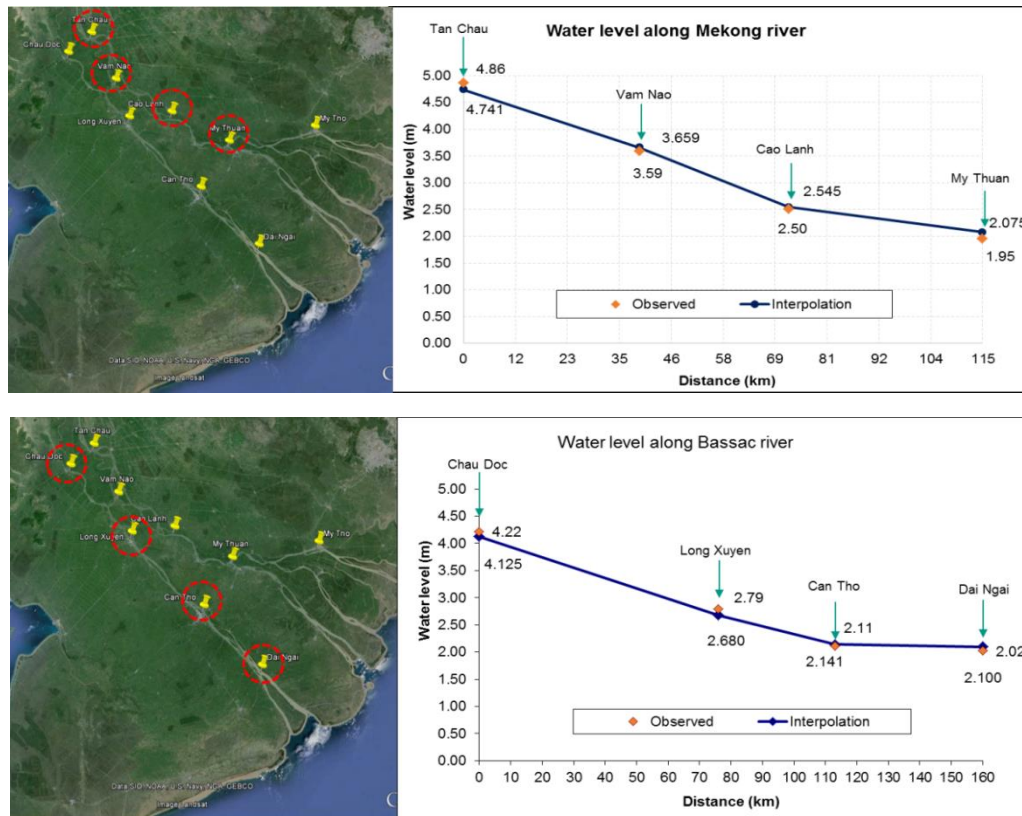


Figure 4.6. Interpolation of flood water level along Mekong and Bassac rivers on 29.09.2011

Table 4.5 and Figure 4.6 show the application of the interpolation method for prediction of water levels along the Mekong and Bassac Rivers on 29.09.2012. The accuracy of the interpolation method was 94% at the My Thuan gauge, 98% at the Cao Lanh gauge, 98% at the Vam Nao gauge, and 98% at the Tan Chau gauge on the Mekong River. Similarly, the accuracy on the Bassac River was 96% at the Dai Ngai gauge, 99% at Can Tho, 96% at Long Xuyen, and 98% at the Chau Doc gauge, respectively. The flood in 2011 was classified as a low flood, yet the results of interpolation method still showed a high level of agreement with the observed data. Also, there

Application of GIF and remote sensing into flood monitoring and land use management for the MD

was accuracy in regards to the locations near the East Sea, such as Dai Ngai and My Thuan, which typically showed lower accuracy than the upstream locations due to the tidal impacts.

4.2.2. Interpolation of flood level for flood in 2012

Table 4.6. Calculation for flood interpolation on 30.09.2012

Q_{\max} Tan Chau = 20300 (m^3/s), Q_{\max} Chau Doc = 5590 (m^3/s); $Q_{\text{total}} = 25890$ (m^3/s)

Compartment	Wet area (ha)	Dry area A^*i (ha)	Total area A_i (ha)	A^*i/A_i	Mekong river				Bassac river			
					ΔZ_i Tanchau (cm)	ΔZ_i Vam Nao (cm)	ΔZ_i Cao Lanh (cm)	ΔZ_i My Thuan (cm)	ΔZ_i Chau Doc (cm)	ΔZ_i Long Xuyen (cm)	ΔZ_i Can Tho (cm)	ΔZ_i Dai Ngai (cm)
A1	9,311	23,918	33,229	0.720	0	0	0	0	1	0	0	0
A2	26,285	88,901	115,186	0.772	1	1	1	0	2	3	0	0
A3	13,019	77,792	90,811	0.857	1	1	0	0	2	1	0	0
A4	38,343	21,090	59,434	0.355	0	0	0	0	0	0	0	0
A5	13,502	25,024	38,526	0.650	0	1	0	0	0	1	0	0
A6	20,398	12,563	32,961	0.381	0	0	0	0	0	0	0	0
A7	51,228	21,283	72,512	0.294	0	0	0	0	0	0	0	0
A8	44,075	28,818	72,893	0.395	0	0	0	0	0	0	0	0
A9	60,137	101,775	161,912	0.629	1	2	0	0	2	7	7	0
A10	16,437	60,609	77,046	0.787	7	3	0	0	0	0	0	0
A11	3,574	34,174	37,748	0.905	2	4	2	0	1	2	-1	-1
A12	40,007	59,654	99,661	0.599	1	3	6	1	1	6	4	-1
A13	21,686	6,971	28,657	0.243	0	1	0	0	0	0	0	0
A14	12,702	7,261	19,963	0.364	0	0	0	0	0	0	0	0
A15	7,594	8,978	16,572	0.542	1	0	0	0	0	0	0	0
A16	33,524	2,522	36,047	0.070	0	0	0	0	0	0	0	0
A17	38,177	16,888	55,065	0.307	1	0	0	0	1	0	0	0
A18	68,900	10,599	79,499	0.133	0	0	0	0	0	0	0	0
A19	49,151	18,659	67,811	0.275	0	0	0	0	0	0	0	0
A20	36,272	46,323	82,595	0.561	0	0	0	0	0	0	0	0
A21	33,235	41,585	74,819	0.556	0	0	1	0	0	0	0	0
A22	23,489	72,093	95,582	0.754	0	0	0	0	0	0	0	0
F_full	0	1,448,527	1,448,527	1	17	19	9	0	12	24	11	0
			Total A_i (i=1-22)		15	16	10	1	11	21	10	-2
			$K_c = F_{\text{full}} / \text{sum}(A1:A22)$		1.13	1.19	0.89	-0.01	0.99	1.02	0.96	1.11

Table 4.7. Interpolation of water level along the main rivers for flood on 30.09.2012

Flood 2012	Gauge	Distance (km)	Z_{baseline} (m)	ΔZ_{2012} (m)	Interpolation (m)	Observed water level (m)	Agreement (%)
Mekong river	Tan Chau	0	3.227	0.221	3.448	3.24	94%
	Vam Nao	39	2.365	0.283	2.648	2.56	97%
	Cao Lanh	72	1.929	0.104	2.033	2.02	99%
	My Thuan	115	1.871	0.000	1.871	1.64	88%
Bassac River	Chau Doc	0	2.748	0.127	2.875	2.83	98%
	Long Xuyen	76	1.866	0.333	2.199	2.22	99%
	Can Tho	113	1.730	0.102	1.831	1.78	97%
	Dai Ngai	160	2.071	-0.021	2.050	1.86	91%

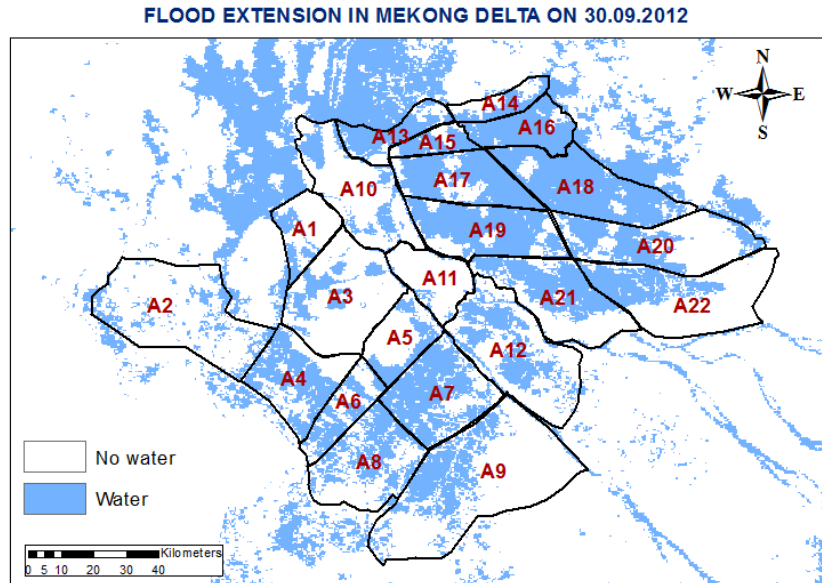


Figure 4.7. Flood extension on 30.09.2012

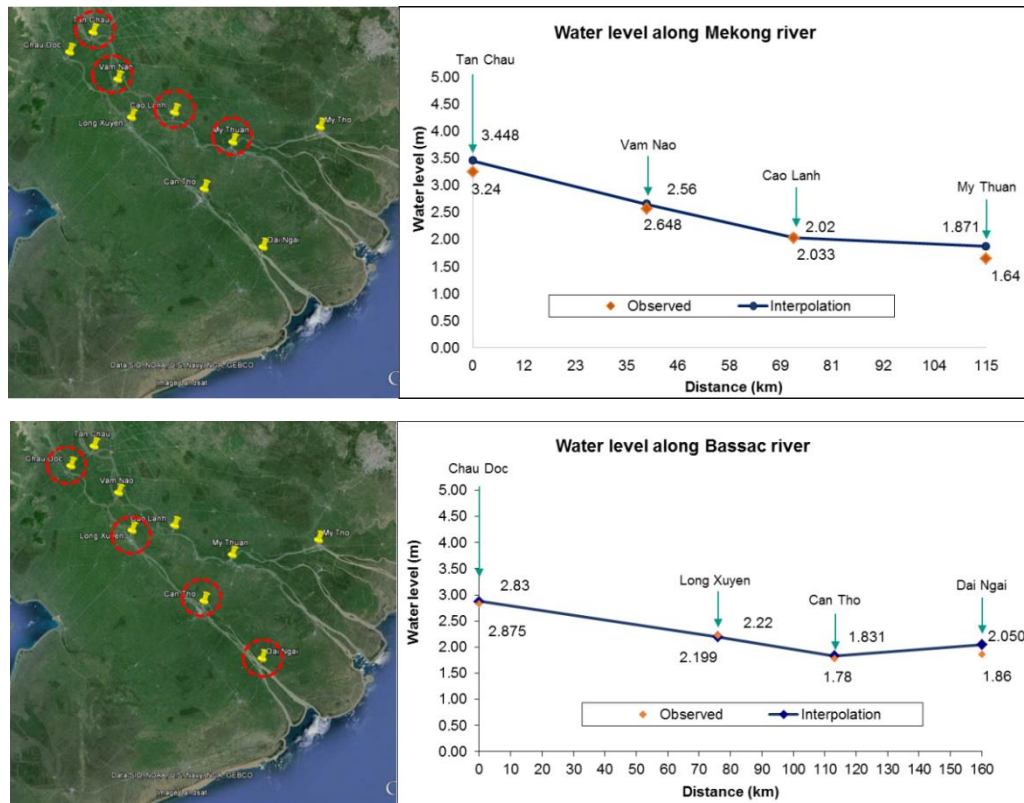


Figure 4.8. Interpolation of flood water level on main rivers for small flood on 30.09.2012

Table 4.7 and Figure 4.8 represent the application of the interpolation method for the prediction of water levels along the Mekong and Bassac Rivers on 30.09.2012. The accuracy of the interpolation method was 88% at the My Thuan gauge, 99% at the Cao Lanh gauge, 97% at the Vam Nao gauge, and 94% at Tan Chau on the Mekong River. On the Bassac River, the accuracy was 91% at the Dai Ngai gauge, 97% at Can Tho, 99% at Long Xuyen, and 98% at the Chau Doc gauge. The flood in 2012 was classified as a low flood, and the results of the interpolation method showed a high level of agreement with the observed data. In contrast, the accuracy at the locations near the East Sea such as Dai Ngai and My Thuan had lower accuracy in comparison

Application of GIF and remote sensing into flood monitoring and land use management for the MD

with the flood in 2011 due to the fact that the impact of tides was stronger than the impact of the dykes with this flood.

4.2.3. Interpolation of flood level for flood in 2013

Table 4.8. Calculation for flood interpolation on 2.10.2013

$Q_{\text{max Tan Chau}} = 25200 \text{ (m}^3/\text{s)}$, $Q_{\text{max Chau Doc}} = 7370 \text{ (m}^3/\text{s)}$; $Q_{\text{total}} = 32570 \text{ (m}^3/\text{s)}$

Compartment	Wet area (ha)	Dry area A*i (ha)	Total area Ai (ha)	A*i/Ai	Mekong river				Bassac river			
					ΔZ_i _Tanchau (cm)	ΔZ_i _Vam Nao (cm)	ΔZ_i _Cao Lanh (cm)	ΔZ_i _My Thuan (cm)	ΔZ_i _Chau Doc (cm)	ΔZ_i _Long Xuyen (cm)	ΔZ_i _Can Tho (cm)	ΔZ_i _Dai Ngai (cm)
A1	7,604	25,625	33,229	0.771	1	1	0	0	2	1	0	0
A2	88,294	26,891	115,186	0.233	0	0	0	0	0	0	0	0
A3	15,922	74,889	90,811	0.825	0	0	0	0	1	0	0	0
A4	45,180	14,253	59,434	0.240	0	0	0	0	0	0	0	0
A5	13,867	25,196	39,063	0.645	0	0	0	0	0	0	0	0
A6	29,108	3,853	32,961	0.117	0	0	0	0	0	0	0	0
A7	60,453	12,058	72,512	0.166	0	0	0	0	0	0	0	0
A8	50,756	22,137	72,893	0.304	0	0	0	0	0	0	0	0
A9	77,202	84,710	161,912	0.523	1	2	1	0	1	4	0	0
A10	19,759	57,287	77,046	0.744	10	2	0	0	5	1	0	0
A11	7,363	30,385	37,748	0.805	2	5	3	0	1	1	0	0
A12	49,956	49,704	99,661	0.499	1	3	8	1	2	5	0	0
A13	21,729	6,928	28,657	0.242	0	0	0	0	1	0	0	0
A14	19,169	794	19,963	0.040	0	1	0	0	0	0	0	0
A15	8,307	8,264	16,572	0.499	1	0	0	0	0	0	0	0
A16	34,812	1,234	36,047	0.034	0	0	0	0	0	0	0	0
A17	37,946	17,119	55,065	0.311	3	2	0	0	3	1	0	0
A18	71,165	8,334	79,499	0.105	0	1	0	0	0	0	0	0
A19	37,367	30,444	67,811	0.449	0	0	0	0	0	0	0	0
A20	38,284	44,311	82,595	0.536	0	0	0	0	0	0	0	0
A21	22,673	52,146	74,819	0.697	0	0	0	0	0	0	0	0
A22	24,358	71,224	95,582	0.745	0	0	0	0	0	0	0	0
F_full	0	1,449,064	1,449,064	1	35	32	15	2	25	26	0	0
			Total_Ai (i=1-22)		18	17	12	1	16	13	0	0
			Kc=F_full/sum(A1:A22)		1.94	1.88	1.25	2.00	1.53	2.02	-	-

Table 4.9. Interpolation of flood water along main rivers on 2.10.2013

Flood 2013	Gauge	Distance (km)	Z_baseline (m)	ΔZ _2013 (m)	Interpolation (m)	Observed water level (m)	Agreement (%)
Mekong river	Tan Chau	0	3.886	0.399	4.285	4.32	99%
	Vam Nao	39	2.901	0.371	3.272	3.10	95%
	Cao Lanh	72	2.173	0.149	2.322	2.41	96%
	My Thuan	115	1.871	0.013	1.884	1.75	93%
Bassac River	Chau Doc	0	3.541	0.174	3.714	3.59	97%
	Long Xuyen	76	2.198	0.317	2.515	2.32	92%
	Can Tho	113	1.870	0.118	1.988	1.90	96%
	Dai Ngai	160	2.080	0.000	2.080	1.83	88%

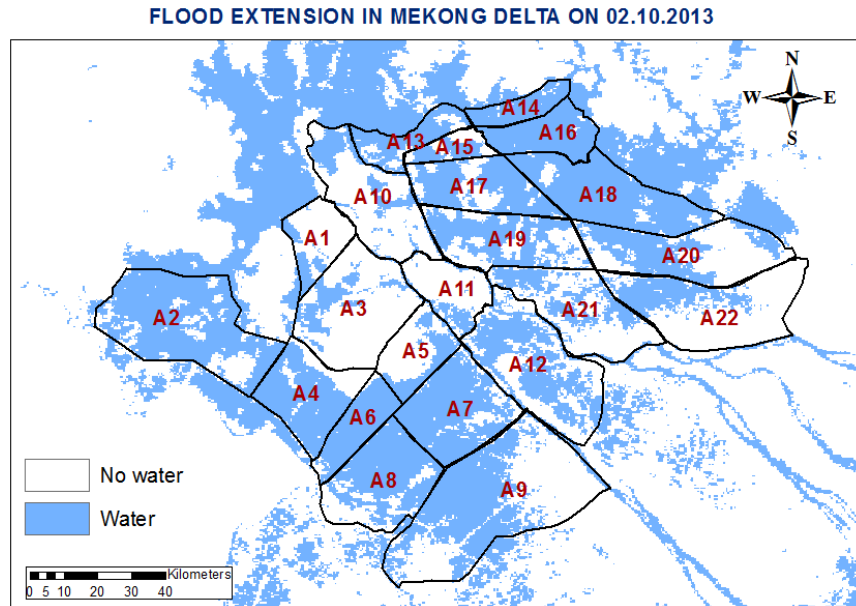


Figure 4.9. Flood extension on 02.10.2013

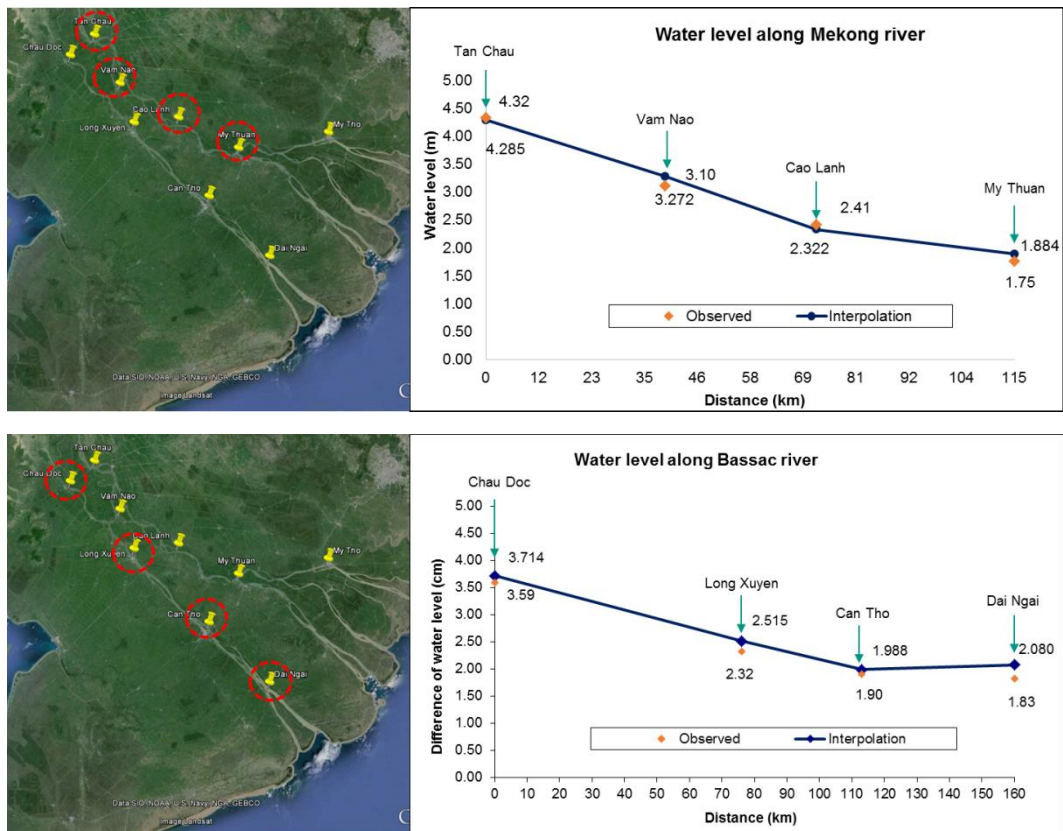


Figure 4.10. Interpolation of flood water level along main rivers on 02.10.2013

Table 4.9 and Figure 4.10 show the application of the interpolation method for prediction of water level along the Mekong and Bassac Rivers on 02.10.2013. The accuracy of the interpolation method as 93% at the My Thuan gauge, 96% at the Cao Lanh gauge, 95% at the Vam Nao gauge, and 99% at Tan Chau on the Mekong River. The accuracy on the Bassac River was 88% at the Dai Ngai gauge, 96% at Can Tho, 92% at Long Xuyen, and 97% at the Chau Doc gauge. The flood in 2013 was classified as a medium flood; the results of interpolation method showed a higher level of agreement with the low flood in 2012 but lower accuracy than the one in 2011.

Application of GIF and remote sensing into flood monitoring and land use management for the MD

Therefore, it can be concluded that the magnitude of the flood plays a major factor when using the interpolation method.

4.2.4. Interpolation of flood level for flood in 2014

Table 4.10. Calculation for flood interpolation on 11.08.2014

Q_{\max} Tan Chau = 20725 (m^3/s), Q_{\max} Chau Doc = 5550 (m^3/s); $Q_{\text{total}} = 26275$ (m^3/s)

Compartment	Wet area (ha)	Dry area A^*i (ha)	Total area Ai (ha)	A^*/Ai	Mekong river				Bassac river			
					$\Delta Zi_{\text{Tanchau}}$ (cm)	$\Delta Zi_{\text{Vam Nao}}$ (cm)	$\Delta Zi_{\text{Cao Lanh}}$ (cm)	$\Delta Zi_{\text{My Thuan}}$ (cm)	$\Delta Zi_{\text{Chau Doc}}$ (cm)	$\Delta Zi_{\text{Long Xuyen}}$ (cm)	$\Delta Zi_{\text{Can Tho}}$ (cm)	$\Delta Zi_{\text{Dai Ngai}}$ (cm)
A1	10,449	22,781	33,229	0.686	0.03	0.05	0.00	0.00	1.05	0.05	0.00	0.00
A2	6,805	108,381	115,186	0.941	0.95	0.95	0.95	0.00	1.89	2.84	0.00	0.00
A3	41,064	49,747	90,811	0.548	0.95	0.95	0.00	0.00	1.95	0.95	0.00	0.00
A4	14,318	45,116	59,434	0.759	0.00	0.00	0.00	0.00	0.00	0.00	0.00	0.00
A5	11,114	27,412	38,526	0.712	0.00	0.95	0.00	0.00	0.00	0.95	0.00	0.00
A6	1,943	31,018	32,961	0.941	0.00	0.00	0.00	0.00	0.00	0.00	0.00	0.00
A7	3,697	68,814	72,512	0.949	0.00	0.00	0.00	0.00	0.00	0.00	0.00	0.00
A8	794	72,098	72,893	0.989	0.00	0.00	0.00	0.00	0.00	0.00	0.00	0.00
A9	2,377	159,534	161,912	0.985	1.00	2.00	0.05	0.00	1.95	6.84	7.05	0.11
A10	19,963	57,083	77,046	0.741	7.16	2.95	0.00	0.00	-0.74	0.24	0.15	0.06
A11	2,984	34,764	37,748	0.921	2.00	4.05	2.05	0.00	1.02	1.95	-1.03	-1.00
A12	8,071	91,589	99,661	0.919	0.97	3.00	6.11	1.00	1.53	5.95	4.05	-0.95
A13	17,731	10,926	28,657	0.381	0.00	0.95	0.00	0.00	0.53	0.00	0.00	0.00
A14	8,254	11,710	19,963	0.587	0.00	0.05	0.09	0.09	0.09	0.19	0.19	0.06
A15	7,588	8,983	16,572	0.542	1.00	0.00	0.00	0.00	0.00	0.00	0.00	0.00
A16	29,886	6,161	36,047	0.171	0.00	0.00	0.00	0.00	0.00	0.00	0.00	0.00
A17	36,170	18,895	55,065	0.343	1.11	0.11	0.00	0.00	1.58	0.05	0.00	0.00
A18	52,253	27,246	79,499	0.343	0.00	0.05	0.00	0.00	0.00	0.00	0.00	0.00
A19	24,514	43,297	67,811	0.638	0.00	0.00	0.00	0.00	0.00	0.00	0.00	0.00
A20	5,731	76,864	82,595	0.931	0.00	0.00	0.00	0.00	0.00	0.00	0.00	0.00
A21	1,771	73,048	74,819	0.976	0.00	0.00	0.95	0.00	0.00	0.00	0.00	0.00
A22	188	95,394	95,582	0.998	0.00	0.00	0.00	0.00	0.00	0.00	0.00	0.00
F_full	0	1,448,527	1,448,527	1	17.97	19.70	9.32	0.11	12.70	24.11	11.22	0.00
Total_Ai (i=1-22)					15.16	16.05	10.20	1.09	10.85	19.99	10.42	-1.72
$Kc=F_{\text{full}}/\text{sum}(A1:A22)$					1.19	1.23	0.91	0.10	1.17	1.21	1.08	0.00

Table 4.11. Interpolation of flood water along main rivers on 11.08.2014

Flood 2014	Gauge	Distance (km)	Z_{baseline} (m)	ΔZ_{2014} (m)	Interpolation (m)	Observed water level (m)	Agreement (%)
Mekong river	Tan Chau	0	3.265	0.239	3.504	3.71	94%
	Vam Nao	39	2.396	0.334	2.731	2.41	88%
	Cao Lanh	72	1.943	0.149	2.092	2.02	97%
	My Thuan	115	1.878	0.001	1.880	1.90	99%
Bassac River	Chau Doc	0	2.793	0.149	2.943	2.96	99%
	Long Xuyen	76	1.885	0.371	2.256	2.27	99%
	Can Tho	113	1.738	0.109	1.847	1.75	95%
	Dai Ngai	160	2.071	0.000	2.071	2.10	99%

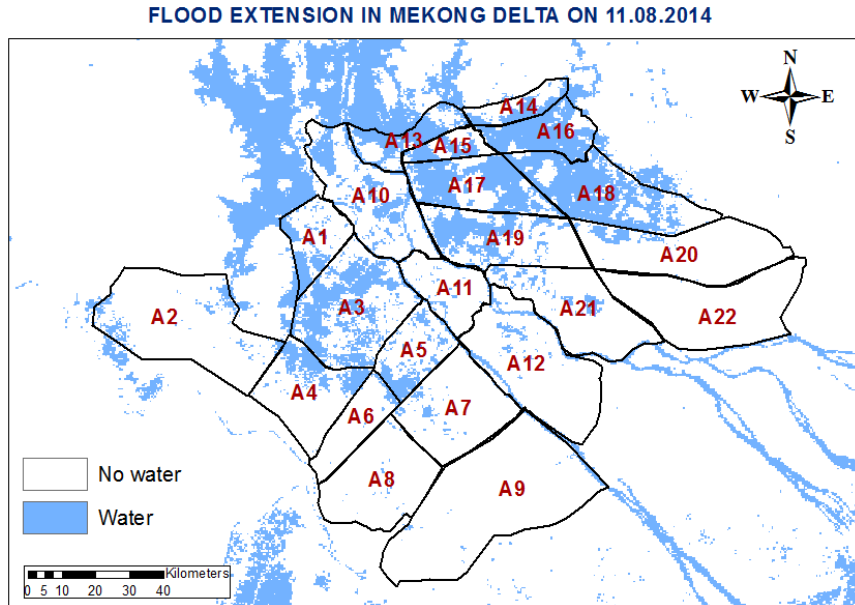


Figure 4.11. Flood extension on 11.08.2014

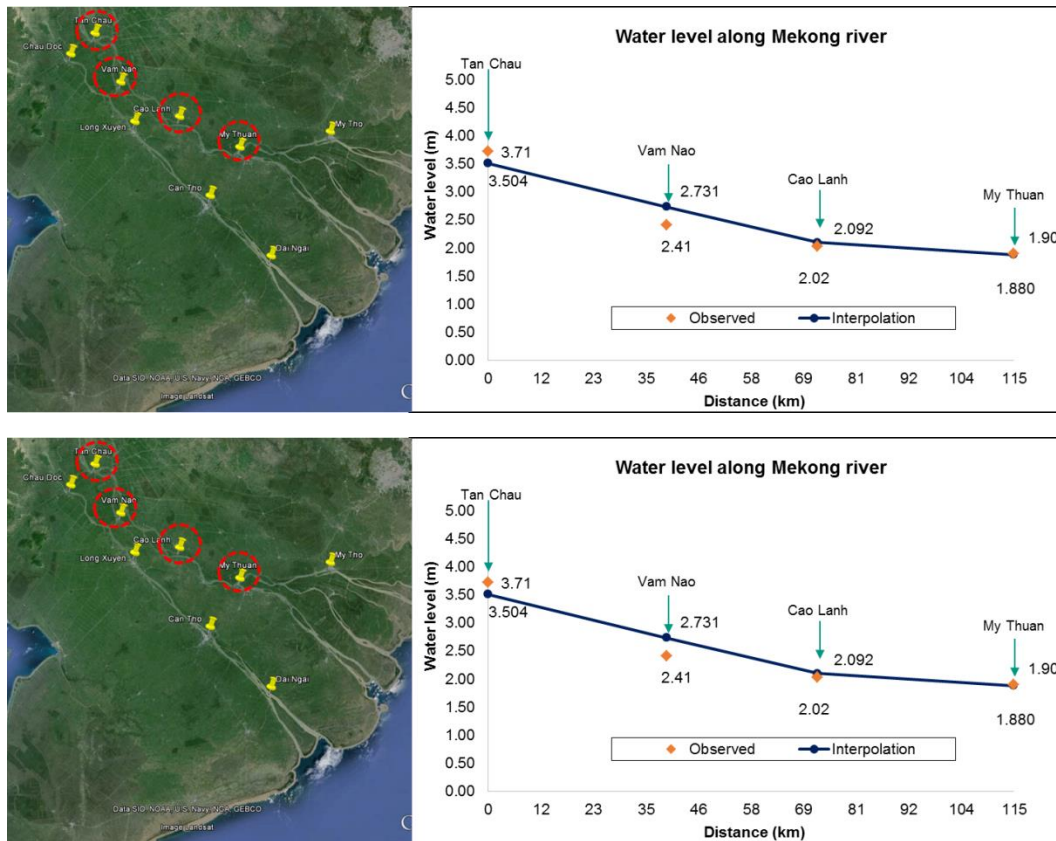


Figure 4.12. Interpolation of flood water level along main rivers on 11.08.2014

Similarly, Table 4.11 and Figure 4.12 showed the application of interpolation method for the prediction of water levels along the Mekong and Bassac Rivers on 11.08.2014. The accuracy of the interpolation method was 99% at the My Thuan gauge, 97% at the Cao Lanh gauge, 88% at the Vam Nao gauge, and 94% at Tan Chau on the Mekong River. Similarly, the accuracy on the Bassac River was 99% at the Dai Ngai gauge, 95% at Can Tho, 99% at Long Xuyen, and 99% at the Chau Doc gauge. The flood in 2014 was classified as a medium flood, so the results of the interpolation method showed a higher agreement with the observed water levels at the gauges.

Application of GIF and remote sensing into flood monitoring and land use management for the MD

4.2.5. Interpolation of flood level for flood in 2015

Table 4.12. Calculation for flood interpolation on 16.8.2015

Q_{\max} Tan Chau = 16526 (m^3/s), Q_{\max} Chau Doc = 2426 (m^3/s); $Q_{\text{total}} = 18952$ (m^3/s)

Compartment	Wet area (ha)	Dry area A^*i (ha)	Total area A_i (ha)	A^*i/A_i	Mekong river				Bassac river			
					ΔZ_i Tanchau (cm)	ΔZ_i Vam Nao (cm)	ΔZ_i Cao Lanh (cm)	ΔZ_i My Thuan (cm)	ΔZ_i Chau Doc (cm)	ΔZ_i Long Xuyen (cm)	ΔZ_i Can Tho (cm)	ΔZ_i Dai Ngai (cm)
A1	6,778	26,451	33,229	0.796	-0.52	-1.03	0.00	0.00	-0.03	-1.03	0.00	0.00
A2	7,733	107,453	115,186	0.933	2.03	2.03	2.03	0.00	4.06	6.10	0.00	0.00
A3	46,581	44,230	90,811	0.487	2.03	2.03	0.00	0.00	3.03	2.03	0.00	0.00
A4	5,087	54,346	59,434	0.914	0.00	0.00	0.00	0.00	0.00	0.00	0.00	0.00
A5	14,699	23,827	38,526	0.618	0.00	2.03	0.00	0.00	0.00	2.03	0.00	0.00
A6	1,454	31,507	32,961	0.956	0.00	0.00	0.00	0.00	0.00	0.00	0.00	0.00
A7	3,622	68,889	72,512	0.950	0.00	0.00	0.00	0.00	0.00	0.00	0.00	0.00
A8	5,018	67,875	72,893	0.931	0.00	0.00	0.00	0.00	0.00	0.00	0.00	0.00
A9	7,030	154,882	161,912	0.957	1.00	2.00	-1.03	0.00	3.03	10.10	5.97	-2.06
A10	18,037	59,010	77,046	0.766	3.90	4.03	0.00	0.00	4.04	1.54	1.23	0.82
A11	10,067	27,680	37,748	0.733	2.00	2.97	0.97	0.00	0.59	3.03	-0.48	-1.00
A12	10,454	89,207	99,661	0.895	1.52	3.00	3.94	1.00	0.98	7.03	2.97	-2.03
A13	7,175	21,482	28,657	0.750	0.00	2.03	0.00	0.00	-0.02	0.00	0.00	0.00
A14	478	19,486	19,963	0.976	0.00	-1.03	0.20	0.10	0.20	0.41	0.41	0.93
A15	2,050	14,522	16,572	0.876	1.00	0.00	0.00	0.00	0.00	0.00	0.00	0.00
A16	8,425	27,621	36,047	0.766	0.00	0.00	0.00	0.00	0.00	0.00	0.00	0.00
A17	9,268	45,797	55,065	0.832	-1.06	-2.06	0.00	0.00	-0.05	-1.03	0.00	0.00
A18	24,777	54,722	79,499	0.688	0.00	-1.03	0.00	0.00	0.00	0.00	0.00	0.00
A19	10,583	57,228	67,811	0.844	0.00	0.00	0.00	0.00	0.00	0.00	0.00	0.00
A20	3,274	79,322	82,595	0.960	0.00	0.00	0.00	0.00	0.00	0.00	0.00	0.00
A21	4,422	70,397	74,819	0.941	0.00	0.00	2.03	0.00	0.00	0.00	0.00	0.00
A22	521	95,062	95,582	0.995	0.00	0.00	0.00	0.00	0.00	0.00	0.00	0.00
F_full	0	1,448,527	1,448,527	1	-1.58	5.58	2.81	-0.03	-1.42	21.94	6.87	0.00
Total A_i (i=1-22)					11.90	14.97	8.14	1.10	16	30	10	-3
$Kc=F_{\text{full}}/\text{sum}(A1:A22)$					-0.13	0.37	0.34	-0.03	-0.09	0.73	0.68	0.00

Table 4.13. Interpolation of water level along the main rivers for flood on 16.8.2015

Flood 2015	Gauge	Distance (km)	Z_baseline (m)	ΔZ_{2014} (m)	Interpolation (m)	Observed water level (m)	Agreement (%)
Mekong river	Tan Chau	0	2.542	-0.022	2.521	2.43	96%
	Vam Nao	39	1.810	0.087	1.896	1.90	100%
	Cao Lanh	72	1.676	0.043	1.719	-	-
	My Thuan	115	1.732	0.000	1.731	-	-
Bassac River	Chau Doc	0	1.924	-0.020	1.904	2.11	90%
	Long Xuyen	76	1.521	0.441	1.962	-	-
	Can Tho	113	1.583	0.110	1.693	1.45	86%
	Dai Ngai	160	2.062	0.000	2.062	-	-

where "-" means no valuable data for calibration and validation

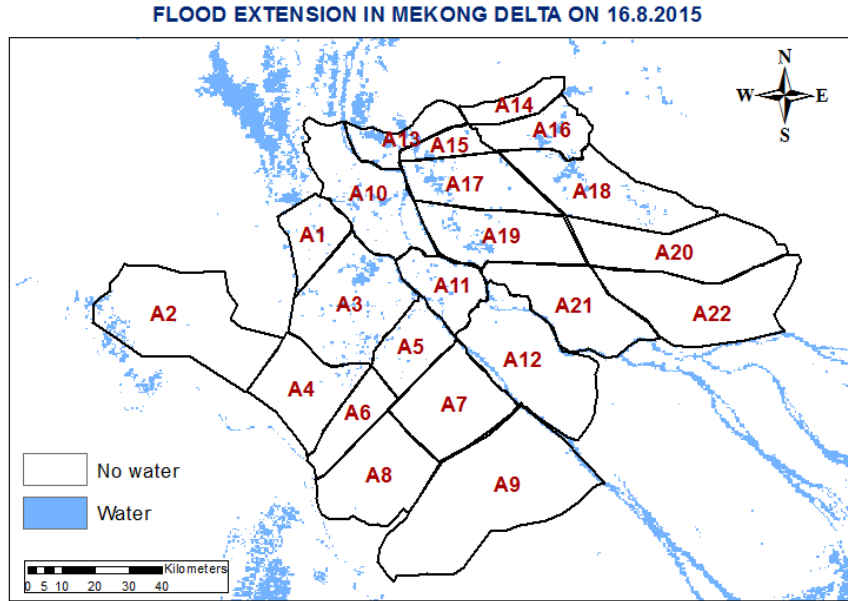


Figure 4.13. Flood extension on 16.08.2015

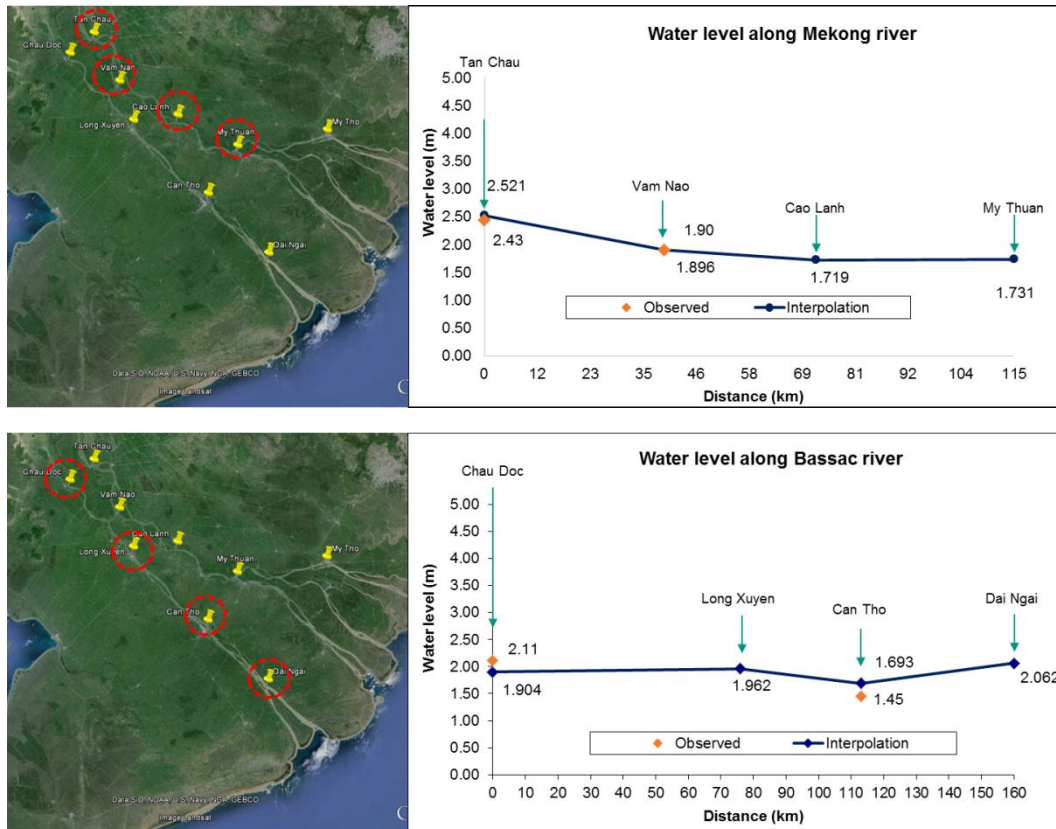


Figure 4.14. Interpolation of flood water level along main rivers on 16.08.2015

Similarly, Table 4.13 and Figure 4.14 show the calculation method of the interpolation water levels along the Mekong and Bassac Rivers on 16.08.2015. The accuracy of the interpolation method is 100% at the Vam Nao gauge and 96% at Tan Chau on the Mekong River. On the other hand, the accuracy on the Bassac River was 86% at Can Tho and 90% at the Chau Doc gauge. The flood in 2015 was classified as a low flood, so the results of the interpolation method showed good agreement with the observed water levels at the gauges. The observed data at My Thuan, Cao Lanh, Long Xuyen and Dai Ngai were missing on the MRC website, so the interpolation method can provide information about the missing data.

Application of GIF and remote sensing into flood monitoring and land use management for the MD

4.2.6. Interpolation of flood level for flood in 2016

Table 4.14. Calculation for flood interpolation on 06.10.2016

Q_{\max} Tan Chau = 21664 (m³/s), Q_{\max} Chau Doc = 4149 (m³/s); Q_{total} = 25813 (m³/s)

Compartment	Wet area (ha)	Dry area A [*] i (ha)	Total area Ai (ha)	A [*] i/Ai	Mekong river				Bassac river			
					ΔZ_i Tanchau (cm)	ΔZ_i Vam Nao (cm)	ΔZ_i Cao Lanh (cm)	ΔZ_i My Thuan (cm)	ΔZ_i Chau Doc (cm)	ΔZ_i Long Xuyen (cm)	ΔZ_i Can Tho (cm)	ΔZ_i Dai Ngai (cm)
A1	5,495	27,734	33,229	0.835	-0.01	-0.01	0.00	0.00	0.99	-0.01	0.00	0.00
A2	13,684	101,501	115,186	0.881	1.01	1.01	1.01	0.00	2.03	3.04	0.00	0.00
A3	8,635	82,177	90,811	0.905	1.01	1.01	0.00	0.00	2.01	1.01	0.00	0.00
A4	19,121	40,313	59,434	0.678	0.00	0.00	0.00	0.00	0.00	0.00	0.00	0.00
A5	11,060	27,680	38,741	0.715	0.00	1.01	0.00	0.00	0.00	1.01	0.00	0.00
A6	21,632	11,329	32,961	0.344	0.00	0.00	0.00	0.00	0.00	0.00	0.00	0.00
A7	48,996	23,516	72,512	0.324	0.00	0.00	0.00	0.00	0.00	0.00	0.00	0.00
A8	35,682	37,211	72,893	0.510	0.00	0.00	0.00	0.00	0.00	0.00	0.00	0.00
A9	60,899	101,013	161,912	0.624	1.00	2.00	-0.01	0.00	2.01	7.04	6.99	-0.03
A10	8,978	68,068	77,046	0.883	6.96	3.01	0.00	0.00	-0.44	0.32	0.21	0.11
A11	3,268	34,480	37,748	0.913	2.00	3.99	1.99	0.00	0.99	2.01	-0.99	-1.00
A12	32,880	66,780	99,661	0.670	1.01	3.00	5.97	1.00	1.49	6.01	3.99	-1.01
A13	16,191	12,466	28,657	0.435	0.00	1.01	0.00	0.00	0.49	0.00	0.00	0.00
A14	10,588	9,375	19,963	0.470	0.00	-0.01	0.10	0.10	0.10	0.20	0.20	0.11
A15	5,635	10,937	16,572	0.660	1.00	0.00	0.00	0.00	0.00	0.00	0.00	0.00
A16	31,668	4,379	36,047	0.121	0.00	0.00	0.00	0.00	0.00	0.00	0.00	0.00
A17	24,176	30,889	55,065	0.561	0.97	-0.03	0.00	0.00	1.48	-0.01	0.00	0.00
A18	57,566	21,933	79,499	0.276	0.00	-0.01	0.00	0.00	0.00	0.00	0.00	0.00
A19	16,985	50,826	67,811	0.750	0.00	0.00	0.00	0.00	0.00	0.00	0.00	0.00
A20	12,058	70,537	82,595	0.854	0.00	0.00	0.00	0.00	0.00	0.00	0.00	0.00
A21	11,613	63,206	74,819	0.845	0.00	0.00	1.01	0.00	0.00	0.00	0.00	0.00
A22	16,432	79,150	95,582	0.828	0.00	0.00	0.00	0.00	0.00	0.00	0.00	0.00
F_full	0	1,448,527	1,448,527	1	16.74	18.81	8.91	-0.03	11.81	23.97	10.94	0.00
			Total_Ai (i=1-22)		15	16	10	1	11	21	10	-2
			Kc=F_full/sum(A1:A22)		1.12	1.18	0.88	-0.03	1.06	1.16	1.05	0.00

Table 4.15. Interpolation of flood water along main rivers on 06.10.2016

Flood 2016	Gauge	Distance (km)	Z _{baseline} (m)	ΔZ_{2016} (m)	Interpolation (m)	Observed water level (m)	Agreement (%)
Mekong river	Tan Chau	0	3.219	0.244	3.463	3.01	87%
	Vam Nao	39	2.359	0.303	2.663	2.47	93%
	Cao Lanh	72	1.926	0.116	2.043	-	-
	My Thuan	115	1.869	0.000	1.869	-	-
Bassac River	Chau Doc	0	2.738	0.156	2.894	2.71	94%
	Long Xuyen	76	1.862	0.405	2.267	-	-
	Can Tho	113	1.728	0.116	1.844	1.76	95%
	Dai Ngai	160	2.071	0.000	2.071	-	-

where "-" means no valuable data for calibration and validation

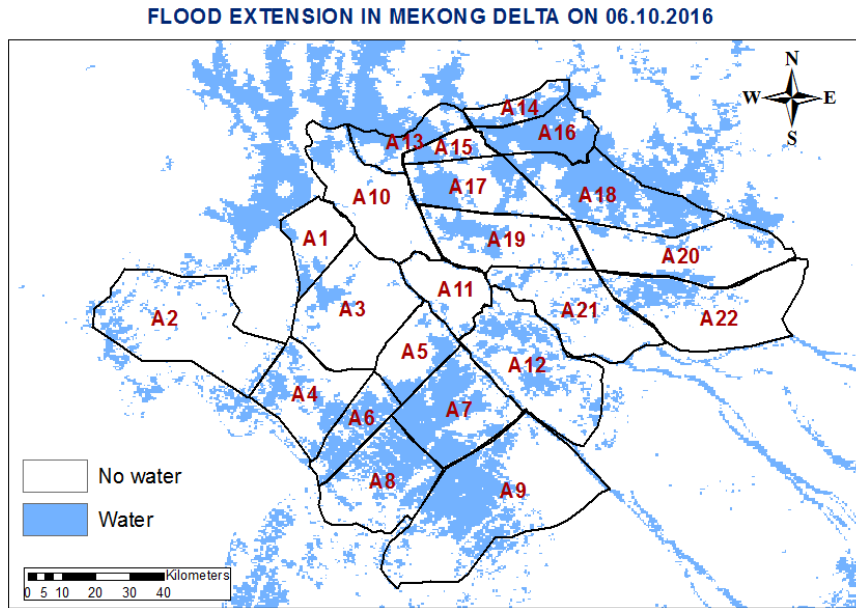


Figure 4.15. Flood extension on 06.10.2016

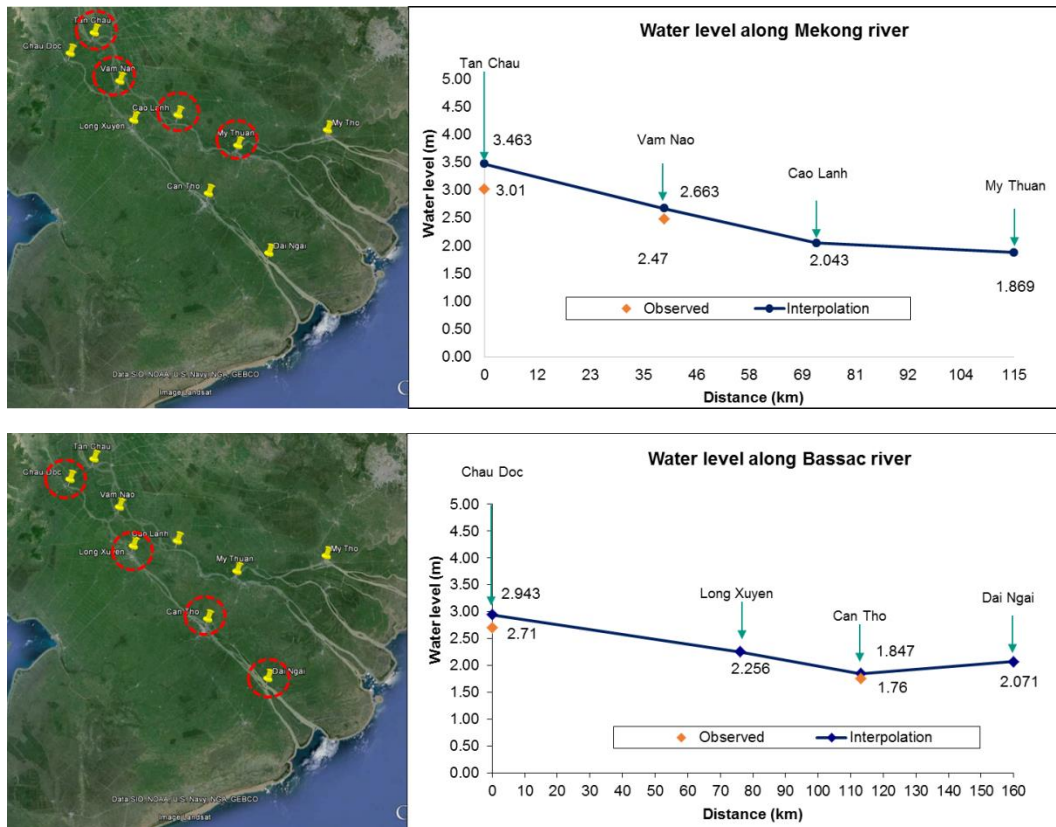


Figure 4.16. Interpolation of flood water level along main rivers on 06.10.2016

Table 4.15 and figure 4.16 show the calculation method for the interpolation of water levels along the Mekong and Bassac Rivers on 06.10.2016. The accuracy of the interpolation was 93% at the Vam Nao gauge and 87% at Tan Chau on the Mekong River. Similarly, the accuracy on the Bassac River was 94% at Can Tho and 95% at the Chau Doc gauge. The flood in 2016 was classified as a low flood, so the results of interpolation method demonstrated good agreement with the observed water levels at the gauges. The observed data on My Thuan, Cao Lanh, Long Xuyen, and Dai Ngai were missing on the MRC website, so the interpolation method can once again provide information about the missing data.

Application of GIF and remote sensing into flood monitoring and land use management for the MD

4.2.7. Interpolation of flood level for flood in 2017

Table 4.16. Calculation for flood interpolation on 10.10.2017

Q_{\max} Tan Chau = 20688 (m³/s), Q_{\max} Chau Doc = 5058 (m³/s); $Q_{\text{total}} = 25746$ (m³/s)

Compartment	Wet area (ha)	Dry area A [*] i (ha)	Total area Ai (ha)	A [*] i/Ai	Mekong river				Bassac river			
					ΔZ_i Tanchau (cm)	ΔZ_i Vam Nao (cm)	ΔZ_i Cao Lanh (cm)	ΔZ_i My Thuan (cm)	ΔZ_i Chau Doc (cm)	ΔZ_i Long Xuyen (cm)	ΔZ_i Can Tho (cm)	ΔZ_i Dai Ngai (cm)
A1	7,755	25,475	33,229	0.767	-0.01	-0.02	0.00	0.00	0.98	-0.02	0.00	0.00
A2	26,752	88,434	115,186	0.768	1.02	1.02	1.02	0.00	2.05	3.07	0.00	0.00
A3	15,117	75,694	90,811	0.834	1.02	1.02	0.00	0.00	2.02	1.02	0.00	0.00
A4	32,065	27,369	59,434	0.460	0.00	0.00	0.00	0.00	0.00	0.00	0.00	0.00
A5	12,214	26,312	38,526	0.683	0.00	1.02	0.00	0.00	0.00	1.02	0.00	0.00
A6	16,733	16,228	32,961	0.492	0.00	0.00	0.00	0.00	0.00	0.00	0.00	0.00
A7	54,695	17,817	72,512	0.246	0.00	0.00	0.00	0.00	0.00	0.00	0.00	0.00
A8	34,426	38,467	72,893	0.528	0.00	0.00	0.00	0.00	0.00	0.00	0.00	0.00
A9	63,367	98,544	161,912	0.609	1.00	1.00	-0.02	0.00	2.02	7.07	6.98	-0.05
A10	20,371	56,675	77,046	0.736	6.93	3.02	0.00	0.00	-0.39	0.33	0.22	0.12
A11	4,030	33,718	37,748	0.893	2.00	4.98	1.98	0.00	0.99	2.02	-0.99	-1.00
A12	44,225	55,436	99,661	0.556	1.01	3.00	5.95	1.00	1.49	6.02	3.98	-1.02
A13	15,455	13,202	28,657	0.461	0.00	1.02	0.00	0.00	0.49	0.00	0.00	0.00
A14	8,007	11,956	19,963	0.599	0.00	0.10	0.10	0.10	0.10	0.20	0.20	0.12
A15	7,572	9,000	16,572	0.543	1.00	0.00	0.00	0.00	0.00	0.00	0.00	0.00
A16	29,859	6,188	36,047	0.172	0.00	0.00	0.00	0.00	0.00	0.00	0.00	0.00
A17	33,943	21,122	55,065	0.384	0.95	-0.05	0.00	0.00	1.46	-0.02	0.00	0.00
A18	64,135	15,364	79,499	0.193	0.00	-0.02	0.00	0.00	0.00	0.00	0.00	0.00
A19	40,291	27,519	67,811	0.406	0.00	0.00	0.00	0.00	0.00	0.00	0.00	0.00
A20	34,646	47,949	82,595	0.581	0.00	0.00	0.00	0.00	0.00	0.00	0.00	0.00
A21	32,000	42,819	74,819	0.572	0.00	0.00	1.02	0.00	0.00	0.00	0.00	0.00
A22	22,571	73,011	95,582	0.764	0.00	0.00	0.00	0.00	0.00	0.00	0.00	0.00
F_full	0	1,448,527	1,448,527	1	16.56	19.68	8.85	-0.05	11.68	23.95	10.90	0.00
			Total_Ai (i=1-22)		14.93	16.00	9.95	1.00	10.88	21.19	9.98	-2.05
			Kc=F_full/sum(A1:A22)		1.11	1.23	0.89	-0.05	1.07	1.13	1.09	0.00

Table 4.17. Interpolation of water level along the main rivers on 10.10. 2017

Flood 2017	Gauge	Distance (km)	Z_baseline (m)	ΔZ _2014 (m)	Interpolation (m)	Observed water level (m)	Agreement (%)
Mekong river	Tan Chau	0	3.213	0.200	3.413	3.35	98%
	Vam Nao	39	2.354	0.271	2.625	2.75	95%
	Cao Lanh	72	1.924	0.108	2.032	-	-
	My Thuan	115	1.868	0.000	1.867	-	-
Bassac River	Chau Doc	0	2.731	0.134	2.864	3.03	95%
	Long Xuyen	76	1.859	0.351	2.210	-	-
	Can Tho	113	1.727	0.111	1.838	1.93	95%
	Dai Ngai	160	2.071	0.000	2.071	-	-

where "-" not valuable data for calibration and validation.

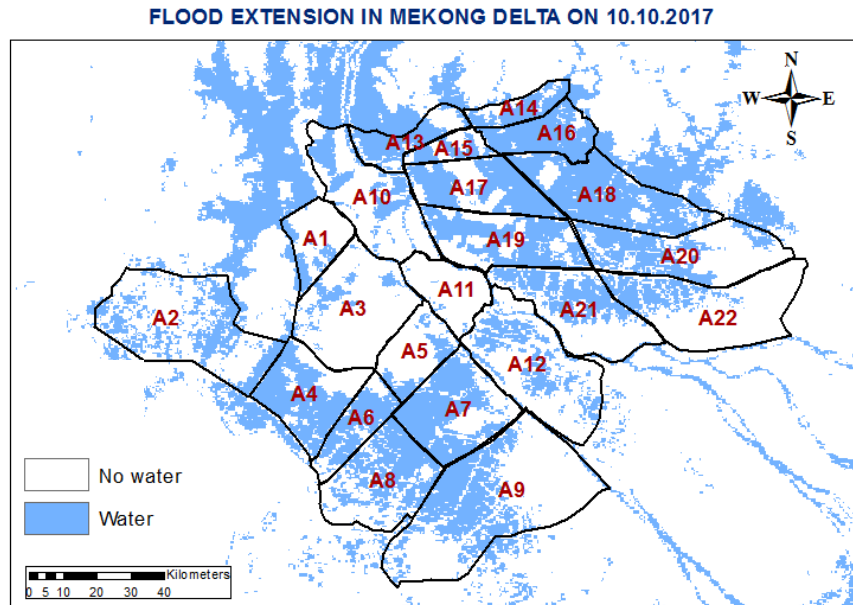


Figure 4.17. Flood extension on 10.10.2017

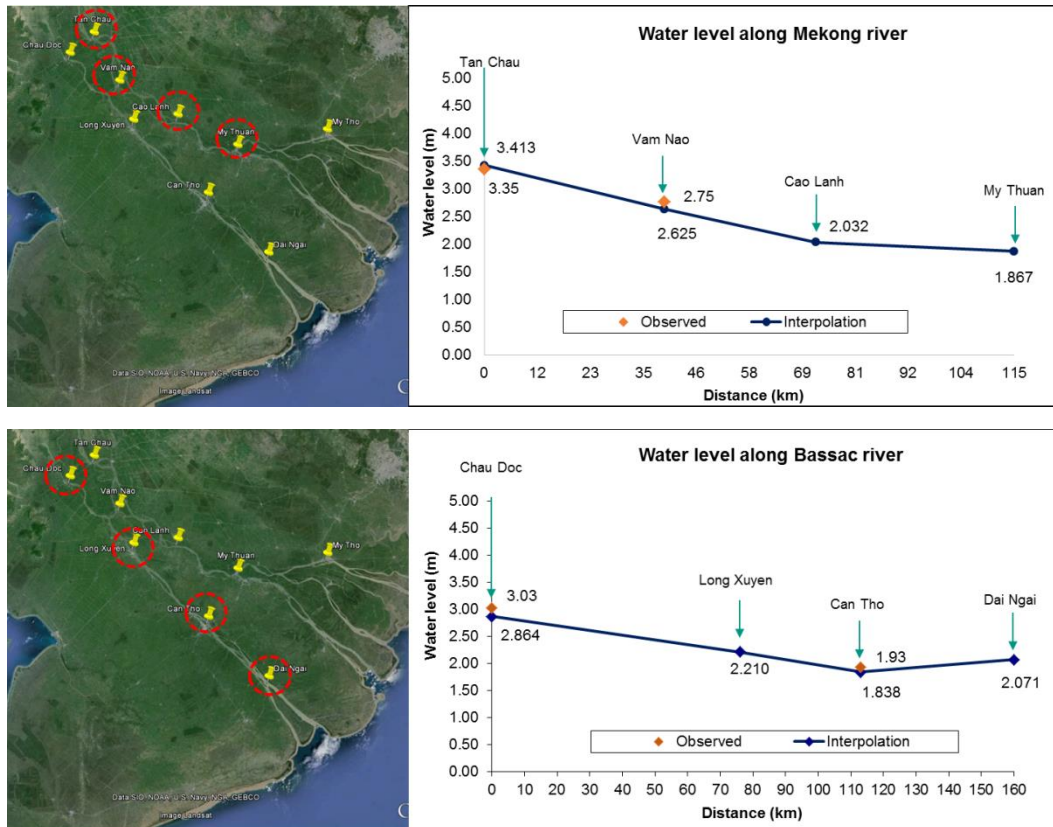


Figure 4.18. Interpolation of flood water level along main rivers on 10.10.2017

Table 4.17 and Figure 4.18 show the calculation method of interpolation of water levels along the Mekong and Bassac Rivers on 10.10.2017. The accuracy of the interpolation method was 95% at the Vam Nao gauge and 98% at Tan Chau on the Mekong River. The accuracy on the Bassac River was 95% at Can Tho and 95% at the Chau Doc gauge. The flood in 2017 was classified as a low flood, so the results of interpolation method demonstrated a high level of agreement with the observed water levels at the gauges. The observed data on My Thuan, Cao Lanh, Long Xuyen, and Dai Ngai were missing on the MRC website. Hence, the interpolation method can provide the unavailable data.

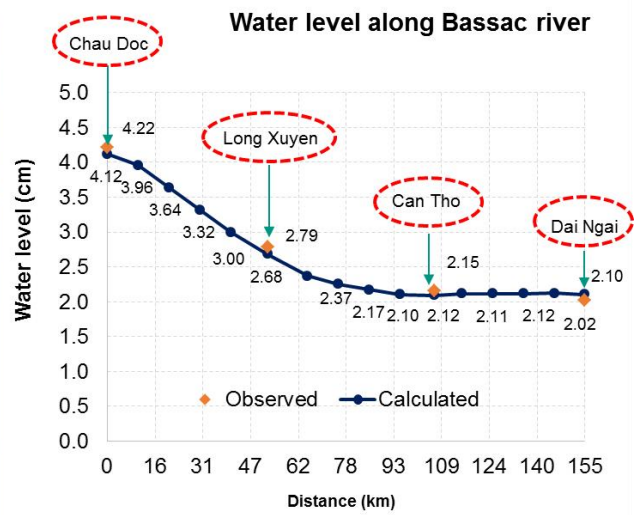
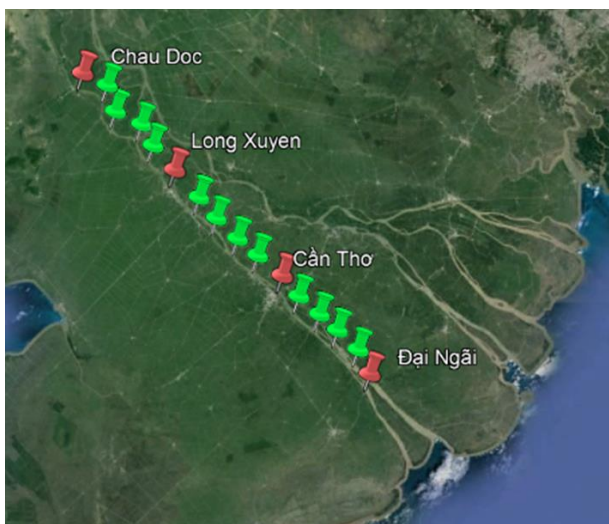
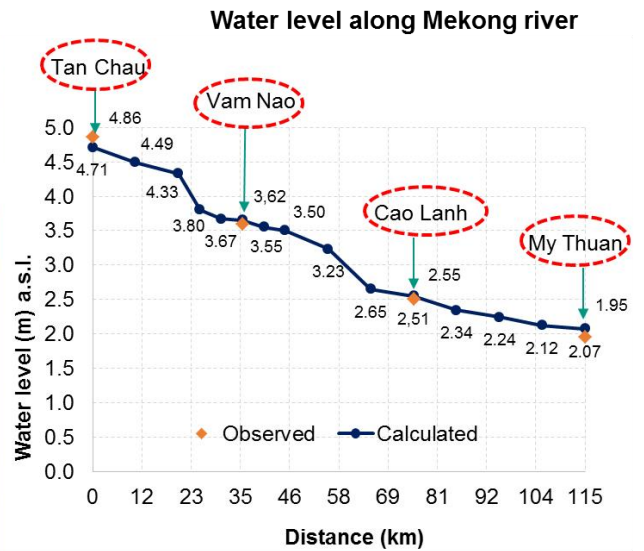
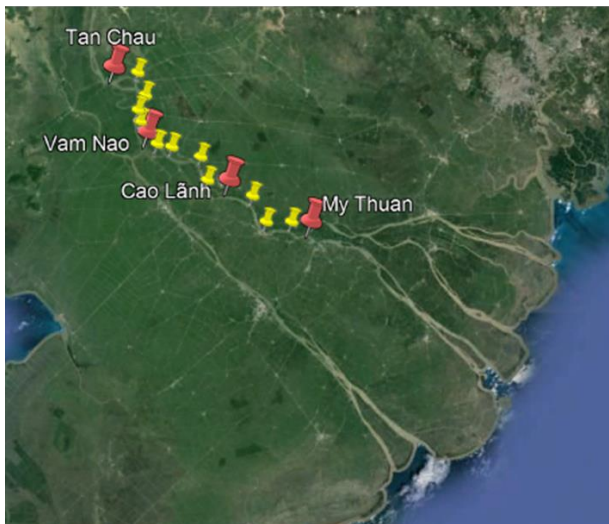
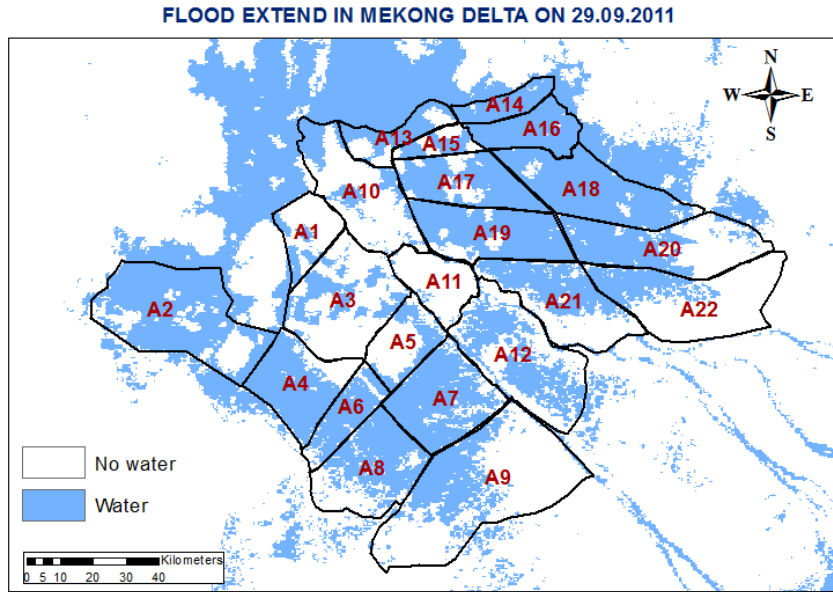


Figure 4.19. Interpolation of unavailable water level along the Mekong and Bassac River on 29.09.2011

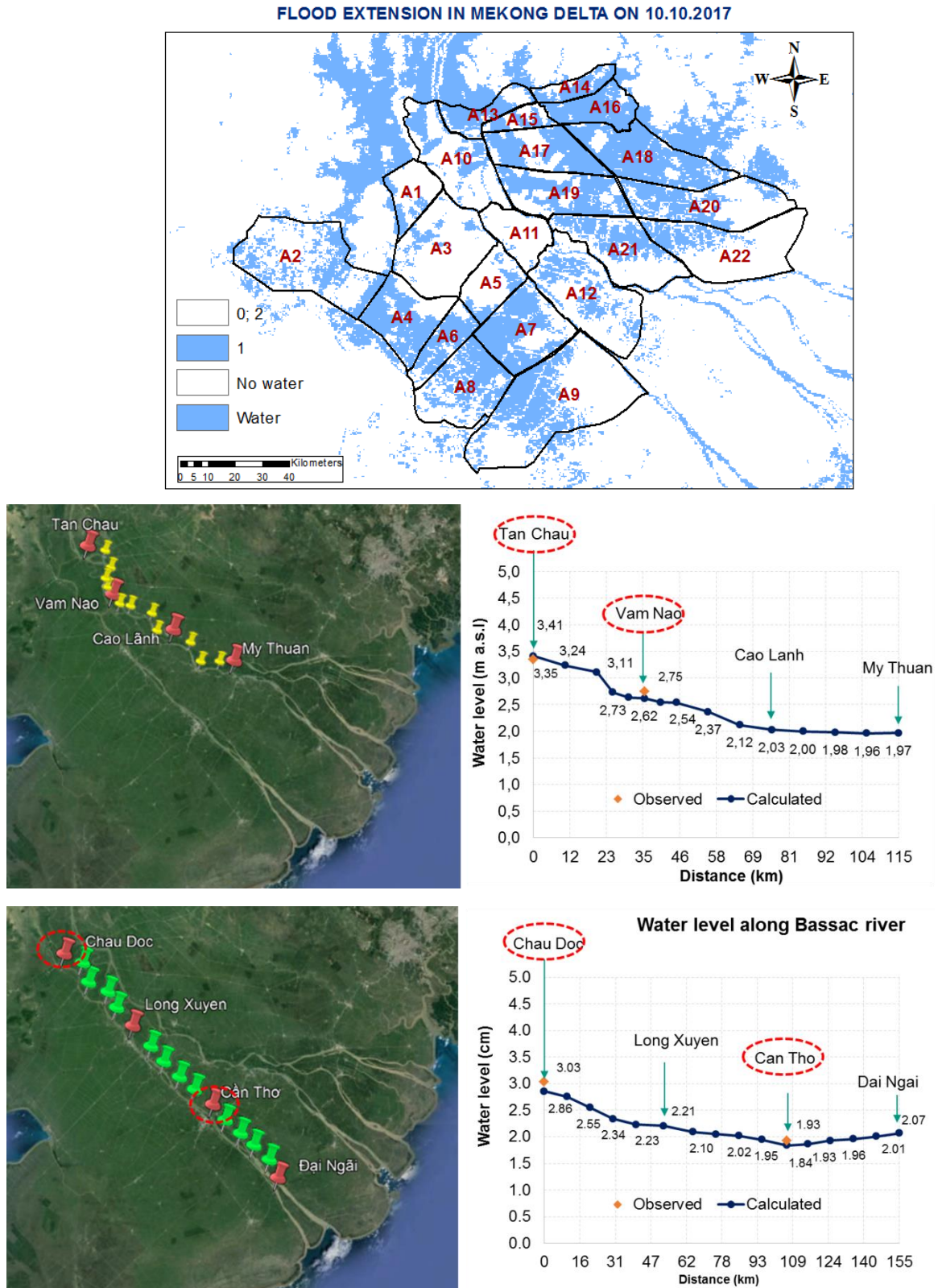


Figure 4.20. Interpolation of unavailable water level along the Mekong and Bassac River on 10.10.2017

Via application the FLEM method, the unavailable water level data on the Mekong and Bassac rivers are calculated on the date 29.9.2011 and 10.10.2017 at any location along the Mekong river with the high accuracy, fast and simple calculation, see Figure 4.19 and Figure 4.20. This is a scientific base for establishment a real-time flood monitoring to support the decision makers in flood management for the MD region.

Application of GIF and remote sensing into flood monitoring and land use management for the MD

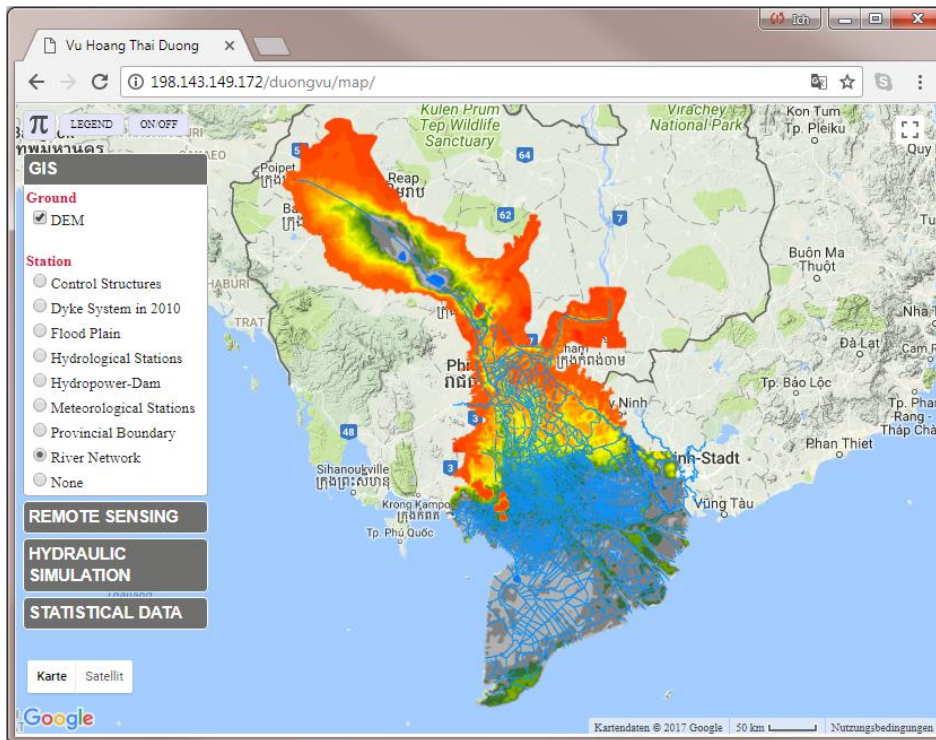


Figure 4.23. Details of GIS menu

A full database of MODIS flood distribution maps (476 maps) in the MD during the flooding seasons from 2000 to 2017, and 7 yearly land use maps (2000, 2003, 2013, 2014, 2015, 2016, 2017) have been interpreted using MODIS satellite products. These satellite products in the MD will be planned to publish online for public access to serve further researches about the Mekong Delta.

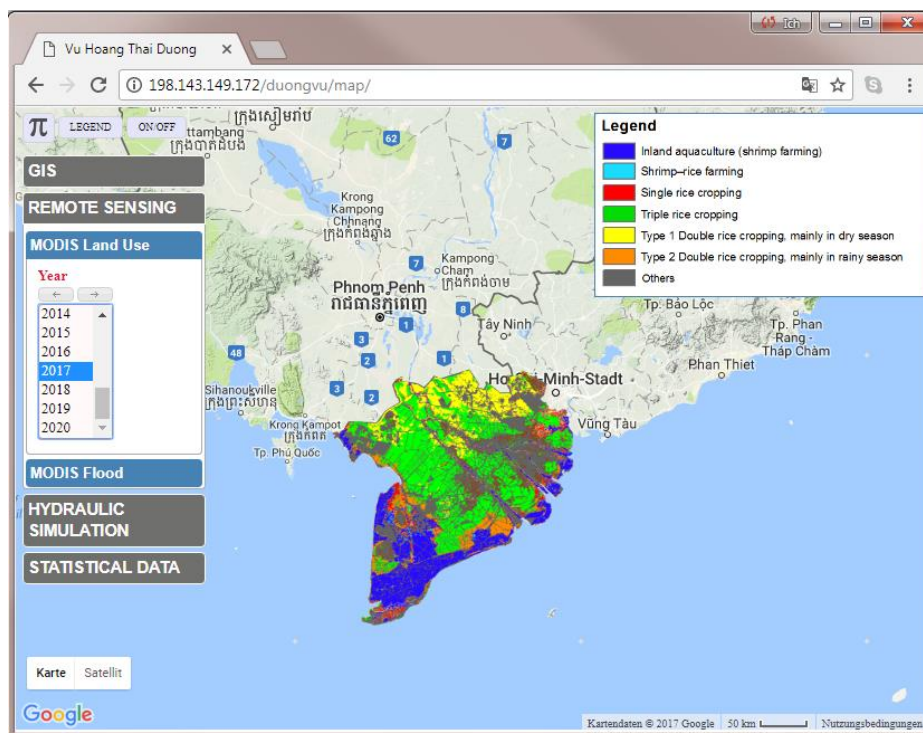


Figure 4.24. Detail of Remote Sensing – Land Use

Application of GIF and remote sensing into flood monitoring and land use management for the MD

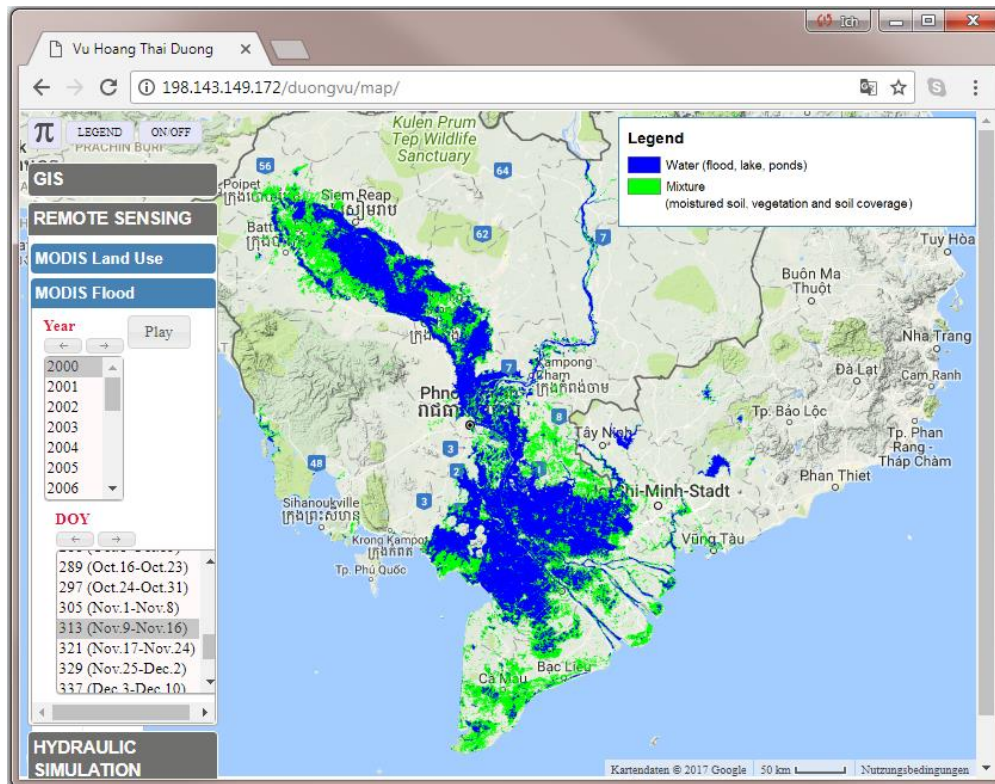


Figure 4.25. Detail of Remote Sensing – Flood Menu

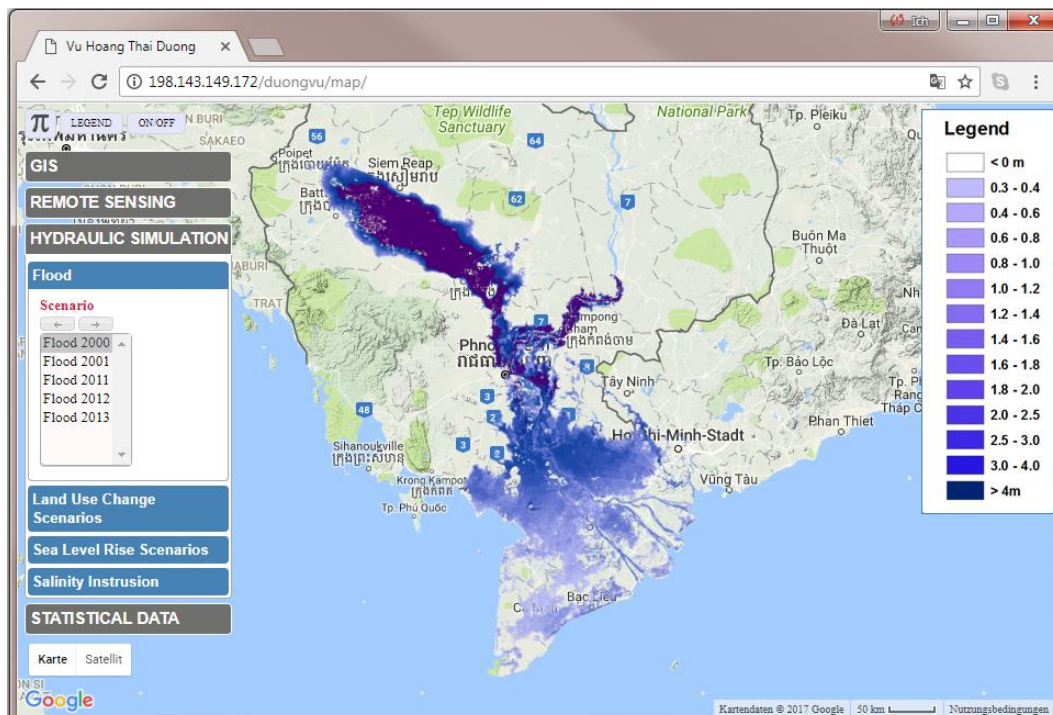


Figure 4.26. Hydraulic Simulation Menu

Application of GIF and remote sensing into flood monitoring and land use management for the MD

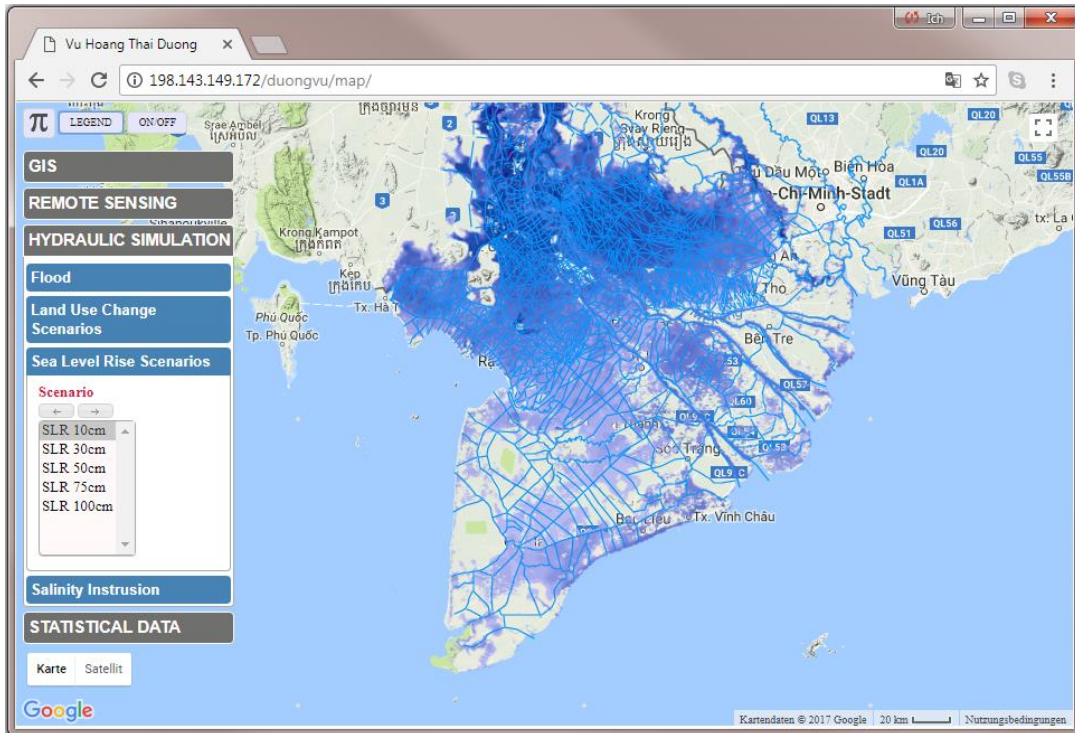


Figure 4.27. Sea level Rice Scenarios

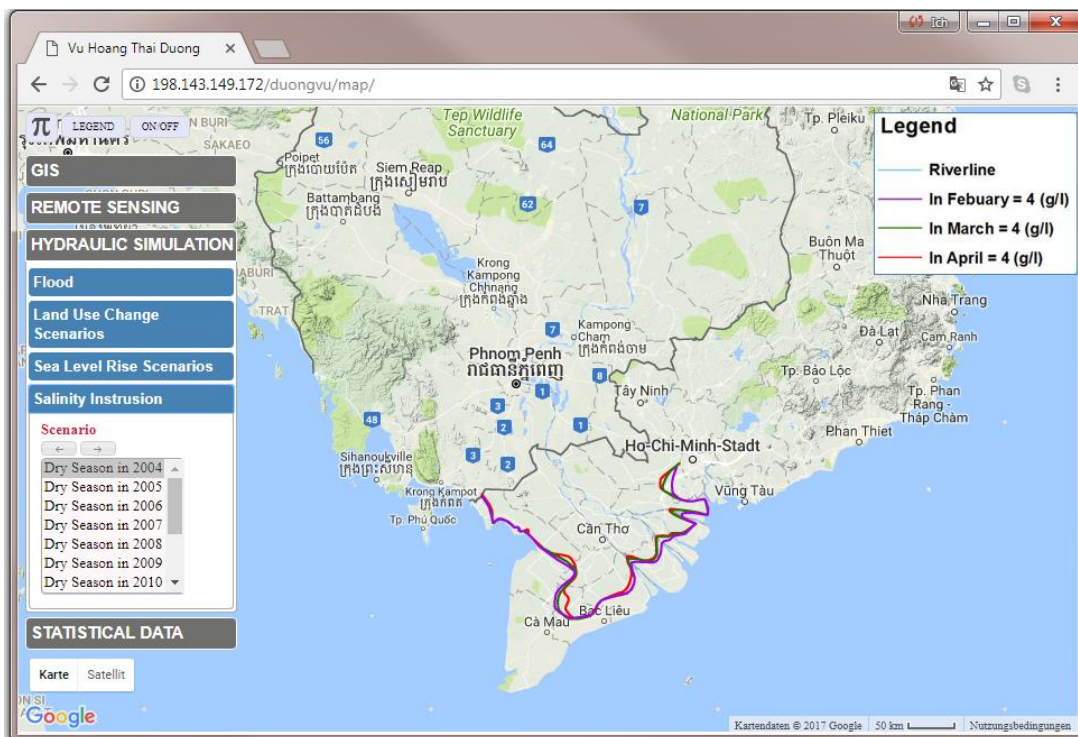


Figure 4.28. Salinity Simulation Menu

4.4. Discussion

The GIF was applied to optimize the locations of dyke measurement for triple rice cropping in the upstream provinces of the MD in terms of the hydraulic sector. However, to have an overall assessment and recommendation for the areas for triple rice cropping in the MD, an evaluation of the impact in regards to society and our economy should be also considered.

Application of GIF and remote sensing into flood monitoring and land use management for the MD

The upper part of the Mekong Delta was divided into 22 compartments along the main canals and rivers in order to evaluate several impacts of full-dyke measurements at the different compartments on the flood water levels by GIF. Flood maps from satellite products and observed hydraulic data from the MRC website were also used for the interpolation method (FLEM). The results of the interpolation method were calibrated for the three different types of floods in 2011 (high flood), in 2012 (low flood), and in 2013 (medium flood) with an accuracy from 90% to 96% in comparison with observed hydraulic data from the Mekong and Bassac Rivers. Afterwards, this method was applied to interpolate water levels on the Mekong and Bassac Rivers for the floods in 2014, 2015, 2016 and 2017, respectively. The results of the interpolation of flood water along the main rivers demonstrated a high level of agreement with the observed water level.

The interpolation method (FLEM) is a simple, alternative option to forecast the water levels at any location along the Mekong and Bassac Rivers. Hence, the results extracted from the interpolation method can also meet the purpose of providing the missing data on water levels along the Mekong and Bassac River which are not measured.

The online implementation system has been developing for interactive purpose that presents the relating information about land use, dyke and sluice system, hydrological and meteorological gauges, flooding situation in the MD from 2000 until now. This can serve as a database for the further studies to establish of a near-real-time flood monitoring system to support authorities and decision-makers in flood management for the MD region.

5. Conclusion and outlooks

5.1. Conclusions

The agricultural development in the Mekong Delta over recent years has had a significant impact in economic terms for Vietnam. With the rapid development of triple rice cropping patterns, especially in the deep flooding zones, the areas for floodplains have decreased. This has caused a change in the annual flood distribution in the Mekong Delta. Places where the flood water would normally have occupied during flooding seasons in the Long Xuyen quadrangle (LXQ) and Plain of Reeds have been reduced, which has made water levels on the main rivers increase and caused negative impacts for downstream areas such as Cantho City.

The Geographical Impact Factor (GIF) could be used as an expression of the influence of dyke measurements on flood water levels along the main rivers. With different geographical locations of dyke compartments, different impacts on flooding situations along the main rivers were analyzed.

The GIF was established to help scientists and planners with various aspects. It could help to anticipate the possible impact of full-dyke measurement on water levels along the main rivers. It will moreover be a scientific basis to develop an interpolation tool for flood water level prediction in the Mekong Delta. Agricultural production plans under full-dyke protection could be assessed and optimized according to the determined acceptable flood water levels along the rivers. The smaller the GIF identified for any full-dike compartment, the better the triple rice production that can potentially be cultivated in that compartment will be.

Satellite products are valuable tools for monitoring flooding and land use detection in the MD. The MODIS land use maps demonstrated a high level of accuracy in comparison with statistical data and were also reconfirmed through field trips in Dong Thap and An Giang provinces. The algorithms for land use detection by Sakamoto et al. (2009) were applied as well for the years from 2013 to 2017. The products of MODIS land use played an important role for the detection of land use patterns in the MD region in order to calibrate the statistical data. These products can provide a rapid, visualized spatial view of land use pattern in the MD in comparison with the statistical data, which only offers the numbers after a lapse of one year. It could be an effective approach for the survey of land use patterns within the MD to replace the more traditional methods of survey. Hence, a lot of manpower and data processing costs could be saved thanks to this more modern approach. The MODIS flood maps have acceptable accuracy in comparison with radar satellite products. They corresponded well with actual flood levels in the Mekong Rivers. Also, the MODIS flooding and land use maps were also confirmed in terms of their appropriateness via field trips to the Mekong Delta. Satellite products should be used as an important input data about dyke compartment for hydraulic modelling in order to evaluate the impact of dyke measurements on flooding waters along the Mekong Rivers.

Conclusion and outlooks

The hydraulic model MIKE11 is an appropriate tool to simulate flood hazards for a large and complex river network such as the Mekong Delta. It has shown acceptable accuracy to the results gathered by the hydraulic gauges and flood distribution as compared with flood mappings created by satellite products. A new database of the Mekong river network has been built in MIKE11 during the period of implementation for this dissertation. This improved MIKE11 network is a valuable database that could simulate the Mekong River network faster and give higher accuracy in comparison with the available Mekong networks that belong to other Vietnamese organizations.

Also, an interpolation calculation method (FLEM) was developed to calculate water levels along the Mekong and Bassac Rivers; this method is an alternative approach to assist engineers in quickly forecasting flood levels for any specific location along the main rivers. This is an important finding of the thesis that can decrease in the future the dependence on the observed data, which is not easy to collect.

5.2. Outlooks

The study provides a scientific basis for flood monitoring in the Mekong Delta based on satellite land use products to support decision-making about flood management in the Delta. The thesis has also discovered the impact of GIFs on the main rivers. Therefore, it is highly recommended that further researches should be conducted in regards to the impact of GIFs on inland canals in order to have a general view of the land use impact of flooding situations in the MD. Base on that, flood hazards projections shall be figured out to assist decision-makers in creating a comprehensive plan for land use management in the Mekong Delta.

6. References

- Aakash Ahamed, John Bolten, Colin Doyle, Fessica Fayne, 2017. Near Real-Time Flood Monitoring and Impact Assessment Systems. DOI.10.1007/978-3-319-43744-6_6, Remote Sensing of Hydrological Extremes, pp.105-118
- Aronica, G., Hankin, B., Beven, K.J. Uncertainty and equifinality in calibrating distributed roughness coefficients in a flood distribution model with limited data. *Advances in Water Resources* 22 (4), 349–365, 1998.
- Bates, P., Anderson, M., Price, D., Hardy, R., Smith, C.. Analysis and development of hydraulic models for floodplain flows, in: Anderson, M.G., Walling, D.E., Bates, P.D. (Eds.), *Floodplain Processes*. Wiley, New York, 1996.
- Beffa, C. (1994): Praktische Lösung der tiefengemittelten Flachwassergleichungen. Mitteilung 133 der Versuchsanstalt für Wasserbau, Hydrologie und Glaziologie. ETH Zürich.
- Beffa, C. (2002): Integration ein- und zweidimensionaler Modelle zur hydrodynamischen Simulation von Gewässersystemen. In: „Moderne Methoden und Konzepte im Wasserbau“. Mitteilung 174 der Versuchsanstalt für Wasserbau, Hydrologie und Glaziologie. ETH Zürich.
- Beven, K. *Rainfall-Runoff Modelling The Primer* (2nd ed.). Wiley-Blackwell, Chichester, UK, 2012.
- Biggs, D. 2004. *Between Rivers and Tides: A Hydraulic History of the Mekong Delta, 1820–1975*. University of Washington, Seattle, WA, 423 pp.
- Bown, S. 2003. *The Effect of Flooding on Livelihoods of Cambodians Living Near the “Vietnam Dam”*. A Report Prepared for Chamroeun Cheit Khmer. Takeo and Oxfam GB, Phnom Penh, Cambodia, 26 pp.
- Brockmann, H. (1999): Einsatz flugzeuggestützter Fernerkundungstechniken zur Bearbeitung hydrologischer Fragestellungen, in: *Beiträge und Unterlagen zum Workshop Ermittlung von Überflutungsflächen an Fließgewässern*, Karlsruhe
- Brocheux, P. 1995. *The Mekong Delta: Ecology, Economy and Revolution, 1860–1960*. University of Wisconsin, Madison, 269 pp.
- Carlos Cotlier, B. Brisco, Maria C. Mondino, Laura Rita Balparda, 2011. Use of Radarsat-2 ultra-fine images in horticulture-intensive farming: Land use detection and crop discrimination. *Canadian Journal of Remote Sensing* 37(1):37-44. DOI 10.5589/m11-019
- Chen, L. Real Coded Genetic Algorithm Optimization of Long Term Reservoir Operation. *Journal of the American Water Resources Association* 39(5), 1157–1165, 2003.
- Claudia Kuenzer, Jianzhong Zhang, Ande Tetzlaff, Wolfgang Wagner, Stefan Voigt, 2008. Automated demarcation, detection and quantification of coal fires in China using remote

References

- sensing data. Spontaneous coal seam fires: mitigating a global disaster., Publisher: Tsinghua University press and Springer, Editors: null UNESCO Beijing, pp.362-380.
- C. Kuenzer et al. (2013). Flood mapping and flood dynamics of the Mekong Delta: ENVISAT-ASAR-WSM based time series analyses. *Remote Sensing* ISSN 2072-4292.
- Coleman J. M, and Roberts H. H., 1989. Deltaic coastal wetlands Coastal Lowlands: Geology and Geotechnology ed W J M van der Linden, S A P L Cloetingh, J P K Kaasschieter, W J E van de Graaff, J Vandenberghe and J A M van der Gun (Dordrecht: Springer Netherlands) pp 1–24 ([https:// doi.org/10.1007/978-94-017-1064-0_1](https://doi.org/10.1007/978-94-017-1064-0_1))
- Crawley, P. D. and Dandy G. C., Optimal operation of multiple reservoir system, *J. Water Resour. Plann. Manage.*, 119(1), 1-17, 1993. Gioia A. Reservoir Routing on Double-Peak Design Flood, *Water* 2016, 8, 553.
- Cunge, J.A., Holly, F.M., Verwey, A. (1980): *Practical Aspects of Computational River Hydraulics*, Pitman Advanced Publishing Program
- Dung N.V., B. Merz, A. Bardossy, T. D. Thang, H. Apel (2011). Multi-objective automatic calibration of hydrodynamic models utilizing inundation maps and gauge data. *Hydrol. Earth Syst. Sci.*, 15, 1339–1354.
- Dung D.T., J. Weger, 2017. Barriers to implementing irrigation and drainage policies in an giang province, mekong delta, Vietnam. *Irrigation and Drainage Irrig. and Drain.* (2017) Published online in Wiley Online Library (wileyonlinelibrary.com) DOI: 10.1002/ird.2172
- Duong, V.H.T., Nestmann, Van T.C, F., Oberle, P., Nam N.T. (2014). Land use based flood hazards analysis for Mekong delta. *Proceedings 19th IAHR Asian and Pacific Regional Division 2014*, Hanoi, Vietnam, September 21–24, 2014, ISBN: 978-604-82-1383-1.
- Duong, V.H.T., Nestmann F., Van T.C, Oberle, P.,Hinz, S., (2016). Geographical Impact of Dyke Measurement for Land Use on Flood Water in the Mekong Delta. *Proceedings of the IWA 8 th Eastern European Young Water Professionals Conference Gdansk, Poland*, 12-14 May, 2016, 308-317.
- Duong V.H.T, F. Nestmann, Van T.C, S. Hinz, P. Oberle, “ Analysis the development of triple rice cropping area and its impact on flooding situation in An Giang province”. *Proceedings in the 10 Eastern European Young Water Professionals Conference, Zagreb, Croatia, May 7-12, 2018.*
- Duong V.H.T, F. Nestmann, Van T.C, S. Hinz, P. Oberle. Introduction about the interpolation method for flood water prediction along Mekong River. *Proceedings in the 10 Eastern European Young Water Professionals Conference, Zagreb, Croatia, May 7-12, 2018.*
- Esat, V., Hall, M.J. *Water Resources System Optimization Using Genetic Algorithms*. In: *Proceedings of the First International Conference on Hydroinformatics*, pp. 225–231, 1994.
- Feldman, A. D., Hydrologic Engineering Center (U.S.), *Hydrologic Modeling System HEC-HMS*, US Army Corps of Engineers, Hydrologic Engineering Center, 2000.
- Fiorentino M., Gioia A., Iacobellis V., Manfreda S. Analysis on flood generation processes by means of a continuous simulation model, *Advances in Geosciences*, ISSN 1680-7340, 7, 231-236, 2006, www.adv-geosci.net/7/231/2006/, doi:10.5194/adgeo-7-231-2006.

References

- Fiorentino M., Gioia A., Iacobellis V. and Manfreda S. Regional analysis of runoff thresholds behaviour in Southern Italy based on theoretically derived distributions, *Advances in Geosciences*, ISSN 1680-7340, 26, 139–144, 2011- www.adv-geosci.net/26/139/2011/, doi:10.5194/adgeo-26-139-2011.
- Fluet-Chouinard, E., Lehner, B., Rebelo, L-M. P. F. and Hamilton, S. K. Development of a global inundation map at high spatial resolution from topographic downscaling of coarse-scale remote sensing data, *Remote Sensing of Environment*, 2014.
- General Statistics Office of Vietnam (2014). Statistical Publishing House, Hanoi. <http://www.gso.gov.vn>.
- Gowing, J.W., Tuong, T.P., Hoanh, C.T. and Khiem, T.T. 2006. Social and environmental impact of rapid change in the coastal zone of Vietnam: An assessment of sustainability issues. In: *Environment and Livelihoods in Tropical Coastal Zones: Managing Agriculture-Fishery-Aquaculture Conflicts*. Hoanh, C.T., Tuong, T.P.,
- G. Sarp, A. Erener, 2008. Land use detection comparison from satellite images with different classification procedures. *The International Archives of the Photogrammetry, Remote Sensing and Spatial Information Sciences*. Vol. XXXVII. Part B4. Beijing 2008
- Hager, W. H. (1986): *Discharge Measurement Structures*. Communication 1, Chaire de Construction Hydrauliques. EPFL Lausanne.
- Heng Dong, Jun Li, Yanbin Yuan, Chao Chen, 2017. A component-based system for agricultural drought monitoring by remote sensing. e0188687. DOI10.1371/journal.pone.0188687
- Henry, J.B., Chastanet, P., Fella, K. and Desnos, Y.L., 2006, Envisat multi-polarized ASAR data for flood mapping, *International Journal of Remote Sensing* vol. 27, no. 10, 1921–1929
- Hoc, D.X., (2016). Mekong Delta Activity living with floods. Integrated water resources management in Mekong Basin Workshop, January 12, 2016, Hochiminh, Vietnam, 11-17.
- Howie, C. 2005. High dykes in the Mekong Delta in Vietnam bring social gains and environmental pains. *Aquacult. News* 32, 15–17.
- Horritt, M. S., and Mason D. C., Flood boundary delineation from Synthetic Aperture Radar imagery using a statistical active contour model, *International Journal of Remote Sensing*, 2001, vol. 22, no. 13, 2489–2507
- Iacobellis V., Castorani A., Di Santo A. R., Gioia A. Rationale for flood prediction in karst endorheic areas. *Journal of Arid Environments*, 2015, 112(PA), pp. 98-108, DOI: 10.1016/j.jaridenv.2014.05.018.
- ICEM, 2009. Mekong Delta climate change forum 2009. International Centre for Environmental Management for Office of Government, MONRE, Australian Embassy, Danish Embassy, World Bank and Asian Development Bank. 12-13 November 2009.
- Imhoff, M.L., Vermillon, C., Story, M.H., Choudhury, M.A., and Gafoor, A., 1987, Monsoon flood boundary delineation and damage assessment using space borne imaging radar and Landsat data, *Photogrammetric Engineering and Remote Sensing*, vol. 53, 405-413
- Islam, M.M. and Sado, K., 2000a, Development of flood hazard maps of Bangladesh using NOAA-AVHRR images with GIS, *Hydrological Sciences Journal*, 45(3), 337-355

References

- Islam, M.M. and Sado, K., 2000b, Flood hazard assessment in Bangladesh using NOAA-AVHRR images with Geographic Information System, *Hydrological Processes*, 14, 605-620
- Islam, M.M. and Sado, K., 2002, Development of priority map for flood countermeasure by remote sensing data with Geographic Information System, *Journal of Hydrologic Engineering*, vol. 7, no. 5, 346-355
- Jain, S.K., Singh, R.D., Jain, M.K., Lohani, A.K. Delineation of Flood-Prone Areas Using Remote Sensing Techniques. *Water Resour Manage* (2005) 19: 333. <https://doi.org/10.1007/s11269-005-3281-5>.
- Johnson, S . A., Stedinger J. R. and StaschusH K. Euristic operating policies for reservoir system simulation, *Water Resour. Res.*, 27(5), 673-685, 1991.
- Joseph Okotto Okotto, Phillip O. Raburu, Kevin Obiero, Elizabeth A. Raburu, 2016. Spatio-Temporal Impacts of Lake Victoria Water Level Recession on the Fringing Nyando Wetland, Kenya. *Wetland DOI* 10.1007/s13157-016-0831-y
- Kakonen, M., Keskinen, M. and Varis, O. 2006. Mekong Delta socio-economic analysis: Interconnections between water and livelihoods in the Mekong Delta of Vietnam. In: WUPFIN Phase II: Hydrological, Environmental and Socio-Economic Modelling Tools for the Lower Mekong Basin Impact Assessment. Mekong River Commission and Finnish Environment Institute Consultancy Consortium, Vientiane, Lao PDR, 177 pp. (<http://www.eia.fi/wup-fin/>)
- Kim, T., Heo, J.-H., Jeong, C.S. Multireservoir System Optimization in the Han River basin using Multi-Objective Genetic Algorithm. *Hydrological Processes* 20, 2057–2075, 2006.
- Lawrence, M.K., Walker, N.D., Balasubramanian, S., Babin, A., and bars, J, 2005. Applications of Radarsat-1 synthetic aperture radar imagery to assess hurricane-related flooding of coastal Louisiana., *International Journal of Remote Sensing*, vol. 26, no. 24, 5359–5380
- Le Coq, J.F., M. Fufumier, G. Trebuil, 2001. History of rice production in the Mekong Delta. Third Euroseas Conference – London, september the 6th – 8th 2001.
- Le Coq, J.F. and Tre buil, G. 2005. Impact of liberalization on rice intensification, agricultural diversification, and rural livelihoods in the Mekong Delta. *Vietnam Southeast Asian Studies*, 42, 519–547.
- Leon T. Hauser , Giang Nguyen Vu, Binh An Nguyen , Emma Dade, Hieu Minh Nguyen, Trang Thi Quynh Nguyen, Toan Quang Le , Long Huu Vu, Ai Thi Huyen Tong, Hoa Viet Pham, 2017. Uncovering the spatio-temporal dynamics of land cover change and fragmentation of mangroves in the Ca Mau peninsula, Vietnam using multi-temporal SPOT satellite imagery (2004 - 2013). *Applied Geography* 86 (2017), P 197-207
- Le T.V. Hoa, Haruyama Shigeko, Nguyen Huu Nhan and Tran Thanh Cong (2008). Infrastructure effects on floods in the Mekong River Delta in Vietnam. *Hydrol. Process* 22, 1359–1372.
- Le T.V. Hoa, Nguyen Huu Nhan, Eric Wolanski, Tran Thanh Cong, Haruyama Shigeko (2007). The combine impact on the flooding in Vietnam's Mekong river delta of local manmade structures, sea level rise, and dams upstream in the river catchment. *Estuarine, Coastal and Shelf Science* 71, 110–116.
- Lian Yeap, Jill Shephard, Anna Le Souef, Kristin Shannon Warren,Christine J Groom, Rick David Dawson, Tony Kirkbym Kristin Shannon Warren, 2015. Satellite tracking of rehabilitated

References

- wild Baudin's cockatoos, *Calyptorhynchus baudinii*: A feasibility trial to track forest black cockatoos January 2015. *Pacific Conservation Biology* 21(2):163-167. DOI 10.1071/PC14917
- Lienhard, P., Molle, F. and Trung, N.H. 2001. Change in Land and Water Use: Micro and Macro Perspectives from the Mekong River Delta. Report to the European Union INCO-DC. Can Tho University, Can Tho, Vietnam, 93 pp.
- Luttrell, C. 2001. Institutional change and natural resource use in coastal Vietnam. *GeoJournal* 54, 529–540.
- Maha Shadaydeh, Andras Zlinszkym Andrea Manno Kovacs, Tamas Sziranyi, 2017. Wetland mapping by fusion of airborne laser scanning and multi-temporal multispectral satellite imagery. *International Journal of Remote Sensing* 38(23): 7422-7440. DOI 10.1080/01431161.2017.1375614
- Manfreda, S., Samela, C., Gioia, A., Consoli, G.G., Iacobellis, V., Giuzio, L., Cantisani, A., Sole, A. Flood-prone areas assessment using linear binary classifiers based on flood maps obtained from 1d and 2d hydraulic models. *Nat. Hazards* 79(2), 735–754, 2015.
- Mekong River Commission (MRC). Available at: <http://www.mrcmekong.org>.
- Mekong River Commission. 2005. Databases of Mekong River Commission. Mekong River Commission (MRC), Vientiane, Lao PDR. (<http://www.mrcmekong.org/>) Commonwealth Scientific and Industrial Research Organization (CSIRO) Marine Research. 2007. (<http://www.marine.csiro.au>)
- MIKE 11 user manual (2004). A Modelling System for Rivers and Channels, DHI.
- Mira Kakonen (2008), Mekong Delta at the Crossroads: More Control or Adaptation? Royal Swedish Academy of Sciences 2008 205, *Ambio* Vol. 37, No. 3, May 2008, 205-212
- Miller, F. 2003. Society-water Relations in the Mekong Delta: A Political Ecology of Risk. University of Sidney, Sidney, 419 pp.
- Mizyed, N. R., Loftis J. C. and Fontane D. G. Operation of large multireservoirs systems using optimal-control theory, *J. Water Resour. Plann. Manage.*, 118(4), 371-387, 1992.
- Minderhoud P. S. J, G. Erkens, V. H. Pham, V T Bui, L Erban, H Kooi and E Stouthamer, 2017. Impacts of 25 years of groundwater extraction on subsidence in the Mekong delta, Vietnam. *Environ. Environmental Research Letters*, Volume 12, Number 6.
- Musall M., Nestmann F., Oberle P., 2010. Hydraulic modelling, Flood Risk Assessment and Management, Editor: A. Schuumann, p. 187-209, Springer Science.
- Musall, M., Kron, A., Oberle, P. (2007): Floodplain modelling for real-time use based on an interlinked numerical 1D/2D model, DKKV-Forum Katastrophenvorsorge
- Musall, M., Kron, A., Oberle, P., Nestmann, F. (2009): GIS-gestütztes HN-Simulationswerkzeug für das operationelle Hochwassermanagement, in: Unterlagen zur DWA-Tagung GIS in der Wasserwirtschaft, Kassel
- Nestmann F., Norra S., Stolpe, Rudolph, (2017). Integrated Solutions for Sustainable Development in the Mekong-Delta – Land, Water, Energy and Climate –ViWaT Mekong. BMBF, Germany.

References

- Nghiem, S.V., Liu, W.T., Tsai, W.Y. and Xie, X., 2000, Flood mapping over the Asian continent during the 1999 summer monsoon season, Proceedings of IGARSS'00. IEEE Publication, pp. 2027-2028
- Ngoc TA., (2016). The effects of sea level rise and upstream development on sediment distribution in the lower Mekong delta, Vietnam. Workshop on Integrated Water resources management in the Mekong Basin, sponsored by Northumbria University Newton Fund (UK), Ho Chi Minh city 12. January 2016.
- NIAPP. 2002. Land Use Map of the Mekong Delta of Vietnam. National Institute for Agricultural Planning and Projection (NIAPP), Ministry of Agriculture and Rural Development (MARD), Hanoi.
- Oberle, P. (2004): Integrales Hochwasserinformationssystem Neckar - Verfahren, Werkzeuge, Anwendungen und Übertragung, Mitteilung 226 des Instituts für Wasser und Gewässerentwicklung, Karlsruhe
- Oliveira, R., Loucks, D.P. Operating Rules for Multireservoir Systems. *Water Resources Research* 33(4), 839–852 (1997).
- Pavel Ukrainski, 2016. Classification accuracy assessment, confusion matrix method. <http://www.50northspatial.org/classification-accuracy-assessment-confusion-matrix-method/>
- Pham, C.D. 1985. Vietnamese Peasants under French Domination 1861–1945. University of California, Berkeley, CA, 220 pp.
- Pham Viet Hoa, N.A. Binh, Leo T. Hauser, Nguyen Vu Giang, Nguyen T. Q. T., Le Q. T., Vu H. L., 2017. Deforestation and drought: integrating remotely sensed indices in a Web-Gis environment for the central highlands of Vietnam. *Geo-Spatial Technologies and Earth Resources*, Publishing House for Science and Technology, Vietnam, ISBN 978-604-913-618-4.
- Philippe Rigo et al., 2005. Design of movable Weirs and Storm Surge Barriers. InCom Working Group 26, Final report Version 6.7. 1st August 2005.
- Popkin, S. 1979. The Rational Peasant. The Political Economy of Rural Society in Vietnam. University of California Press, Berkeley, CA, 306 pp.; and Cummings, R.C.
- Q.M. Nhat (2011). Efficiency Analysis of Selected Farming Patterns: The Case of Irrigated Systems in the Mekong Delta of Vietnam, *Advances in Global Change Research*, ISBN 9789400709331.
- Rajat Subhra Chatterjee, Parth sarathi Roy, Vinay Kumar Dadhwal, R. Saha, T. X. Quang, R. Saha, 2007. Assessment of land subsidence phenomenon in Kolkata city, India using satellite-based D-InSAR technique. *Current science* 93(1):85-93
- Rigon, R., Bertoldi, G. and Over T. M.GEOtop: A Distributed Hydrological Model with Coupled Water and Energy Budgets. *J. Hydrometeor*, 7, 371–388. doi: <http://dx.doi.org/10.1175/JHM497.1>, 2006.
- Shailaja Thapa, Rajat Subhra Chatterjee, K. B. Singh, D. Kumar, 2016. Land subsidence monitoring using ps-insar technique for l-band sar data. DOI. 10.5194/isprs-archives-XLI-B7-995-2016. Conference: ISPRS - International Archives of the Photogrammetry, Remote Sensing and Spatial Information Sciences.

References

- S. Benedikter (2013). *The Vietnamese Hydrocracy and the Mekong Delta*. PhD Dissertation. ISBN 9793643904379
- SCS (USDA Soil Conservation Service), 1972. *National Engineering Handbook, Section 4: Hydrology*. U.S. Department of Agriculture, Washington, DC, USA.
- Scott, J.C. 1998. *Seeing Like a State: How Certain Schemes to Improve the Human Condition Have Failed*. Yale University Press, New Haven, CT, pp. 184, 264.
- Scott, J.C. 1976. *The Moral Economy of the Peasant: Rebellion and Subsistence in Southeast Asia*. Yale University Press, New Haven, CT, 445 pp.
- Sordo-Ward, A., Gabriel-Martin, I., Bianucci P and Garrote L. A Parametric Flood Control Method for Dams with Gate-Controlled Spillways, *Water* 2017,9, 237; doi:10.3390/w904023.
- Statistical yearbook – An Giang province from 2000 to 2016. Statistical Office of An Giang province.
- Statistical yearbook – Bac Lieu province from 2000 to 2016. Statistical Office of Bac Lieu province.
- Statistical yearbook – Ben Tre province from 2000 to 2016. Statistical Office of Ben Tre province.
- Statistical yearbook – Ca Mau province from 2000 to 2016. Statistical Office of Ca Mau province.
- Statistical yearbook – Can Tho province from 2000 to 2016. Statistical Office of Can Tho province.
- Statistical yearbook – Dong Thap province from 2000 to 2016. Statistical Office of Dong Thap province.
- Statistical yearbook – Hau Giang province from 2005 to 2016. Statistical Office of Hau Giang province.
- Statistical yearbook – Kien Giang province from 2000 to 2016. Statistical Office of Kien Giang province.
- Statistical yearbook – Long An province from 2000 to 2016. Statistical Office of Long An province.
- Statistical yearbook – Soc Trang province from 2000 to 2016. Statistical Office of Soc Trang province.
- Statistical yearbook – Tien Giang province from 2000 to 2016. Statistical Office of Tien Giang province.
- Statistical yearbook – Tra Vinh province from 2000 to 2016. Statistical Office of Tra Vinh province.
- Statistical yearbook – Vinh Long province from 2000 to 2016. Statistical Office of Vinh Long province.
- T. Sakamoto, Cao V.P., Khang D. N., M. Yokozawa, 2009. Analysis of rapid expansion of inland aquaculture and triple rice-cropping areas in a coastal area of the Vietnamese Mekong Delta using MODIS time-series imagery. *Landscape and Urban Planning* 92 (2009), P 34-46
- T. Sakamoto, Nhan Van Nguyen, Akihiko Kotera, Hiroyuki Ohno, Naoki Ishitsuka, Masayuki Yokozawa (2007). Detecting temporal changes in the extent of annual flooding within the

References

- Cambodia and the Vietnamese Mekong Delta from MODIS time-series imagery. *Remote Sensing of Environment* 109, 295–313.
- T. Sakamoto, Phung Cao Van, Aikihiko Koreta, Khang Nguyen Duy and Masayuki Yokozawa (2009). Detection of Yearly Change in Farming Systems in the Vietnamese Mekong Delta from MODIS Time-Series Imagery. *JARQ* 43(3), 173–185.
- Teegavarapu, R.S.V., Simonovic, S.P. Optimal Operation of Reservoir Systems using Simulated Annealing. *Water Resources Management* 16, 401–428, 2002.
- Thanh T.V. (2013). Discussion about historical flooding hazards 2000 and 2011 in Mekong delta (internal presentation), SIWRR.
- Thanh D.D., Thomas A. C., Mauricio, Van P.D.T, (2017). Future hydrological alterations in the Mekong Delta under the impact of water resources development, land subsidence and sea level rise. *Journal of Hydrology: Regional Studies* 15 (2018) 119–133
- Thuc, T. and Tuyen, H.M. 2005. Hydraulic computation for the Lower Mekong Basin to study flood drainage for the Plain of Reeds in Vietnam. In: *Conference of Role of Water Sciences in Transboundary River Basin Management*. Ubon Ratchathani, Thailand, 9 pp.
- Townsend, P. A., (2002), Relationships between forest structure and the detection of flood inundation in forested wetlands using C-band SAR, *International Journal of Remote Sensing*, vol. 23, no. 3, 443–460
- Van T.C. (2010). Impacts of rising sea level on the Mekong Delta, *The International Journal on Hydropower & Dam*, 3, 73–76
- Van Te Chow (2009). *Open channel hydraulics book*, ISBN 07-010776-9
- Van P.D. Tri, N.H. Trung, N. T. Tuu (2012). Flow dynamics in the Long Xuyen Quadrangle under the impacts of full-dyke systems and sea level rise. *VNU Journal of Science, Earth Sciences* 28, 205–214.
- Vinh N.T. (2010). Flooding regime in Long Xuyen quadrangle, SIWRR.
- Vietnamese Villages in the Mekong Delta: Their Articulations with the Wider Society and the Local Implications for Local Social Organization*, (1978). State University of New York at Binghamton, Binghamton, NY, 301 pp.
- Vögtle, T., Steinle, E. (2001): Erfahrungen mit Laser-Scanner-Daten zur automatisierten 3D-Modellierung von Gebäuden, in: *Deutscher Verein für Vermessungswesen (DVW), Landesverein Baden-Württemberg, Mitteilung H. 2, 48 Jg.*
- Wang, Y., Colby, J. D., and Mulcahy, K. A., 2002. An efficient method for mapping flood extent in a coastal floodplain using Landsat TM and DEM data, *International Journal of Remote Sensing*, vol. 23, no. 18, 3681–3696
- Wang, Y., 2004, Using Landsat 7 TM data acquired days after a flood event to delineate the maximum flood extent on a coastal floodplain, *International Journal of Remote Sensing*, vol. 25, no. 5, 959–974
- Wardlaw, R., Sharif, M. Evaluation of Genetic Algorithms for Optimal Reservoir System Operation. *Journal of Water Resources Planning and Management*, ASCE 125(1), 25–33, 1999.

References

- WISDOM project, the portal website <http://www.wisdom.caf.dlr.de/>
- Worldfish Center, 2002. Increasing and sustaining the productivity of fish and rice in seasonally flooded ecosystem in South and Southeast Asia. IFAD, final report.
- Xiaofeng Liu, Xiufang Zhu, Yaozhong Pan, Yuqi Ma, 2016. Agricultural drought monitoring: Progress, challenges, and prospects. *Journal of Geographical Sciences* 26(6):750-767. DOI10.1007/s11442-016-1297-9
- Xing Li, J. Paul Liu, Yoshiki Saito, Van Lap Nguyen, 2017. Recent evolution of the Mekong Delta and the impact of dams. *Earth Science Reviews* 175 (2017), P 1-17.
- Xuan V.T., Matsui S. 1998. Development of farming systems in the Mekong delta, Vietnam. Ho Chi Minh City Publishing House 13: 314. <https://doi.org/10.1002/ldr.494>.
- Zubair, A. O., 2006. Change detection in land use and land cover using remote sensing data and GIS, a case study of Ilorin and its environs in Kwara State. University of Ibadan, Ibadan.

7. Appendix

7.1. Day of year (DOY) calendar

Table 7.1. DOY for normal year

Jan	Feb	Mar	Apr	May	Jun	Jul	Aug	Sep	Oct	Nov	Dec
1	32	60	91	121	152	182	213	244	274	305	335
2	33	61	92	122	153	183	214	245	275	306	336
3	34	62	93	123	154	184	215	246	276	307	337
4	35	63	94	124	155	185	216	247	277	308	338
5	36	64	95	125	156	186	217	248	278	309	339
6	37	65	96	126	157	187	218	249	279	310	340
7	38	66	97	127	158	188	219	250	280	311	341
8	39	67	98	128	159	189	220	251	281	312	342
9	40	68	99	129	160	190	221	252	282	313	343
10	41	69	100	130	161	191	222	253	283	314	344
11	42	70	101	131	162	192	223	254	284	315	345
12	43	71	102	132	163	193	224	255	285	316	346
13	44	72	103	133	164	194	225	256	286	317	347
14	45	73	104	134	165	195	226	257	287	318	348
15	46	74	105	135	166	196	227	258	288	319	349
16	47	75	106	136	167	197	228	259	289	320	350
17	48	76	107	137	168	198	229	260	290	321	351
18	49	77	108	138	169	199	230	261	291	322	352
19	50	78	109	139	170	200	231	262	292	323	353
20	51	79	110	140	171	201	232	263	293	324	354
21	52	80	111	141	172	202	233	264	294	325	355
22	53	81	112	142	173	203	234	265	295	326	356
23	54	82	113	143	174	204	235	266	296	327	357
24	55	83	114	144	175	205	236	267	297	328	358
25	56	84	115	145	176	206	237	268	298	329	359
26	57	85	116	146	177	207	238	269	299	330	360
27	58	86	117	147	178	208	239	270	300	331	361
28	59	87	118	148	179	209	240	271	301	332	362
29		88	119	149	180	210	241	272	302	333	363
30		89	120	150	181	211	242	273	303	334	364
31		90		151		212	243		304		365
Jan	Feb	Mar	Apr	May	Jun	Jul	Aug	Sep	Oct	Nov	Dec

(Source: https://nsidc.org/data/tools/doy_calendar.html)

Appendix

Table 7.2. DOY for Leap Year

Jan	Feb	Mar	Apr	May	Jun	Jul	Aug	Sep	Oct	Nov	Dec
1	32	61	92	122	153	183	214	245	275	306	336
2	33	62	93	123	154	184	215	246	276	307	337
3	34	63	94	124	155	185	216	247	277	308	338
4	35	64	95	125	156	186	217	248	278	309	339
5	36	65	96	126	157	187	218	249	279	310	340
6	37	66	97	127	158	188	219	250	280	311	341
7	38	67	98	128	159	189	220	251	281	312	342
8	39	68	99	129	160	190	221	252	282	313	343
9	40	69	100	130	161	191	222	253	283	314	344
10	41	70	101	131	162	192	223	254	284	315	345
11	42	71	102	132	163	193	224	255	285	316	346
12	43	72	103	133	164	194	225	256	286	317	347
13	44	73	104	134	165	195	226	257	287	318	348
14	45	74	105	135	166	196	227	258	288	319	349
15	46	75	106	136	167	197	228	259	289	320	350
16	47	76	107	137	168	198	229	260	290	321	351
17	48	77	108	138	169	199	230	261	291	322	352
18	49	78	109	139	170	200	231	262	292	323	353
19	50	79	110	140	171	201	232	263	293	324	354
20	51	80	111	141	172	202	233	264	294	325	355
21	52	81	112	142	173	203	234	265	295	326	356
22	53	82	113	143	174	204	235	266	296	327	357
23	54	83	114	144	175	205	236	267	297	328	358
24	55	84	115	145	176	206	237	268	298	329	359
25	56	85	116	146	177	207	238	269	299	330	360
26	57	86	117	147	178	208	239	270	300	331	361
27	58	87	118	148	179	209	240	271	301	332	362
28	59	88	119	149	180	210	241	272	302	333	363
29	60	89	120	150	181	211	242	273	303	334	364
30		90	121	151	182	212	243	274	304	335	365
31		91		152		213	244		305		366
Jan	Feb	Mar	Apr	May	Jun	Jul	Aug	Sep	Oct	Nov	Dec

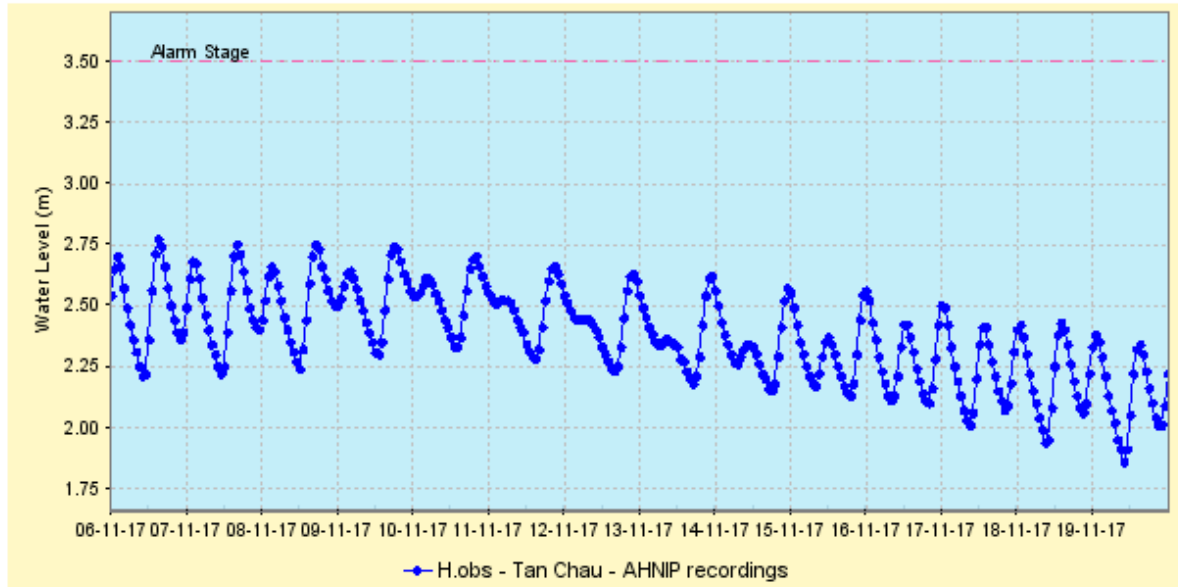
(https://nsidc.org/data/tools/doy_calendar.html)

7.2. Telemetry data from MRC website

Telemetry Data at Tan Chau

Time of Report 20/11/2017 15:18 GMT+07:00
 Datum level (m msl) 0.00
 Flood level (m) 4.5
 Alarm level (m) 3.5

Water Level (metres above zero gauge)



Rated Discharge (cumecs)

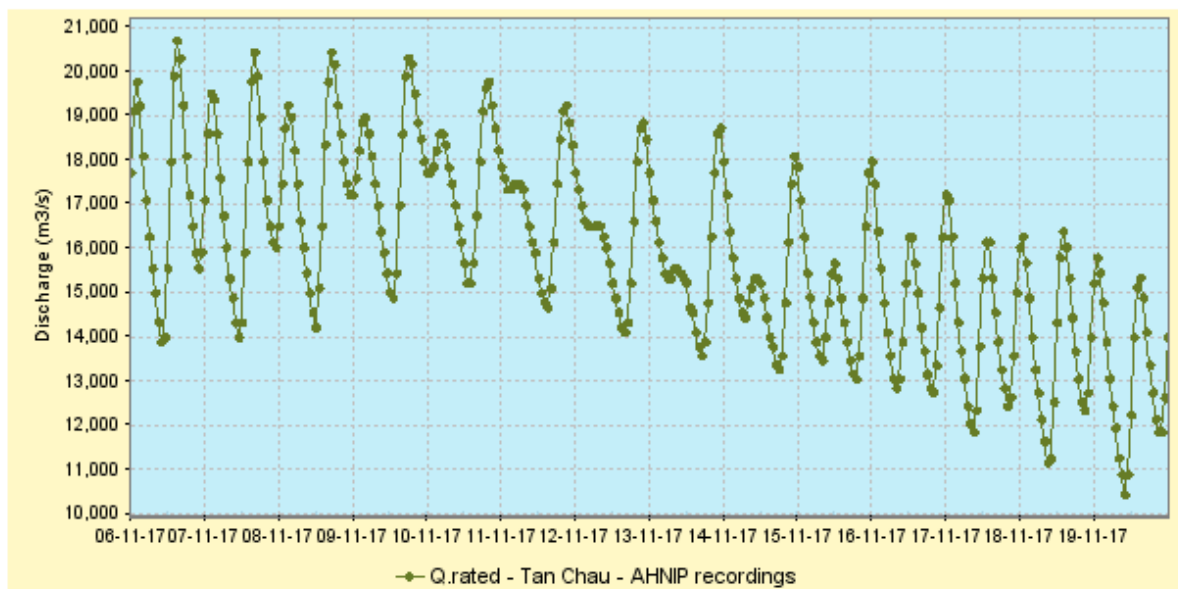


Figure 7.1. Online observed water level and discharge at Tan Chau gauge on MRC website.

(Source: Telemetry data at Tan Chau, MRC, 2017)

Appendix

7.3. Accuracy analysis for Land use flood map by MODIS satellite

7.3.1. The accuracy of total rice in year and aquaculture areas vs statistical data

Table 7.3. Comparison of total rice area between MODIS and statistical data in the MD

An Giang	2000	2001	2002	2003	2004	2005	2006	2007	2008	2009	2010	2011	2012	2013	2014	2015	2016
MODIS satellite	545.46	499.49	523.71	554.32	581.93	586.41	545.10	570.67	605.98	597.01	630.18	642.67	687.85	700.17	708.27	715.25	731.27
Statistical data	464.40	459.10	477.20	503.90	523.00	529.70	503.50	520.30	564.50	557.30	586.60	603.90	625.10	641.40	625.80	644.20	-
difference	15%	8%	9%	9%	10%	10%	8%	9%	7%	7%	7%	6%	9%	8%	12%	10%	-
Dongthap	2000	2001	2002	2003	2004	2005	2006	2007	2008	2009	2010	2011	2012	2013	2014	2015	2016
MODIS satellite	508.24	442.65	467.99	483.42	497.31	516.54	486.12	487.70	501.44	492.93	505.14	520.19	488.46	585.41	602.05	616.96	618.66
Statistical data	408.40	408.30	426.40	436.40	453.00	467.70	454.00	447.10	468.10	450.80	465.10	501.10	487.60	541.80	528.60	546.00	-
difference	20%	8%	9%	10%	9%	9%	7%	8%	7%	9%	8%	4%	0%	7%	12%	12%	-
Longan	2000	2001	2002	2003	2004	2005	2006	2007	2008	2009	2010	2011	2012	2013	2014	2015	2016
MODIS satellite	567.63	411.76	419.19	412.08	421.57	405.92	398.79	422.89	418.48	446.44	456.32	476.05	500.21	519.18	482.69	539.95	569.21
Statistical data	453.10	440.90	433.30	424.10	433.40	429.30	433.20	428.40	457.00	463.60	471.10	486.50	499.60	527.70	519.20	525.10	-
difference	20%	7%	3%	3%	3%	5%	8%	1%	8%	4%	3%	2%	0%	2%	7%	3%	-
Kiengiang	2000	2001	2002	2003	2004	2005	2006	2007	2008	2009	2010	2011	2012	2013	2014	2015	2016
MODIS satellite	561.90	466.16	524.29	481.21	504.79	506.90	472.49	452.01	468.00	488.04	495.27	537.79	583.22	620.00	601.28	635.42	633.68
Statistical data	541.00	550.60	575.90	563.00	570.30	595.80	595.10	582.90	609.20	622.10	642.70	686.90	725.10	770.40	753.60	769.50	-
Difference	4%	15%	9%	15%	11%	15%	21%	22%	23%	22%	23%	22%	20%	20%	20%	17%	-
Cantho	2000	2001	2002	2003	2004	2005	2006	2007	2008	2009	2010	2011	2012	2013	2014	2015	2016
MODIS satellite	224.59	191.94	205.72	208.71	215.01	223.79	204.28	199.19	203.45	194.19	202.69	215.18	230.65	204.52	200.36	201.32	211.15
Statistical data	206.70	220.55	228.30	226.70	229.90	232.00	222.80	207.90	218.60	208.80	209.40	224.70	228.20	236.60	232.30	237.90	-
difference	8%	13%	10%	8%	6%	4%	8%	4%	7%	7%	3%	4%	1%	14%	14%	15%	-
Hau Giang	2000	2001	2002	2003	2004	2005	2006	2007	2008	2009	2010	2011	2012	2013	2014	2015	2016
MODIS satellite	191.19	153.48	174.34	160.82	165.06	177.63	158.07	149.42	162.86	151.80	166.88	164.05	183.67	189.86	159.10	166.79	176.01
Statistical data	206.70	220.55	228.30	226.70	228.40	228.40	227.10	189.30	202.90	191.20	210.70	212.70	214.10	212.00	205.30	207.00	-
difference	8%	30%	24%	29%	28%	22%	30%	21%	20%	21%	21%	23%	14%	10%	23%	19%	-
Vinh Long	2000	2001	2002	2003	2004	2005	2006	2007	2008	2009	2010	2011	2012	2013	2014	2015	2016
MODIS satellite	231.17	195.29	199.90	197.46	177.88	193.87	188.24	162.55	177.83	173.23	179.32	182.63	203.45	204.52	200.36	201.32	211.15
Statistical data	208.60	216.30	209.80	207.00	208.10	203.10	196.50	158.30	177.40	176.70	170.00	181.50	185.90	181.90	180.20	180.50	-
difference	10%	10%	5%	5%	15%	5%	4%	3%	0%	2%	5%	1%	9%	11%	10%	10%	-

Appendix

Tien giang	2000	2001	2002	2003	2004	2005	2006	2007	2008	2009	2010	2011	2012	2013	2014	2015	2016
MODIS satellite	276.53	246.49	240.90	232.09	208.29	223.65	205.83	225.88	225.62	220.16	218.18	209.75	211.77	217.24	197.15	213.62	202.77
Statistical data	282.40	276.10	265.00	260.80	259.40	251.90	247.80	246.80	244.90	246.40	244.00	241.10	241.40	235.60	230.60	224.70	-
difference	2%	11%	9%	11%	20%	11%	17%	8%	8%	11%	11%	13%	12%	8%	15%	5%	-
Ben Tre	2000	2001	2002	2003	2004	2005	2006	2007	2008	2009	2010	2011	2012	2013	2014	2015	2016
MODIS satellite	99.05	68.13	65.93	62.83	60.69	61.54	55.42	57.95	54.87	58.85	55.33	56.11	50.97	60.96	74.47	57.89	47.85
Statistical data	101.60	100.80	99.60	95.50	90.50	83.50	81.80	79.70	79.20	81.10	80.20	76.90	75.80	72.20	66.60	63.00	-
difference	3%	32%	34%	34%	33%	26%	32%	27%	31%	27%	31%	27%	33%	16%	11%	8%	-
Tra Vinh	2000	2001	2002	2003	2004	2005	2006	2007	2008	2009	2010	2011	2012	2013	2014	2015	2016
MODIS satellite	288.97	210.98	233.78	217.34	202.34	205.22	187.25	212.79	218.30	220.15	228.32	227.39	237.83	265.97	271.93	263.74	251.37
Statistical data	237.00	240.40	235.80	236.20	235.60	232.40	228.20	224.00	226.90	231.90	232.70	233.00	227.40	235.60	235.80	237.30	-
difference	18%	12%	1%	8%	14%	12%	18%	5%	4%	5%	2%	2%	4%	11%	13%	10%	-
Soc trang	2000	2001	2002	2003	2004	2005	2006	2007	2008	2009	2010	2011	2012	2013	2014	2015	2016
MODIS satellite	419.09	316.38	333.13	319.20	306.16	311.19	305.28	312.33	318.46	337.79	360.79	354.39	385.61	397.10	387.69	419.09	368.98
Statistical data	370.40	348.80	354.90	349.60	315.20	321.60	324.40	325.40	322.30	334.60	349.60	348.90	365.90	373.50	363.90	367.00	-
difference	12%	9%	6%	9%	3%	3%	6%	4%	1%	1%	3%	2%	5%	6%	6%	12%	-
Bac Lieu	2000	2001	2002	2003	2004	2005	2006	2007	2008	2009	2010	2011	2012	2013	2014	2015	2016
MODIS satellite	231.04	138.11	143.88	114.72	109.81	115.62	123.60	119.40	127.36	143.47	133.06	144.92	147.45	168.29	171.37	167.56	165.27
Statistical data	217.30	178.10	169.80	150.40	137.30	141.30	144.10	149.90	155.00	166.50	158.30	162.40	178.70	181.80	180.20	180.80	-
difference	6%	22%	15%	24%	20%	18%	14%	20%	18%	14%	16%	11%	17%	7%	5%	7%	-

Appendix

Table 7.4. Comparison of aquaculture area between MODIS and statistical data in the MD

(Unit thousand ha)

MODIS	2000	2001	2002	2003	2004	2005	2006	2007	2008	2009	2010	2011	2012	2013	2014	2015	2016
An Giang	8.6	9.7	11.1	11.5	10.6	12.2	12.0	12.1	13.9	12.1	12.0	11.7	10.9	6.8	2.3	4.2	4.8
Bac Lieu	58.6	104.9	110.2	127.3	129.1	131.1	131.1	134.5	131.9	124.4	127.7	123.8	124.9	111.7	106.9	115.7	118.0
Ben tre	41.0	59.8	60.4	60.9	61.2	61.4	61.4	61.7	61.5	60.3	60.1	59.7	59.6	43.5	41.2	49.9	46.1
Ca Mau	146.5	274.3	281.8	290.7	297.9	303.2	310.8	320.4	324.5	314.0	311.2	307.8	305.3	275.5	251.5	280.4	284.3
Can Tho	2.6	4.6	4.8	4.9	4.9	4.9	5.3	5.5	6.1	5.5	5.0	5.3	4.9	3.2	2.1	0.4	3.3
Dong Thap	7.8	14.0	15.0	15.5	15.9	16.3	16.0	16.5	19.2	16.5	16.6	16.4	15.6	8.7	3.6	6.6	6.1
Hau Giang	0.2	2.3	0.8	0.7	0.5	0.5	1.1	0.9	0.7	0.6	0.7	0.8	0.5	0.2	0.1	0.0	0.2
Kien Giang	29.7	50.3	48.3	75.3	75.3	83.6	94.4	99.2	102.9	90.2	94.8	93.4	88.5	72.2	52.0	85.2	96.0
Long An	13.4	24.2	28.0	19.8	20.7	26.7	24.2	24.9	36.0	22.3	21.0	22.5	18.6	16.6	3.3	11.0	11.9
Soc Trang	34.0	58.4	57.8	67.9	67.9	69.9	69.3	69.6	69.9	67.5	68.1	67.5	67.0	53.2	52.9	36.3	58.7
Tien Giang	9.2	15.3	15.5	15.1	15.4	15.7	16.2	16.1	16.6	16.0	15.3	16.0	15.7	10.1	9.4	11.7	10.7
Tra Vinh	30.2	48.8	47.8	51.8	53.8	54.2	54.9	56.3	56.5	55.7	55.3	54.7	53.9	39.2	20.0	40.9	43.8
Vinh Long	5.2	9.5	8.8	8.6	8.5	8.6	8.9	8.8	9.1	9.0	8.8	9.0	8.5	5.1	3.1	1.1	4.4
Mekong delta	387.1	676.3	690.3	749.9	761.7	788.4	805.5	826.6	848.9	794.0	796.6	788.5	773.9	645.9	548.3	643.4	688.4

Table 7.5. Total area of inland aquaculture by statistical data (Unit: thousand ha)

Statistical data	2000	2001	2002	2003	2004	2005	2006	2007	2008	2009	2010	2011	2012	2013	2014	2015	2016
An Giang	1.3	1.3	1.8	1.6	1.9	1.8	1.9	3.0	2.8	2.5	2.4	1.8	1.8	2.5	2.4	2.5	-
Bac Lieu	54.0	83.0	100.6	112.3	118.8	118.7	120.2	122.2	125.6	126.3	125.4	125.2	117.8	127.9	127.5	130.6	-
Ben tre	29.3	25.6	36.0	37.7	41.1	42.3	41.0	41.9	42.1	42.0	42.5	43.1	47.7	44.8	47.1	42.4	-
Ca Mau	204.4	254.2	271.4	277.7	277.7	279.2	275.2	290.8	293.2	294.7	296.1	296.5	296.5	295.8	298.1	299.8	-
Can Tho	12.6	13.6	16.5	10.0	11.0	12.5	13.6	14.0	12.9	13.1	12.8	12.6	11.7	11.0	11.4	10.9	-
Dong Thap	1.9	2.3	2.6	2.6	3.2	3.6	4.5	5.0	5.8	5.0	4.8	5.5	5.7	5.9	6.0	5.8	-
Hau Giang	0.0	0.0	0.0	7.5	8.3	8.9	7.4	8.4	6.1	6.2	6.4	6.4	6.6	6.5	7.1	6.8	-
Kien Giang	34.6	42.6	49.7	62.1	79.2	82.2	95.5	106.2	134.6	121.7	123.1	114.6	115.5	126.9	132.9	136.2	-
Long An	3.4	6.6	7.3	10.2	12.4	13.2	11.6	12.6	10.0	9.0	9.4	10.8	8.9	9.0	8.7	8.7	-
Soc Trang	41.4	53.2	48.3	57.1	59.0	64.9	64.3	62.0	67.7	69.2	71.5	67.1	64.8	68.2	68.4	68.8	-
Tien Giang	8.4	8.8	9.6	10.8	11.9	12.1	12.4	12.9	12.6	12.6	13.1	14.1	14.4	15.4	15.7	12.6	-
Tra Vinh	52.6	54.3	25.2	30.2	32.5	38.7	41.3	42.5	36.4	34.0	32.8	29.1	40.4	37.0	30.8	29.5	-
Vinh Long	1.4	1.3	1.4	1.5	1.6	1.8	2.3	2.3	2.4	2.5	2.4	2.5	2.4	2.6	2.4	2.4	-
Mekong delta	445.3	546.8	570.4	621.3	658.6	679.9	691.2	723.8	752.2	738.8	742.7	729.3	734.2	753.5	758.5	757.0	-

Appendix

7.3.2. Accuracy analysis of Triple rice cropping area

Table 7.6. Comparison of Triple rice cropping between MODIS vs Statistical data (Unit: Thousand ha.)

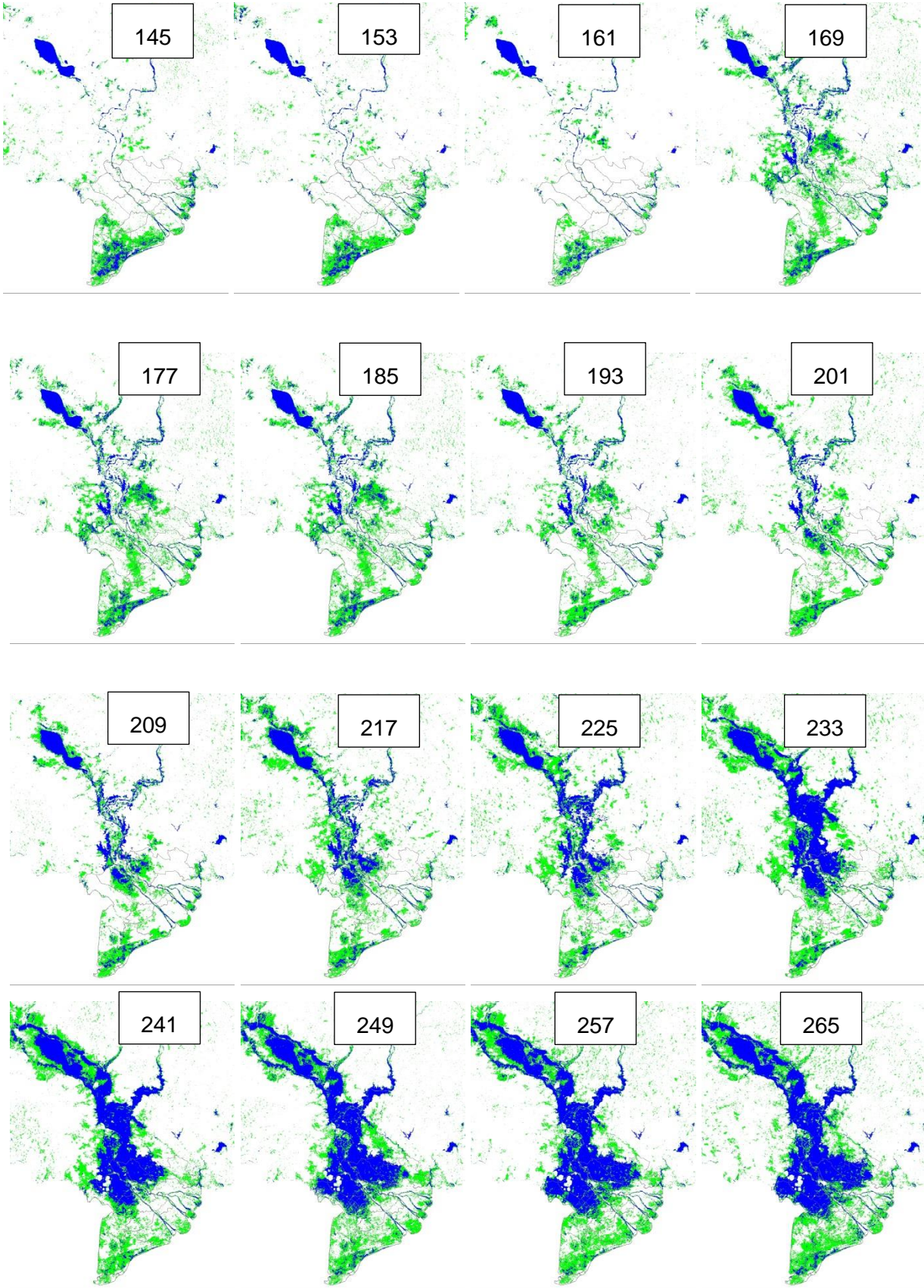
An Giang	2000	2001	2002	2003	2004	2005	2006	2007	2008	2009	2010	2011	2012	2013	2014	2015	2016
Statistic data	21.01	18.86	35.35	63.00	80.34	83.39	43.15	58.86	94.42	84.25	115.04	133.72	149.54	163.18	157.23	-	-
Modis	30.37	18.02	37.14	63.97	85.97	87.89	48.07	65.75	106.71	92.34	127.12	139.26	180.60	189.17	194.93	208.25	215.7
Difference	31%	4%	5%	2%	7%	5%	10%	10%	12%	9%	10%	4%	17%	14%	19%	-	-
Dong Thap	2000	2001	2002	2003	2004	2005	2006	2007	2008	2009	2010	2011	2012	2013	2014	2015	2016
Statistic data	23.40	23.40	39.32	44.71	62.74	78.17	50.49	44.67	63.82	47.33	60.29	98.52	142.00	134.97	-	-	-
Modis	23.74	20.75	37.39	48.40	61.59	77.01	44.57	46.06	61.66	47.75	64.42	77.68	122.57	136.27	150.22	173.28	168.2
Difference	1%	11%	5%	8%	2%	1%	12%	3%	3%	1%	6%	21%	14%	1%	-	-	-
Kien Giang	2000	2001	2002	2003	2004	2005	2006	2007	2008	2009	2010	2011	2012	2013	2014	2015	2016
Statistic data	4.60	7.01	30.58	29.77	38.09	41.46	35.17	1.99	9.15	5.29	14.32	47.00	70.04	-	-	-	-
Modis	14.27	14.81	36.57	28.08	45.33	48.29	23.40	3.82	13.52	5.57	23.18	47.97	83.48	80.00	78.38	128.24	142.9
Difference	68%	53%	16%	6%	16%	14%	33%	48%	32%	5%	38%	2%	16%	-	-	-	-
Long An	2000	2001	2002	2003	2004	2005	2006	2007	2008	2009	2010	2011	2012	2013	2014	2015	2016
Statistic data	-	-	-	-	-	-	-	-	-	-	-	-	22.49	-	49.27	-	-
Modis	23.22	28.75	29.17	26.19	29.38	25.30	17.49	24.85	28.97	28.06	30.06	31.07	51.79	62.74	58.35	108.26	112.6
Difference	-	-	-	-	-	-	-	-	-	-	-	-	57%	-	-	-	-
Can Tho	2000	2001	2002	2003	2004	2005	2006	2007	2008	2009	2010	2011	2012	2013	2014	2015	2016
Statistic data	19.67	33.07	40.16	37.87	44.42	50.20	41.04	30.44	41.38	32.50	33.66	54.40	58.28	-	-	-	-
Modis	22.23	19.51	32.42	35.77	45.78	51.28	36.56	30.55	35.49	26.09	32.80	46.45	59.12	69.70	35.21	77.48	81.1
Difference	12%	41%	19%	6%	3%	2%	11%	0%	14%	20%	3%	15%	1%	-	-	-	-
Vinh Long	2000	2001	2002	2003	2004	2005	2006	2007	2008	2009	2010	2011	2012	2013	2014	2015	2016
Statistic data	-	-	-	-	-	66.21	62.00	25.50	44.75	46.12	40.33	54.14	61.80	58.12	59.77	-	-
Modis	68.60	53.89	60.81	60.86	44.94	61.59	56.41	25.98	43.68	35.84	45.85	53.69	65.65	66.04	64.35	66.55	69.4
Difference	-	-	-	-	-	7%	9%	2%	2%	22%	12%	1%	6%	12%	7%	-	-
Hau Giang	2000	2001	2002	2003	2004	2005	2006	2007	2008	2009	2010	2011	2012	2013	2014	2015	2016
Statistic data	38.30	38.30	50.74	62.69	65.35	64.36	65.71	65.49	34.26	45.47	31.14	48.81	52.33	58.81	50.59	49.77	-
Modis	42.20	30.49	47.34	36.95	43.34	45.39	33.12	22.60	29.50	16.78	30.57	25.02	39.97	49.15	29.05	40.43	41.1
Difference	9%	20%	7%	41%	34%	29%	50%	65%	14%	63%	2%	49%	24%	16%	43%	19%	-
Tien Giang	2000	2001	2002	2003	2004	2005	2006	2007	2008	2009	2010	2011	2012	2013	2014	2015	2016

Appendix

Statistic data	-	-	-	-	-	42.24	40.97	41.66	41.53	41.55	41.90	40.97	39.91	38.02	-	-	-
Modis	82.94	78.91	77.46	73.72	54.08	70.47	62.95	71.88	72.53	70.45	69.84	65.11	68.00	66.14	53.76	50.39	57.2
Difference	-	-	-	-	-	40%	35%	42%	43%	41%	40%	37%	41%	43%	-	-	-
Soc Trang	2000	2001	2002	2003	2004	2005	2006	2007	2008	2009	2010	2011	2012	2013	2014	2015	2016
Statistic data	-	-	-	-	-	20.24	-	1.32	11.33	2.20	-	-	-	-	-	-	-
Modis	95.02	36.45	42.56	40.22	29.35	29.47	29.47	29.52	31.31	42.04	69.03	59.12	84.67	92.05	79.22	95.02	62.9
Difference	-	-	-	-	-	31%	-	96%	64%	95%	-	-	-	-	-	-	-
Bac Lieu	2000	2001	2002	2003	2004	2005	2006	2007	2008	2009	2010	2011	2012	2013	2014	2015	2016
Statistic data	-	-	-	-	-	64.07	0.00	62.68	65.82	68.52	32.36	62.72	34.04	76.06	77.96	78.96	79.96
Modis	26.17	4.58	7.97	4.59	2.38	9.38	17.02	20.68	22.12	27.40	21.17	28.31	32.23	36.44	34.35	36.59	29.7
Difference	-	-	-	-	-	85%	100%	67%	66%	60%	35%	55%	5%	52%	56%	54%	-
Tra Vinh	2000	2001	2002	2003	2004	2005	2006	2007	2008	2009	2010	2011	2012	2013	2014	2015	2016
Statistic data	-	-	-	-	-	-	-	-	45.46	93.37	91.76	90.91	89.01	-	-	-	-
Modis	84.81	48.19	49.23	50.59	37.52	45.01	40.96	47.18	53.90	56.78	63.03	59.24	62.86	79.32	82.31	81.41	64.6
Difference	-	-	-	-	-	-	-	-	16%	39%	31%	35%	29%	-	-	-	-
Ben Tre	2000	2001	2002	2003	2004	2005	2006	2007	2008	2009	2010	2011	2012	2013	2014	2015	2016
Statistic data	-	-	-	-	-	-	-	24.23	24.55	24.16	23.24	23.14	22.23	-	-	-	-
Modis	25.61	18.09	17.74	17.61	17.32	17.57	15.71	17.05	16.49	17.15	14.95	16.54	15.36	17.65	20.04	16.59	9.3
Difference	-	-	-	-	-	-	-	30%	33%	29%	36%	28%	31%	-	-	-	-

7.4. Flood distribution in Mekong Delta - MODIS satellite

7.4.1. Flood distribution in 2001



Appendix

Flood distribution in 2001 (continue)

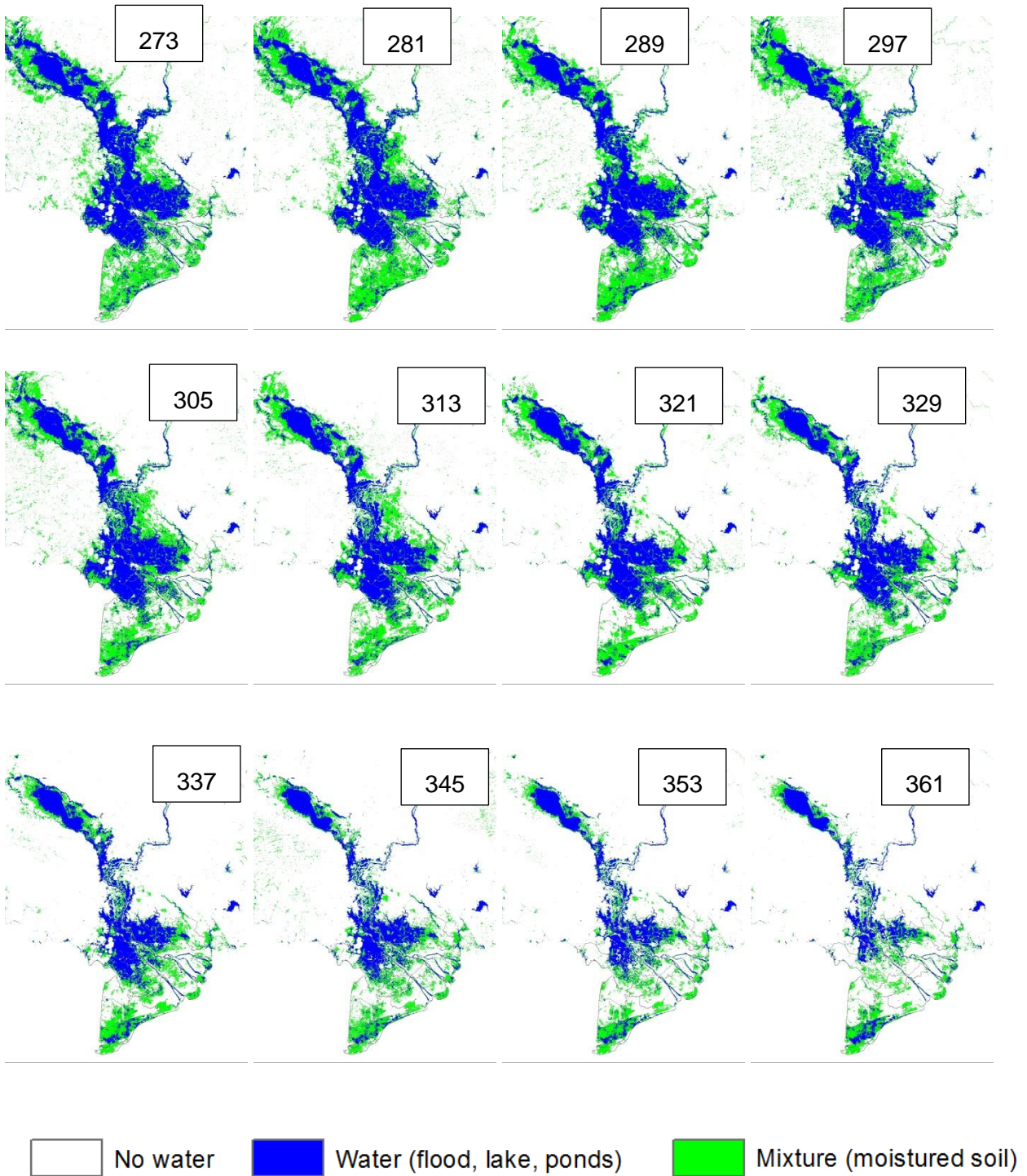
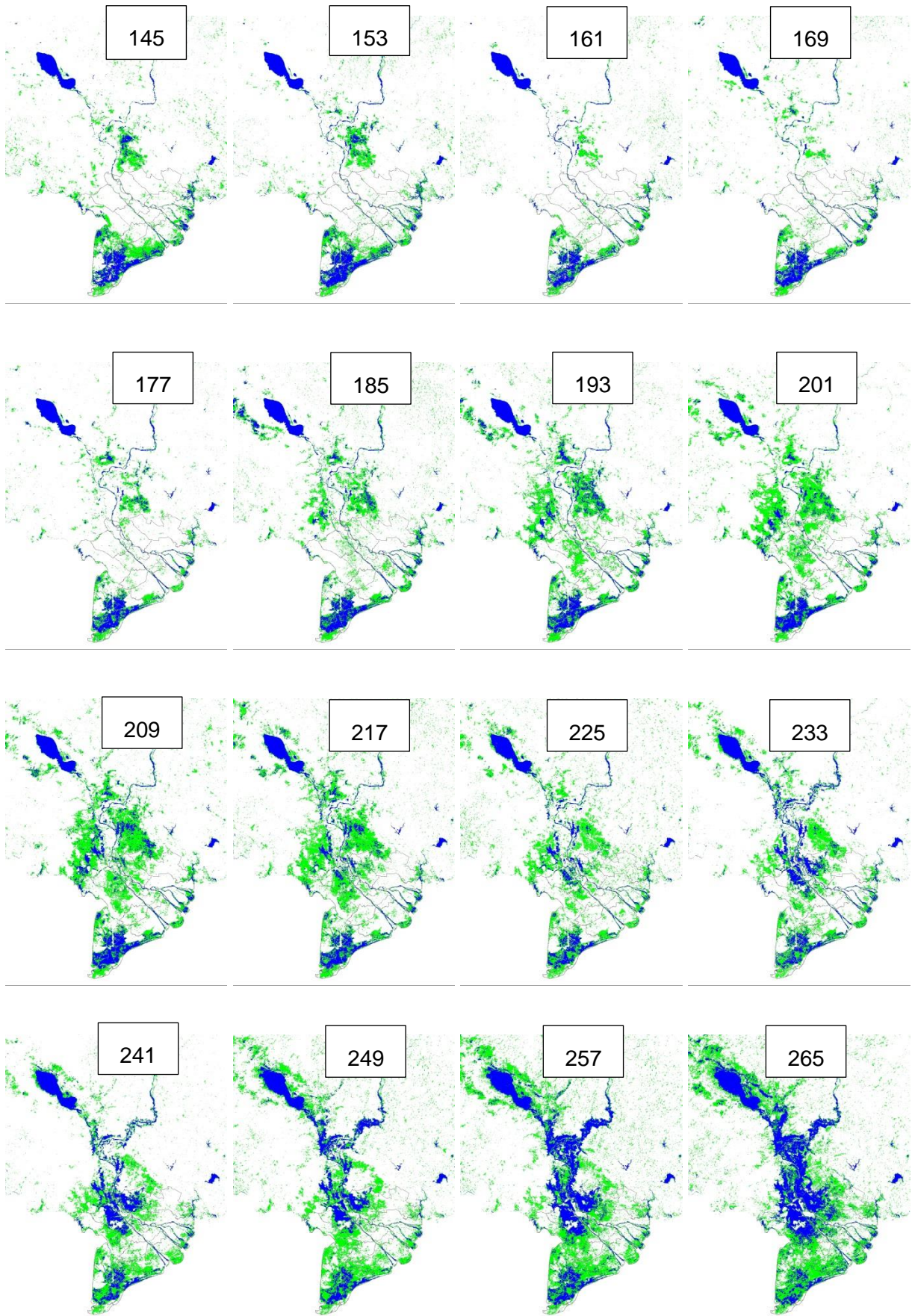


Figure 7.2. Flood distribution in Mekong delta in 2001 – MODIS satellite

7.4.2. Flood distribution in 2002



Appendix

FLOOD DISTRIBUTION IN 2002 (continue)

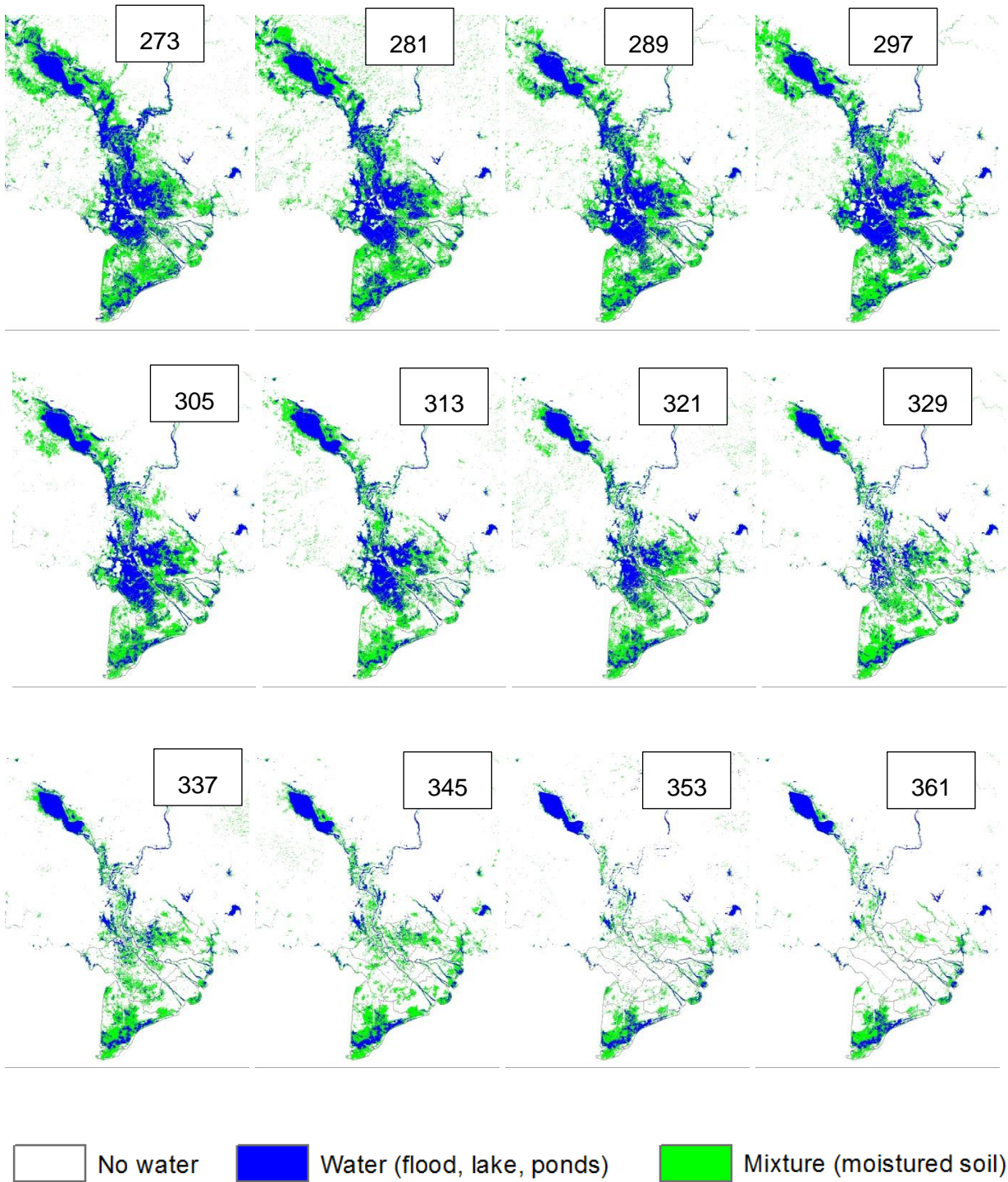
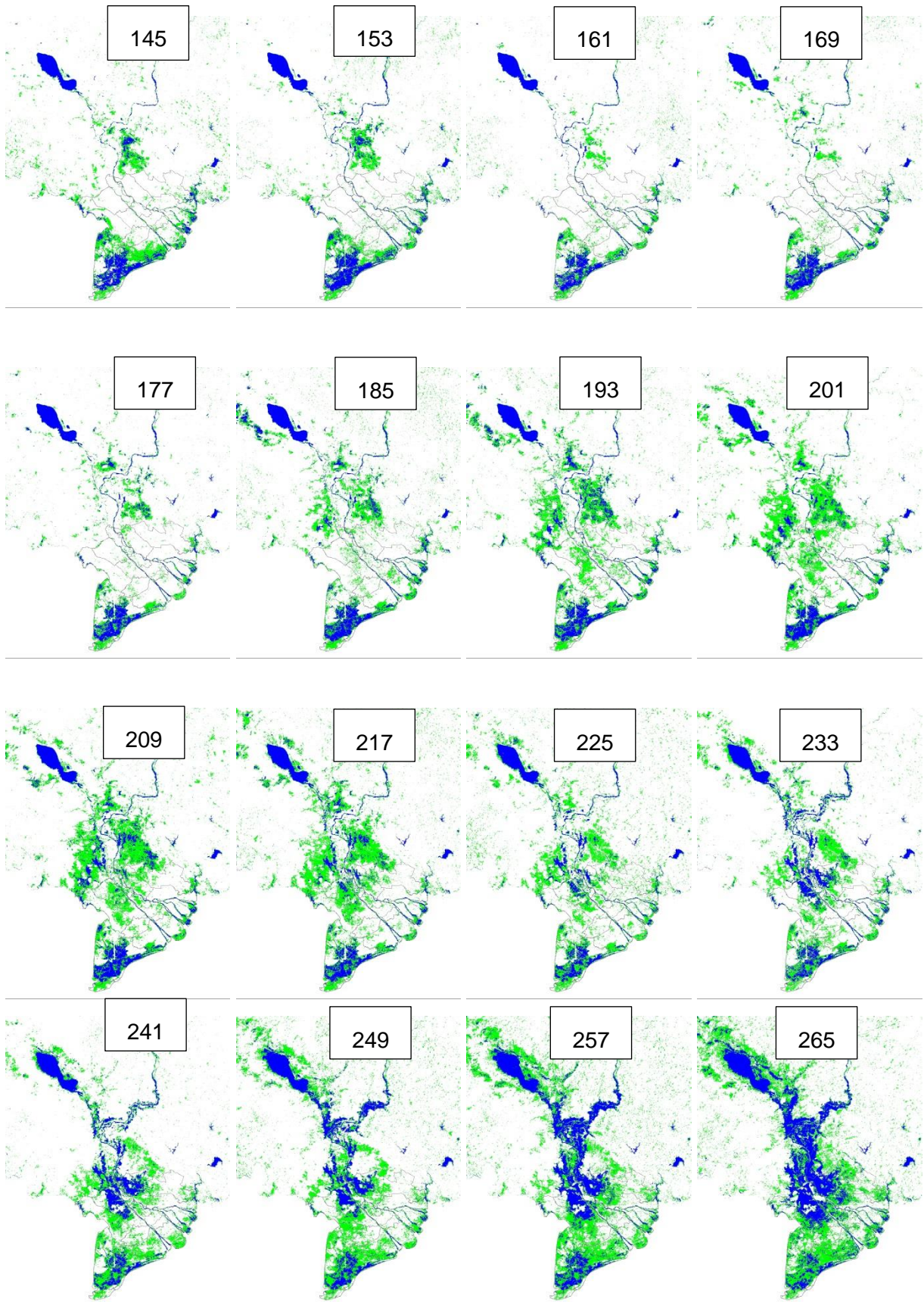


Figure 7.3. Flood distribution in Mekong delta in 2002 – MODIS satellite

7.4.3. Flood distribution in 2003



Flood distribution in 2003 (continue)

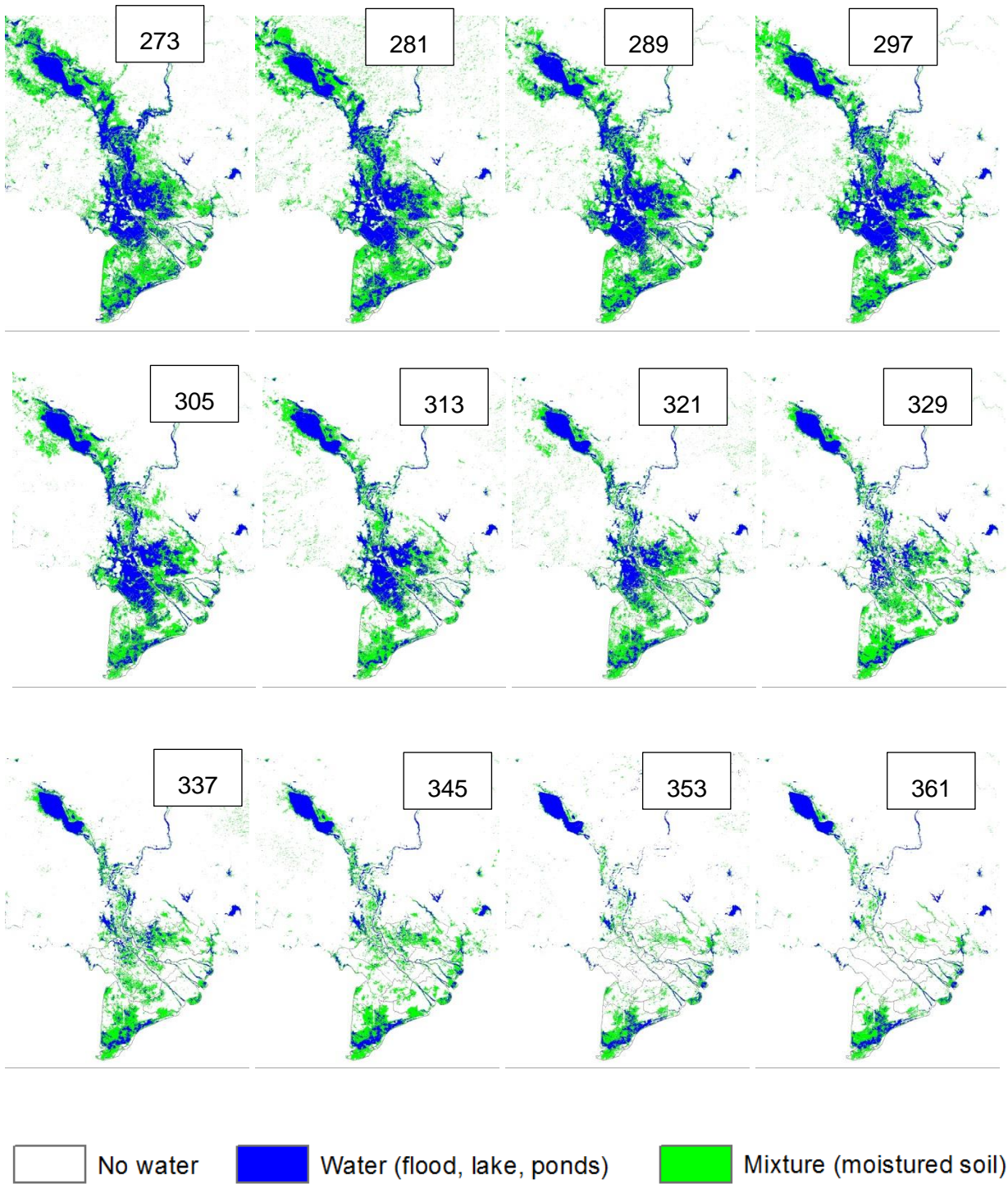
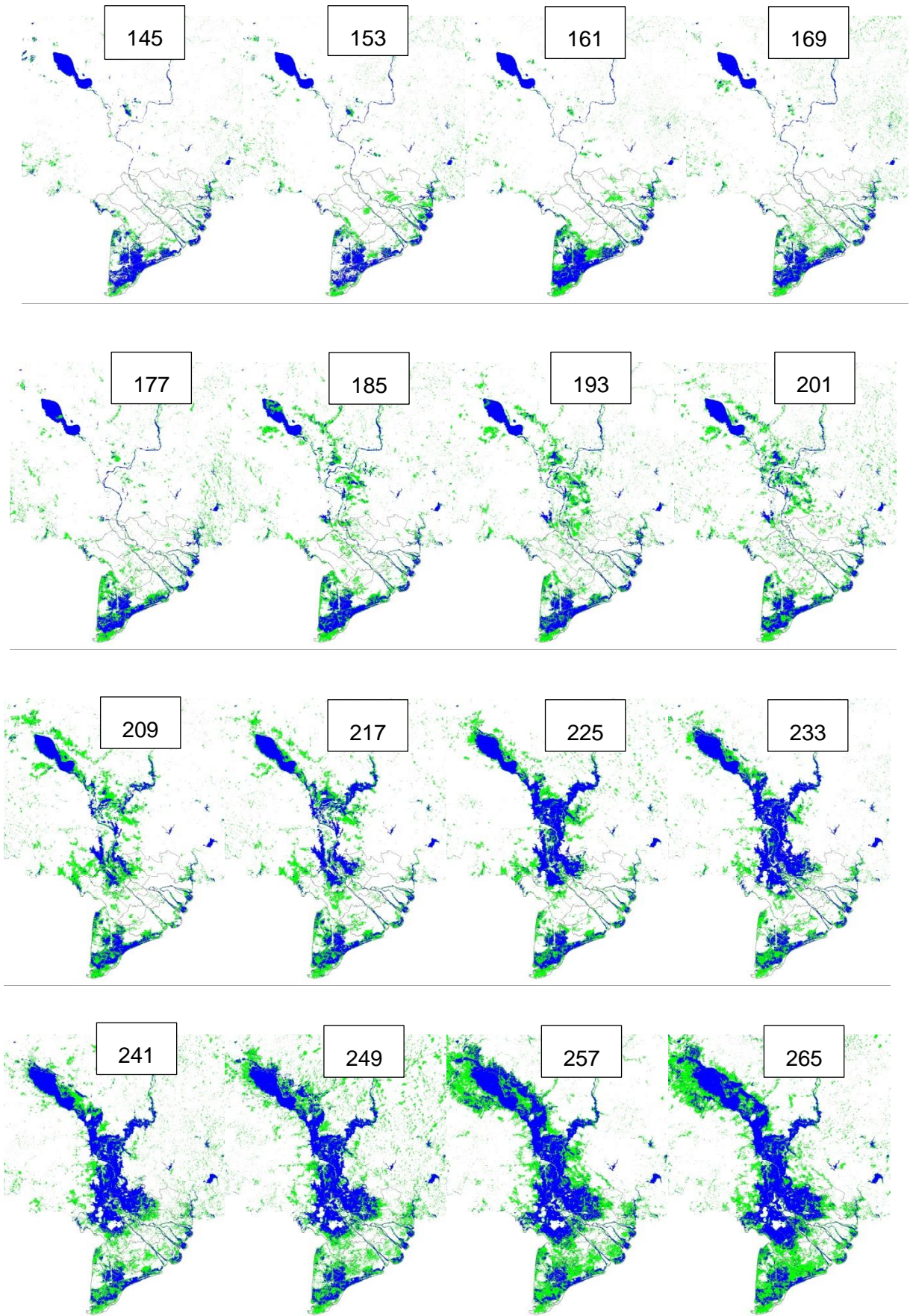


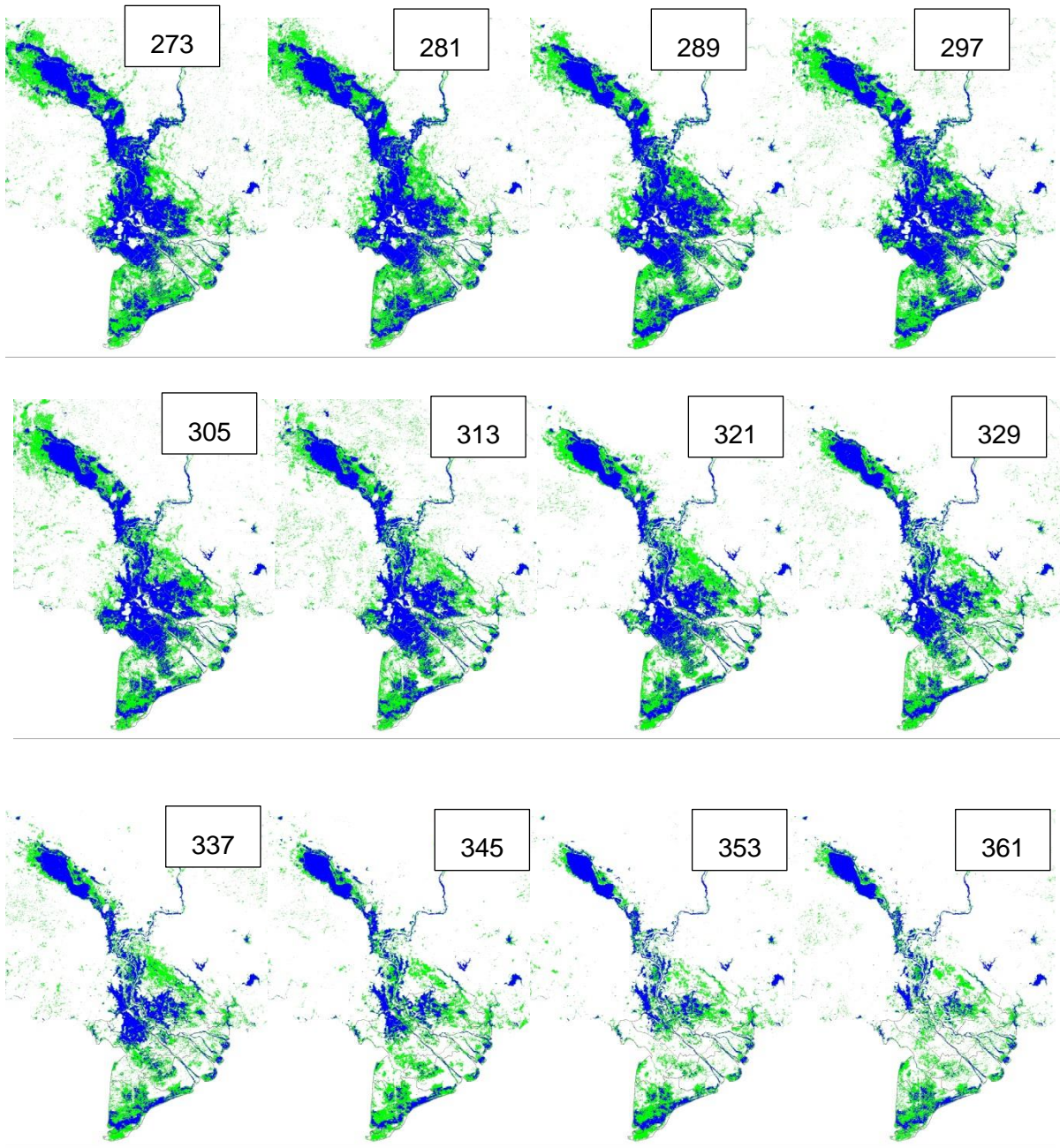
Figure 7.4. Flood distribution in Mekong delta in 2003 – MODIS satellite

7.4.4. Flood distribution in 2004



Appendix

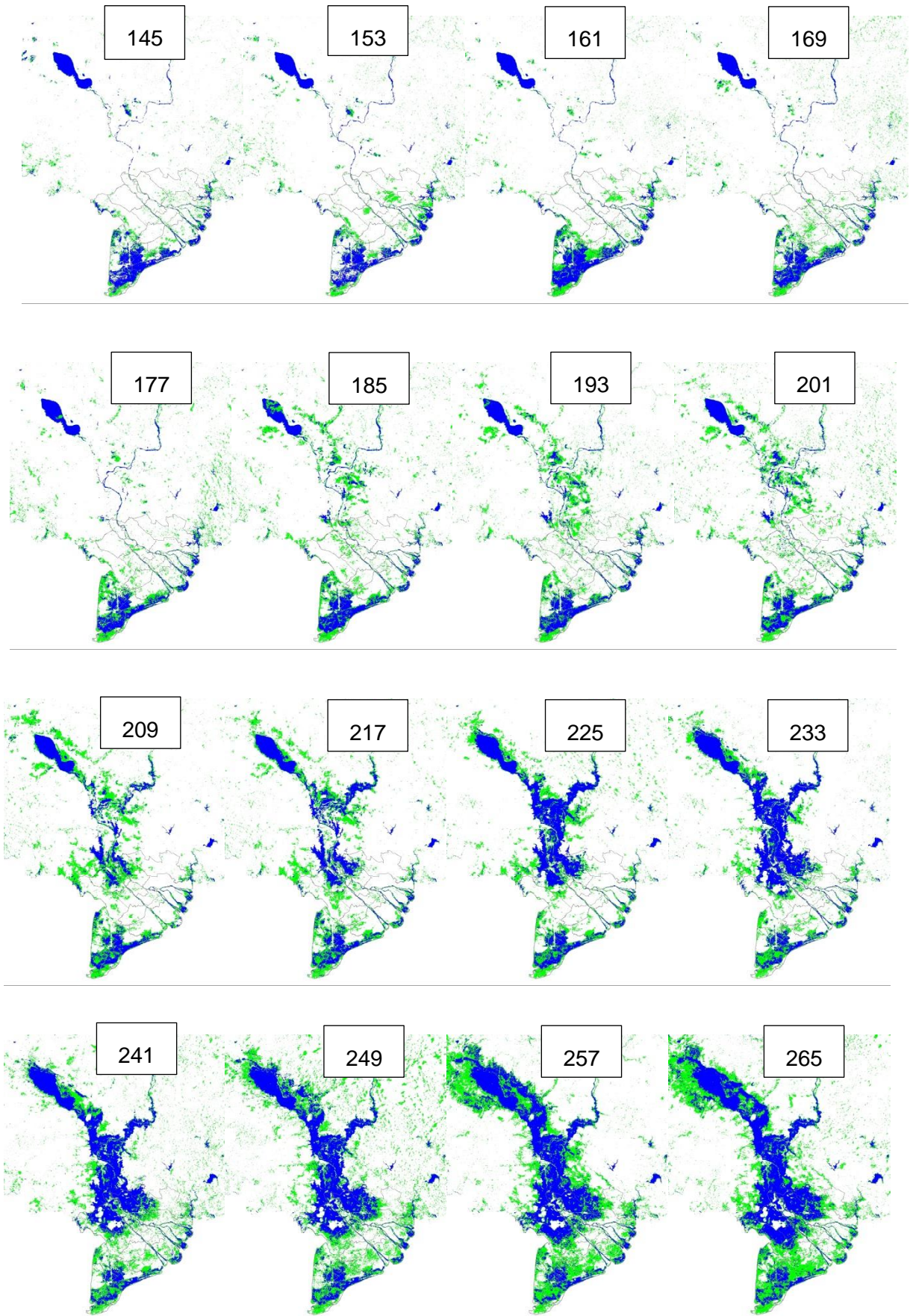
Flood distribution in 2004 (continue)



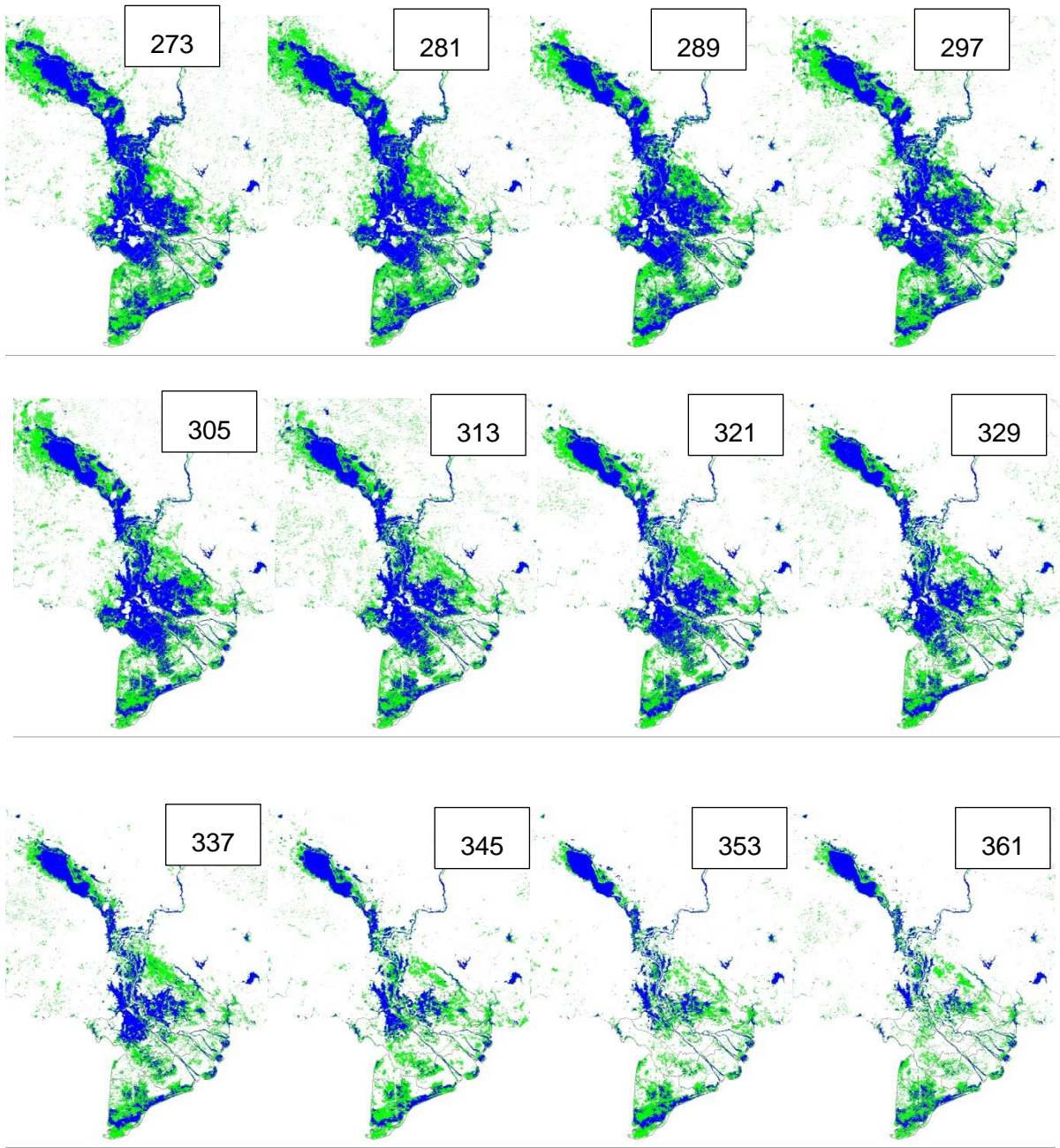
 No water  Water (flood, lake, ponds)  Mixture (moistured soil)

Figure 7.5. Flood distribution in Mekong delta in 2004 – MODIS satellite

7.4.5. Flood distribution in 2005



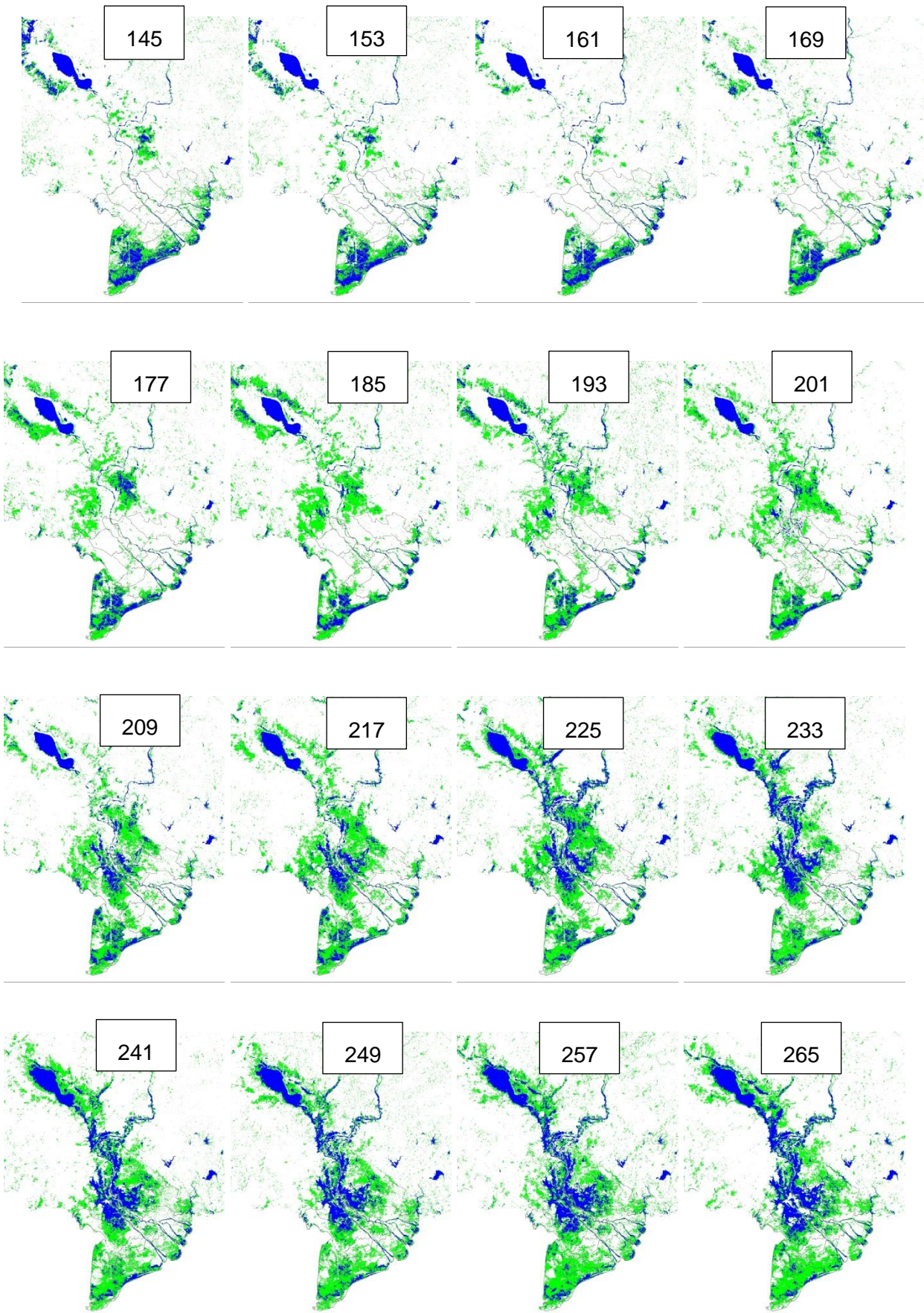
Flood distribution in 2005 (continue)



 No water  Water (flood, lake, ponds)  Mixture (moistured soil)

Figure 7.6. Flood distribution in Mekong delta in 2005 – MODIS satellite

7.4.6. Flood distribution in 2006



FLOOD DISTRIBUTION IN 2006 (continue)

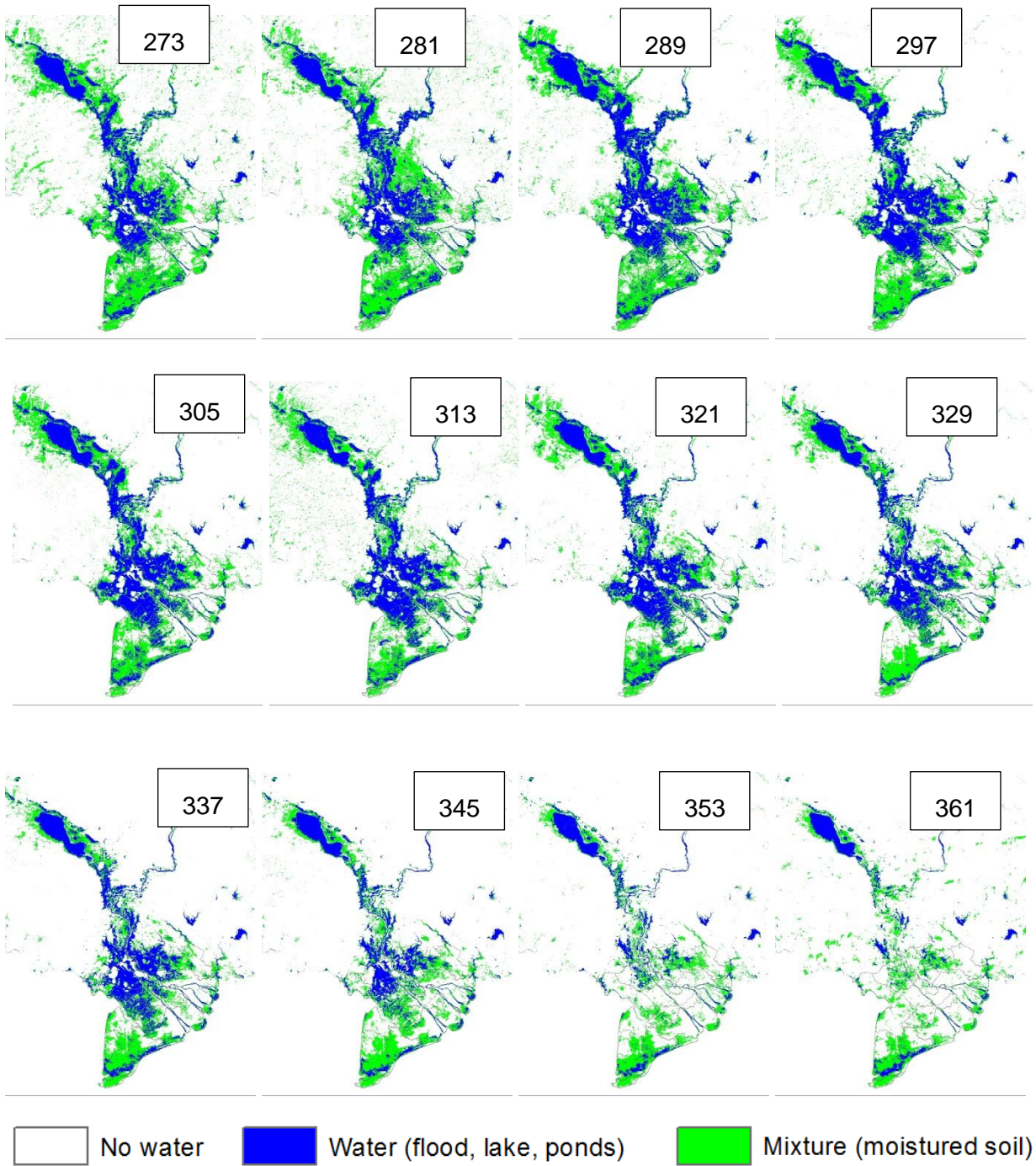
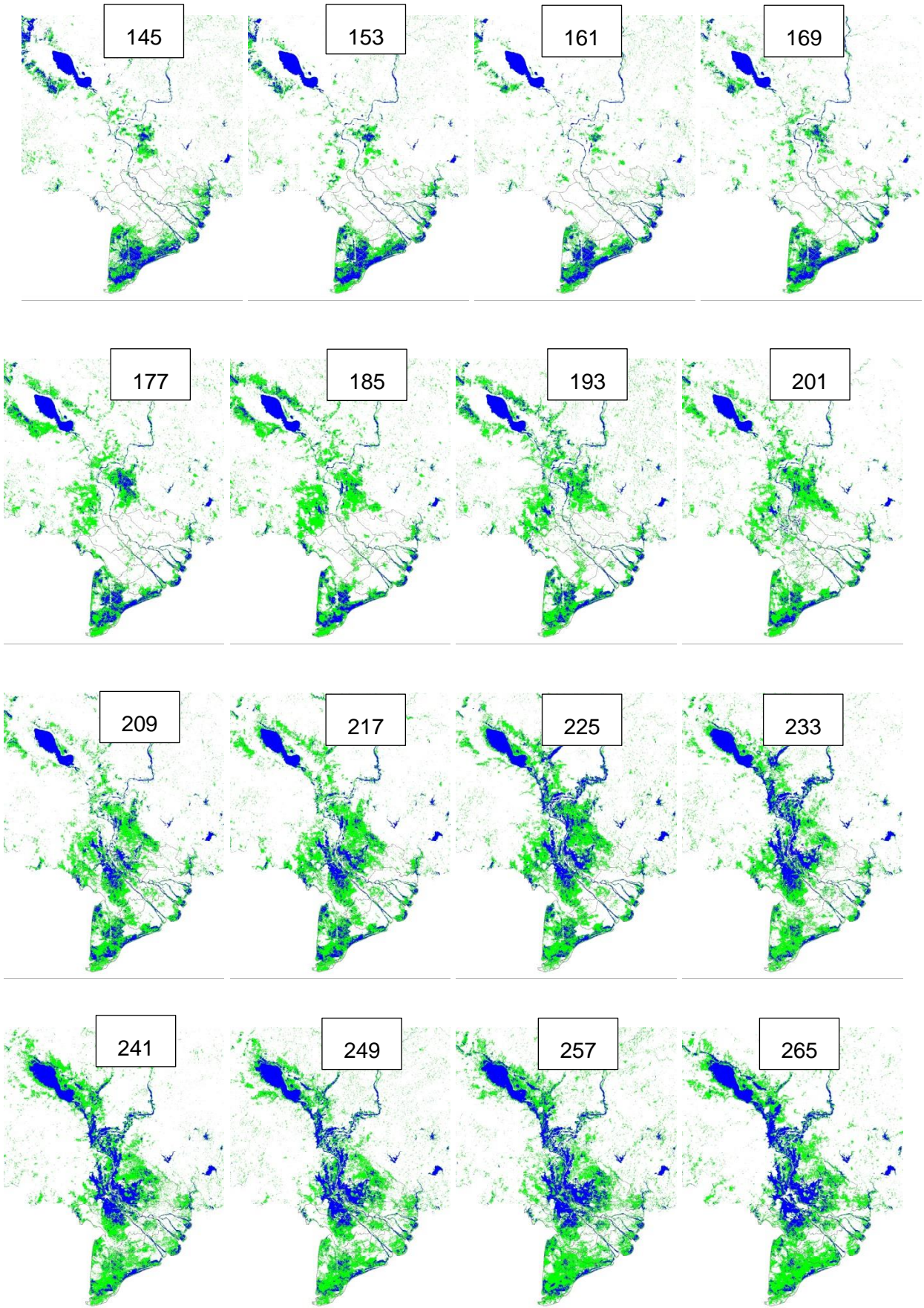
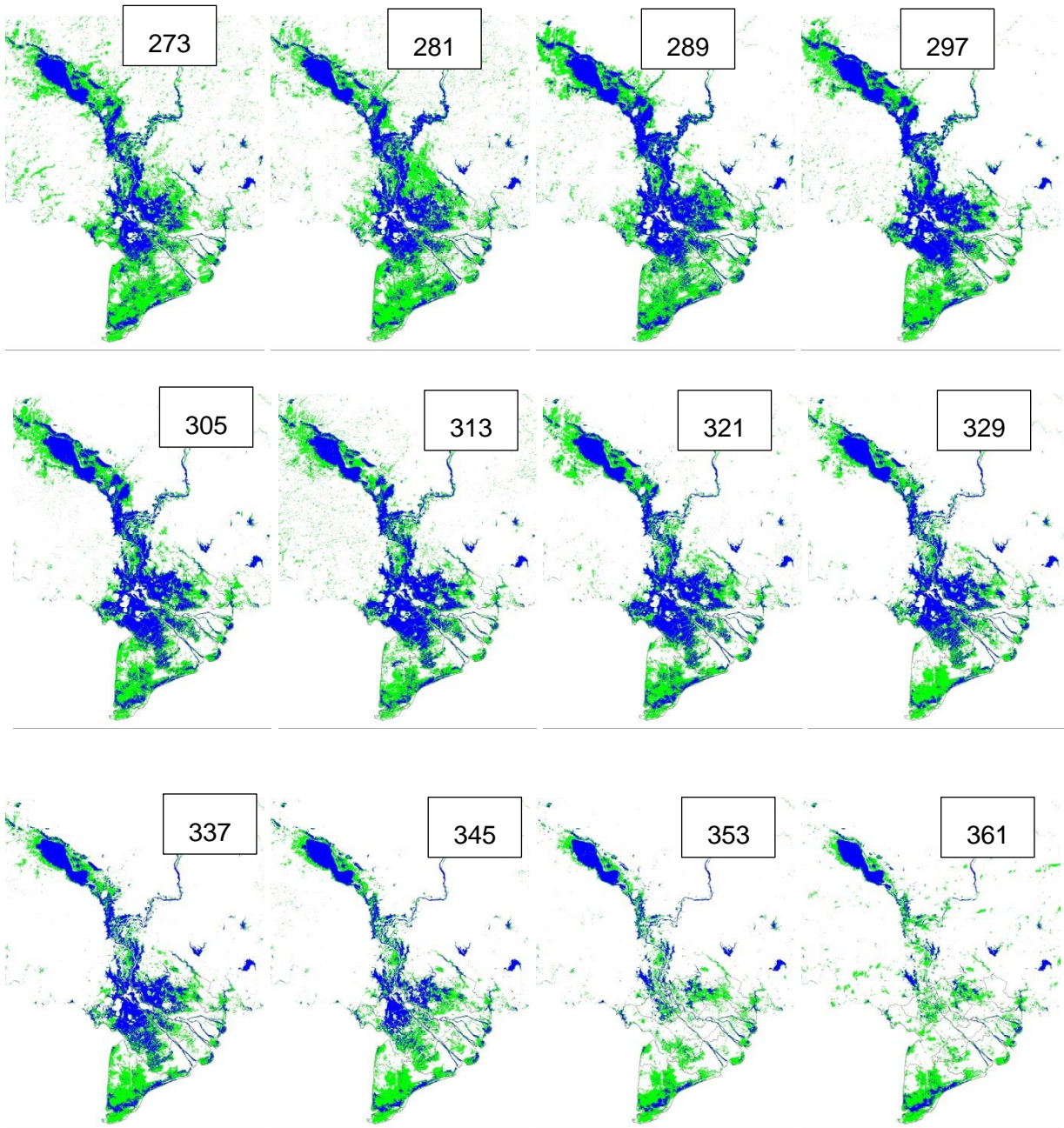


Figure 7.7. Flood distribution in Mekong delta in 2007 – MODIS satellite

7.4.7. Flood distribution in 2007



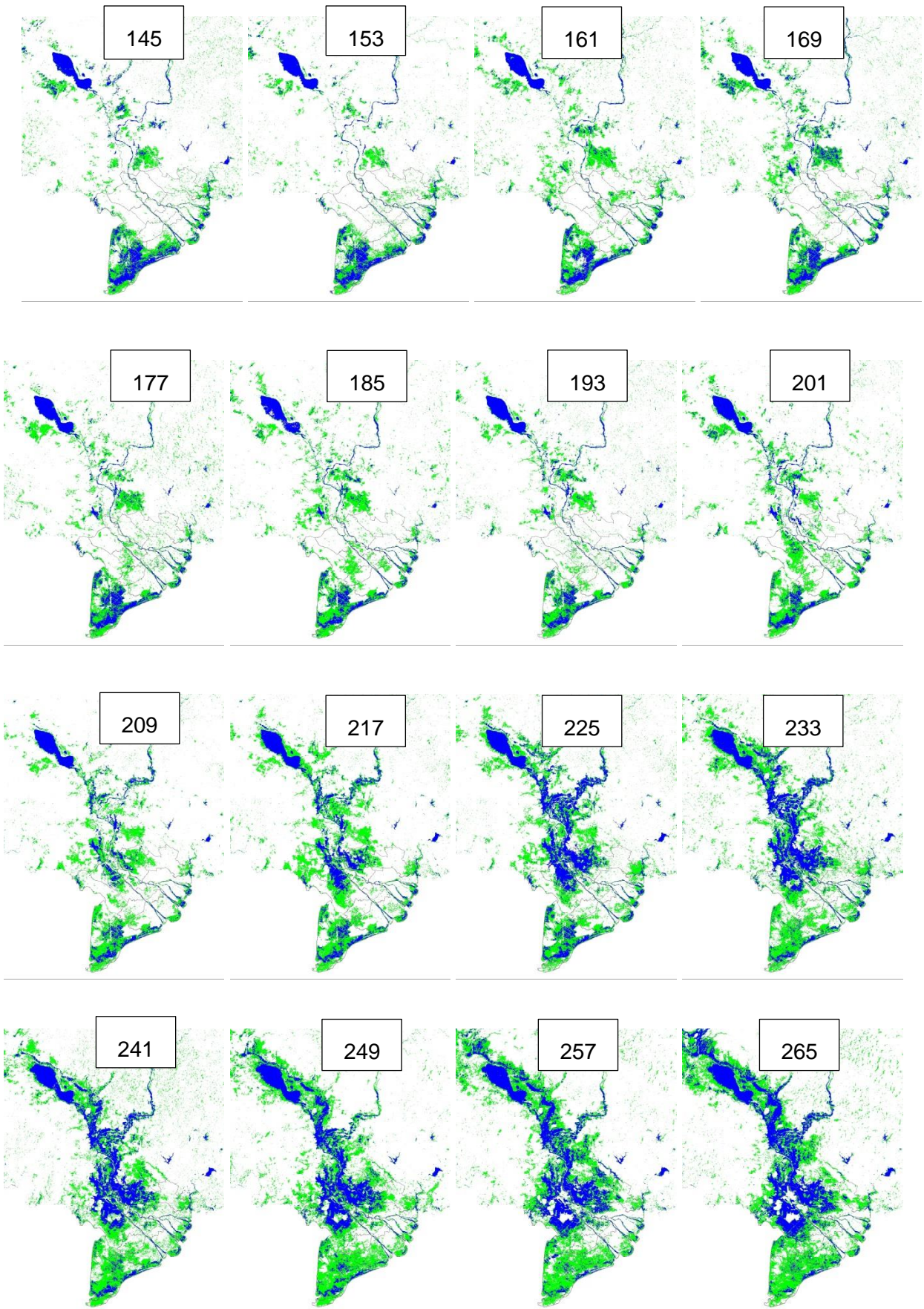
FLOOD DISTRIBUTION IN 2007 (continue)



 No water  Water (flood, lake, ponds)  Mixture (moistured soil)

Figure 7.8. Flood distribution in Mekong delta in 2007 – MODIS satellite

7.4.8. Flood distribution in 2008



FLOOD DISTRIBUTION IN 2008 (continue)

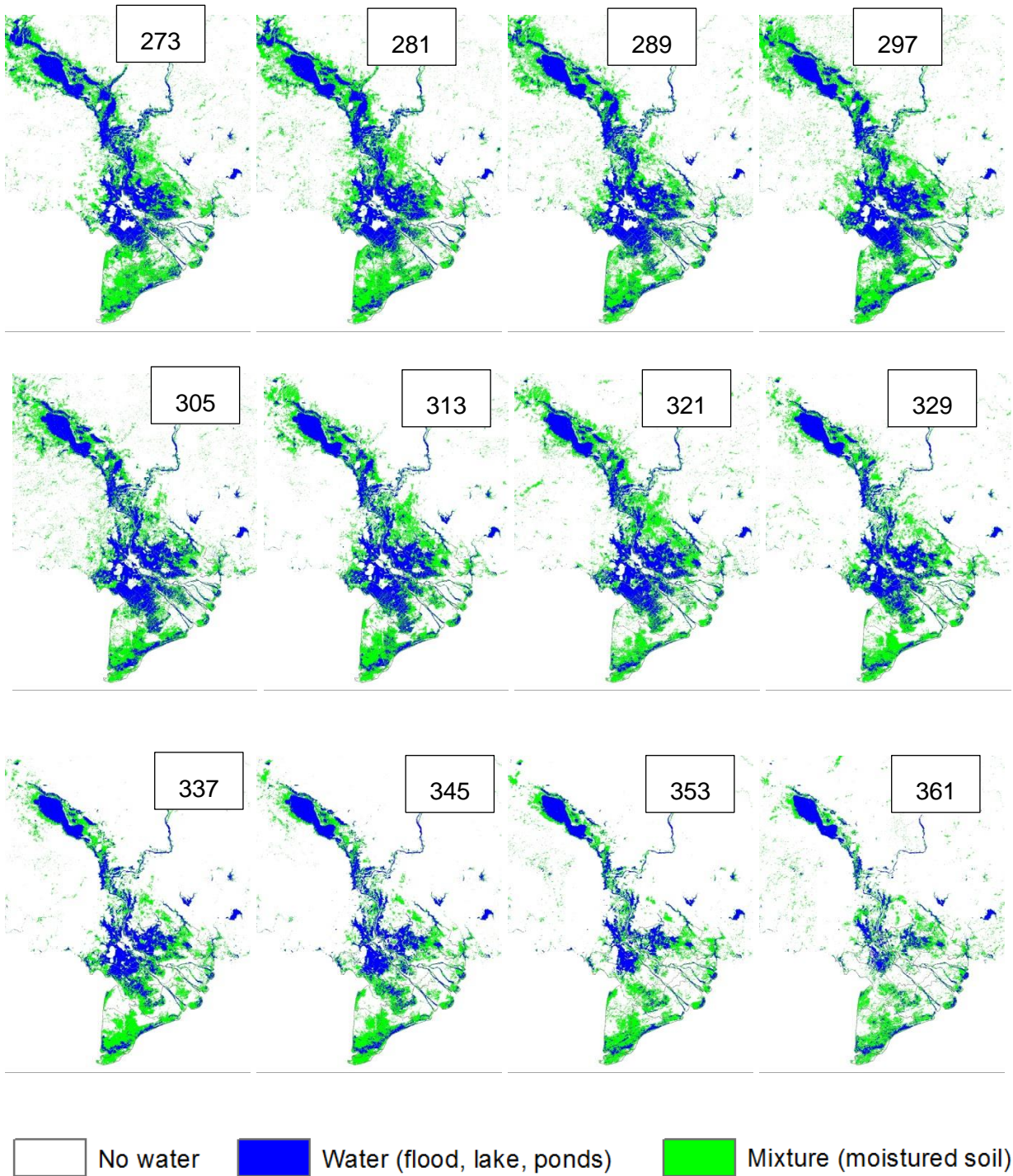
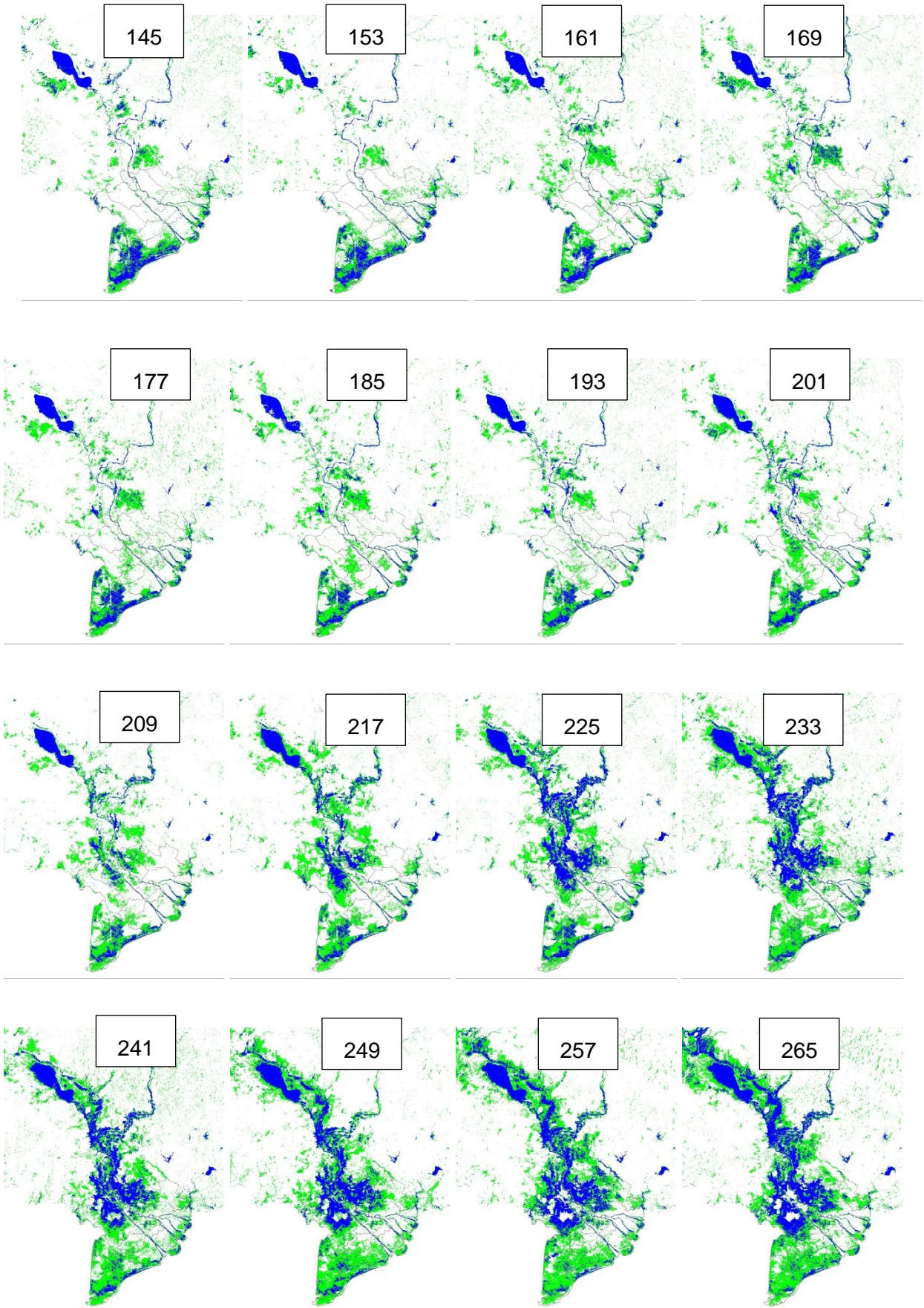


Figure 7.9. Flood distribution in Mekong delta in 2008 – MODIS satellite

7.4.9. Flood distribution in 2009



FLOOD DISTRIBUTION IN 2009 (continue)

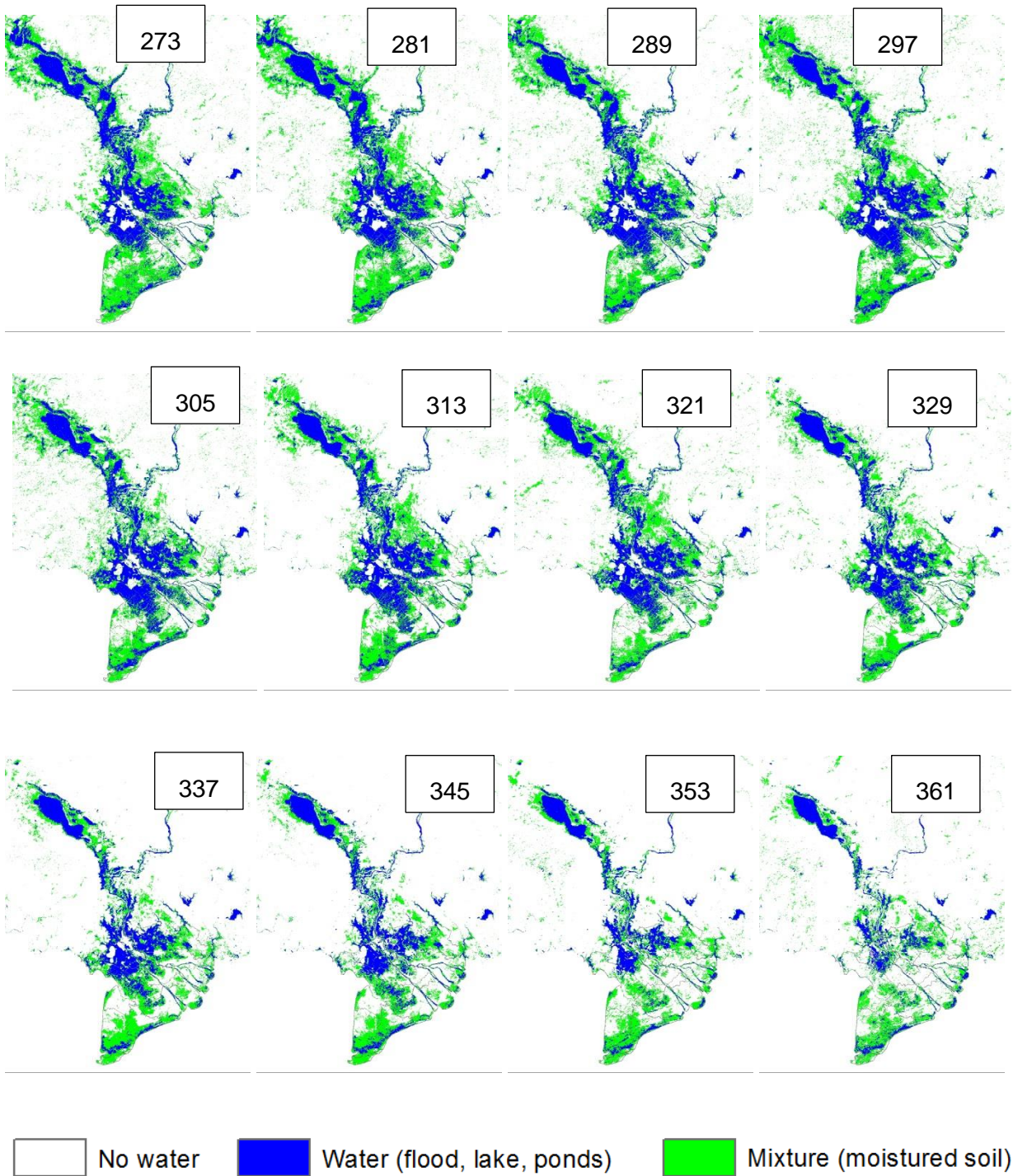
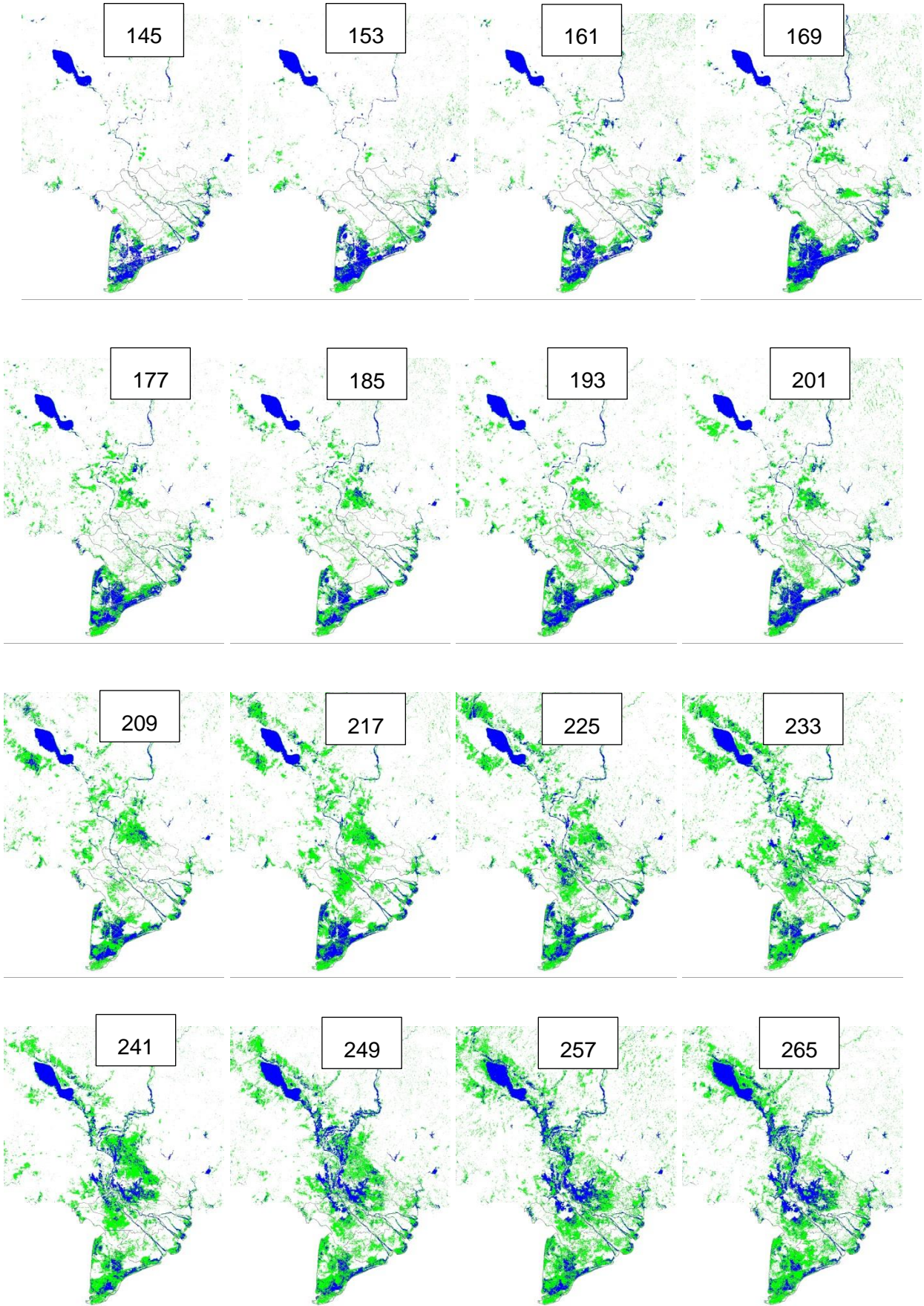


Figure 7.10. Flood distribution in Mekong delta in 2009 – MODIS satellite

7.4.10. Flood distribution in 2010



Appendix

Flood distribution in 2010 (continue)

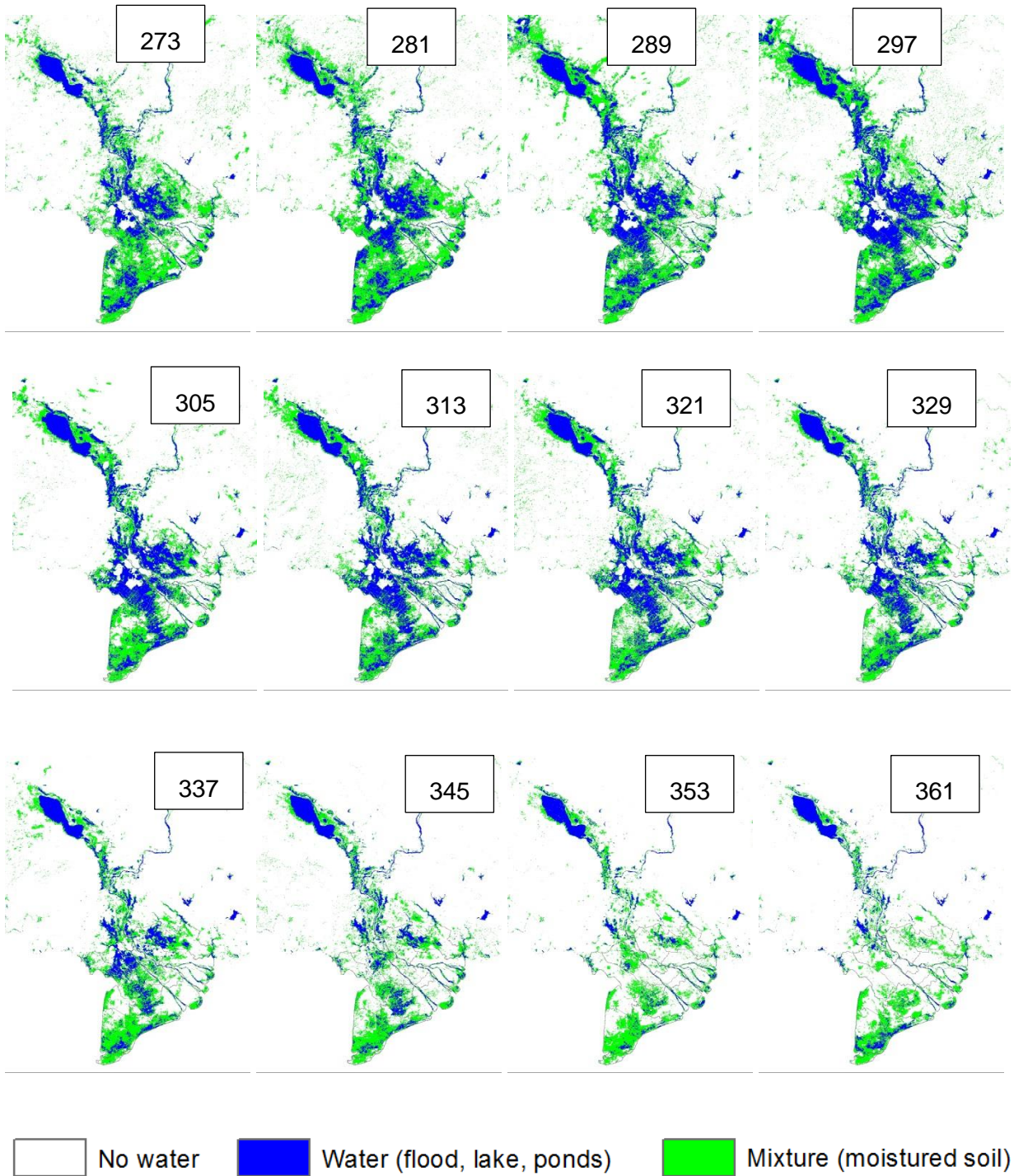
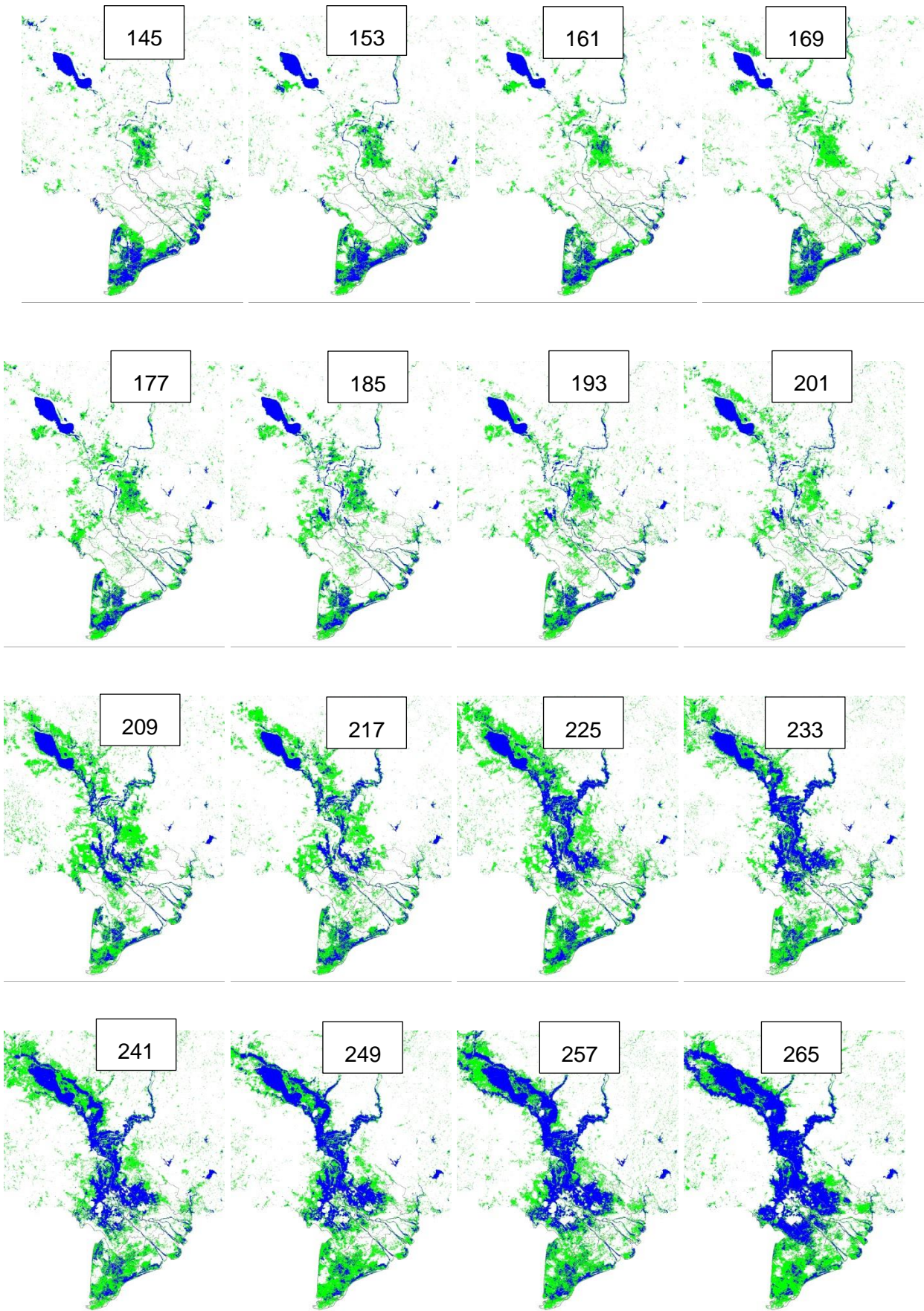


Figure 7.11. Flood distribution in Mekong delta in 2010 – MODIS satellite

7.4.11. Flood distribution in 2011



Flood distribution in 2011 (continue)

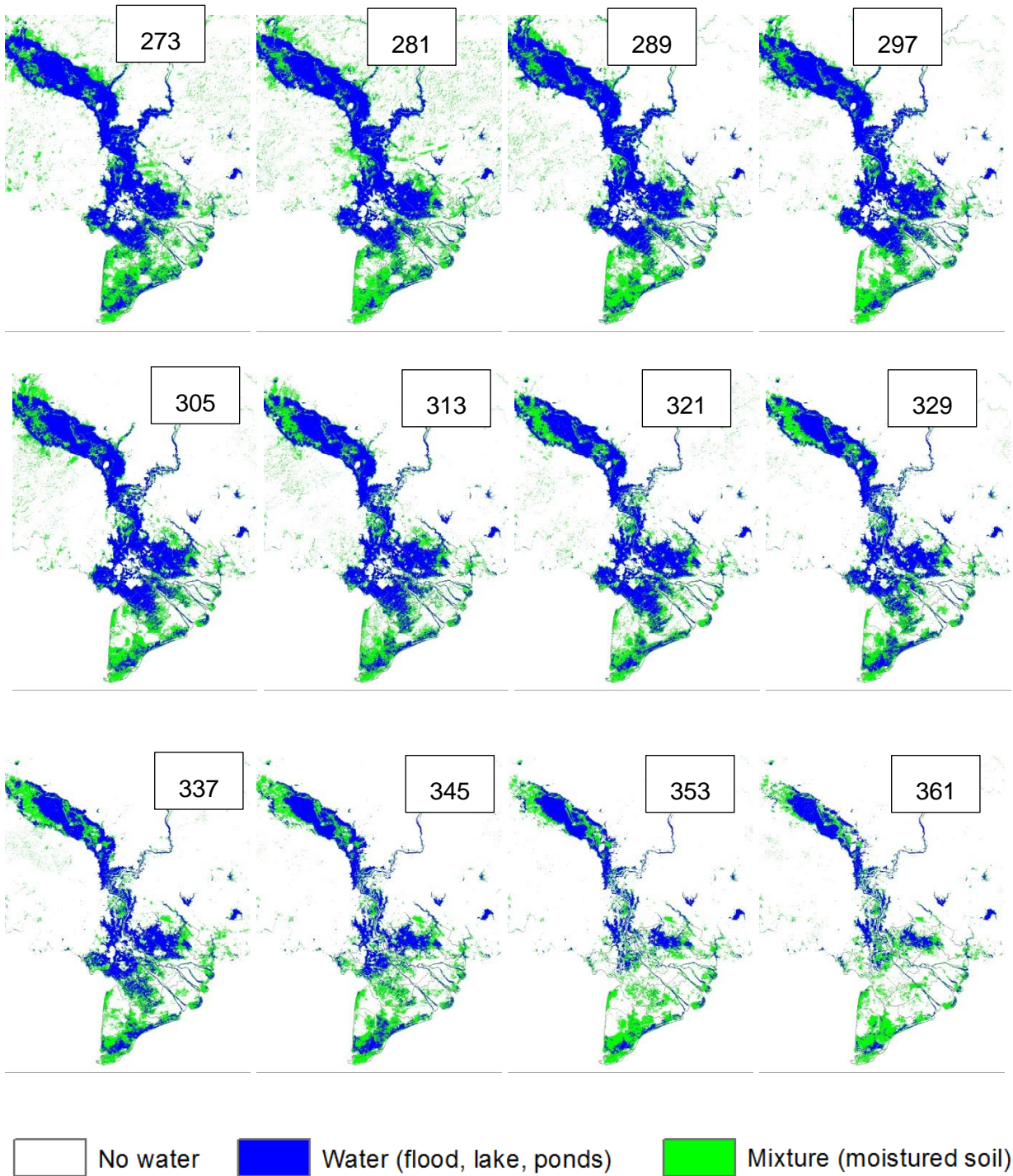
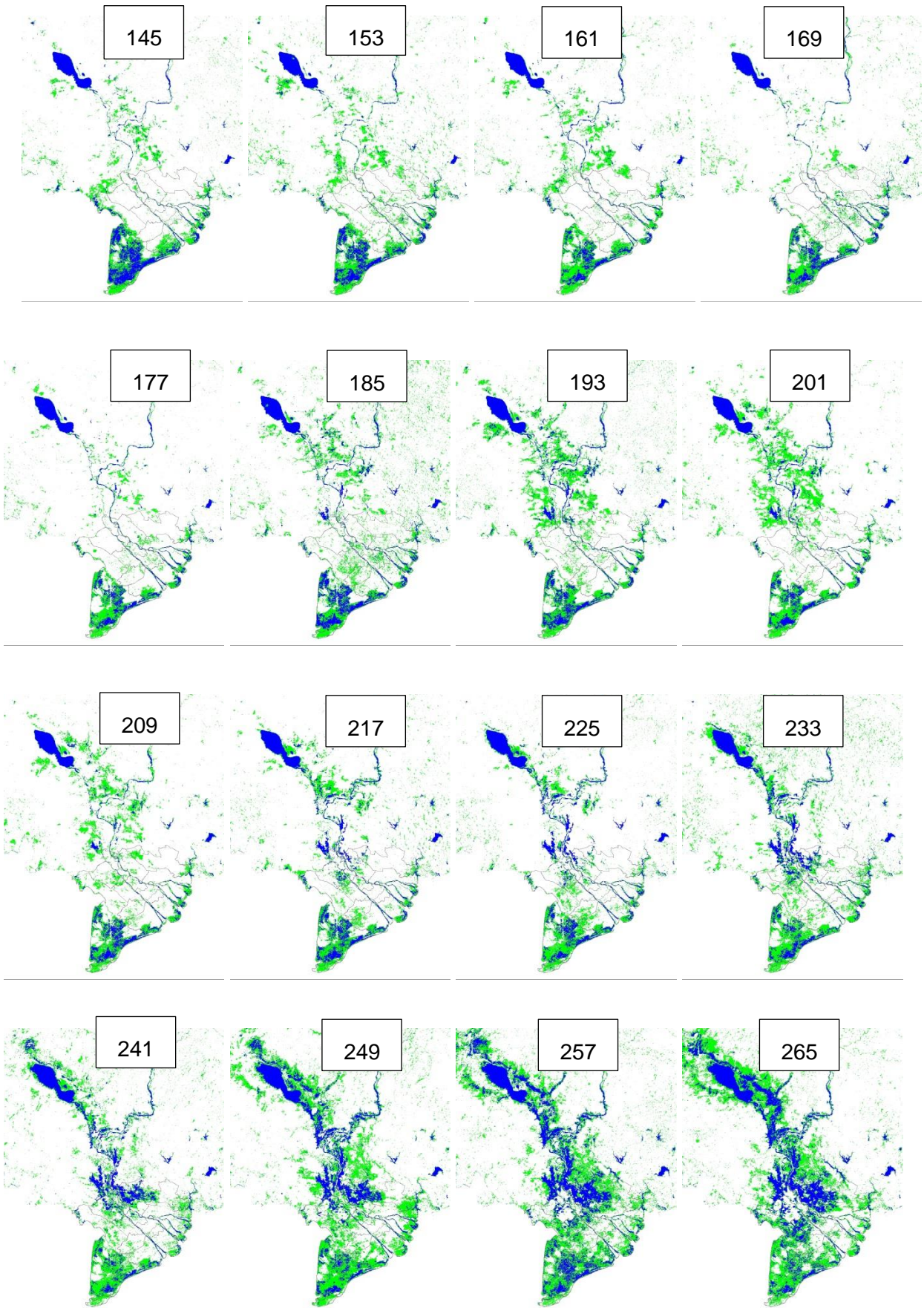


Figure 7.12. Flood distribution in Mekong delta in 2011 – MODIS satellite

7.4.12. Flood distribution in 2012



Flood distribution in 2012 (continue)

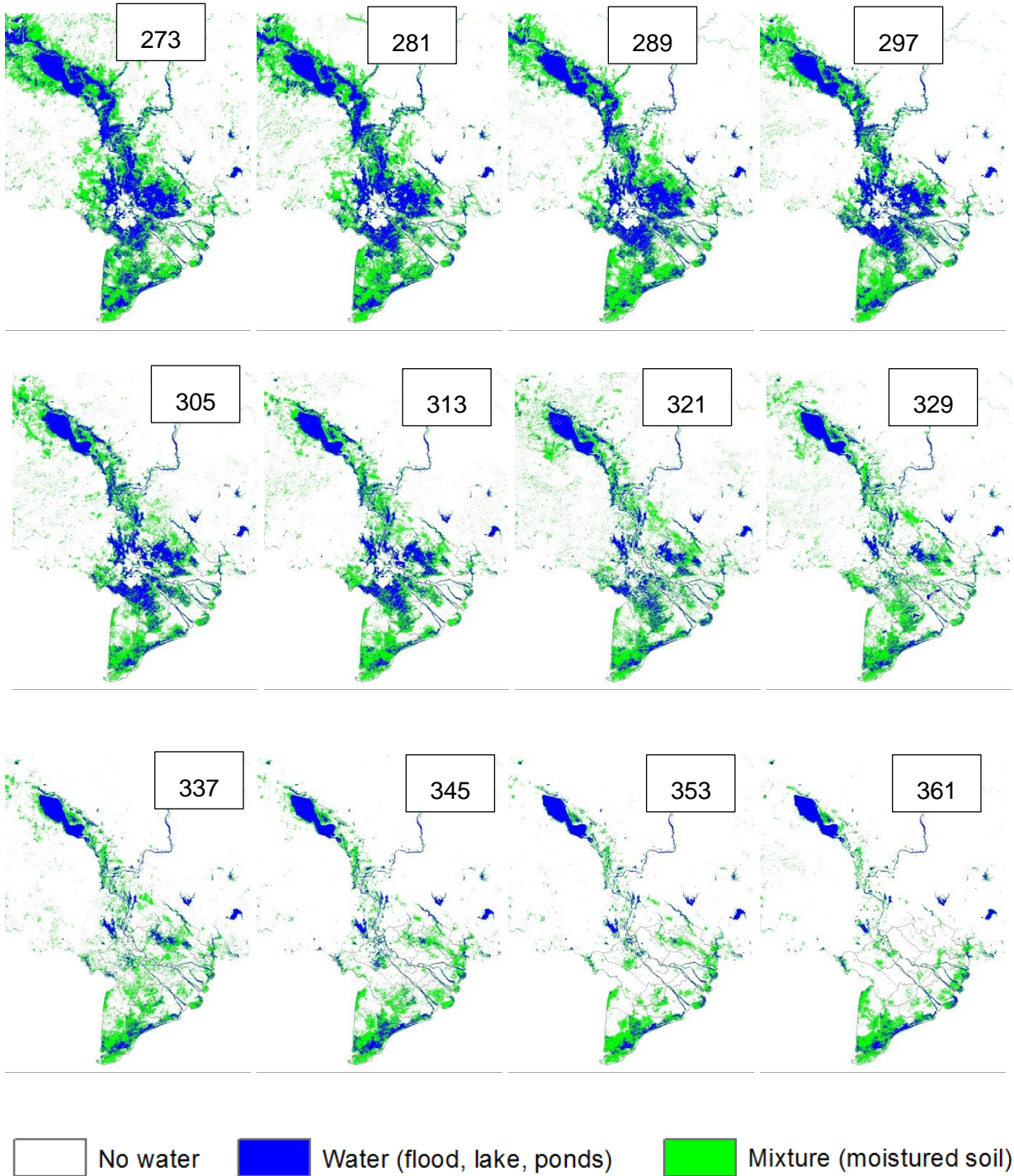
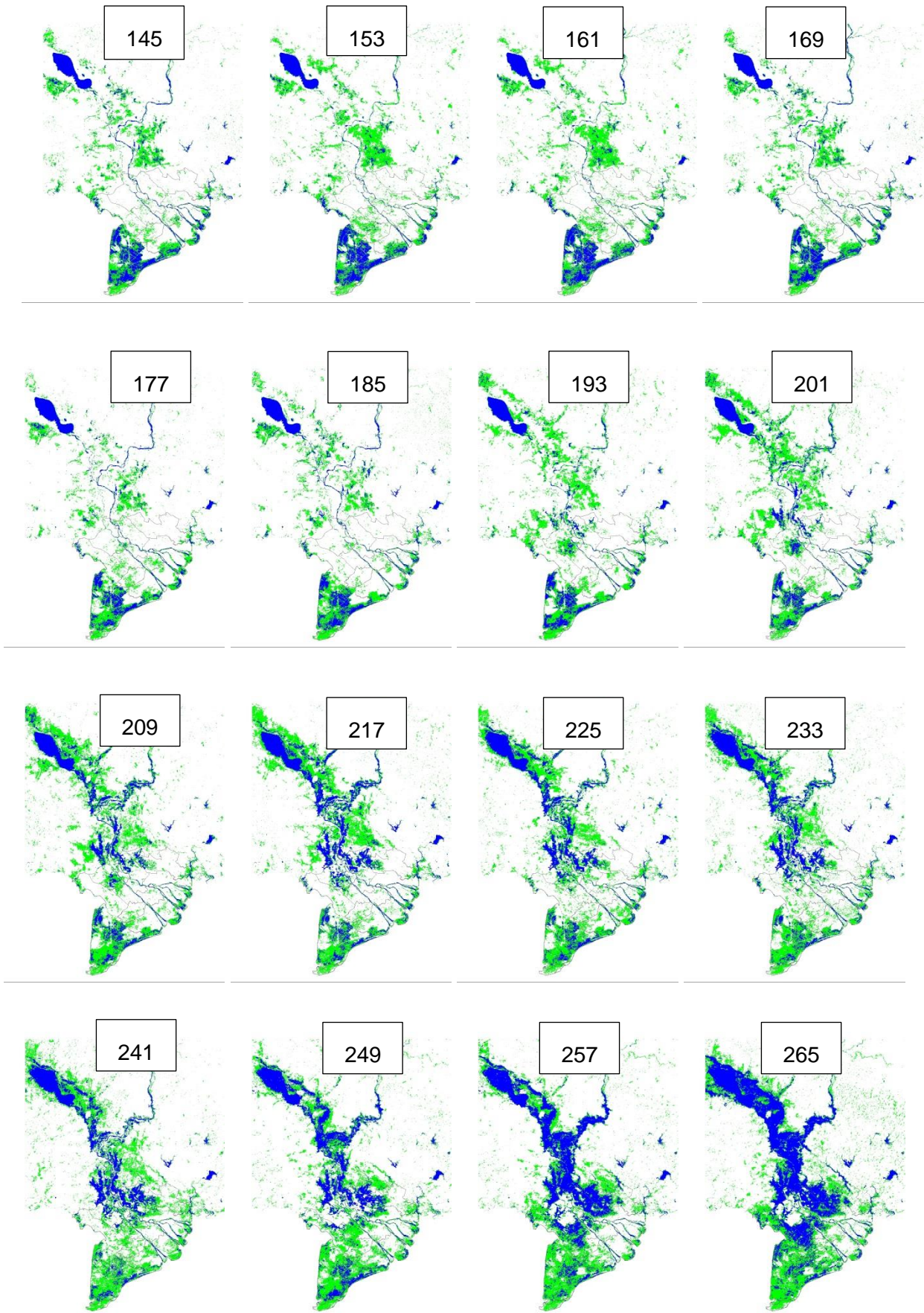


Figure 7.13. Flood distribution in Mekong delta in 2012 – MODIS satellite

7.4.13. Flood distribution in 2013



flood distribution in 2013 (continue)

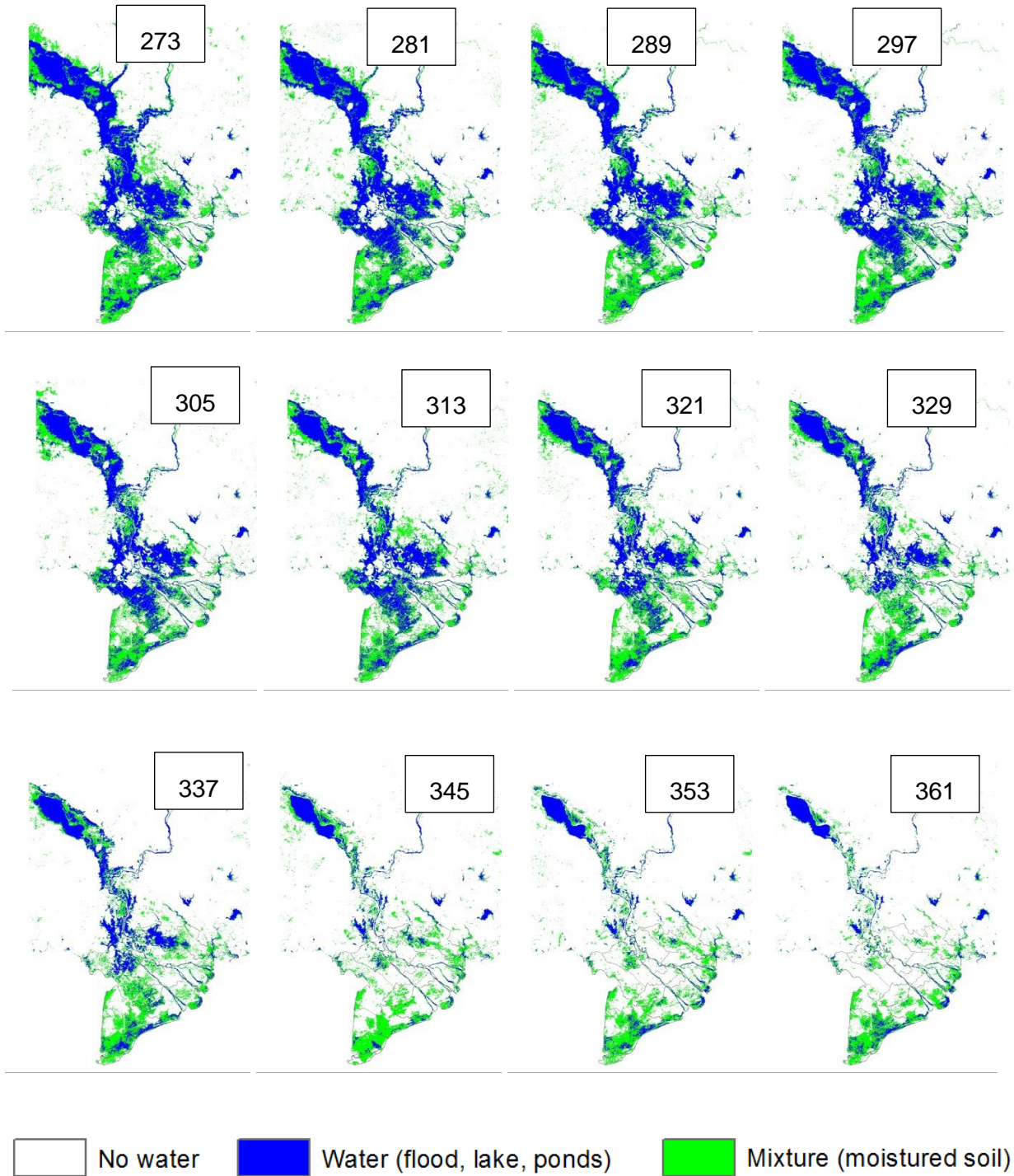
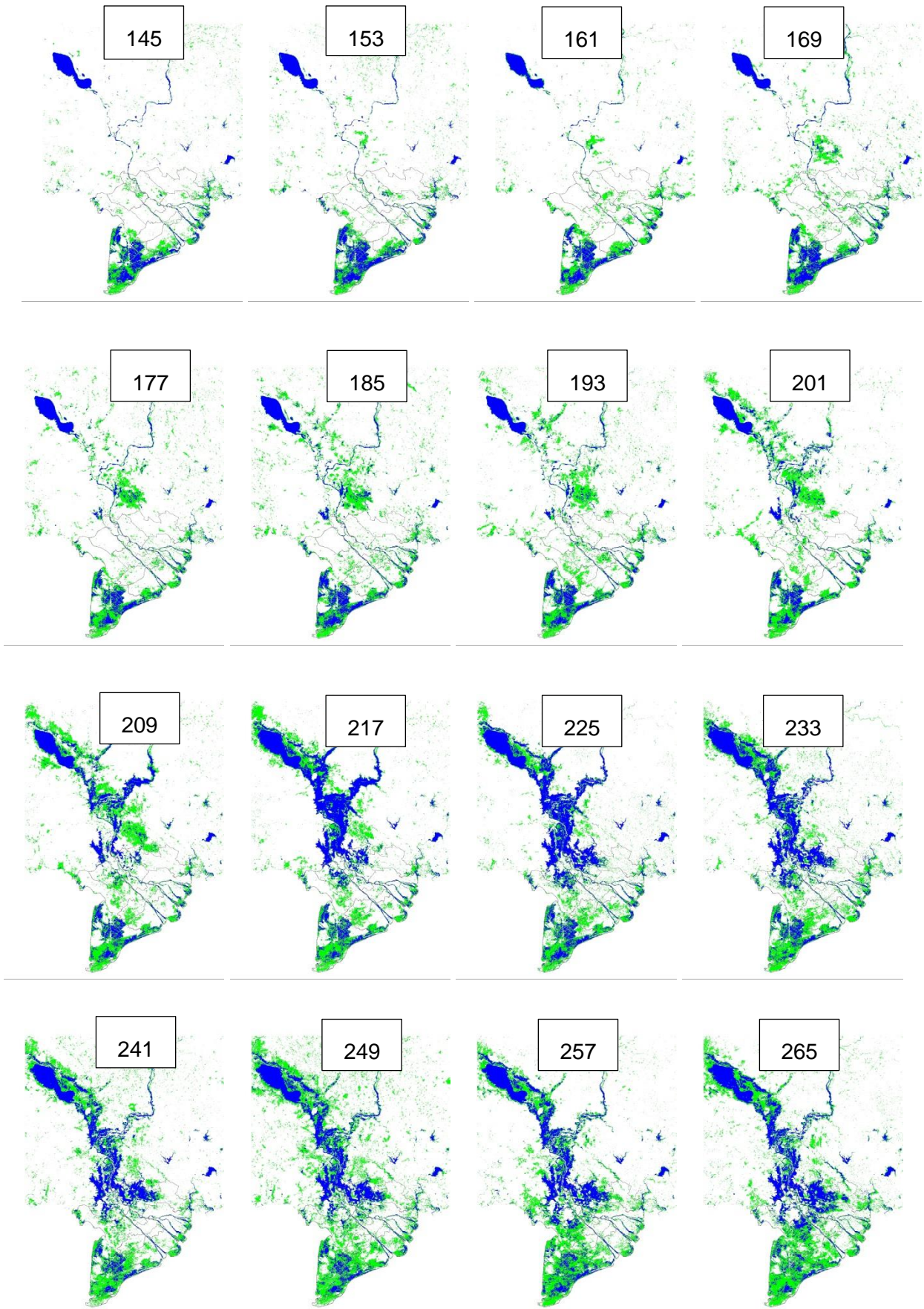


Figure 7.14. Flood distribution in Mekong delta in 2013 – MODIS satellite

7.4.14. Flood distribution in 2014



Flood distribution in 2014 (continue)

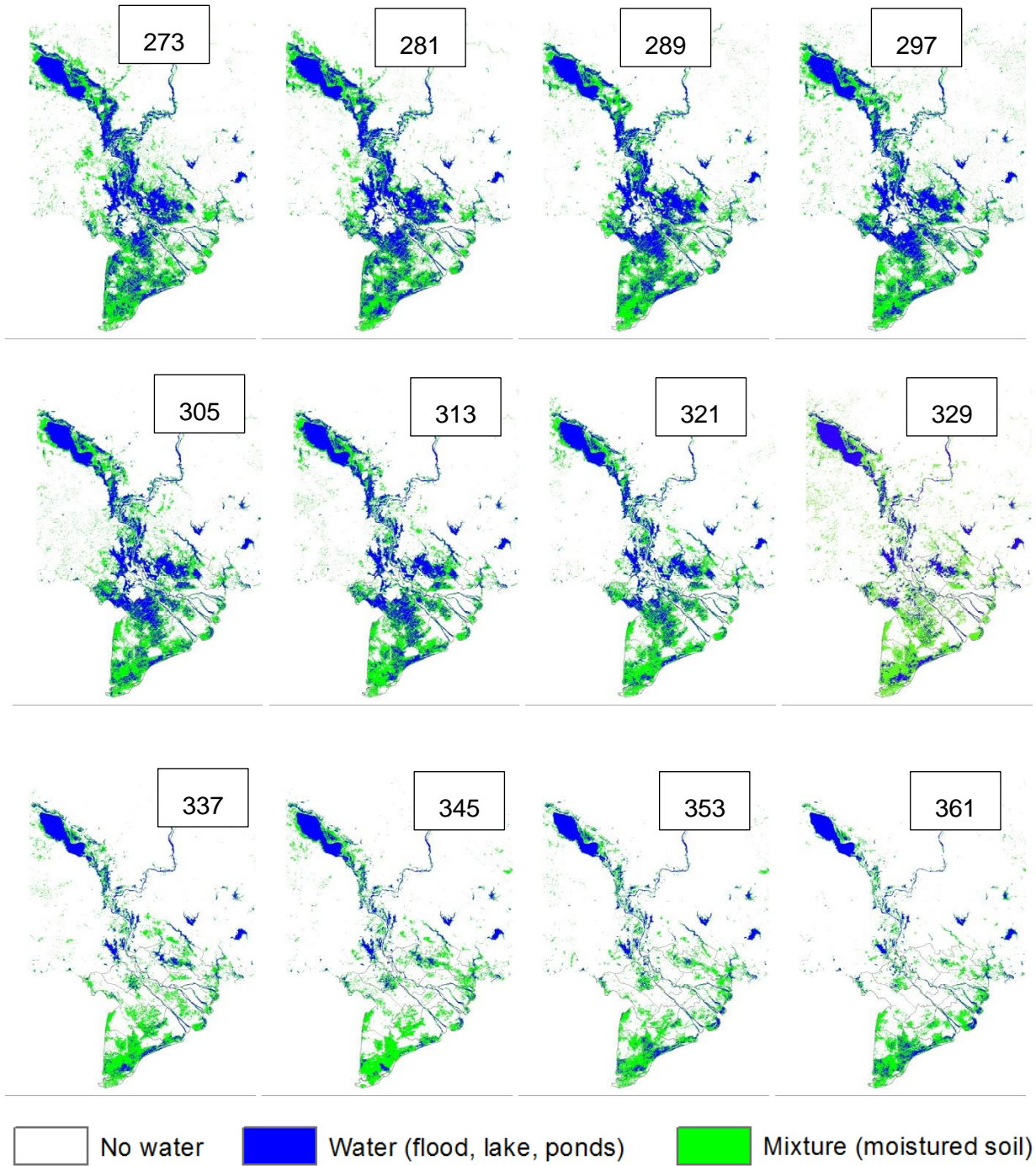
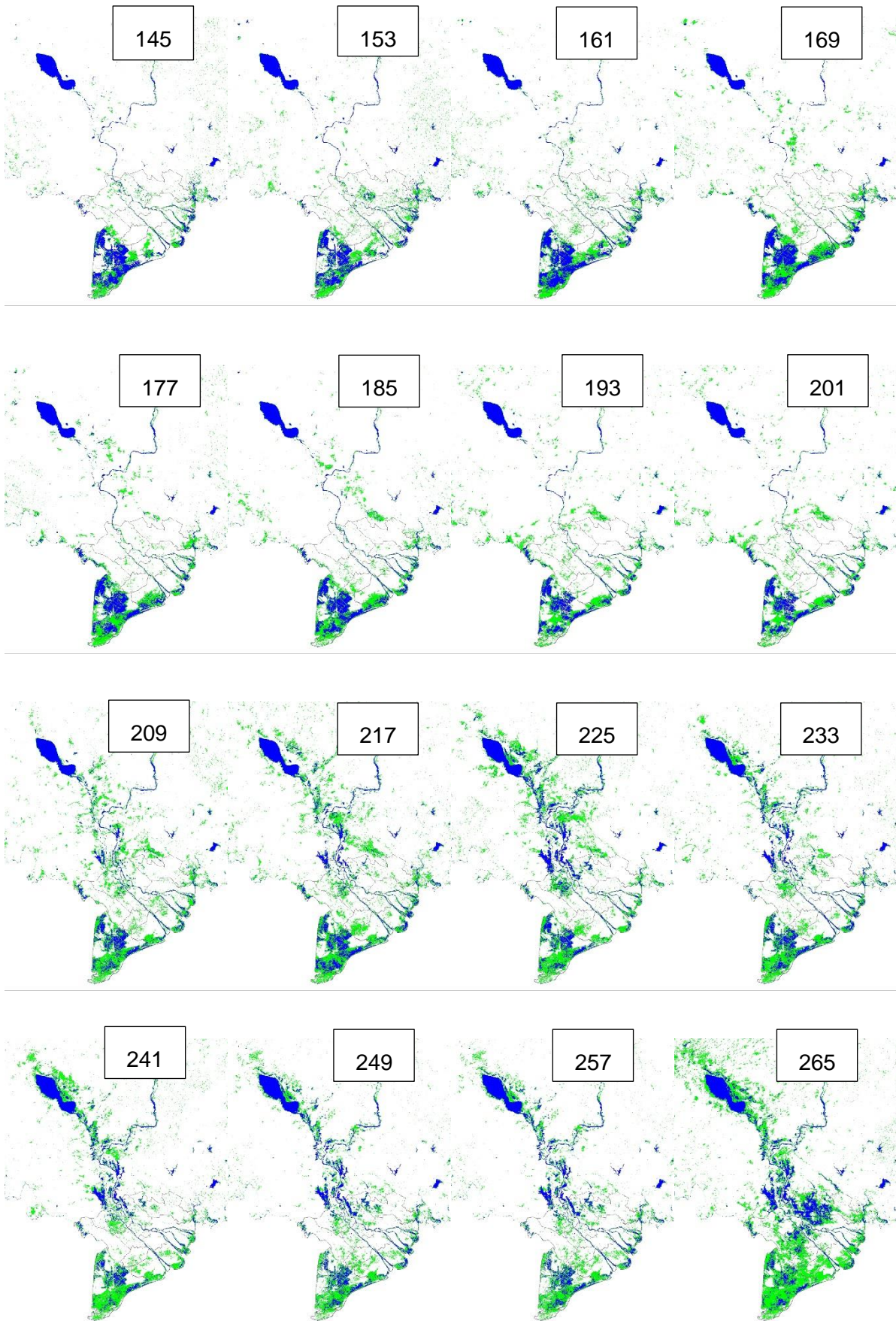


Figure 7.15. Flood distribution in Mekong delta in 2014 – MODIS satellite

7.4.15. Flood distribution in 2015



Flood distribution in 2015 (CONTINUE)

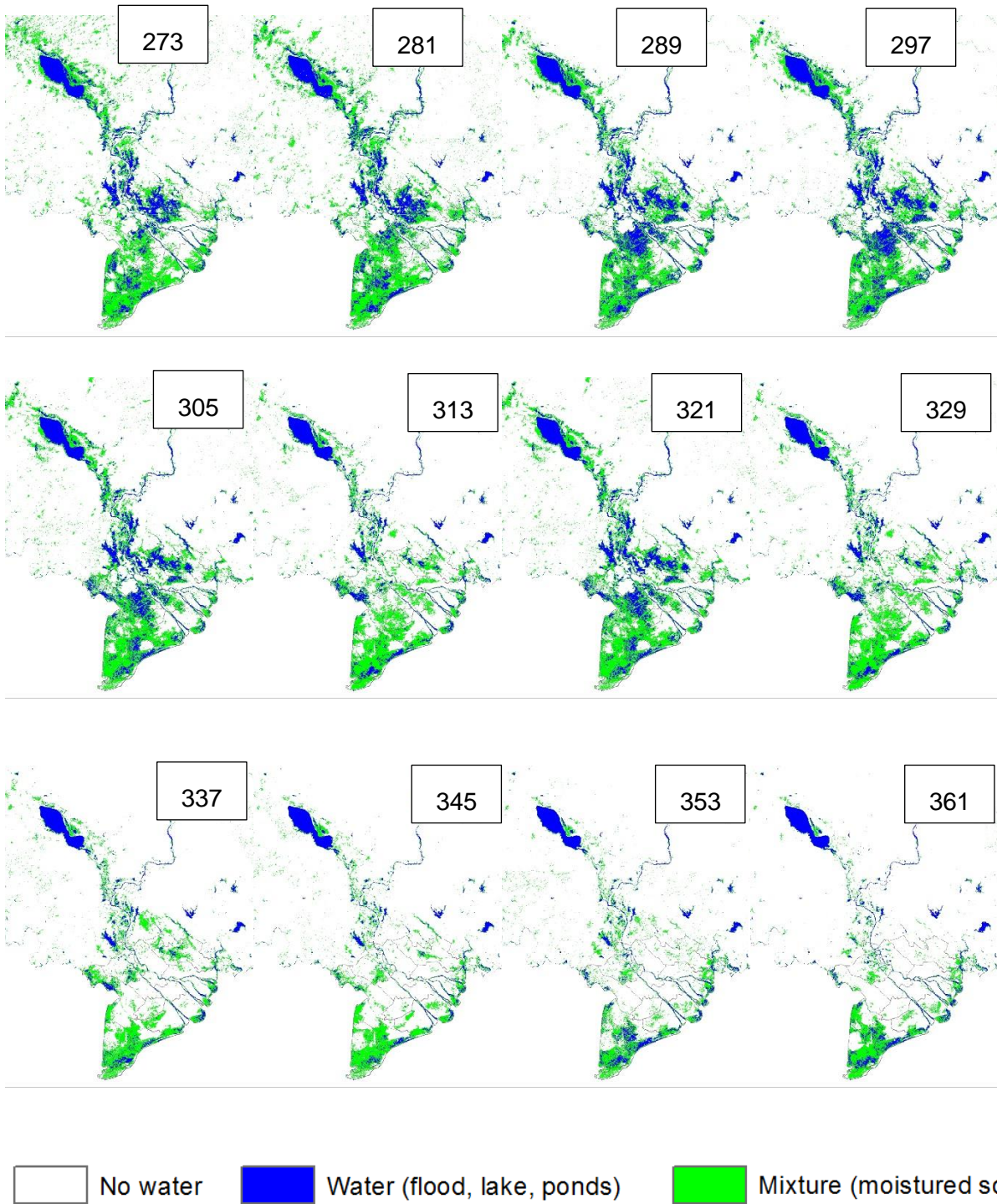
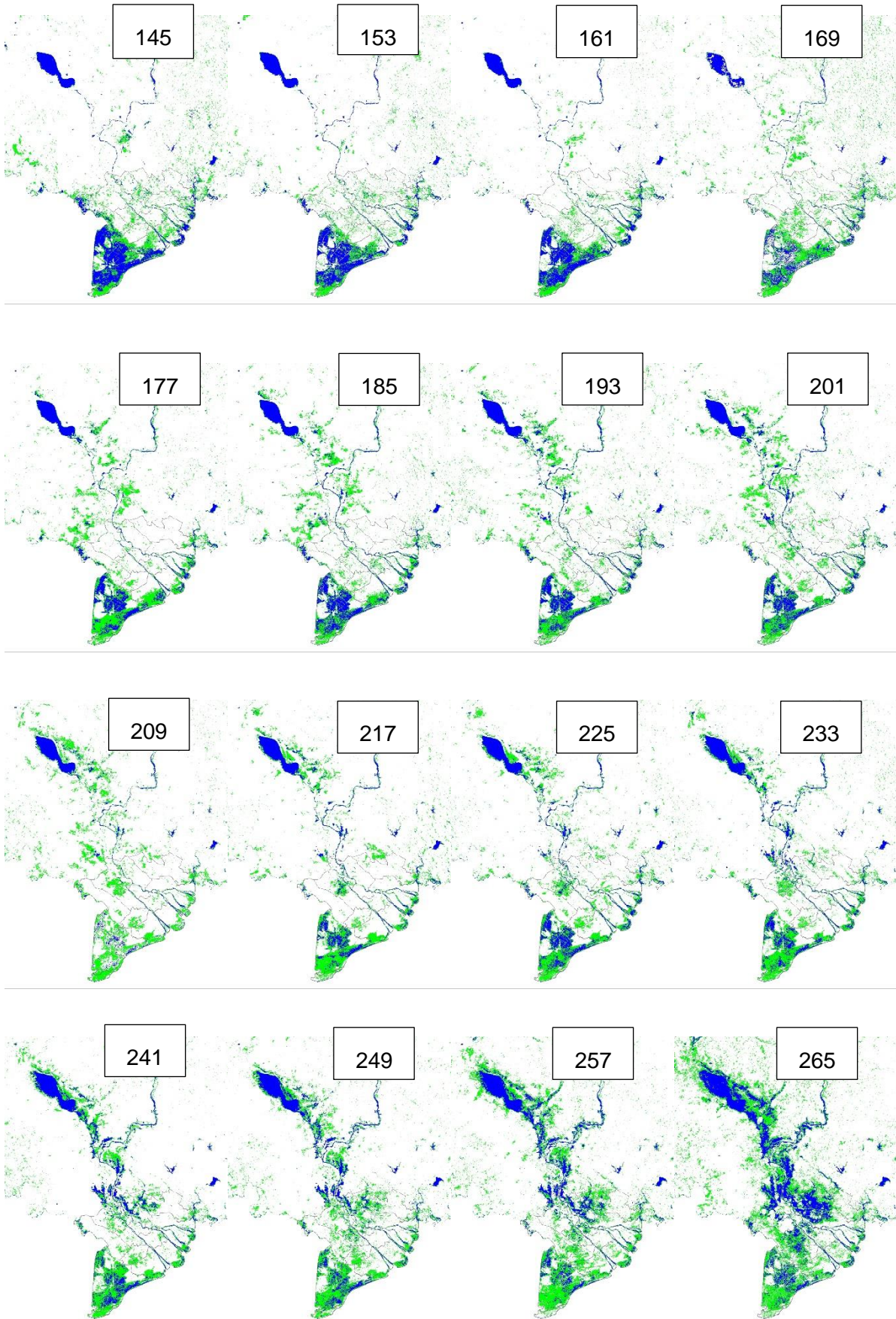


Figure 7.16. Flood distribution in Mekong delta in 2015 – MODIS satellite

7.4.16. Flood distribution in 2016



Flood distribution in 2016 (continue)

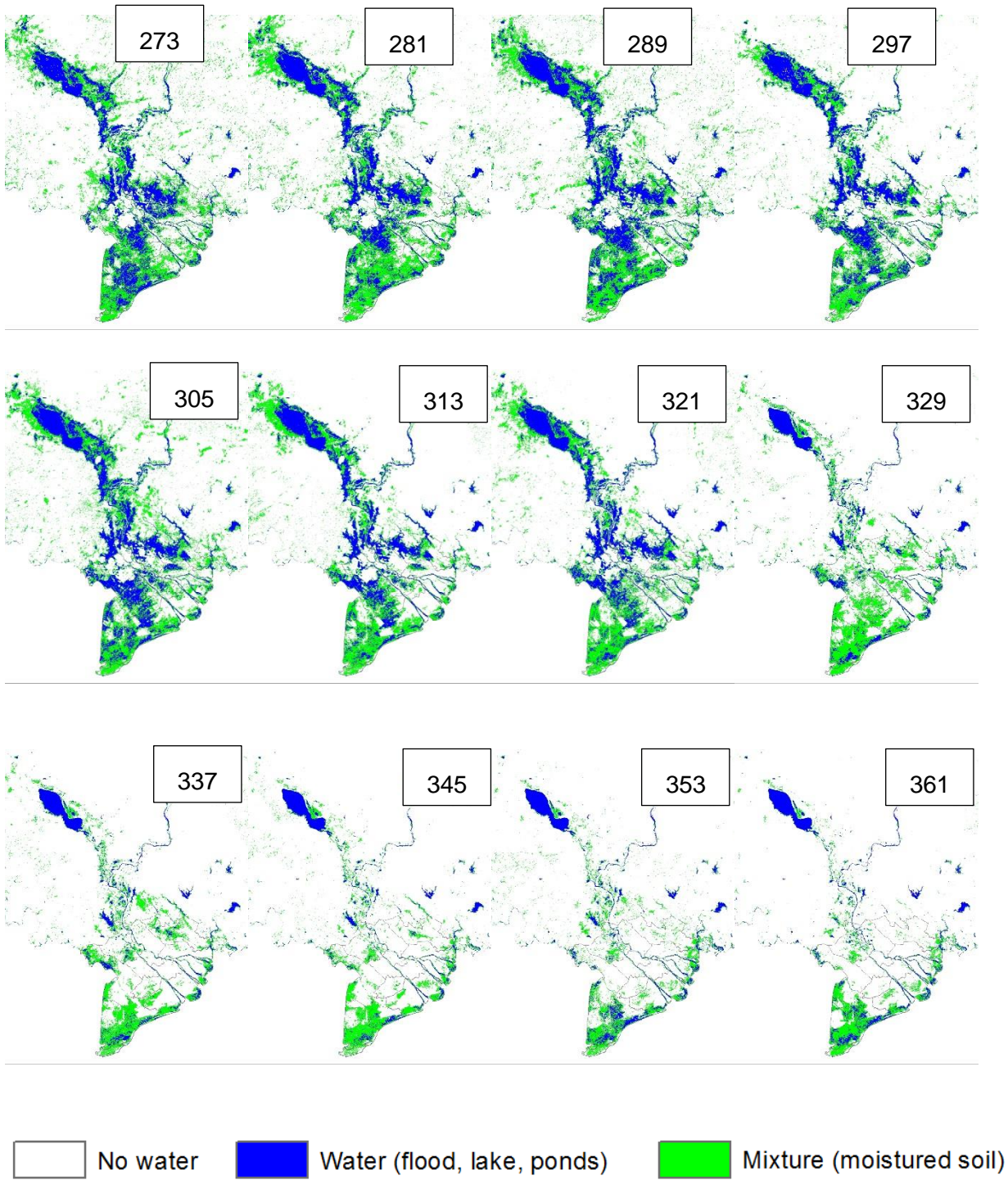
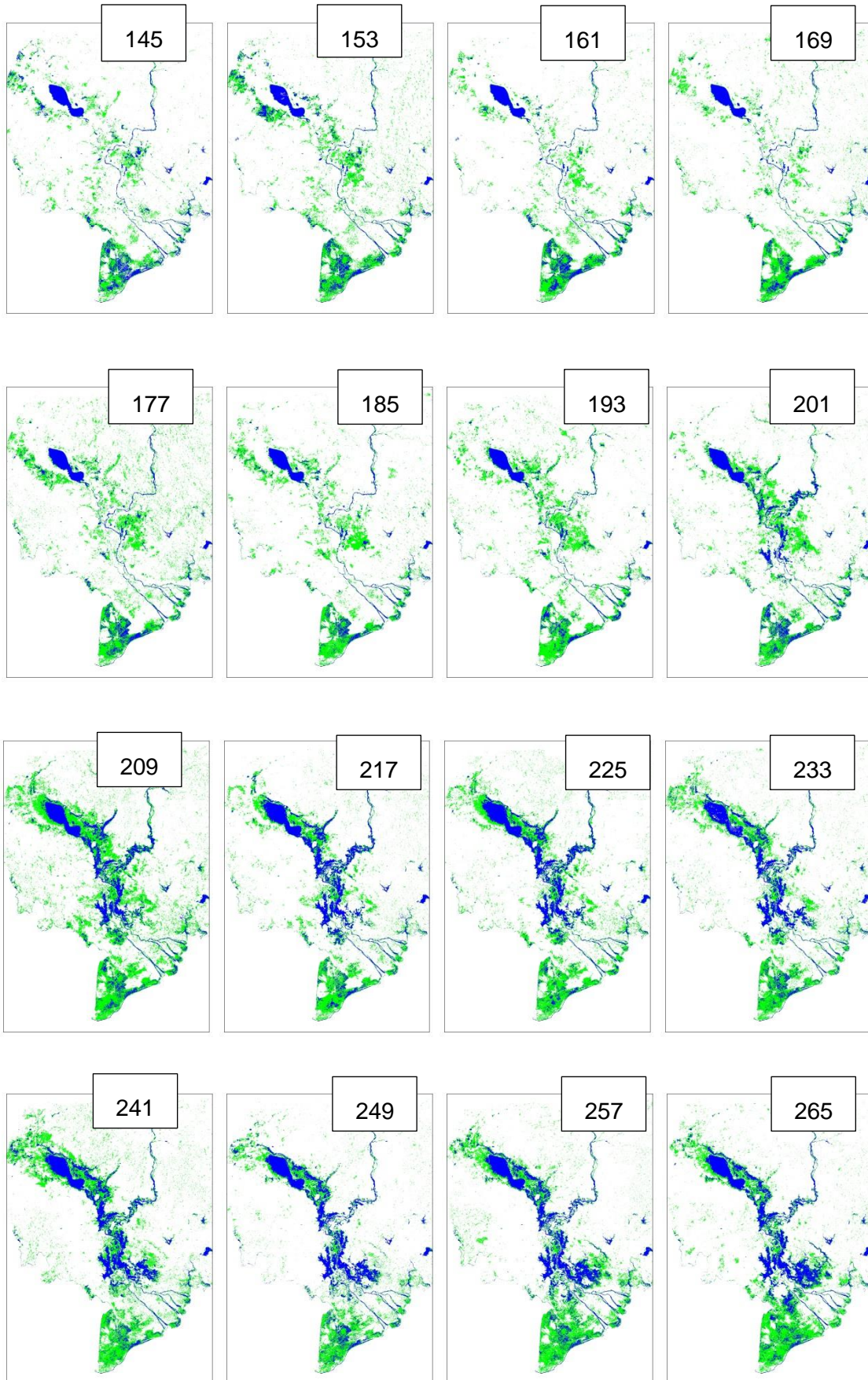


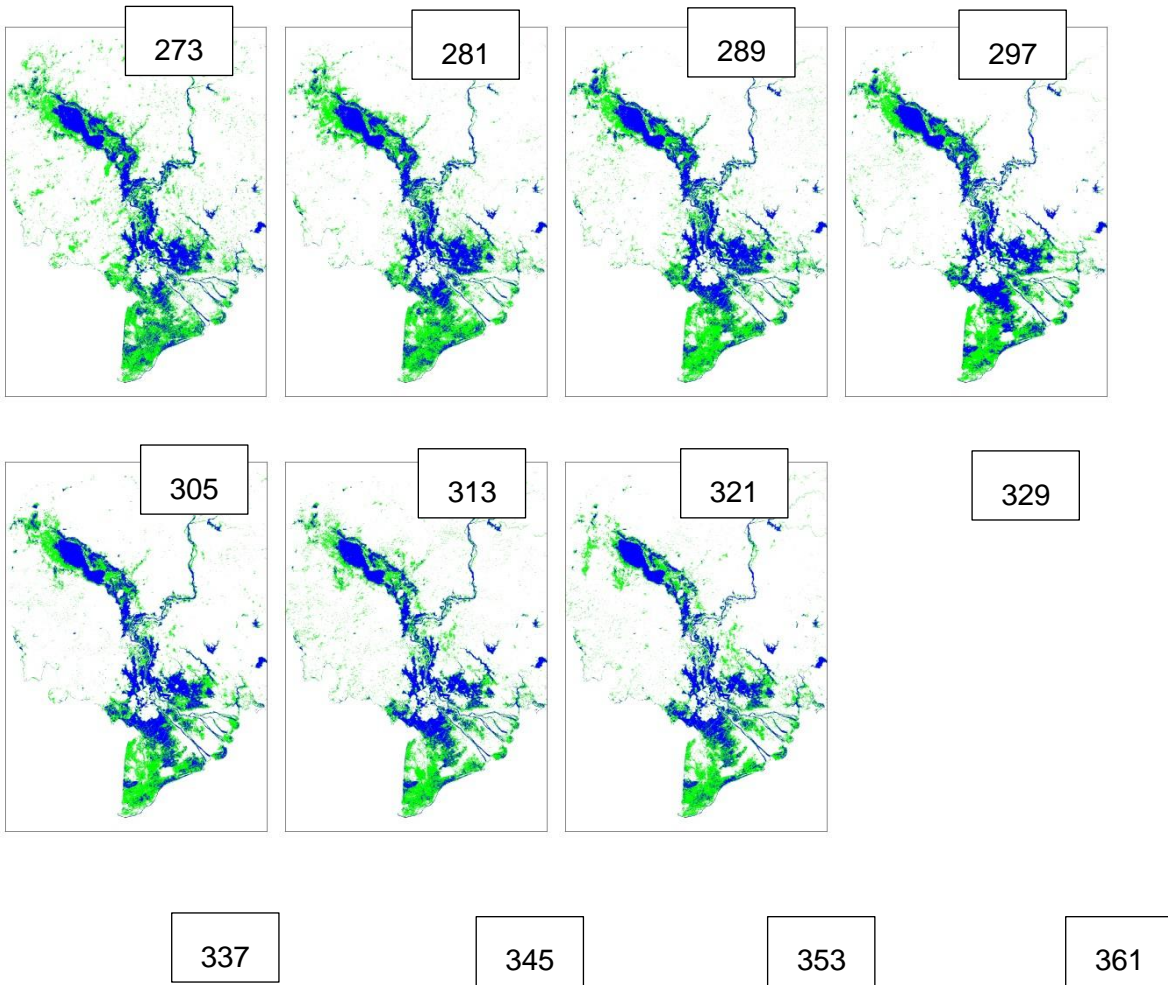
Figure 7.17. Flood distribution in Mekong delta in 2016 – MODIS satellite

7.4.17. Flood distribution in 2017



Appendix

FLOOD DISTRIBUTION IN 2017 (continue)



 No water  Water (flood, lake, ponds)  Mixture (moistured soil)

Figure 7.18. Flood distribution in Mekong delta in 2017 – MODIS satellite

7.5. Accuracy analysis of flood maps from MODIS satellite

7.5.1. Comparison with flood maps by ENVISAT-ASAR Satellite (source: DLR, 2015)

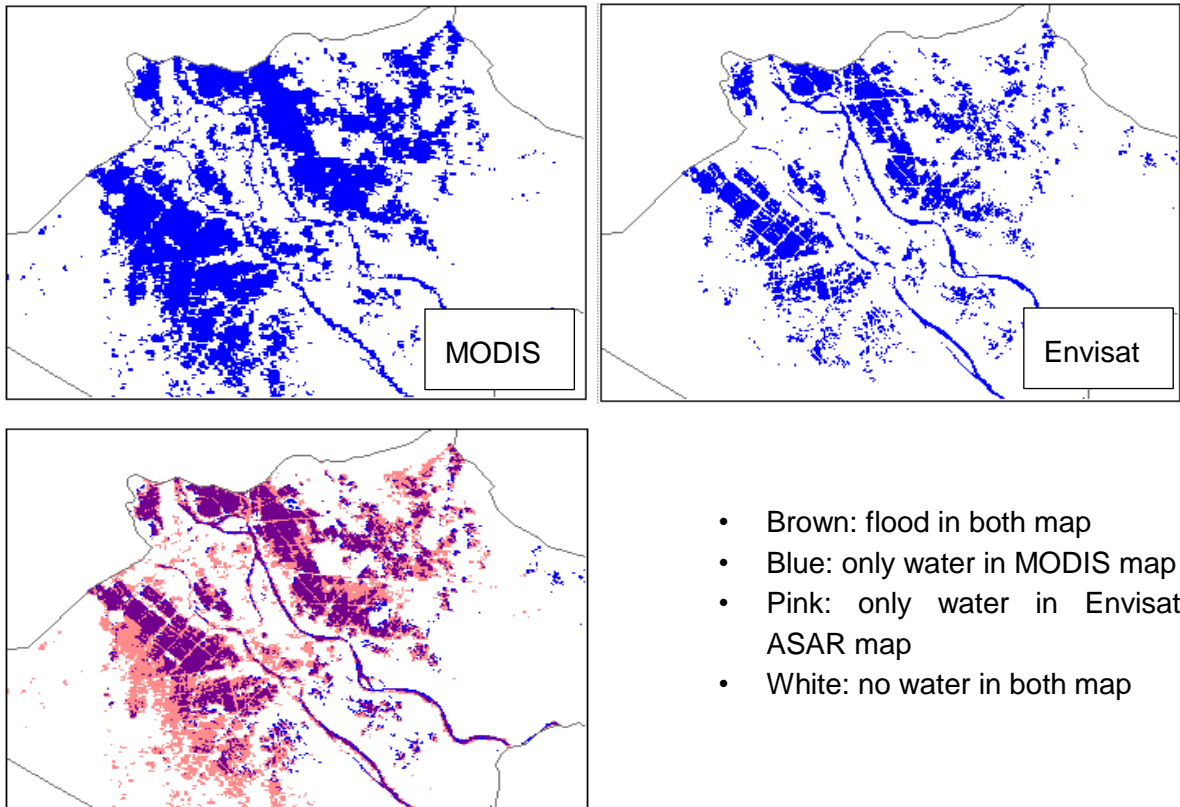


Figure 7.19. Comparison of flood mapping between Envisat ASAR vs MODIS on 14.08.2007

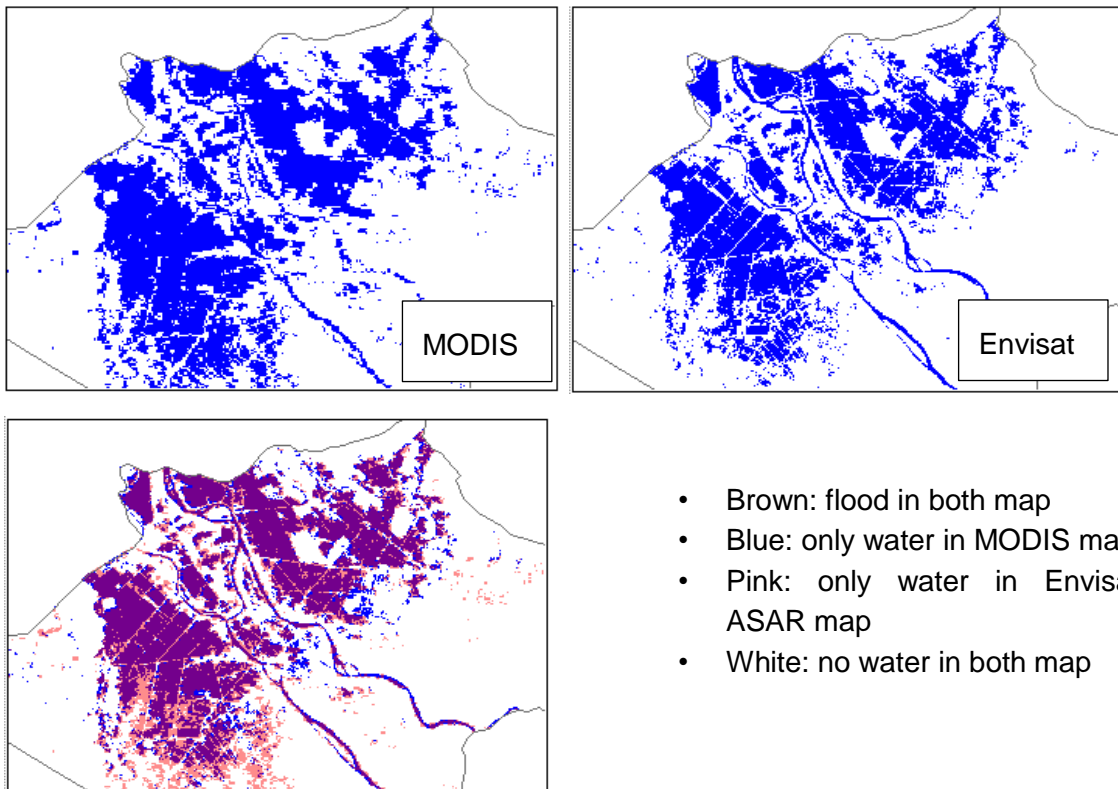


Figure 7.20. Comparison of flood mapping between *Envisat ASAR vs MODIS on 19.07.2007*

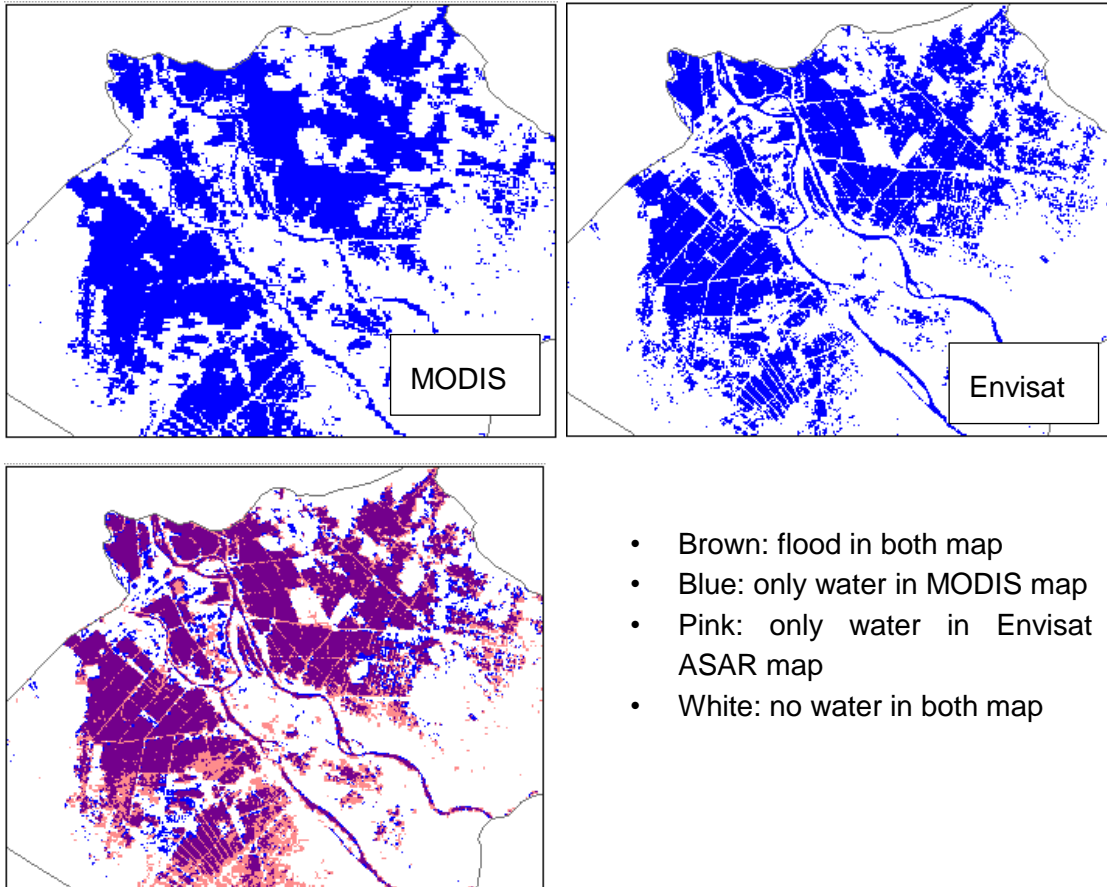


Figure 7.21. Comparison of flood mapping between *Envisat ASAR* vs *MODIS* on 11.09.2007

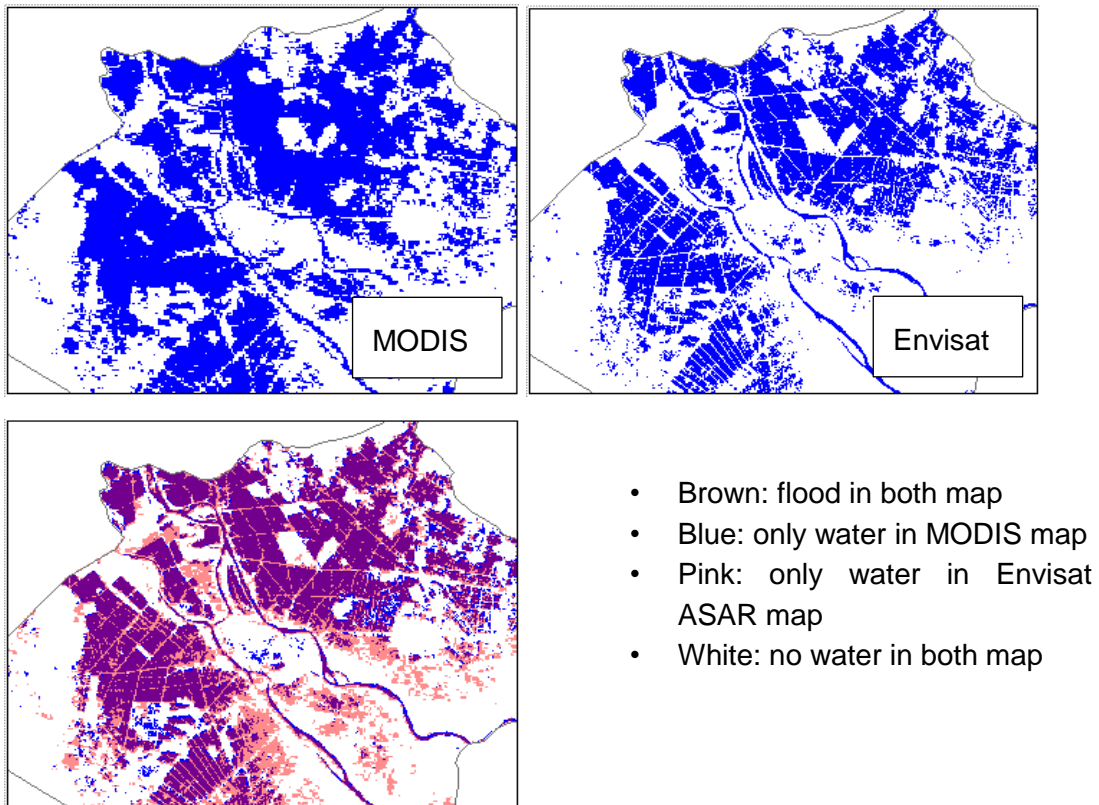


Figure 7.22. Comparison of flood mapping between *Envisat ASAR* vs *MODIS* on 18.09.2007

Appendix

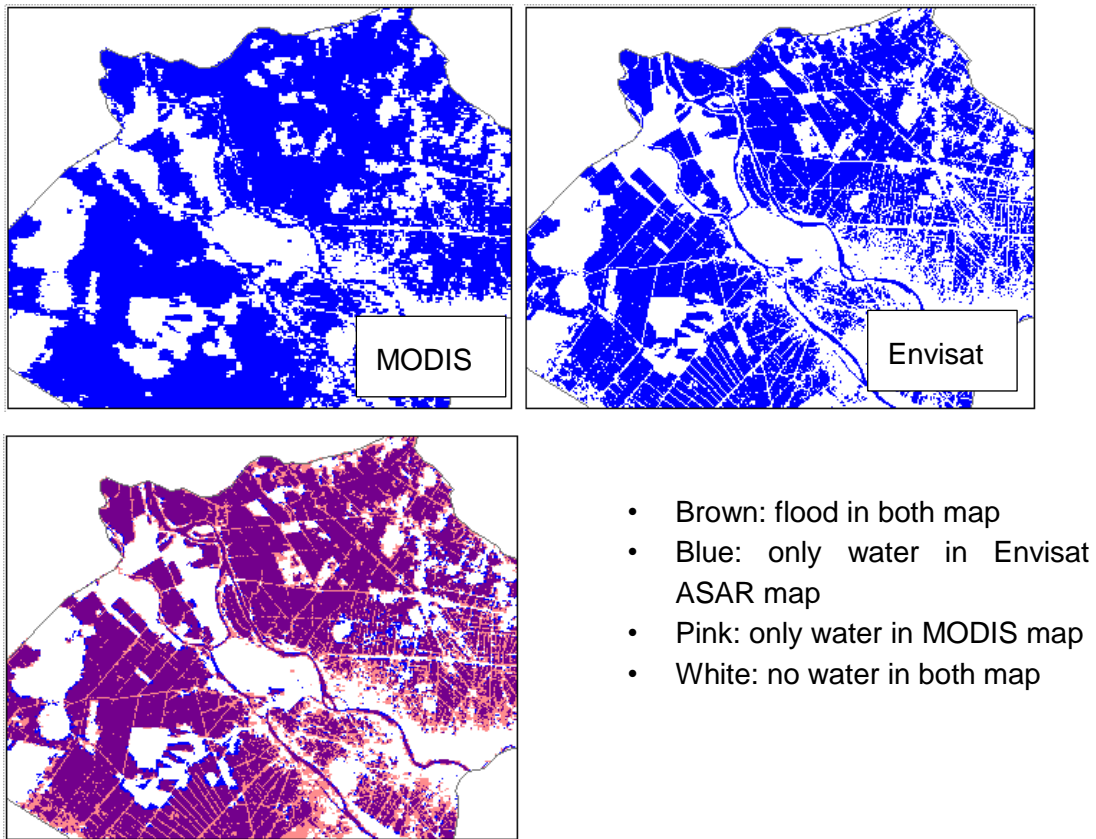


Figure 7.23. Comparison of flood mapping between *Envisat ASAR vs MODIS* on 16.10.2007

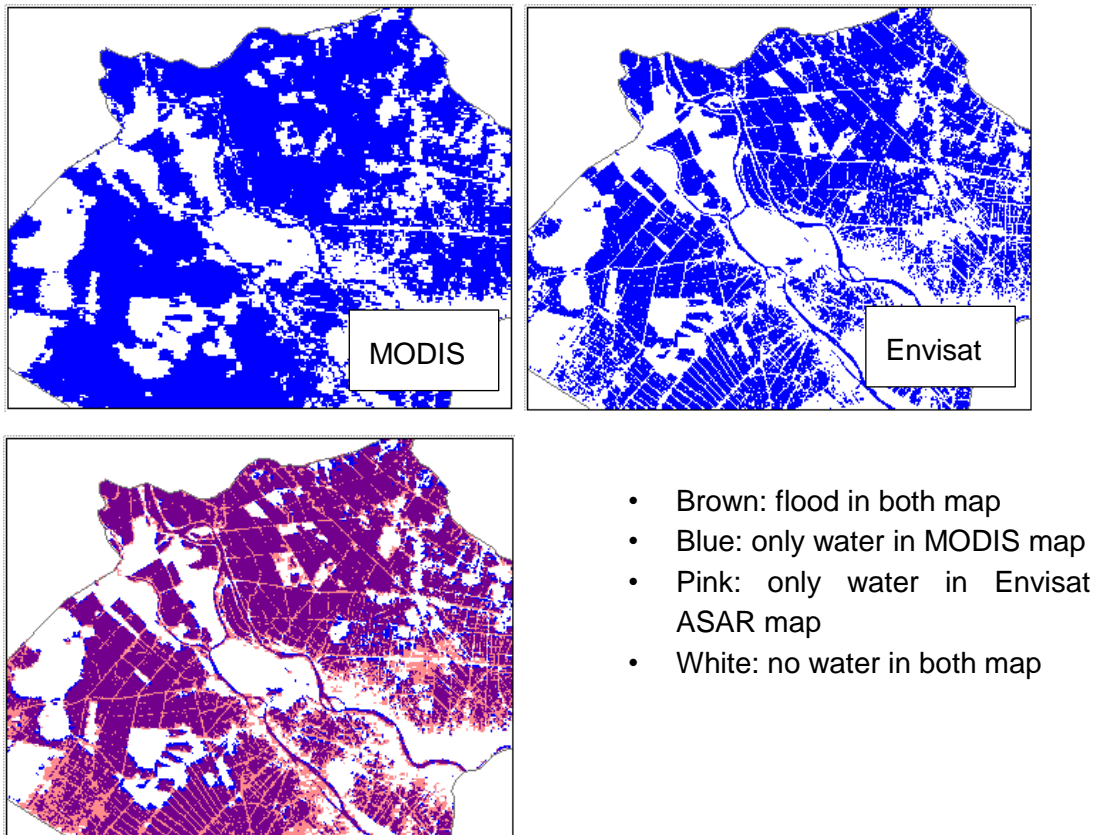


Figure 7.24. Comparison of flood mapping between *Envisat ASAR vs MODIS* on 23.10.2007

Appendix

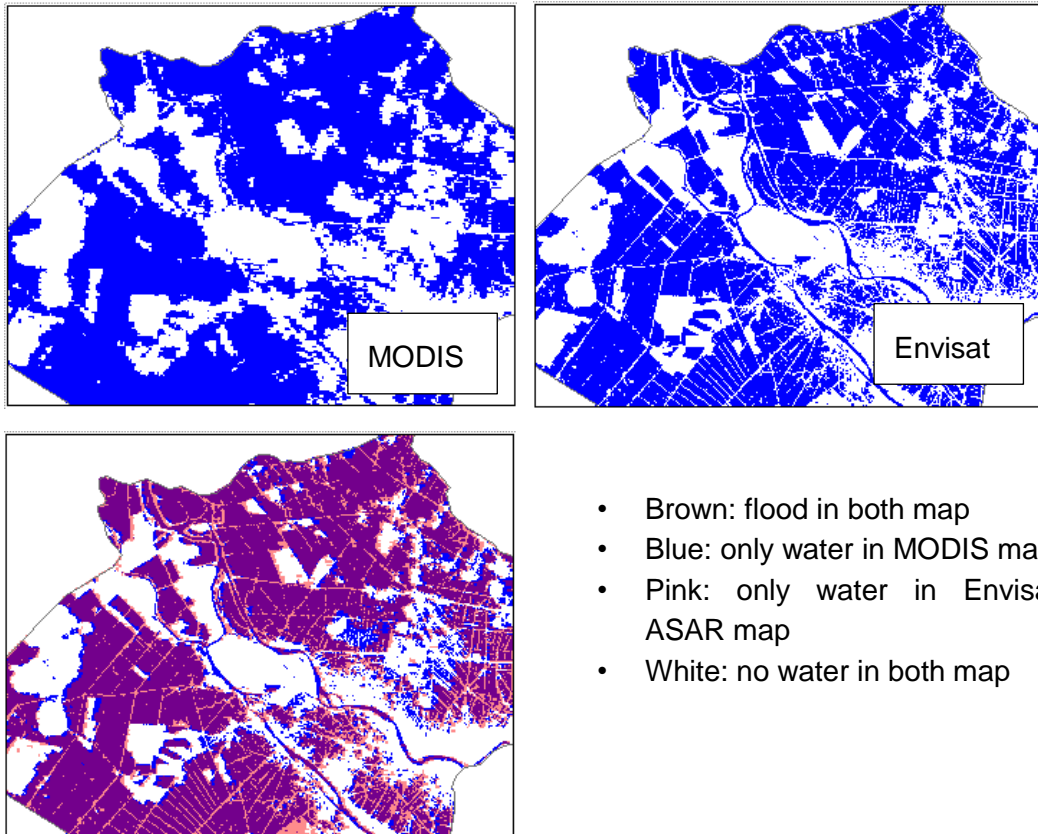


Figure 7.25. Comparison of flood mapping between *Envisat ASAR vs MODIS on 01.11.2007*

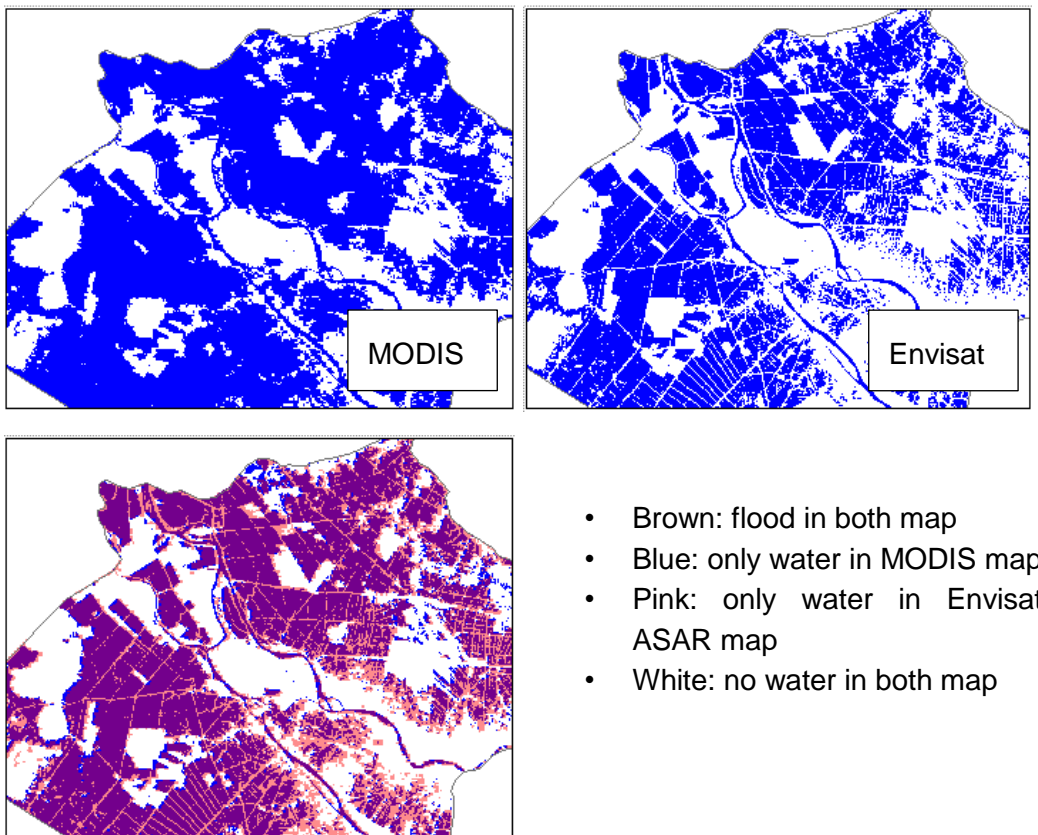


Figure 7.26. Comparison of flood mapping between *Envisat ASAR vs MODIS on 20.11.2007*

Appendix

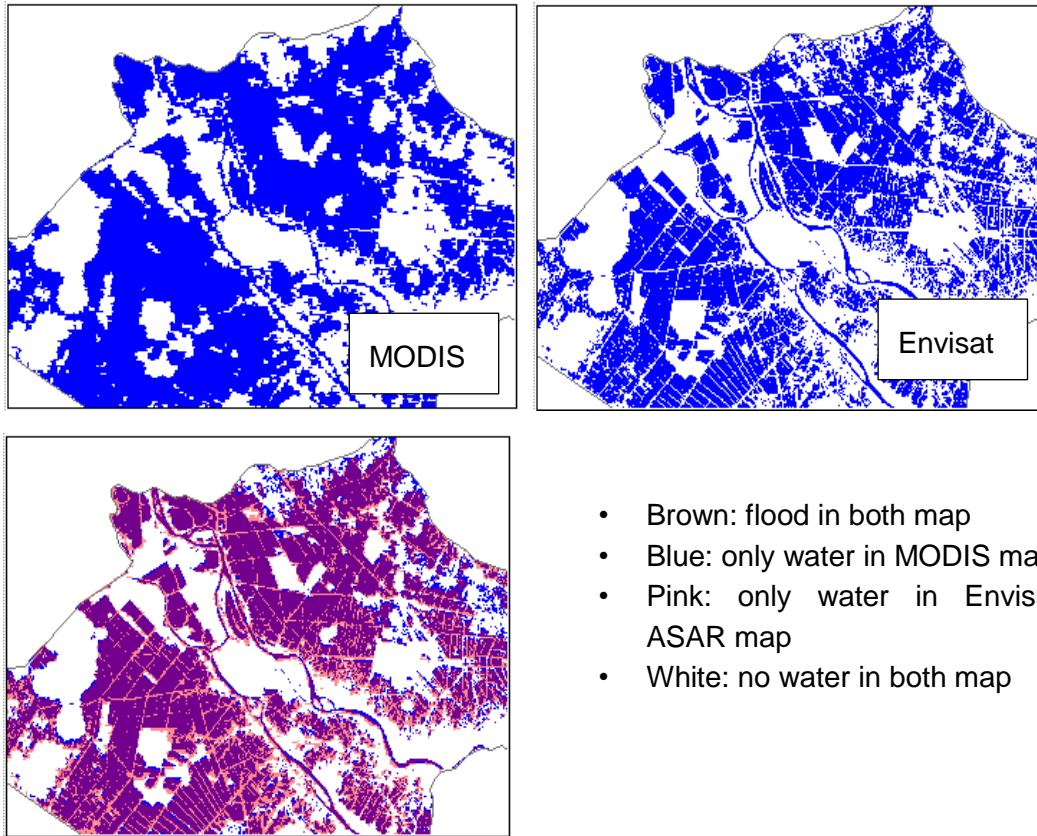


Figure 7.27. Comparison of flood maps by *Envisat ASAR vs MODIS* on 27.11.2007

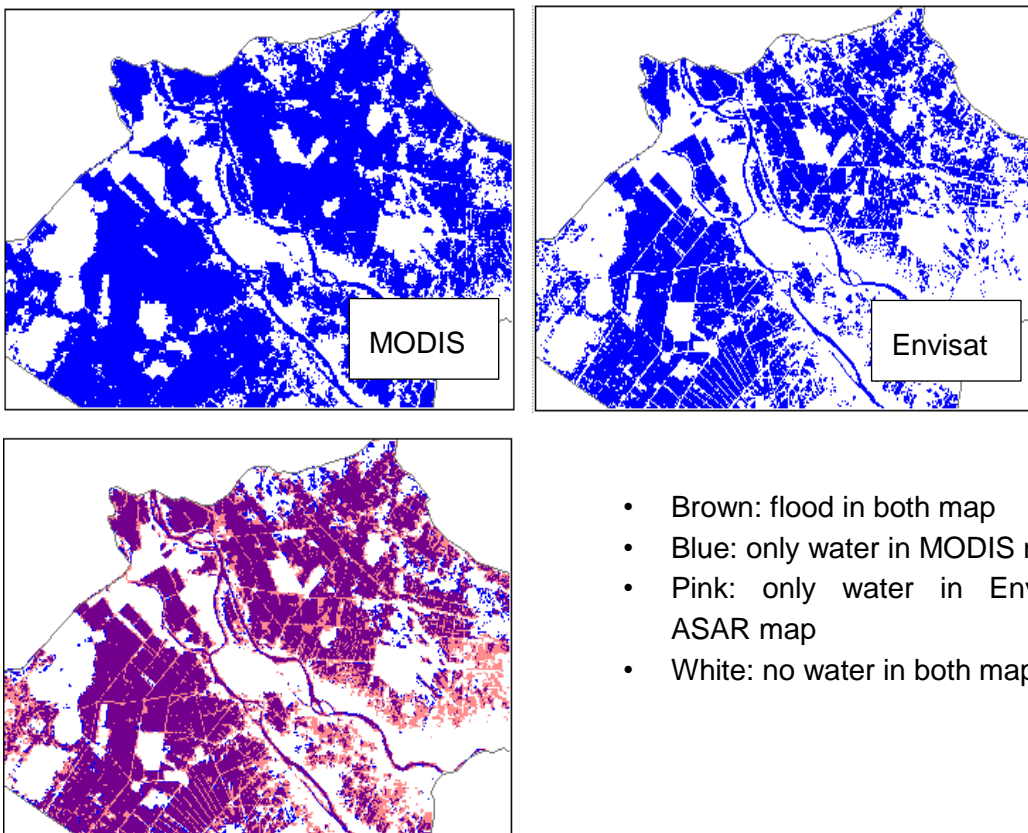


Figure 7.28. Comparison of flood mapping between *Envisat ASAR vs MODIS* on 06.12.2007

7.5.2. Comparison with flood map of TERRA-X-Scan SAR satellite (source: DLR, 2015)

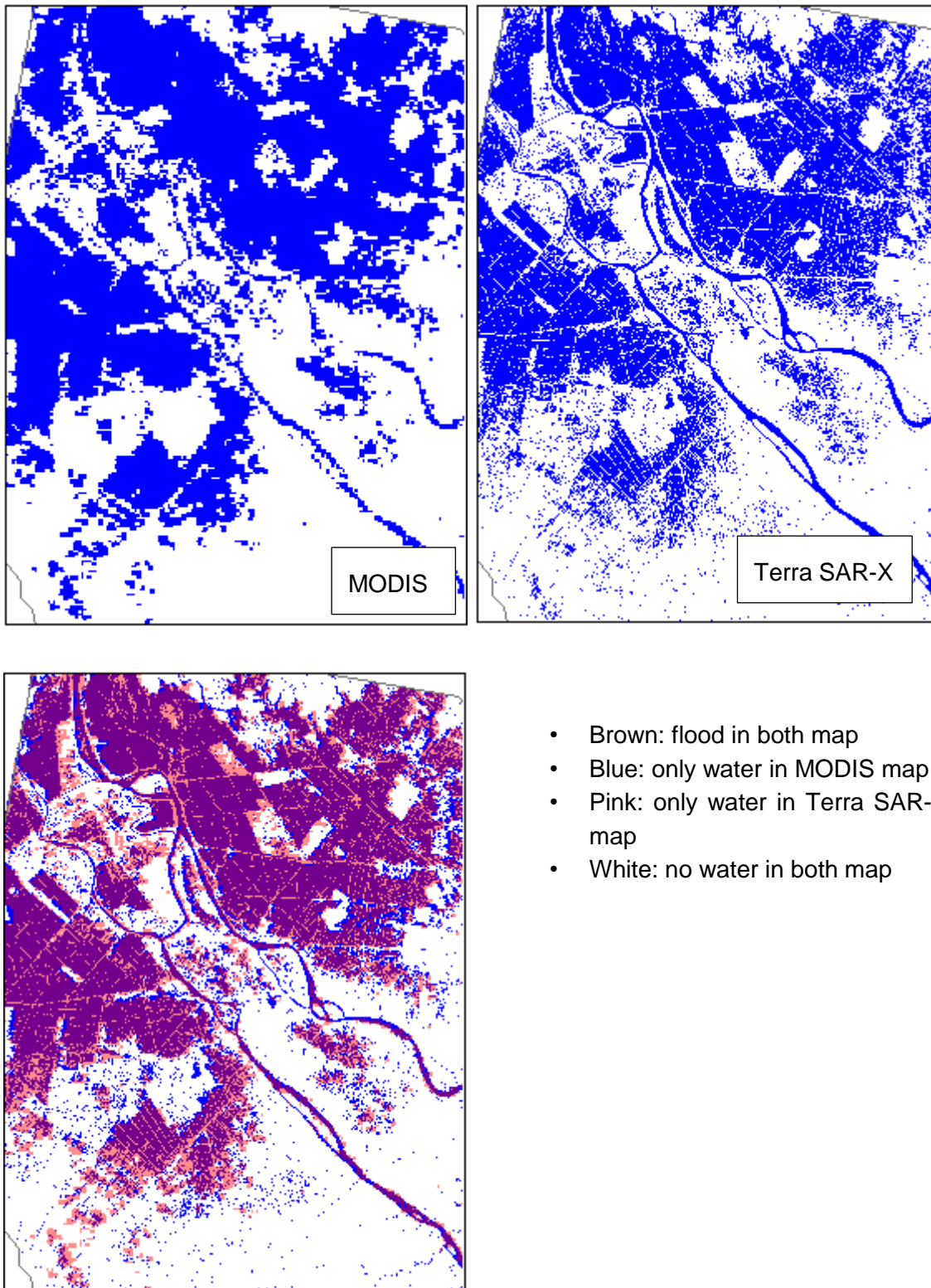
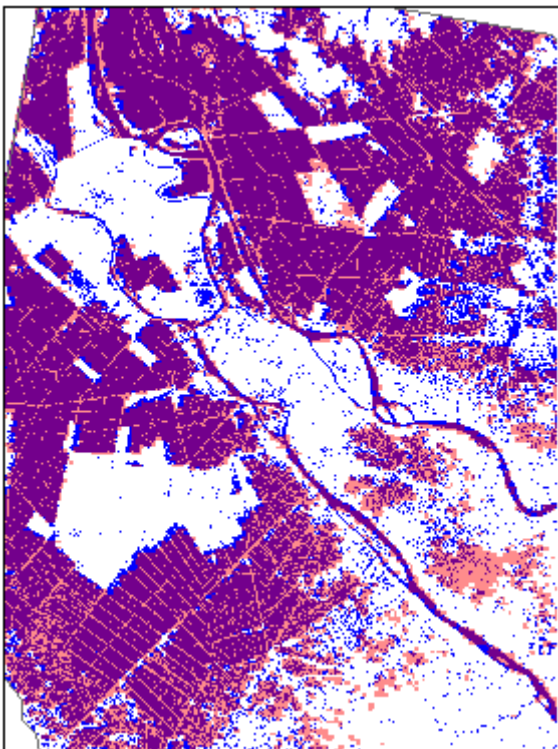
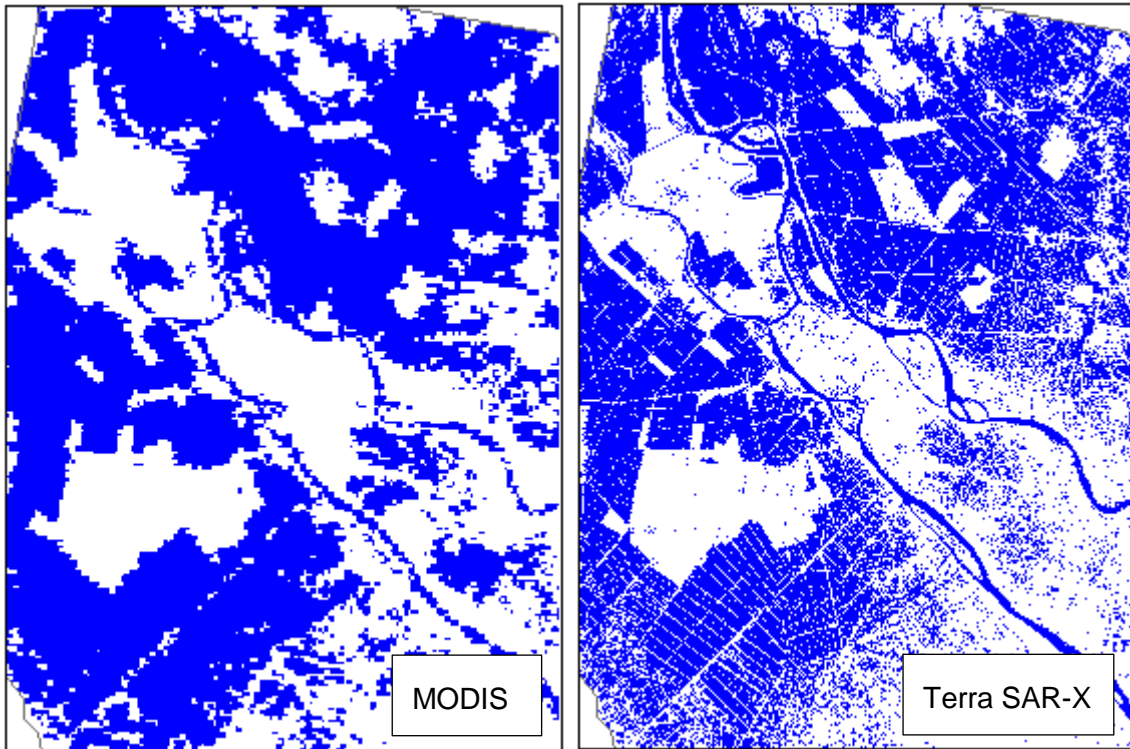
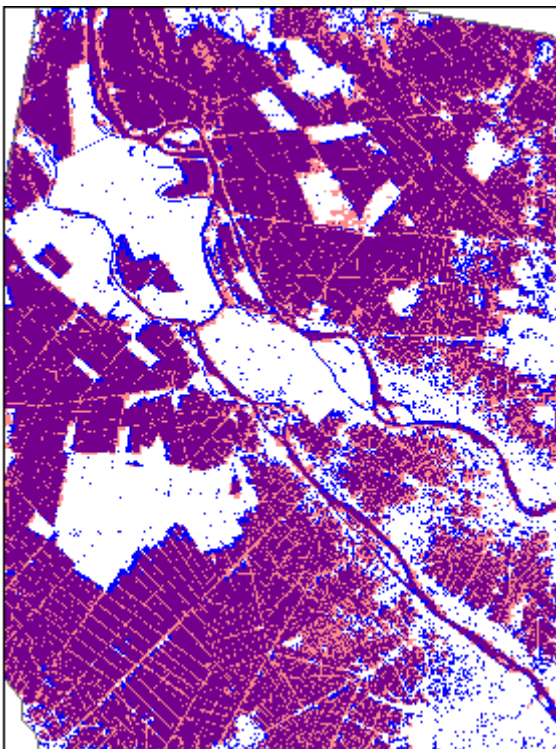
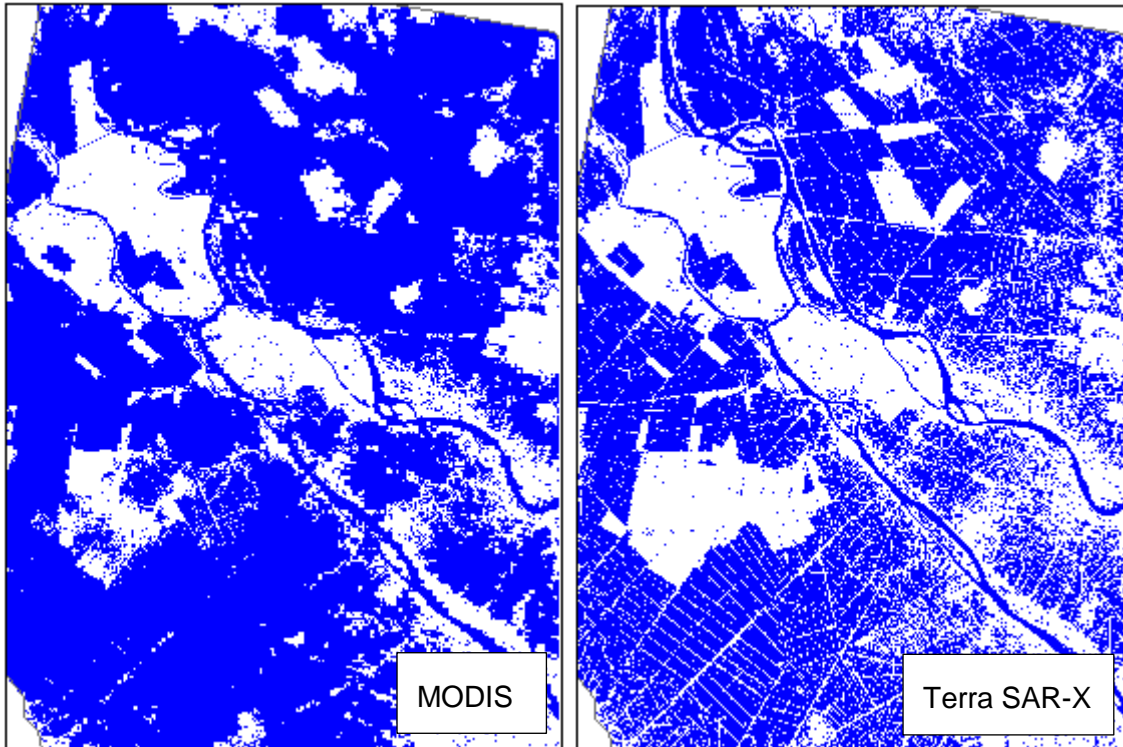


Figure 7.29. Comparison of flood mapping between Terra SAR-X vs MODIS on 23.08.2008



- Brown: flood in both map
- Blue: only water in MODIS map
- Pink: only water in Terra SAR-X map
- White: no water in both map

Figure 7.30. Comparison of flood mapping between Terra SAR-X vs MODIS on 25.09.2008



- Brown: flood in both map
- Blue: only water in MODIS map
- Pink: only water in Terra SAR-X map
- White: no water in both map

Figure 7.31. Comparison of flood mapping between Terra SAR-X vs MODIS on 28.10.2008

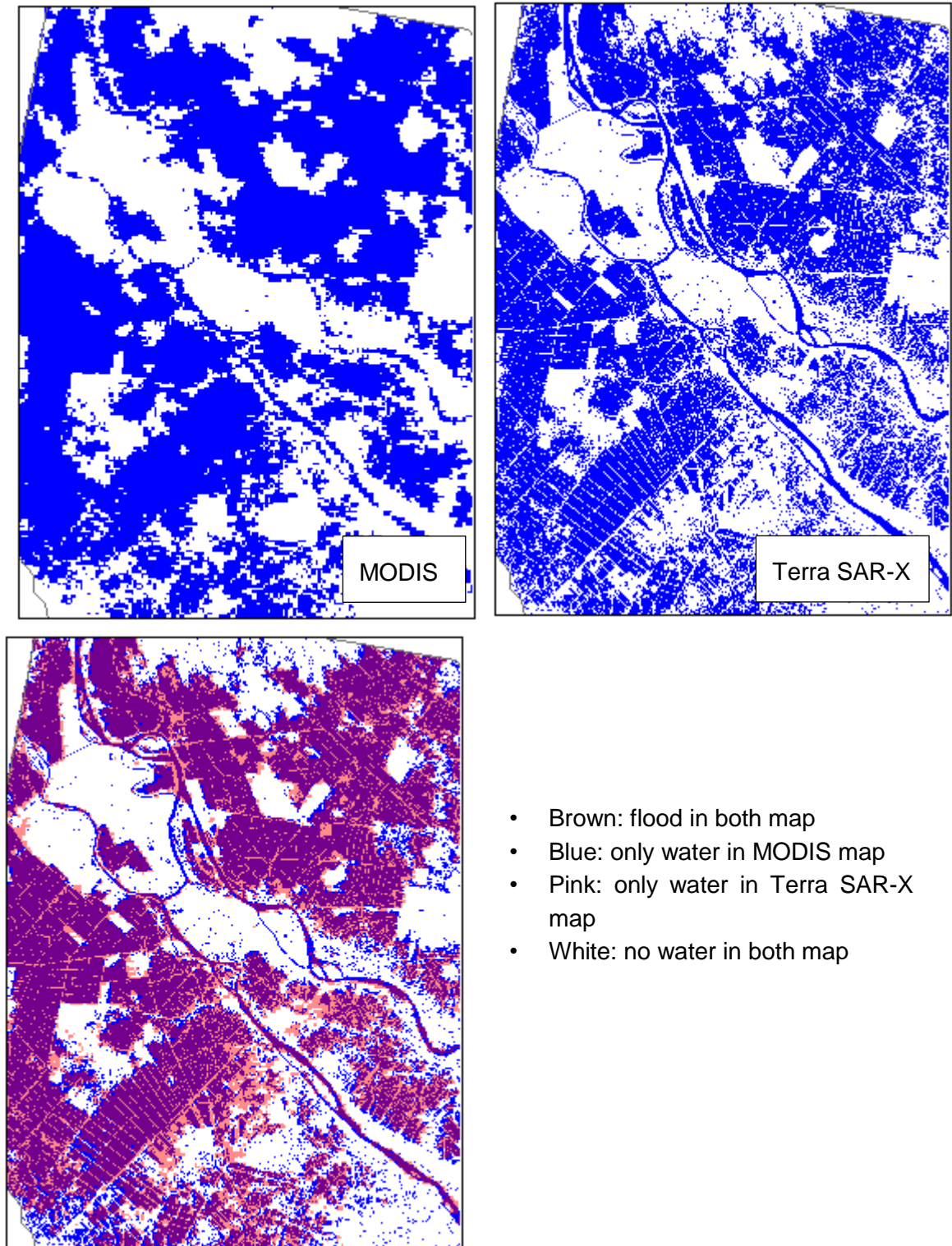
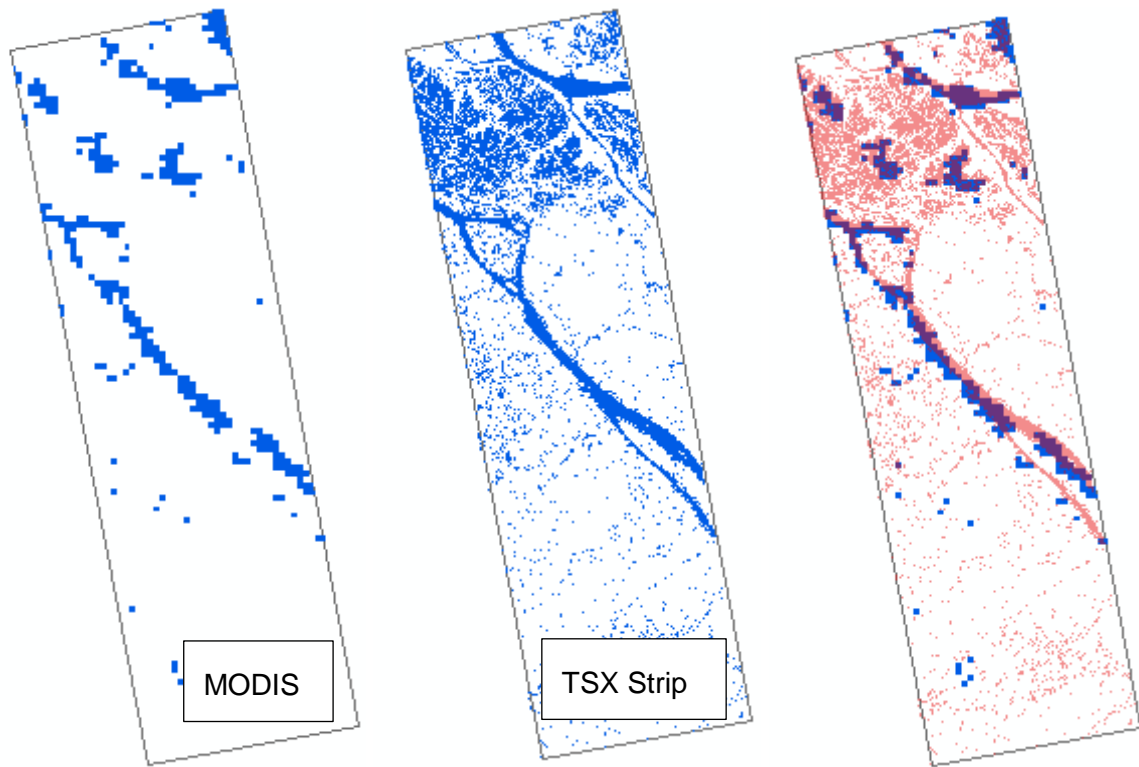


Figure 7.32. Comparison of flood mapping between Terra SAR-X vs MODIS on 30.11.2008

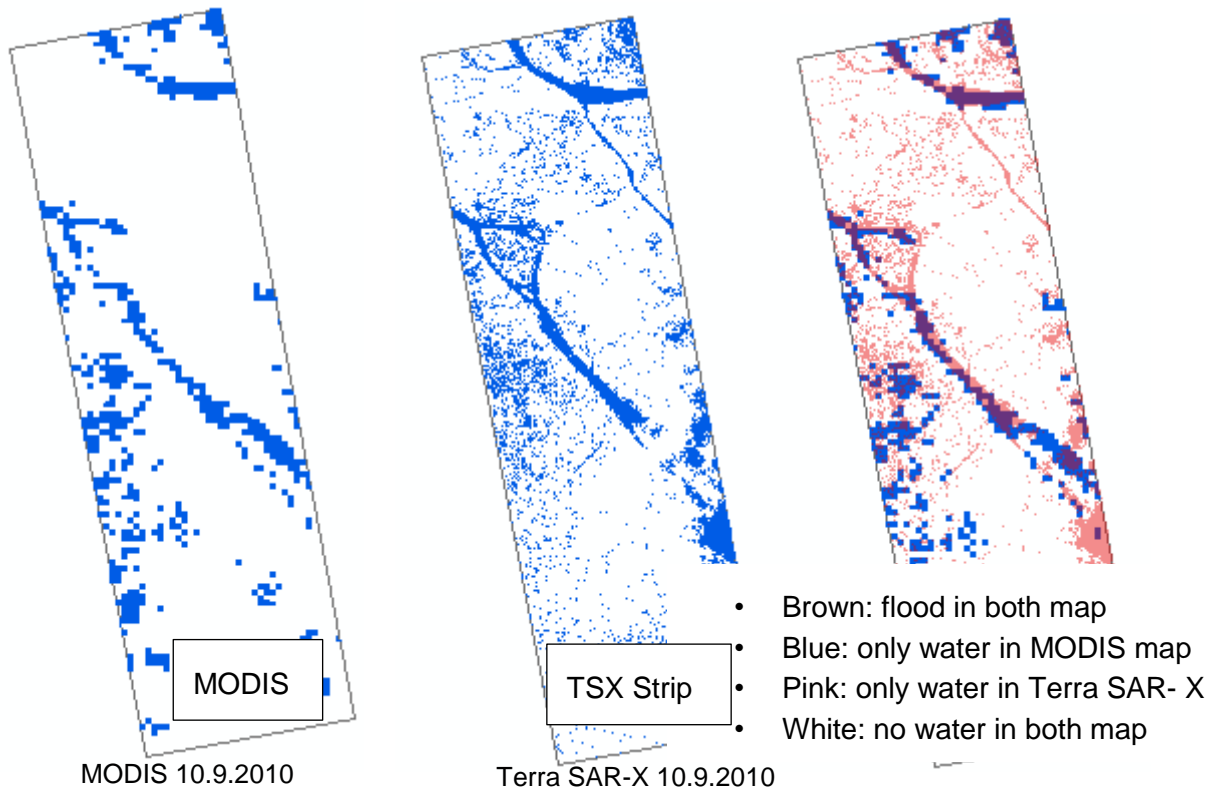
7.5.3. Comparison with flood map of TSX Strip satellite (source: DLR, 2015)



MODIS 30.8.2010

Terra SAR-X 30.8.2010

Figure 7.33. Comparison of flood mapping between Terra SAR-X vs MODIS on 30.8.2010



MODIS 10.9.2010

Terra SAR-X 10.9.2010

Figure 7.34. Comparison of flood mapping between Terra SAR-X vs MODIS on 10.9.2010

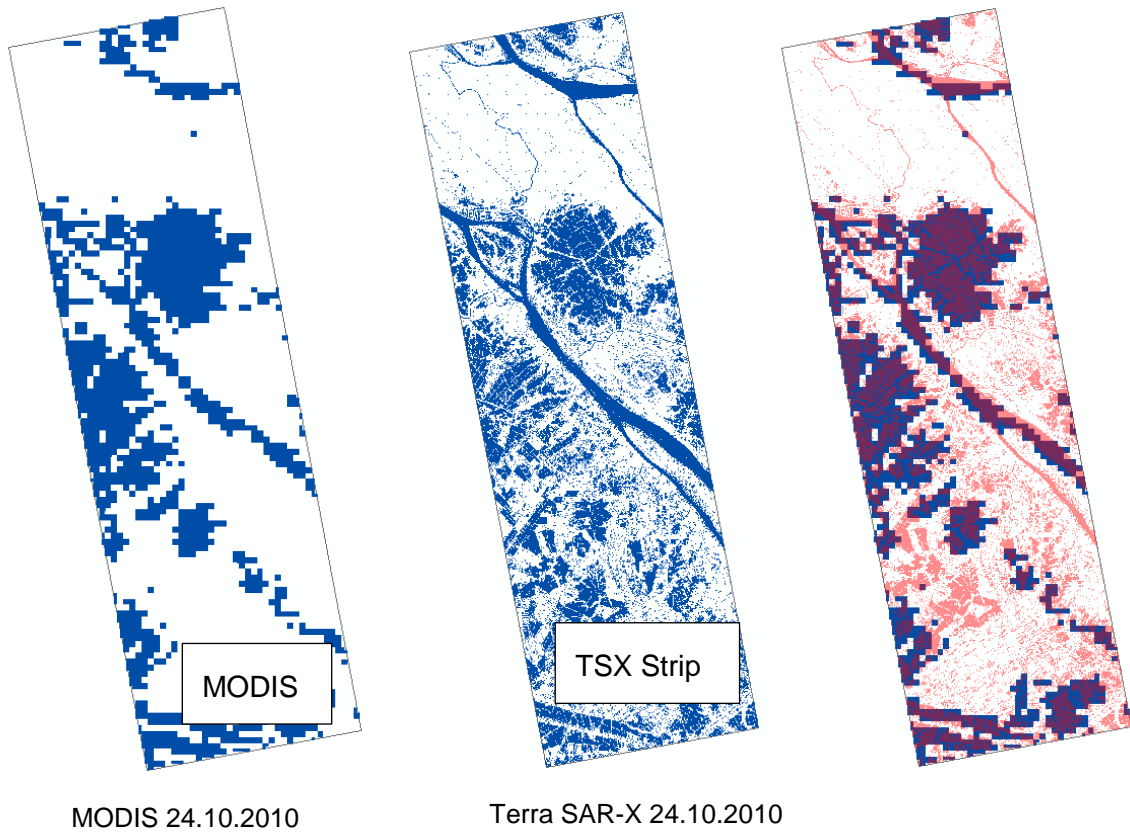


Figure 7.35. Comparison of flood mapping between Terra SAR-X vs MODIS on 24.10.2010

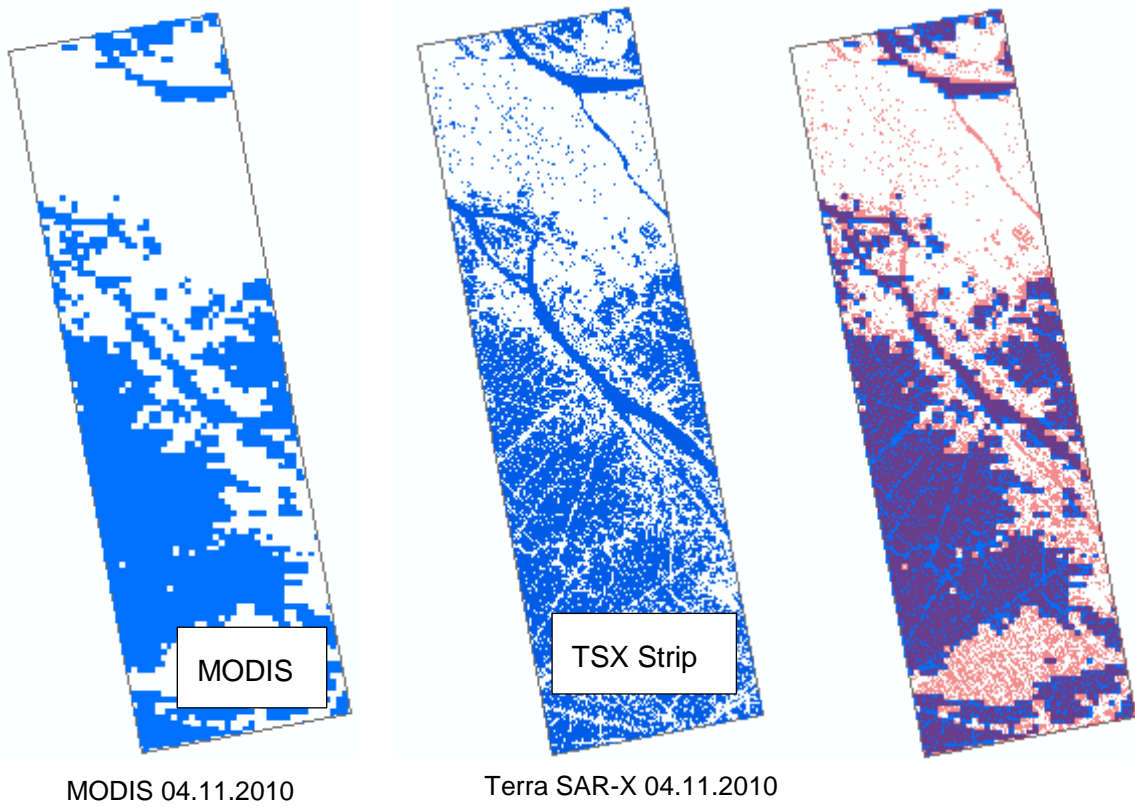
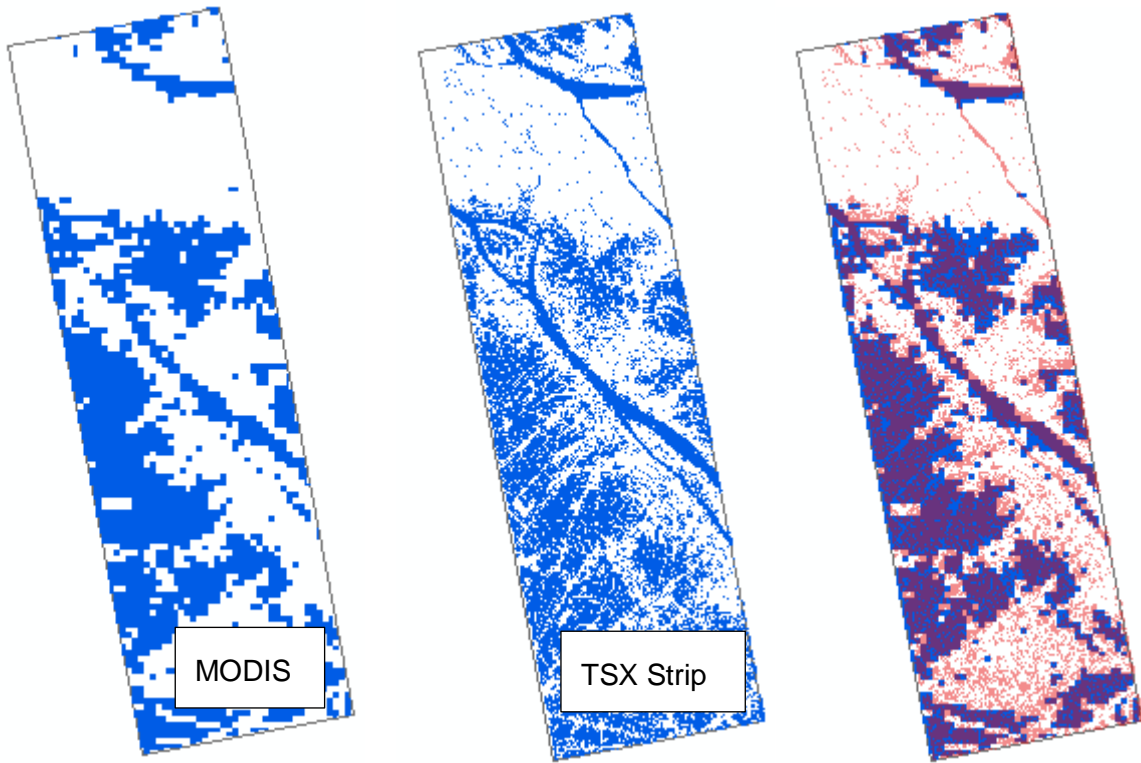


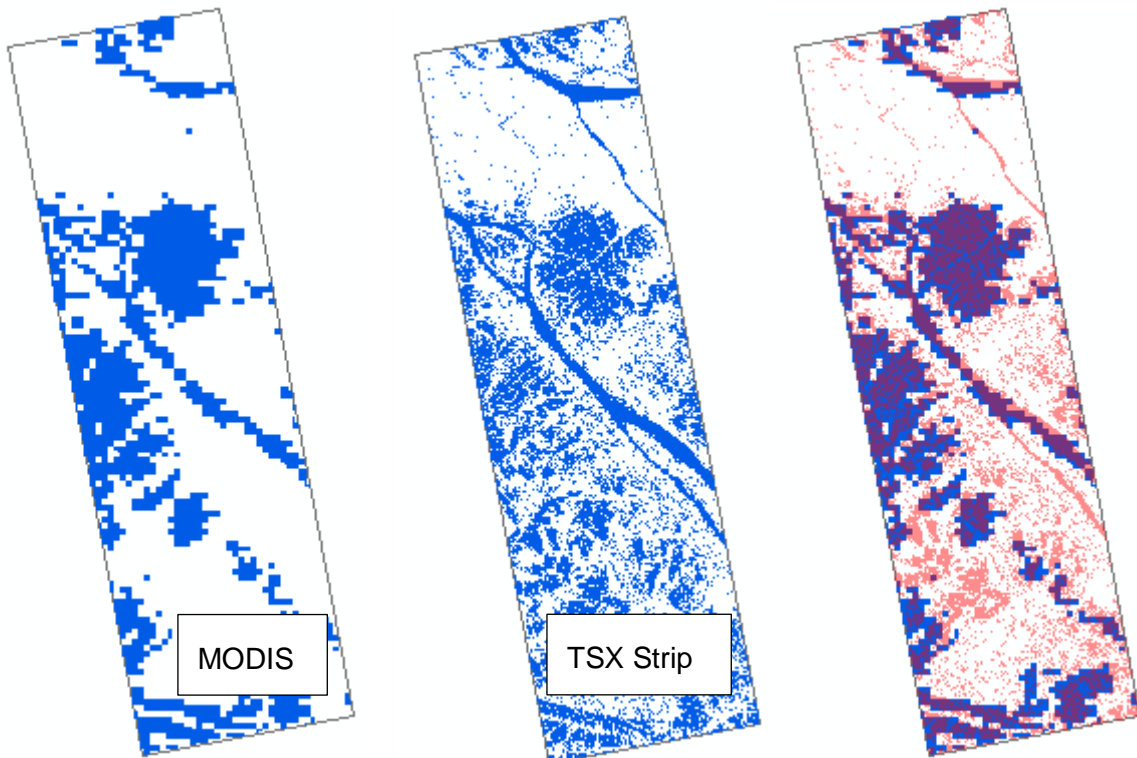
Figure 7.36. Comparison of flood maps between Terra SAR-X vs MODIS on 04.11.2010



MODIS 15.11.2010

Terra SAR-X 15.11.2010

Figure 7.37. Comparison of flood mapping between Terra SAR-X vs MODIS on 15.11.2010



MODIS 26.11.2010

Terra SAR-X 26.11.2010

Figure 7.38. Comparison of flood mapping between Terra SAR-X vs MODIS on 26.11.2010

8. Information about the author

Name: Vu, Hoang Thai Duong
Geburtsdatum: 02.11.1984 Geschlecht : Männlich
Nationalität: vietnamesisch
Beruf: Ingenieur
Adresse: Nancystrasse 24, 76187, Karlsruhe
Handys Nummer: 015734788130
Mailbox: hoang.vu@kit.edu
Sprache: Englisch, Deutsch

Studium:
2003 - 2008 Bachelor an der Water Resources Universität, Hochiminh Stadt
2010 – 2012 Master an der Universität of Liege, Belgien
2013 - 2018 Doktorand am Institut für Wasser und Gewässerentwicklung (IWG)
Karlsruhe Institut für Technologie (KIT)

Beruf:
2008 – 2012 Wissenschaftliche Angestellte an der Water Resources Universität
2013 – 2018 Stipendiat am Institut für Wasser und Gewässerentwicklung (IWG)
Karlsruhe Institut für Technologie (KIT)
Seit 2018 Wissenschaftlicher Mitarbeiter am IWG - KIT

Publications:

- Duong, V.H.T., Nestmann, Van T.C, F., Oberle, P., Nam N.T. (2014). Land use based flood hazards analysis for Mekong delta. Proceedings 19th IAHR Asian and Pacific Regional Division 2014, Hanoi, Vietnam, September 21–24, 2014, ISBN: 978-604-82-1383-1.
- Duong, V.H.T., Nestmann F., Van T.C, Oberle, P.,Hinz, S., (2016). Geographical Impact of Dyke Measurement for Land Use on Flood Water in the Mekong Delta. Proceedings of the IWA 8 th Eastern European Young Water Professionals Conference Gdansk, Poland, 12-14 May, 2016, 308-317.
- Duong V.H.T, F. Nestmann, Van T.C, S. Hinz, P. Oberle, “ Analysis the development of triple rice cropping area and its impact on flooding situation in An Giang province”. Proceedings in the 10 Eastern European Young Water Professionals Conference, Zagreb, Croatia, May 7-12, 2018.
- Duong V.H.T, F. Nestmann, Van T.C, S. Hinz, P. Oberle. Introduction about the interpolation method for flood water prediction along Mekong River. Proceedings in the 10 Eastern European Young Water Professionals Conference, Zagreb, Croatia, May 7-12, 2018.